Discovery and Mechanisms of Small Molecule Amyloid Formation Inhibitors

Paul William Velander

Dissertation submitted to the faculty of the Virginia Polytechnic Institute and State University in partial fulfillment of the requirements for the degree of

Doctor of Philosophy
In Biochemistry

Bin Xu, Committee Chair

David Bevan

Mike Klemba

Pablo Sobrado

December 6th, 2017
Blacksburg, VA

Academic Abstract

Current dogma suggests modulating or preventing amyloid assembly will prove critical to the armamentarium of therapeutic interventions that will likely be required to overcome the multifaceted pathology associated with amyloid diseases. The work described in this dissertation reveals substantial gains in understanding key aspects relating to the anti-amylin amyloid activities associated with both individual and broad groups of small molecule amyloid inhibitors. A main observation was the important role that the catechol functional group plays in modulating and preventing amyloid formation. In this context, each chapter provides unique yet complementary mechanistic insight that delineates a wide range of anti-amyloid activities associated with preventing amylin amyloid formation by mainly catechol-containing structural scaffolds. Structure activity studies show that the catechol moiety present within baicalein, oleuropein and rosmarinic acid are critical for their anti-amyloid functions, including exerting cell rescue effects against amylin induced cytotoxicity. We also demonstrate that in general, autoxidation enhances the anti-amyloid potency associated with many catechol containing amyloid inhibitors that may be mechanistically linked to a covalent mode of action. For example, we demonstrate that the O-quinone form of baicalein conjugates with amylin via a Schiff base mechanism. In contrast, we also show that catechol mediated formation of protein denaturant resistant aggregates, which requires autoxidation and that also stems from a predicted covalent mode of action, does not necessarily correlate with the enhanced anti-amyloid activities that occur upon catechol autoxidation. Regardless of the chemical mechanism(s) that drive catechol mediated anti-amyloid activity *in vitro,* the observed cell rescue effects exhibited by catechol containing molecules against amylin amyloid induced cytotoxicity is congruent with several recent *in vivo* studies that indicate polyphenols prevent toxic amyloid deposition as well as decades of population based studies that show regular consumption of diets rich in

polyphenols are linked to a reduce incidence of age-related neurodegenerative amyloid disease. Indeed, advances in structure based drug discovery against amyloid formation may provide new avenues to optimize various catechol containing scaffolds that could be readily leveraged into improving diagnostic tools or perhaps accelerate the effort of discovering anti-amyloid therapeutics.

General Audience Abstract

From causing dementia in diseases like Alzheimer's disease (AD) to potentiating type 2 diabetes (T2D), amyloid diseases represent some of the most devastating and increasingly more common human diseases. Amyloids themselves mainly consist of an aggregated mass of a specific type of protein that is believed to be either directly or indirectly toxic. Currently, there are no known cures for preventing amyloid diseases, and so far, efforts to discover anti-amyloid therapeutics have been largely unsuccessful. Many studies indicate regular consumption of plant-based diets, like the Mediterranean diet, that includes foods such as olives, vegetables and red wine leads to reduced incidence of age related amyloid diseases. Guided by these data, scientists have begun to uncover specific molecules within these diets that are able to prevent amyloid formation. A main emphasis in this dissertation was to understand the details of how these molecules prevent toxic amyloid formation. The insights gained from these studies have elucidated key chemical structural features present within these molecules that convey unique effects on perturbing amyloid formation. Excitingly, we also found that the presence of oxygen within the air we breathe, interacts with and enhances the ability of these compounds to exhibit stronger anti-amyloid functions! These data can be used to engineer better amyloid inhibitors that could lead to drugs.

Acknowledgments

I dedicate this work to all the family, friends and colleagues that have provided instrumental support to me throughout the duration of my dissertation work. I would like to acknowledge my mother Paula, my father Bill, my brother Chris, and my two sisters Lauren and Claire. I consider myself *extremely* fortunate to have such a dedicated, enduring, and loving family. I also would like to thank my lifelong friends and surrogate parents George and Suzan Mauney for their love and guidance during my dissertation work. In addition, I also thank Breanna Renee for her love and support during all my academic pursuits leading up to and during my dissertation work at Virginia Tech. Finally, I am grateful for the guidance and support continually provided by the biochemistry community at Virginia Tech, not the least of which includes my advisor Bin Xu, the Xu lab group and my committee members, David Bevan, Pablo Sobrado and Mike Klemba.

Table of Contents

List of Abbreviations

hIAPP	Human amylin
$A\beta_{42}$	42 residue amyloid beta peptide
tau 2N4R	Isoform of human tau containing 4 microtubule binding domains and 2 amino terminus inserts
($PAP_{248–286}$)	Phosphatase-cleaved amyloid precursor peptide
T2D	Type 2 diabetes
AD	Alzheimer's disease
PD	Parkinson's disease
DPBS	Dulbecco's phosphate buffer saline
DMSO	Dimethyl sulfoxide
HFIP	Hexafluoroisopropanol
TCEP	Tris(2-carboxyethyl) phosphine
ThT	Thioflavin T
RFU	Relative florescence units
$T_{1/2}$	Time required to reach half-maximum ThT RFU
UV-Vis	Ultraviolet-visible (light)
PICUP	Photo-induced cross linking of unmodified proteins
TEM	Transmission electron microscopy
MTT	3-(4,5-Dimethylthiazol-2-yl)-2,5-Diphenyltetrazolium Bromide
MD	Molecular Dynamics
RMSD	Root mean square deviation
SASA	Solvent accessible surface area
LC-MS	Liquid chromatography-mass spectrometry

List of Abbreviations (Continued)

NMR	Nuclear magnetic resonance
SDS-PAGE	Sodium dodecyl sulfate-polyacrylamide gel electrophoresis
HIP rats	Sprague-Dawley rats transgenic for human IAPP
GSIS	Glucose stimulated insulin secretion
MAPK/ERK	Mitogen-activated protein kinases/ Extracellular signal-regulated kinases
PAINS	Pan-assay interference compounds
Ole	Oleuropein
3-HT	2-(3-hydroxyphenyl) ethanol
RA	Rosmarinic acid
RA-A	Rosmarinic acid-amide
CA	Caffeic acid
SAA	Salvianic acid A
EGCG	Epigallocatechin gallate
Cat	Catechol
Nor	Norepinephrine

Thesis Overview

The focus of this thesis was to identify small molecule (mainly natural product based) *amylin amyloid inhibitors* and to gain insights into their anti-amyloid activities. Provided below is a brief outline of each chapter.

Chapter 1: Background information on protein amyloid and amylin amyloid-induced pathophysiology are provided. An overview of common approaches utilized to identify small molecule amyloid inhibitors is discussed. Broad classes of natural compound small molecule amyloid inhibitors are identified and a detailed discussion of their chemical modes of action against amyloid formation *in vitro* are provided.

Chapters 2-5: Each chapter begins with and includes a drug discovery component. Thioflavin T (ThT) assay screens were conducted on a variety of small molecule libraries to identify individual compounds or functional groups that display anti-amyloid activities. Utilizing identified lead compounds from these screens as tools, Chapters 2-4 focused on individual case studies that differentially emphasized a variety of mechanistic questions linked to their observed anti-amylin amyloid activities. In contrast, Chapter 5 emphasizes the identification and characterization of broad classes of amyloid inhibitors that are effective against amylin, $A\beta_{42}$ and tau 2N4R aggregation. Below is a brief synopsis of each chapter that highlights major findings and comments on potential applications stemming from each study.

Chapter 2: Structure activity studies of the natural compound anti-amylin amyloid inhibitor baicalein highlights essential roles of its vicinal dihydroxy groups, that are linked chemically to its ability to mediate covalent adducts with amylin. As technologies for rational drug design approaches against amyloid formation further develop, this work may be useful for applications of lead compound optimization efforts for flavonoid-based amyloid inhibitors.

Chapter 3: Dual anti-diabetes properties were discovered for natural compound polyphenol oleuropein. Structure activity studies determined that ligstroside and 3-hydroxytyrosol served as key underlying structural components responsible for enhanced glucose stimulated insulin secretion and anti-amylin amyloid activities, respectively. Future studies that elucidate the potential benefits of multifunctional amyloid inhibitors like oleuropein may be useful in engineering drugs that can address the multi-faceted nature of amyloid diseases.

Chapter 4: The natural compound rosmarinic acid (RA) was found to potently inhibit amylin amyloid formation and to neutralize amylin amyloid-induced cytotoxicity. Numerous anti-amylin amyloid activities associated with RA were shown to be chemically linked to its underlying structural components, salvianic acid A and caffeic acid. Excitingly, both RA and a synthetic amide-linked RA analogue (RA-A), which exhibited even stronger anti-amyloid potency compared to RA, disrupted pre-formed amylin oligomers present in the serum taken from both transgenic rats overexpressing human amylin (HIP rats) as well as from humans afflicted with T2D. We are currently conducting *in vivo* studies to determine if RA can prevent amylin amyloid deposition in HIP rats as well as assess if RA can halt T2D progression and rescue against neurocognitive deficits that develop in this animal model system. This work epitomizes how basic science efforts to identify and characterize small molecule amyloid inhibitors can be leveraged into animal studies that could potentially have a translational impact.

Chapter 5: A drug repurposing platform identified several broad classes of amyloid inhibitors capable of preventing amyloid formation against microtubule-associated protein tau 2N4R, $A\beta_{42}$ and amylin. Herein catechol-containing inhibitors are highlighted. We found that autoxidation is a general determinant for enhancing catechol-containing compound anti-amyloid activities. Data are presented that also suggest amyloid "remodeling" may not be a general requirement

linked to the anti-amyloid activities of catechol-containing inhibitors. Identifying key structural features of the ligands and clarifying the mechanisms that confer their anti-amyloid activities will provide useful information for future rational drug design efforts. Moreover, the initial repurposing screening platform utilized in this study could also be potentially employed to uncover protein specific amyloid inhibitors. The latter could be used to further elucidate structure function amyloid toxicity that may be associated with unique amyloid polymorphisms as well as optimized to aid in clinical diagnostics.

Chapter 6: Summary conclusions and future perspectives are discussed.

Manuscript Attributions

I would like to acknowledge the following pleasant and fruitful collaborations that contributed to the work contained in this dissertation: Dr. Ling Wu for her work for all cell based assays and Western blotting analysis of rat and human sera samples as described in Chapters 2, 3 and 4 as well as her novel finding of glucose stimulated insulin secretion effect of oleuropein; Dr. Sherry Hildreth, Dr. Keith Ray and Dr. Rich Helm for their mass spectrometry work as described in Chapters 2 and 5; Dr. Shijun Zhang's group from the Department of Medicinal Chemistry at Virginia Commonwealth University for synthetic amyloid inhibitors including the rosmarinic acid amide-linked analogue as described in Chapter 4; Drs. Anne Brown and David Bevan for their molecular dynamics simulation work as described in Chapter 4; Dr. Nancy Vogelaar for her assistance and technical support in executing the semi-high throughput ThT assays as described in Chapter 5 and Ms. Kathy Lowe for her assistance in transmission electron microscope data collection as described in Chapters 2-5. I would also like to thank Dr. Biswarup Mukhopadhyay and his group for training and usage of their anaerobic chamber as described in Chapter 5 and Drs. Dan Slade and Pablo Sobrado and the Virginia Tech Center for Drug Discovery for access to their spectrophotometers that contributed to work in Chapters 2-5.

Chapter 1 Literature Review: Protein Amyloid, Amylin pathophysiology and Natural Product-Based Amyloid Inhibitors

Portions of this review are adapted from:

Paul Velander, Ling Wu, Francis Henderson, Shijun Zhang, David Bevan, Bin Xu. (2017) *Biochem. Pharmacol. 139*, 40-55.

Amyloid Background

Amyloidosis is associated with the largest class of protein misfolding diseases that includes a broad spectrum of neurological, metabolic and aging related diseases including Alzheimer's disease (AD), prion disease, Parkinson's disease, and type 2 diabetes (T2D). The pathological hallmarks of amyloidosis are structurally conserved intracellular and extracellular insoluble proteinaceous deposits termed amyloid fibrils.[1-3]. Protein amyloid aggregation proceeds through a nucleation dependent process wherein seed competent precursor species initiate an aggregation cascade that results in equilibrium between mature amyloid fibrils and their small precursor aggregates. Mature amyloid fibrils are comprised of several unbranched protofilament segments, which are in turn made up of β-sheet rich protein structures. These structures stack upon one another, forming the conserved amyloid "cross beta spine", characterized by individual β-strand units being positioned perpendicular to the long axis of the protofilament[2]. Even though certain physicochemical properties conferred by amino acid sequence such as hydrophobicity, charge and β-sheet propensity can affect amyloidogenicity of natively unfolded proteins, extensive literature suggests that amyloid formation is facilitated by backbone interactions [2]. Over the last two decades, increasing evidence indicates that the primary pathological amyloid species are non-fibrillar precursor aggregates that range from unstructured oligomers (as small as dimers) to β-sheet rich aggregates termed protofibrils (as small as 20-mers) [2, 4-9].

Generic mechanisms of amyloid induced cytotoxicity include cell membrane damage, organelle dysfunction, and impaired proteostasis that can ultimately lead to cell death [10-13]. Protein amyloid-specific pathology can also arise due to the cellular and physiological processes that are perturbed in specific tissues. For example, insulin resistance and reduced β-cell mass may result from amylin amyloid formation in T2D. Other amyloid pathology may stem from unique consequences linked to losing the native function of the aggregating protein. For example, amyloid formation that occurs in AD and tauopathies may result in microtubule dysfunction because of a depleted source of functional tau. Currently amyloid disease can be classified based on if the amyloid deposits are localized or systemic and if the underlying pathologies are neuropathic. Using these criteria, Dobson and colleagues delineated amyloid diseases into three categories: neurodegenerative, non-neuropathic systemic and non-neuropathic localized amyloidosis [1-2]. Over fifty human protein misfolding diseases and their associated proteins and peptides have been described, including several physiologically important peptide hormones such as insulin [14] and amylin [15].

Pathophysiology of amylin amyloid

Human islet amyloid polypeptide (hIAPP), is also called and hereon referred to as amylin. It is a 37-residue natively unfolded peptide hormone that is co-expressed and co-secreted with insulin by pancreatic beta cells. Amylin plays a regulatory role in glucose homeostasis and in inducing post-prandial satiety[15]; however, human amylin is also highly amyloidogenic. Sequence analysis between human and non-amyloidogenic isoforms, such as rodent amylin, as well as high resolution structural data using various human amylin fragments indicate residues 20-29 are essential determinants of human amylin amyloidogenicity [16-17] (Fig 1A,). Human amylin amyloid pancreatic deposition occurs is estimated to occur between 80-95% of humans with T2D, and several animal studies validate its association with numerous clinicopathological features of T2D, including reduced pancreatic beta cell mass[18-19]. Furthermore, it is established that soluble oligomers and fibrils of aggregated amylin are toxic against numerous cell lines *in vitro*, including rat insulinoma INS-1, human neuroblastoma SH-SY5Y, mouse neuroblastoma Neuro-2A and mouse smooth vascular muscle cells (Fig 1C). These cytotoxic effects which can lead to reduced cell viability and or apoptosis are linked to a variety of perturbed cellular processes including membrane ion leakage [20-21], perturbed intracellular calcium levels[22-23], reactive oxygen species [21], and impaired proteostasis linked to a dysfunctional ubiquitin proteasome system or autophagy[11, 15]. These data implicate amylin amyloid formation as a contributing factor to T2D pathology. Moreover, recent validation of the presence of amylin amyloid in both the heart and brain tissue in humans suggest a wider pathological influence [23-25]. Despa and colleagues showed a significant difference in amylin oligomer accumulation occurs within failing hearts of obese and T2D individuals but not in healthy controls. A transgenic rat model further elucidated that amylin can perturb myocyte

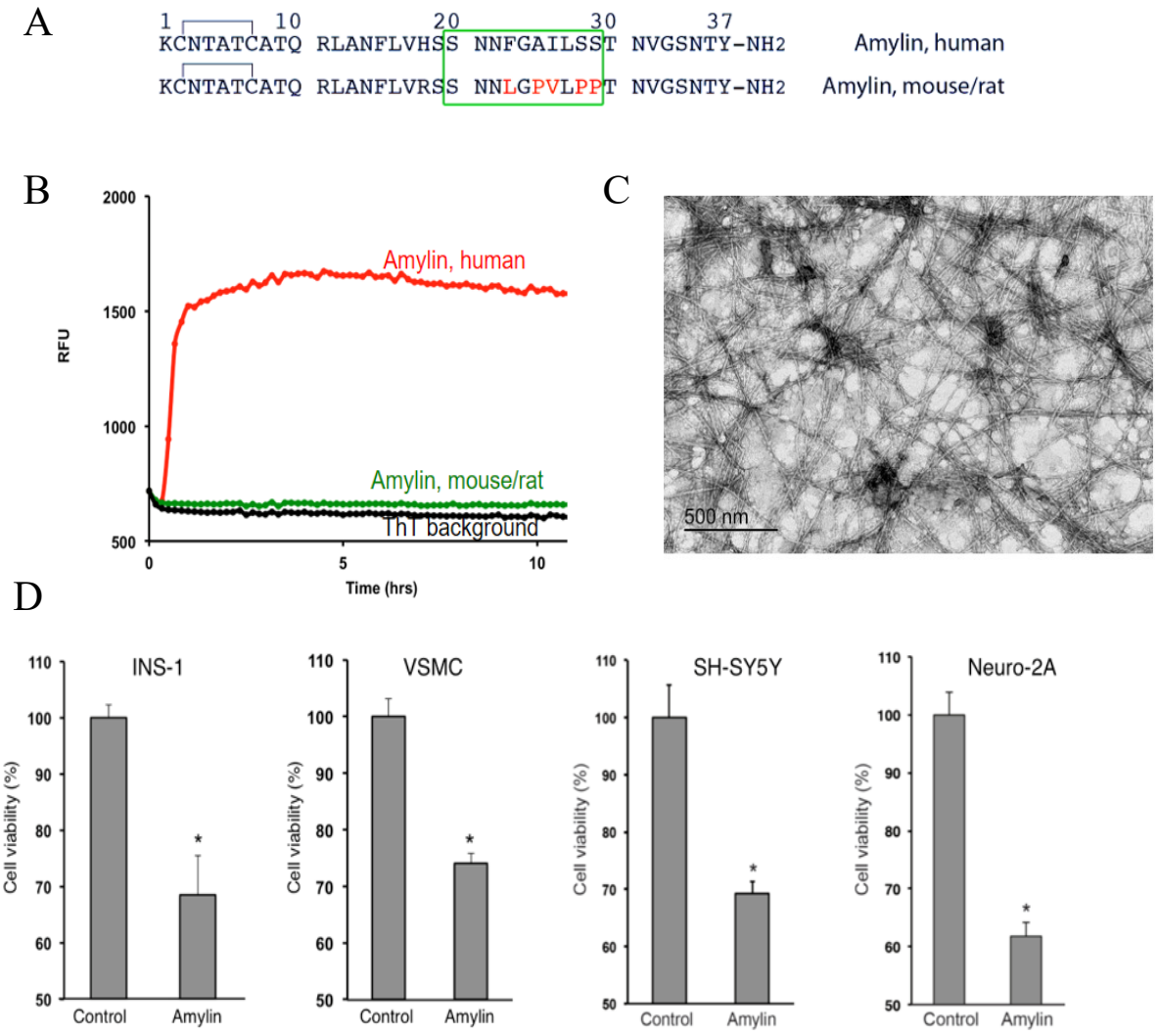

Figure 1. Amylin sequences, cytotoxicity and biochemical characterizations

(A) human and rodent amylin sequences are shown. Green box indicates a key region that determines amyloidogenicity where residue differences in rat amylin are highlighted in red. (B) ThT fluorescence assay indicates that human but not rat amylin forms amylin amyloid (C) TEM images of human amylin fibrils (D) MTT cell viability assays demonstrate the toxic effects of 15 μM amylin on rat insulinoma INS-1, human neuroblastoma (SH-SY5Y), mouse neuroblastoma (Neuro-2A) and mouse vascular smooth muscle cells (VSMC) (unpublished results, Xu lab).

calcium homeostasis and induce diastolic dysfunction[22]. Immunohistochemistry and western blot analysis from two separate groups that examined human brain tissue specimens obtained from healthy controls, individuals diagnosed with T2D-with dementia or those with AD alone, confirmed that diseased but not healthy controls exhibit amylin (and Aβ) amyloid and oligomer deposition within blood vessels and brain parenchyma[24-25]. Amylin amyloid also altered brain microvasculature and appeared to co-localize with apolipoprotein E, which has previously been observed in pancreatic arteriosclerotic lesions[26]. Within the context of established dogma that the mechanisms of cytotoxicity of amyloidogenic peptides are conserved [2, 7, 12, 27-28], validation of amylin amyloid/oligomer deposition in the brain suggests the possibility that amylin could also potentiate cerebral amyloid angiopathy (CAA) and stroke. This rationale stems from epidemiological studies that link Aβ brain deposition to CAA and stroke [2, 7, 12, 27-31]. In summary, these data suggest that amylin amyloid may potentiate T2D, is toxic to neuronal, heart and pancreatic beta cells *in vitro*, and may contribute to chronic cardiovascular and neurodegenerative diseases. These findings suggest an important need to develop anti-amylin amyloid inhibitors.

At least *in vitro*, many kinds of molecules have been found to recognize/bind, perturb or prevent amyloid formation. Some molecules are protein-based, which include antibodies, enzymes, or small peptides[7, 32-37]. Others are nucleotide-based such as DNA or RNA aptamers[38-39]. Additionally, both carbohydrates such glycosaminoglycans as well as membrane lipids have been shown to accelerate amyloid formation[40-43]. Another group of molecules includes structurally diverse small molecules such as antibiotics, sulfonated anions, molecular tweezers, and polyphenols[44-47]. Since the work in this dissertation has primarily focused on characterizing small molecule natural compound amyloid inhibitors, the remainder of this review provides a

detailed overview of these compounds (Figure 2) as well as in-depth analysis of their mechanisms of inhibition.

Natural Product-based Amyloid Inhibitors

Natural compounds that exhibit anti-amyloid effects have distinct advantages over other synthetic compounds: they are often naturally consumed as part of a healthy diet wherein they offer general nutraceutical benefits such as reduced risk for AD and T2D [48]. Several polyphenols including curcumin, resveratrol and epigallocatechin-3-gallate (EGCG), have progressed to clinical trials for AD treatment (see Section: *in vivo* efficacy and clinical studies). Moreover, based on their multiple functions including anti-oxidant, anti-inflammatory and metal chelating capacities, polyphenols are a rich source for a variety of different structural backbones that can be utilized in rational drug design efforts to find multifunctional anti-amyloid agents [49-50] (see Section: Natural Product—Metal—amyloid protein complexes and Chapter 3).

Using PubMed and other public databases, we conducted a general search for a comprehensive list of natural compound amyloid inhibitors. Because natural compounds could be identified based on a wide variety of beneficial activities against amyloid diseases such as inhibiting amyloid indirectly by attenuating amyloid protein expression levels or influencing other key biochemical targets associated with amyloid, only natural compounds that directly prevented or modulated amyloid aggregation are included in our list. Of the 72 compounds identified, 44 are phenolic compounds that include 16 flavonoids, 4 anthraquinones, 13 alkaloids (including 3 indoles, 3 pyridines, and 2 porphyrins), terpenes, and steroids. Figures 2a-c provides the chemical structures of these compounds.

Many of the phenolic compounds identified from our search are present in the diets that are epidemiologically linked with reduced risk of aging-associated amyloid pathologies [51-53].

Examples include oleuropein and oleocanthal found in olive oil, resveratrol found in fruit and red wine, curcumin found in turmeric, as well as EGCG and myricetin found in green tea. Additional polyphenols identified that are present in healthful foods include caffeic acid and rosmarinic acid found in culinary herbs, cinnamaldehyde found in cinnamon, and genistein found in legumes. In contrast to the flavonoids or phenolic acid derivatives that comprised the majority of structures found within polyphenol amyloid inhibitors, several inhibitors with strikingly different structures were identified: cyclodextrin, a cyclic carbohydrate byproduct formed from enzymatic starch breakdown; squalamine, an amino sterol isolated from dogfish with previously documented anti-viral and anti-bacterial activities [54-55]; vitamin A, a fat soluble vitamin [56]; hematin, a porphyrin employed as a therapeutic against porphyria [57]; rifampicin, an antibiotic for treating bacterial infections; and scyllo-inositol, a plant sugar alcohol found abundantly in coconut palm. Caution must be taken since the amyloid-inhibitory functions of many of these compounds have not been validated *in vivo*.

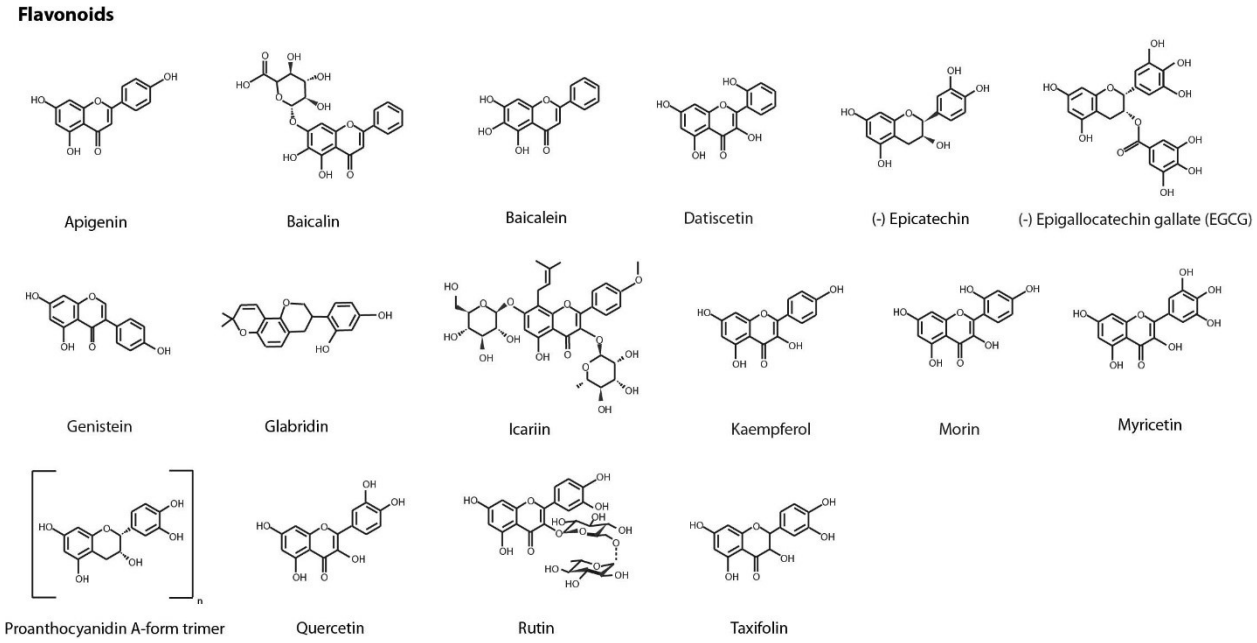

Figure 2a. Chemical structures of identified flavonoid natural product protein amyloid inhibitors. Additional structures of other natural compounds are shown on the next two pages.

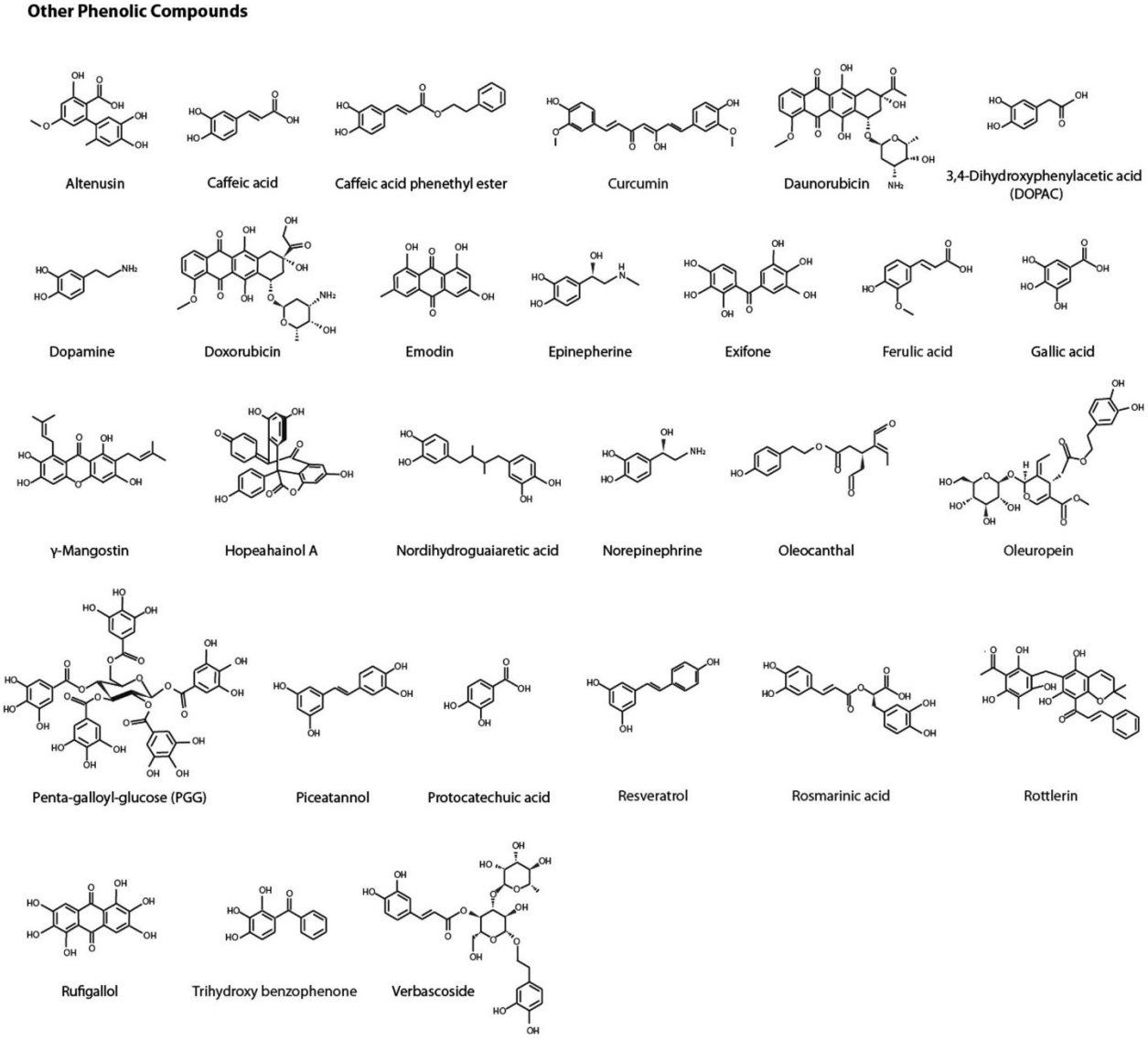

Figure 2b. Chemical structures of identified phenolic natural product protein amyloid inhibitors. Additional structures of other natural compounds are shown on the next page.

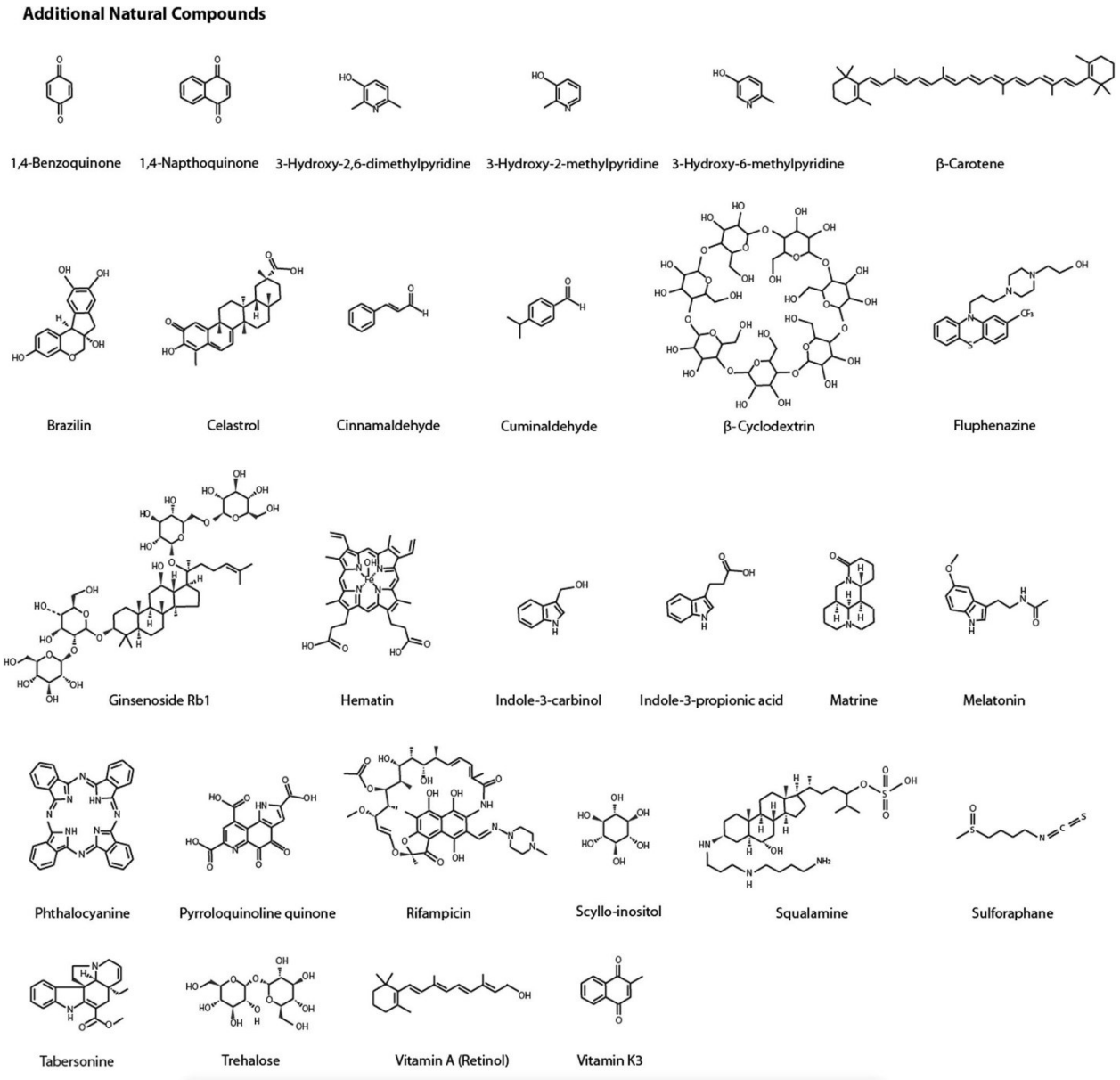

Figure 2c. A wide range of chemical structures of identified natural product protein amyloid inhibitors. Some representative structures shown above include quinones, pyridines, aldehydes, sugar alcohols, and terpenes.

Drug Discovery Strategies against Amyloidosis

There are multiple therapeutic strategies to identify disease-modifying agents against protein amyloidosis (for a recent review, see [58]). For natural compound identification, one source of information comes from epidemiological studies that suggest preventative effects against dementia, AD, or diabetes may be associated with the diets containing high intake of flavonoids and polyphenolic compounds [53]. The Mediterranean diet, featuring by a high intake of vegetables, fruits, cereals, and olive oil, was reported to be associated with reduced risk for AD and mild cognitive impairment in multiethnic community studies in New York [59-60]. Several cohort studies suggested that moderate intake of red wine (containing resveratrol) was associated with a reduction in risk of dementia, AD, or cognitive decline [61-62]. Curcumin, found in yellow curry spice turmeric in traditional Southeast Asian diets, and EGCG and myricetin, polyphenolic compounds present in green tea, have been associated with cognitive health [53]. However, the protective effects of diet are not the same as the specific effects of a single compound. How diet-specific natural compounds may provide health effects are not well known. Nevertheless, information from these epidemiological sources as well as information reported by alternative and complementary medicine led to testable hypotheses and experimental efforts that successfully identified numerous natural compound amyloid inhibitors [63-66].

One of the current strategies aimed at identifying therapeutic lead compounds for amyloidosis focuses on inhibiting amyloid aggregation by (i) inhibiting toxic amyloid formation and/or stabilizing its native form from aggregating and (ii) remodeling or degrading toxic amyloid oligomers and/or insoluble fibrils. Various approaches have been used. A variety of platforms, including *in vitro* [67] and cell based approaches [68], have been used in a semi-to-high throughput capacity to screen for small molecules that prevent or modulate amyloid aggregation.

One selection criterion used to choose the library of compounds for screening emphasizes the overall quantity and diversity of compounds rather than any specific underlying physicochemical features [67]. For instance, Chen and colleagues developed a high throughput small molecule microarray assay capable of identifying amyloid inhibitors by assessing binding affinity with amyloid β-peptide with ~11,000 different small molecule leads per array slide. Activities were assessed from a range of synthetic and natural compounds as well as compounds derived from diversity-oriented synthesis. Several high-resolution crystal structures of fragment sequences of amyloidogenic proteins [17, 69] in concert with atomic structural analysis on small molecules that bind these structures [46, 70-71] have revealed a variety of molecular scaffolds that either inhibit or modulate amyloid formation. These structures, some of which have been proposed as potential pharmacophores [46] that can presumably target the generic cross beta spine architecture common to all amyloids, are currently being used for structure-based drug design efforts. For example, Eisenberg's group, utilizing Orange G, an amyloid binding dye, developed a high throughput screening platform that utilized iterative computational and experimental approaches, and investigated and fine-tuned structure activity relationships for lead compounds with optimized activity against Aβ amyloid [72]. In addition, molecular docking and molecular dynamics simulation are commonly used approaches to screen small molecule libraries, to gain mechanistic insights into target – drug interactions, and to optimize lead compounds [72-74].

Mechanisms of Inhibition

The specific stages of aggregation and amyloid species that are targeted by natural product inhibitors, as well as the resulting biochemical and biomolecular processes that are linked to amyloid induced cytotoxicity, are not yet fully understood. However, recent work has begun to elucidate a detailed understanding of the chemical mechanisms that underlie these

processes. Anti-aggregation agents can exert their actions by forming covalent bonds [75-78] and/or non-covalent interactions (i.e. π-π interactions, hydrogen bonding, or charge-charge interactions between an inhibitor and the backbone or side chain residues of the target protein) [46, 79-81] that may affect one or all stages of the aggregation processes. Eisenberg's group has elucidated at least two different binding modes of amyloid pharmacophores whose non-covalent interactions can be delineated by relatively "tight" (i.e. co-crystal structure of Orange G bound to Aβ fibril fragment KLVFFA) or "less tight" binding (i.e., co-crystal structure of curcumin bound to Tau fibril fragment VQIVYK) within the cross beta spine of single crystal structures of amyloid fragment sequences from Aβ and Tau [46]. However, formation of a common amyloid pharmacophore mediated by predominantly non-covalent bonding interactions fails to explain why in some cases these forces, which typify EGCG mediated anti-amyloid activities in many amyloid systems, are ineffective in others [82]. Accordingly, a series of papers have demonstrated that covalent adduct formation can occur between the nucleophilic side chain thiols and amines (as well as the amino terminal amine) and the electrophilic carbonyls within o-quinone intermediates and/or aldehyde moieties [75-76, 78]. Covalent adduct formation significantly affects anti-aggregation effects of baicalein on α-synuclein [76, 83-84] and likely also on amylin [66]. Adduct formation also affects EGCG's binding affinity and remodeling of Aβ as well as amylin$_{8-24}$ fibrils [77]. Such a mechanism appears to be essential to inhibiting phosphatase-cleaved amyloid precursor peptide (PAP)$_{248-286}$ amyloid formation [82]; Similar mechanisms have been proposed in the observed anti-aggregation effects of taxifolin on Aβ aggregation as well as for cinnamaldehyde and oleocanthal on tau amyloid formation [75, 85-86]. The following sections focus on numerous case studies to provide a detailed discussion of the non-covalent and covalent

mechanisms that mediate natural compound-amyloidogenic protein interactions, and importantly, their association with observed inhibitory effects on amyloid induced cytotoxicity.

Non-covalent Inhibition Mechanisms

The type and specificity of the non-covalent interactions that mediate amyloid inhibitor activity can vary depending upon the protein or stage of aggregation that is targeted [79, 82, 87-90]. Thus, many of the non-covalent interactions described below are not meant to be a comprehensive description of all non-covalent interactions that may mediate the anti-amyloid activities of an inhibitor. Rather it is a summary of some of the key interactions that have been shown to be important for each inhibitor within the specified context. We will use two extensively studied compounds, curcumin and EGCG, as showcase examples.

Curcumin has been documented to modulate amyloid assembly in various amyloid systems. Because curcumin has been suggested as a potential pan-assay interference compound (PAINS) [91], it is especially important to have multiple orthogonal assays to validate the bioactivities of curcumin. Nonetheless, extensive literature shows that curcumin prevents amyloid formation, amyloid induced cytotoxicity, and provides beneficial *in vivo* effects including reduced plaque burden (for a recent review, see [92]; Table 1) via (i) inhibiting amyloid aggregation in the instances of amylin or Aβ [90, 93–95] (ii) Accelerating α-synuclein aggregation that results in less toxic intermediates and insoluble aggregates [89, 96]. Using experimental structure information, computational simulation work has provided insights into key non-covalent interactions between curcumin and the generic cross beta spine structure present in amyloid fibrillar structures as detailed below.

Docking simulations with amyloidogenic "steric zipper" hexapeptide amyloid beta fragment and full length $A\beta_{1-40}$ showed that curcumin binds within the interstrand space

(maintained at characteristic 10 Å distance of protein fibrils; Figure 2A) in a planar fashion, with its phenyl heads oriented in parallel with the fibril axis [71]. Subsequent analysis revealed that curcumin formed key inter-residue side chain interactions that targeted the bolded residues within segment **KLV**F**F**A of the hexapeptide octamer assembly and residues **HQK**L**V**F**F**A in full-length amyloid β peptide [71]. In both cases, interatomic distances between these residues and specific regions of the curcumin molecule were indicative of a variety of important non-covalent contacts that were mediated by hydrophobic and hydrogen bonding interactions (Figure 2A). These include interactions between aromatic phenyl rings of curcumin and His14 (π stacking) and between the phenyl ring of curcumin and Val18 (π-alkyl stacking). Other interactions include hydrogen bonding between two separate flanking Lys16 residues (projected inward from opposite strands of the cross-beta spine) [71]. Furthermore, data from molecular dynamics (MD) trajectories (at 1 ns duration) indicate much larger root mean square fluctuations for residues HQKLVF (1.4-3.6 Å) in full-length Aβ fibrils with curcumin bound than for controls with no curcumin bound (0.9-2.1 Å). Binding of curcumin results in β-sheet perturbations within the cross beta spine that may have important implications experimentally relevant to fibril inhibition [88-89, 94-96]. Indeed, a similar mechanism of "binding and destabilization" has recently been described with curcumin-bound tau hexapeptide VQIVYK [70]. Eisenberg's group recently solved curcumin-bound tau hexapeptide crystal structure that demonstrated curcumin intercalates within the inter-β-sheet pocket of four interacting oligomeric chains, with curcumin oriented in a planar-lengthwise fashion parallel to the fibril axis [46]. Using this complex structure as the starting point, a 20 ns MD trajectory was performed that showed curcumin-bound tau disrupts inter-strand beta sheet chain interactions that preclude ordered fibril assembly [70].

Another recent study utilized MD simulations to investigate the molecular contacts that mediate amylin-curcumin interactions. MD simulations showed that multiple curcumin molecules self-associate, forming a nucleation site, characterized by exposed hydrophobic and hydrogen bonding contacts that bind to and stabilize small order amylin oligomeric "nano-assemblies" that attenuate higher order amyloid aggregation [93]. Helical structures have been proposed to play an important role in facilitating downstream β-sheet rich secondary changes that precede fibrillar amylin amyloid assembly [40-41, 97-99]. Moreover, these data indicate that curcumin can target more than just the cross-beta spine motif. Residues in the amylin sequence that are targeted most frequently by curcumin included Leu12, Phe15, Phe23, Leu27 and Tyr37 (which includes all aromatic residues within amylin). Discrete MD simulations (DMD) data supported the presence of π-π stacking between these aromatic residues and the phenyl rings of curcumin. These simulation results are consistent with the hypothesis that π-π interactions are an important force mediating anti-amyloid effects of polyphenols [100-101]. DMD also suggested the presence of hydrogen bonding between both 4-hydroxy-3-methoxy phenyl substituents on curcumin and backbone/polar residues of amylin. Importantly, these curcumin-nucleated amylin "nano-assemblies" displayed fewer amylin-amylin contacts, which was attributed to formation of several smaller assemblies versus the one cluster seen in the control [93]. The possibility that curcumin nucleates and stabilizes small oligomeric assemblies that leads to fewer amylin-amylin interactions provides mechanistic insights into the experimentally confirmed ability of curcumin to significantly delay and prevent amylin amyloid formation *in vitro* [90].

A common phenomenon observed in each study was that curcumin intercalated within the hydrophobic core of all amyloid assemblies regardless of the type of peptide or the quaternary structure of each complex. The non-covalent interactions observed within these

complexes give not only mechanistic insights into how curcumin exerts its anti-amyloid effects [88-89, 95], but also show how the molecular scaffold of curcumin is capable of targeting the cross beta spine present in all amyloid fibrillar structures, as well as α-helical oligomers that may play an important role during the early events of amyloid aggregation [40, 97].

EGCG exerts powerful anti-amyloid effects against many amyloidogenic proteins. It has the ability to prevent the formation of toxic prefibrillar oligomers (while stabilizing non-toxic off pathway oligomers), as well as inhibit amyloid fibril formation and remodel previously existing amyloid fibrils into less toxic insoluble aggregates [77, 80, 82, 87, 102-104]. Numerous studies have elucidated some of the key non-covalent binding events and interactions that mediate these effects. Multiple studies suggest that EGCG undergoes non-specific hydrophobic and hydrogen bonding interactions that can mediate its anti-amyloid activities: (i) Nitro blue tetrazolium (NBT) dye staining analysis as well as NMR data suggest that EGCG can bind to natively unstructured α-synuclein and amyloid β peptide or denatured bovine serum albumin but not other native globular proteins [87]. These data suggest that EGCG may have a propensity to target unfolded or natively unstructured proteins, presumably via non-specific backbone interactions [87]. (ii) EGCG can remodel preformed amyloid generated by the mutant form of acetylated fragment of yeast prion protein Sup35 (GNNQQN**F**QQ**F**) but not the native fragment (GNNQQ**Y**QQ**Y**). Such differential effects may be due to the mutant fragment possessing more hydrophobic binding regions that can interact with EGCG [77]. (iii) Using a series of amylin mutants, Raleigh's group investigated the importance of residue-specific aromatic/hydrophobic or covalent interactions that may mediate EGCG-induced amyloid inhibition and/or remodeling activities. They concluded that neither was critical, and that backbone hydrogen bonding/hydrophobic interactions likely mediate the effects of EGCG [79]. Other studies indicate that the ability of

EGCG to inhibit amylin amyloid aggregation or remodel preformed amylin$_{8\text{-}24}$ fibrils is attenuated in the presence of negatively charged lipid bilayers [77, 104]. These data suggest that key polar and non-polar regions of amylin that mediate the non-specific hydrophobic interactions and hydrogen bonding as suggested by Raleigh and colleagues [79], are sequestered by both lipid bilayers and detergent, leading to fewer interactions with EGCG.

The anti-amyloid activities of EGCG may also be facilitated by protein specific regions and/or residue binding: (i) Data from biochemical assays, ion mobility mass spectrometry, 2D NMR spectroscopy, and computational simulations suggest that EGCG-Aβ binding results in compact monomeric and dimeric conformations, as well as higher order SDS-stable Aβ oligomers that are mediated by polar and non-polar interactions between EGCG and the aromatic hydrophobic core of Aβ [103, 105]. Hyung and colleagues also suggested from molecular modeling studies that EGCG may interact with metal binding residues His6, His13, and His14 in the Aβ sequence [105]. (ii) NMR spectrometric data on prostatic acid phosphatase-cleaved amyloid precursor peptide (PAP$_{248-286}$) with EGCG indicate that EGCG binding is selective for charged residues Lys, Arg, His along with Met but not its hydrophobic core [82]. Furthermore, EGCG did not exhibit anti-amyloid activity against acetylated PAP, indicating that non-specific hydrophobic interactions or hydrogen bonding cannot alone mediate the anti-amyloid activity of EGCG towards this amyloid peptide (See Section 3.2.3 for further discussion). MD simulations have also been applied in studying the interaction of EGCG with amyloidogenic peptides. In one study, MD simulations were used in combination with MM-PBSA calculations to examine interactions between EGCG and the Aβ$_{42}$ monomer [106]. EGCG molecules were observed to expel water from the surface of the peptide and bind directly to it. Free energy decomposition revealed that the dominant terms contributing to binding involved nonpolar interactions, with polar

interactions playing a minor role. In another study, MD simulations were used to examine the effect of EGCG on aggregation of amylin [107]. Replica exchange MD was used to study the conformation of amylin dimers. Initial conformations were extended and contained a three-stranded antiparallel β-sheet and the β-hairpin characteristic of cross-beta amyloid. When EGCG was present, the hydrophobic and interpeptide interactions that stabilized the extended β-sheet structures were blocked, resulting in the formation of conformations containing predominantly coil structure.

In summary, the anti-amyloid activities of EGCG are mediated by a broad spectrum of non-covalent interactions whose specificity and overall contribution to the observed anti-amyloid activity is determined by the interacting protein: in the case of amylin, non-specific interactions (i.e., hydrophobic/hydrogen bonding interactions) were sufficient to facilitate the anti-amyloid activity of EGCG; this contrasts sharply with its inhibition of PAP amyloid, wherein specific interactions are essential. This dichotomous behavior is also a departure from an inhibitory mechanism that is characterized by a common phenolic pharmacophore, as suggested by studies conducted with curcumin and Orange G [46]. To our knowledge, high-resolution structural information has not been obtained for EGCG in complex with an amyloid peptide.

Covalent Interaction Mechanisms

Multiple studies have suggested or confirmed the presence of o-quinone mediated covalent adduct formation from certain flavonoid or catechol-containing phenolic compounds with amyloid proteins [66, 75-77, 82, 84]). Additional covalent mechanisms have also been reported between nucleophilic amines and thiols of amyloidogenic proteins and electrophilic reactive groups on inhibitors such as aldehydes (Figure 2B, Middle and Lower Panels; [85-86]). Major covalent inhibition mechanisms and selected cases are presented below.

O-quinone Mediated Covalent Mechanisms

We will use EGCG, taxifolin, baicalein, and catecholamines to showcase examples for o-quinone mediated covalent mechanisms. A series of NBT binding assays, transmission electron microscopy (TEM), and NMR analyses confirmed that site specific adduct formation to lysine residues within $(PAP)_{248-286}$ is essential for EGCG-mediated anti-amyloid activity as well as SDS-stable insoluble aggregate formation of $(PAP)_{248-286}$ [82]. Furthermore, mass spectrometry indicates that gallocatechin (GC), which lacks the gallic ester moiety presented in EGCG but retains the three contiguous hydroxyl groups on the B-ring, undergoes less conjugation with $(PAP)_{248-286}$ and neither stabilizes low molecular weight SDS-stable PAP oligomers nor inhibits PAP amyloid formation. This suggests that the gallic ester moiety present in EGCG is essential for yielding a sufficient amount of adduct formation (i.e., 35% in EGCG-PAP samples versus 10% observed in GC-PAP samples) necessary to confer anti-amyloid activities. These effects may be attributed to higher stoichiometric amounts of gallol functional groups capable of o-quinone formation in EGCG (versus GC). Alternatively, the gallo ester may facilitate initial non-covalent EGCG-PAP interactions as suggested by NMR experiments that places EGCG in a more favorable position and orientation (as compared to GC) for covalent conjugation [82]. The latter explanation is similar to the idea of how aromatic/hydrophobic residues within the hydrophobic amyloid core may facilitate proper pharmacophore positioning of certain polyphenols along the cross beta spine of amyloid fibrils [100].

Taxifolin does not inhibit monomeric or seeded amyloid beta fibril formation in anaerobic conditions or in the presence of a mild reducing reagent [75]. However, when incubated

under aerobic conditions, taxifolin attenuates beta sheet rich secondary changes and prevents $A\beta_{42}$ fibril formation, a phenomenon that was accelerated in the presence of an oxidizing reagent, sodium periodate [75]. Studies using mass spectrometry and site directed mutagenesis confirmed that the chemical mechanism responsible for taxifolin mediated anti-amyloid activity occurs via site specific covalent adduct formation, through Michael addition at residues Lys16 and Lys28 [75]. Further characterizations with catechol-type (myricetin and quercetin) and non-catechol type (morin, kaempferol and datiscetin) flavonoid compounds suggested that all compounds exhibited anti-amyloid activity against $A\beta_{1-42}$. But in the presence of Lys16Nle, Lys28Nle, and Lys16Nle/Lys28Nle mutants, only non-catechol-type molecules showed anti-amyloid activity [75]. These results indicate that myricetin and quercetin direct their anti-amyloid activities through o-quinone-Lys covalent adduct formation similar as taxifolin but that such a mechanism may not be generalized to all flavonoid molecules.

In a similar case, baicalein prevents α-synuclein amyloid formation and the primary chemical mechanism responsible for this activity is believed to be via formation of baicalein- α-synuclein covalent adducts [76, 83]. Anti-amyloid activities of baicalein against α-synuclein aggregation are significantly enhanced when it is autoxidized into the quinone form of baicalein versus freshly prepared baicalein, but significantly weakened under anaerobic conditions [76, 83]. Disrupting free radical cycling essential to o-quinone auto-oxidation via 5,5-dimethyl-1-pyrroline-N-oxide radical quenching reagent significantly reduced anti-amyloid effects of baicalein [83]. Finally, results from mass spectrometry confirmed that the o-quinone form of baicalein forms covalent adducts with α−synuclein [76, 83]. Inhibitory effects of baicalein against amylin oligomerization, fibril formation and amylin amyloid-induced toxicity have also been characterized and validated using a variety of analytical approaches [66]. In addition, systematic

structure activity studies using a series of baicalein analogues provided strong evidence for an essential role for its catechol moiety in mediating these effects. Importantly, Schiff-base mediated baicalein-amylin adducts were demonstrated by mass spectrometric evidence [66]. The latter mechanism can readily be explained by the ability of baicalein to undergo auto-oxidation to the o-quinone form and in turn to form covalent adducts with amylin.

Several studies suggest that numerous quinones and amino chromes derived from oxidized catecholamines undergo o-quinone mediated protein covalent adduct formation that leads to the dissolution of both preformed Aβ and α-synuclein amyloid fibrils [108-110]. Dopamine (DA), its precursor 3,4-dihydroxyphenylacetic acid (DOPAC), as well as other catecholamines such as norepinephrine and epinephrine were shown to bind to α−synuclein monomers and prevent β sheet secondary structural changes [109] and also inhibited fibril formation [109-110]. In agreement with spectroscopic based techniques that indicated dopamine could break up preformed Aβ and α-synuclein fibrils, elegant microscopy work tracked the time course of dopamine-mediated dissolution of a single fibrillar species of α-synuclein [109]. Further characterizations suggested that these effects are o-quinone mediated: administration of the anti-oxidant sodium metabisulifite prevented catecholamines from inhibiting fibril formation [110]; the oxidized products of catecholamines were significantly more effective versus the "fresh" parent catechol compounds in inhibiting fibril formation (albeit in this study, validation of polymerized oxidation products was not addressed); the importance for the catechol moiety was suggested by numerous related catecholamine analogues that did not confer anti-amyloid activities [109-110]; the presence of long wavelength fluorescence in samples containing DA and α-synuclein which indicates Tyr-derived radical coupling (i.e., a phenomenon that can serves as an indicator of potential DA- α-synuclein adduct formation at the Tyr residues) was noted [109-110]; the presence of

SDS- and heat-treatment stable DA-α-synuclein monomers and oligomers suggest very stable DA- α-synuclein interactions, potentially mediated by covalent binding [108, 110].

Non-catechol Derived Covalent Mechanisms

Cinnamomum (tree) verum extract has been shown to inhibit amyloid fibril formation from tau and hen egg-white lysozyme [111-112]. Recently it was confirmed that cinnamaldehyde, the major component of cinnamon bark oil, prevents Tau187 amyloid formation without affecting tau mediated microtubule assembly [85]. Further characterizations confirmed that the unsaturated beta carbon on CA undergoes reversible nucleophilic attack by Tau187 cysteine thiols (Figure 2B, Middle Panel; [85]). Amyloid formation from the double cysteine knock out Tau187 mutant C291S/C322S was not affected by cinnamaldehyde, suggesting that cysteine adduct formation was essential to anti-amyloid activity of cinnamomum.

Oleocanthal prevents tau from undergoing beta sheet secondary structure changes and inhibits tau amyloid formation in a concentration dependent manner [86]. Utilizing mass spectrometry (MS), further work established that oleocanthal forms a covalent adduct via Schiff base formation with the lysine residue of the hexapeptide VQIVYK sequence in the tau protein [86]. MS also suggested oleocanthal-tau (full length) adduct formation, but confirmation of the adduct was not possible due to inherent ambiguity related to oleocanthal-crosslinked products as well as because the MS spectra contained a low signal-to-noise ratio. Nonetheless, other data strongly suggests that covalent adduct formation is necessary for anti-amyloid activity of oleocanthal: systematic structure activity studies showed that the two aldehyde groups within oleocanthal are essential for its observed anti-amyloid activity (Figure 2B, Lower Panel; [86]); Titration of lysine into the mixtures containing both tau and oleocanthal reduces tau amyloid formation, in a lysine concentration dependent manner. Such reduction is consistent with the

ability of lysine to form adducts with the aldehyde reactive-functional groups in oleocanthal (maybe more readily than tau), which results in fewer oleocanthal molecules available to inhibit tau amyloid [86].

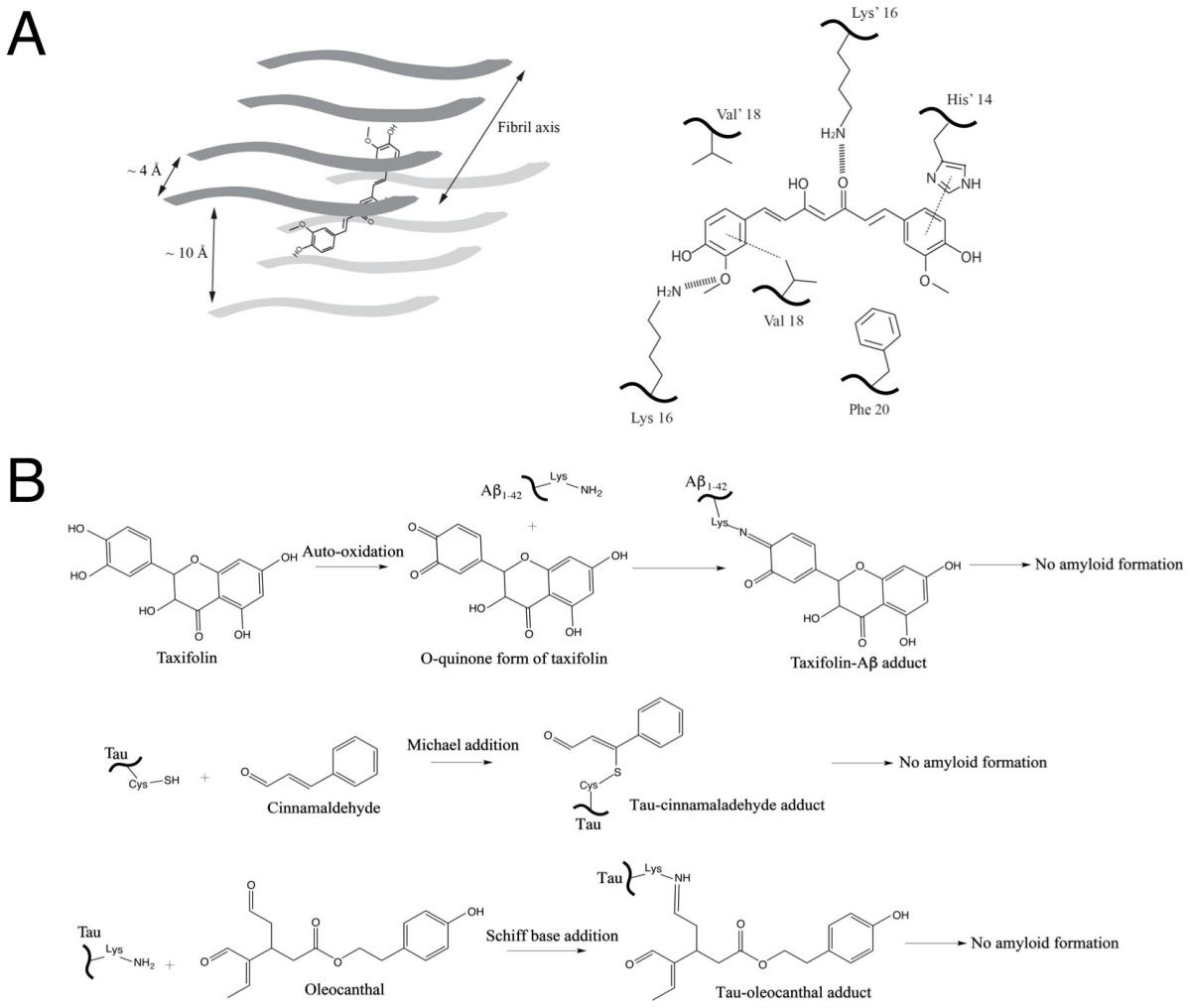

Figure 3. Schematic representations of several proposed mechanisms between inhibitors and amyloid proteins. (A) Non-covalent interaction mechanisms with curcumin as an example. Left panel: The planar curcumin molecule is depicted by a cartoon schematic within the cross-beta spine of an octomeric fibrillar backbone. This representation is based on the structural model of curcumin bound to the VQIVYK segment from the tau protein as well as MD simulation results of curcumin docking onto Aβ hexapeptide KLVFFA [46]. Right panel: key non-covalent interactions occur within *(continued next page)*

the cross-beta spine of full-length amyloid β peptide and curcumin, as depicted from a recent MD simulation study [71]. His14 undergoes π-π stacking (dotted line) with one end of the aromatic heads of curcumin, which is also positioned in a hydrophobic area near Phe20 (bottom right). The central keto-enol functional groups and as well as the aromatic head (bottom left) undergo hydrogen bonding with lysine residues located on opposite sides of the cross-beta spine (hashed lines). Additionally, π-alkyl interactions (depicted by dotted line) were seen between the aromatic head of curcumin (bottom left) and Val18 residues. (B) Covalent interaction mechanisms. Small molecule natural compounds containing electrophilic functional groups such as o-quinones and aldehydes form covalent adducts with amyloidogenic proteins and prevent amyloid formation. (Top panel) Taxifolin forms covalent adducts with the side chain amine group of lysine in $A\beta_{42}$ via Schiff base formation via o-quinone intermediates. (Middle and Lower panels) Tau is covalently modified by the aldehyde functional groups in the case of cinnamaldehyde (middle panel) and oleocanthal (lower panel) via Michael addition and Schiff base respectively. Such conjugation prevents protein amyloid growth and formation.

Natural Product – Metal – Amyloid Protein Complexes

Transition metals, including copper, iron, and zinc are believed to play important roles in contributing to various amyloid diseases [113-116]. While there are still debates about the inhibitory or accelerating effects these metals may have on amyloid formation *in vitro* [115, 117-118], it is well known that metal dyshomeostasis is associated with neurodegenerative amyloid diseases [115, 119]. Furthermore, metals have been shown to directly bind to and exacerbate amyloid plaque load and toxicity *in vivo*. A primary mechanism of toxicity has been attributed to redox active metals such as copper that are sequestered in the amyloid plaques and contribute to cytotoxic reactive oxygen species production in the presence of hydrogen peroxide and reducing agents [115]. Recent work showed that by combining molecular scaffolds or functional groups from individual compounds that chelate metals, interact with amyloid or both, it is possible to engineer multifunctional small molecules with improved activity and selectivity against metal-induced amyloid formation and toxicity [49].

Metal chelating activities of EGCG against various metals, including Zn(II), Cu(I/II), Fe(II/III), and Al(III), directly attenuate metal-catalyzed amyloid formation *in vitro*. For example, EGCG can form compact ternary complexes with Aβ and either Zn(II) or Cu(I/II) that lead to formation of SDS-resistant non-toxic oligomers [105]. Results from NMR and docking simulations showed that these ternary complexes are mechanistically related, at least in part, by the capacity of EGCG to chelate metals separately in solution, and, at the same time, compete (against metals) for binding with the metal binding His residues in amyloid beta peptide (Hyung et al., 2013 [105]). Importantly, these ternary complexes prevent metal-accelerated amyloid formation and are associated with EGCG-mediated cell rescue effects against metal-amyloid beta induced cytotoxicity [105]. Al(III) ion can accelerate amylin amyloid formation *in vitro*, but when

EGCG and Al(III) are present at a 1:1 ratio in the presence of amylin, aggregation is more potently inhibited than in EGCG treated-metal free conditions [120].

Several studies indicate that curcumin can chelate various biologically active metals including redox-active Cu(I/II) and Fe(II/III) [121-124]. Curcumin can inhibit cytotoxic Cu(II)-triggered $A\beta_{42}$ aggregation and remodel preformed Aβ fibrils in the presence of Cu(II) [122]. Mechanistically, these effects are associated with curcumin forming a ternary complex with Cu(II) and Aβ peptide that is facilitated by simultaneous Cu(II) chelation and peptide binding [123]. Curcumin binds Cu(II) and Fe(II) with similar μM-range affinity [121]. It appears that curcumin more readily binds the redox-active metals copper and iron than redox-inactive zinc [121, 125], which has been related to the role of curcumin in suppressing metal-induced oxidative neurotoxicity.

Verbascoside has similar structural and chemical properties as curcumin (Figure 1). It was recently shown to inhibit Aβ fibrillation *in vitro* in metal-free conditions [126]. Recent biochemical and biophysical characterizations have further clarified how verbascoside and its esterified derivative, VPP, interact with freshly dissolved or preformed Aβ aggregates in the presence or absence of $CuCl_2$ or $ZnCl_2$ [50]. Verbascoside showed minimal effects on remodeling preformed aggregates in the absence of metal ions, but interestingly, it was selective for remodeling Aβ aggregates in the presence of $CuCl_2$ but not $ZnCl_2$. In contrast, VPP remodeled preformed Aβ aggregates formed in metal free or in conditions containing either $ZnCl_2$ or $CuCl_2$. In addition, metal binding for both compounds was supported by data from UV-Vis and NMR titration experiments and residue specific peptide binding was suggested [50]. The latter showed evidence that both compounds interacted with the metal binding region of $A\beta_{1-42}$. Furthermore, saturation transfer difference (STD) NMR was utilized to elucidate the atomic details of which

aspects of each compound interacted with preformed fibrils. These data suggested fibrillar $A\beta_{42}$ interacted strongly with the glucose and rhamnose rings of verbascoside, in contrast to the ethyl ester moieties and hydrogens within the aromatic functional groups in VPP[50]. Future studies such as these, that provide atomic details regarding the nature of interactions for different molecular scaffolds on various amyloid targets, will enhance our understanding on the roles of metals in relation to inhibitors and target proteins and also our ability to utilize multifunctional molecular scaffolds to reduce metal-mediated amyloid toxicity.

Non-toxic Off Pathway Aggregates

It has been shown that some natural compounds exert their anti-amyloid activities by inhibiting early oligomerization events as well as preventing mature fibril formation [66]. Others may actually accelerate amyloid formation that result in structural modulation and attenuated oligomer/fibril induced cytotoxicity [96]. Interestingly, it has also been confirmed in multiple cases that natural compounds exert their anti-amyloid effects by modulating amyloid formation and/or preformed fibrils towards the production of both inhibitor-bound soluble and insoluble aggregates [76-77, 84, 87, 96, 103, 127-128]. These aggregates have been reported to display a wide range of size distributions that include soluble low molecular weight oligomers (as small as dimers) as well as high-molecular-weight insoluble amorphous aggregates (HMAA) that sediment under similar conditions as amyloid fibrils and are unable pass through 0.2 μM filters [77]. Several noteworthy biochemical and biophysical characteristics have been associated with these species. (i) *Stability*: both oligomers and HMAA remain stable in the presence of SDS denaturing conditions. Also, resistance to heat or high concentrations of denaturant have been observed in some cases [77, 84, 87, 129] (ii) *Off-(amyloid) pathway nature:* the low molecular weight oligomers do not act as nucleation or template "seeds" for fibril elongation nor do they form amyloid fibrils

themselves [84, 87]. (iii) *Non-toxic:* both oligomers and high molecular weight (HMW) aggregates are inert in cell viability assays and are not recognized by conformation specific and toxic prefibrillar antibodies [87, 96, 127-128]. These characteristics contrast sharply with toxic prefibrillar intermediates that are believed to be one of the major (if not primary) contributors to amyloid induced toxicity [2, 6-7, 130]. We will discuss a few recent findings regarding inhibitor bound protein oligomeric or HMAA complexes, with an emphasis on the chemical mechanisms responsible for their formation.

As discussed earlier, EGCG inhibits PAP mediated fibril formation that results in the formation of insoluble SDS-resistant and EGCG-bound oligomeric PAP complexes [82]. EGCG directs similar formation of SDS- and heat-stable complexes in several other amyloid systems: (i) EGCG forms strong interactions with Aβ and α-synuclein that prevents amyloid formation and at the same time results in formation of EGCG-bound off-pathway complexes that were neither cytotoxic nor recognized by conformational-specific A11 antibody [87]; (ii) EGCG directs formation of high molecular weight insoluble light chain immunoglobulins (isolated and purified from nine different humans diagnosed with light chain amyloidosis or multiple myeloma) that are heat- and SDS-treatment stable [129]. It is unclear in these studies the chemical mechanism(s) that are responsible for the formation of these complexes. (iii) Using microscopic and filter retardation assays, both covalent and non-covalent mechanisms were shown to play a role in the ability of EGCG to remodel preformed amyloid fibrils from numerous amyloid systems (i.e., amylin$_{8-24}$, Aβ or Sup35NM$_{7-16}$) [77].

Baicalein can also stabilize an off pathway population of soluble α-synuclein oligomers that are robustly stable [76, 84]: It took greater than 2M guanidinium hydrochloride (GuHCl) to cause noticeable changes in the secondary structure as determined by thermodynamic stability

studies [84]; at the highest concentration tested (6M GuHCl), baicalein-oligomers are not completely dissociated based on size exclusion chromatography data; at 37 °C baicalein-bound oligomers were shown to be stable for over a month (the longest duration investigated) [84]. Amazingly, these oligomers were determined not only to be "off pathway", but also, in a concentration dependent manner, they inhibited monomeric α-synuclein amyloid fibril formation and showed only minor lipid membrane perturbation against unilamellar vesicles *in vitro* [84]. The unusual stability of these oligomers compounded with the previously confirmed adduct formation and its importance in mediating the anti-amyloid activity of baicalein against α-synuclein suggests that covalent modification plays a role in forming these species.

A recent study showed that nordihydroguaiaretic acid (NDGA), resveratrol, and myricetin remodeled both preformed soluble Aβ oligomers and fibrils towards SDS-stable aggregates that exhibited attenuated cytotoxicity compared to controls and were not recognized by prefibrillar oligomer and fibril conformation-specific antibodies [128]. Another study showed that resveratrol-remodeled fibril aggregates were off pathway and that surprisingly, resveratrol was able to remodel unstructured and toxic prefibrillar oligomers, as identified by circular dichroism and A11 antibodies respectively [127]. Curiously, it did not remodel unstructured, non-toxic soluble oligomers. Since NDGA-, resveratrol-, and myricetin-directed SDS-stable oligomers did not form when samples were boiled prior to SDS-PAGE, it is likely that the chemical mechanism conferring their SDS stability is non-covalent.

Following ultra-centrifugation sedimentation assays, natural compound polyphenol derivatives of rufigallol, trihydroxy benzophenone and exifone, as well as the porphyrin, hematin, were shown to inhibit tau fibril assembly as determined by maintaining a significantly larger portion of tau in the soluble fraction compared to untreated controls (also confirmed by

orthogonal TEM and ThT assays) [131]. At the same time, these compounds directed the formation of SDS-stable soluble and, to a lesser extent, SDS-stable insoluble high molecular weight oligomers. Other sedimentation assays showed that porphyrin phthalocyanine also was able to significantly disaggregate preformed tau filaments into SDS-stable soluble tau oligomers [131]. Further investigations regarding the chemical mechanisms responsible for formation of these soluble HMW oligomers were not performed.

***In vivo* Efficacy and Clinical Studies**

Our detailed analyses of "Mechanisms of Inhibition" in Section 3.2. are based primarily on *in vitro* biochemical and pharmacological studies. While mechanistic insights from *in vitro* studies may still be applicable to *in vivo* cases such as the interactions between directly injected inhibitor drugs with protein amyloid/oligomers in the circulation, such as hyperamylinemia [15]. To our knowledge, there are very few studies that address the mechanisms of amyloid inhibition by small molecules at cellular or *in vivo* levels. We envision a variety of confounding factors will come into play, such as cell membrane permeability/drug delivery, cellular environment, and drug metabolism. Furthermore, how amyloids induce cytotoxicity and lead to cell death are also not completely understood. For all the *in vivo* animal studies, most studies have been focused on examining relevant amyloid plaques using immunohistochemistry approach, quantifying amyloid oligomer levels, and testing basic neurobehavioral functions of the animals (Table 1). We expect future molecular mechanistic studies in the cellular or *in vivo* contexts will emerge as the field further develops.

Currently, there are about two dozen *in vivo* animal studies and only three human clinical trials that have been performed to test selected natural product inhibitors for their efficacy against amyloid diseases (Table 1). Several clinical trials have been registered in the U.S.

National Institutes of Health (NIH) website (ClinicalTrials.gov), but either they are in progress or the final results of completed trials have not been reported[53]. Ongoing clinical trials include tests on resveratrol, genistein, and rosmarinic acid (RA) in AD or mild cognitive impairment patients [53]. Most of these compounds are well studied flavonoids or phenolic compounds, such as EGCG, quercetin, curcumin, oleuropein, and resveratrol, except for rifampicin [132], an antibiotic used to treat bacterial infections, and scyllo-inositol [133], a naturally occurring plant sugar alcohol. Almost all *in vivo* studies have targeted amyloid β peptide. However, EGCG has also been used to target α-synuclein [134] and transthyretin [135]. Most of the animal studies were conducted on transgenic mouse models, though several studies chose *C. elegans* worm as a model. *C. elegans* is known for its simplicity and short lifespan; additionally, deposition of Aβ amyloid in its muscles is age-dependent, as it is in humans, and leads to the paralysis of the worm, a phenotype that can be easily and clearly scored[136-137].

Typical effects observed by these primarily Aβ-targeted inhibitors are summarized in Table 1. Reduced Aβ plaque burden and lowered toxic oligomer levels were observed in the brain of the animal models. Furthermore, memory dysfunction symptoms were often ameliorated. Additional beneficial effects that were reported included reduced microglial activation, increased autophagic responses, reduced inflammatory cytokine levels, and better redox homeostasis. EGCG, curcumin, and rifampicin also targeted tau protein, and these compounds led to reduced phosphorylated tau. In contrast to the animal studies, very few human trials have been completed and reported. EGCG and curcumin had been tested to target Aβ, tau or transthyretin. However, no significant beneficial effects were observed in curcumin-based clinical trials. Noticeably, levels of two inhibitors (curcumin in a clinical trial and resveratrol in an animal study) were undetectable in the brain, suggesting limited bioavailability of some

natural compounds [138-139]. This problem arises for some natural products relevant to their solubility and whether they can efficiently pass blood brain barrier, which will be further addressed in the next section. It is desirable that the bioavailability issue is addressed before more expensive and time-consuming *in vivo* trials are initiated. If a promising lead compound has unsatisfactory bioavailability to reach its target tissue, additional lead optimization steps may be required using medicinal chemistry and/or engineered drug delivery approaches.

Natural Product	Targeted- Protein / Animal Model / Human Trial	Effects	Reference
***In vivo* Animal Studies**			
Curcumin	Aβ / Tg2576 mouse	● Low and high doses of curcumin significantly lowered oxidized proteins and proinflammatory cytokine IL-1β ● With low-dose but not high-dose, soluble and insoluble Aβ, plaque burden, and the astrocytic marker GFAP were significantly reduced	[129]
Curcumin	Aβ / Tg2576 mouse	● Curcumin labeled plaques and reduced amyloid levels and plaque burden	[65]
Curcumin	Aβ / Tg2576 mouse	● Tris buffer saline (TBS)-soluble, A11-positive oligomers in the mice brain significantly reduced ● Aβ plaque depositions in mice brains had decreased tendency but not statistically significant	[130]
Epigallocatechin gallate (EGCG)	Aβ / Tg2576 mouse	● Decreased Aβ levels and plaques	[131]
EGCG	Aβ and tau; Tg2576 mouse	● Decreased plaque burdens in the brain, reduced soluble and insolubleAβ40 and Aβ42 ● Reduced sarkosyl-soluble phosphorylated tau ● Improved working memory	[132]
EGCG	α–synuclein / N-methyl-4-phenyl-1,2,3,6-tetrahydropyridine- and 6-hydroxydopamine-induced neurodegenerative C57-BL mice	● EGCG prevented the accumulation of iron and α-synuclein in the substantia nigra pars compacta.	[133]
Ferulic acid	Aβ / Tg2576 mouse	● No significant changes in the Aβ profile	[130]
Ferulic acid	Aβ / APP/PS1 mouse	● Decreased in brain parenchymal and cerebral vascular β-amyloid deposits as well as Aβ oligomer abundance	[134]

		• Reversed transgene-associated behavioral deficits including hyperactivity, object recognition, spatial working, and reference memory	
Hopeahainol A	Aβ / APP/PS1 mouse	• Protected against mitochondrial dysfunction and suppressed oxidative stress • Rescued synaptic dysfunction and memory impairment	[135]
Myricetin	Aβ / Tg2576 mouse	• Aβ plaque depositions in mice brains significantly decreased • TBS-soluble, A11-positive oligomers in the mice brain significantly reduced • TBS-insoluble Aβ monomers was reduced	[130]
Nordihydroguaiaretic acid	Aβ / Tg2576 mouse	• Aβ plaque depositions in mice brains significantly decreased • TBS-soluble, A11-positive oligomers in the mice brain increased • No changes in TBS-soluble or TBS-insoluble Aβ	[130]
Oleuropein	Aβ / TgCRND8 mouse	• Reduced β-amyloid levels and plaque deposits • Significantly improved cognitive performance • Reduced astrocyte reactions	[136]
Oleuropein	Aβ / TgCRND8 mouse	• Ameliorated memory dysfunction • Enhanced autophagic response	[137]
Oleuropein	Aβ / C. elegan CL2006	• Reduced Aβ plaque deposition, less abundant Aβ oligomers • Decreased paralysis and increased lifespan	[108]
Scyllo-inositol	Amyloid β peptide (Aβ) / TgCRND8 mouse	• Inhibit Aβ high-molecular – weight oligomers in the brain • Ameliorate several AD-link phenotypes: Impaired cognition, Altered synaptic physiology, Cerebral Aβ pathology, Accelerated mortality	[105]

Quercetin	Aβ / C. elegan CL2006	● Decreased the amount of aggregated proteins in solution and also paralysis in CL2006 ● Increased proteasomal activity and the flow of proteins through the macroautophagy pathway	[109]
Resveratrol	Aβ / Tg19959 mouse	● Reduced plaques in medial cortex, striatum, and hypothalamus ● Brain glutathione reduced and brain cysteine increased ● Neither resveratrol nor its conjugated metabolites were detectable in brain	[110]
Resveratrol	Aβ / APP/PS1 mouse	● Lowered Aβ plaque density in the cortex, caudoputamen, and hippocampus ● Reduced average microglial activation	[138]
Resveratrol	Aβ / APP/PS1 mouse	● Long-term treatment significantly prevented memory loss ● Reduced the amyloid burden in the brain	[139]
Rifampicin	Aβ and tau; APP_{OSK} mouse, Tg2576 mouse, Tau609 mouse	APP_{OSK} mouse ● Reduced accumulation of Aβ oligomers, tau hyperphosphorylation, synapse loss, and microglial activation ● Improved memory Tg2576 mouse ● Reduced accumulation of Aβ oligomers, tau hyperphosphorylation, synapse loss, and microglial activation ● No change in amyloid deposition Tau609 mouse ● Reduced accumulation of Aβ oligomers, tau hyperphosphorylation, synapse loss, and microglial activation ● Improved memory	[104]

Rosmarinic acid	Aβ / Tg2576 mouse	● Aβ plaque depositions in mice brains significantly decreased ● TBS-soluble Aβ monomers was increased ● TBS-soluble, A11-positive oligomers in the mice brain significantly reduced	[130]
Rutin	Aβ / APP/PS1 mouse	● Reduced oligomeric Aβ level, increased glutathione/glutathione disulfide ratio ● Attenuated memory deficits ● Reduced microgliosis and astrocytosis, and inflammatory IL-1β and IL-6 levels in brain	[140]
Clinical Studies			
Curcumin	Aβ / Clinical trial	● No changes in Mini-Mental state Examination or plasma Aβ40 levels ● No significant side effects	[141]
Curcumin	Aβ and tau; Clinical trial	● No changes in the AD Assessment Scale-cognitive Subscale, Aβ40 and Aβ42 levels in plasma, levels of Aβ42 and total and phosphorylated tau in cerebrospinal fluid (CSF) ● Suggested limited bioavailability: levels of native curcumin were undetectable in the CSF	[111]
EGCG/Green Tea/Green Tea Extract	Transthyretin / Clinical trial	● No increase of left ventricular (LV) wall thickness and LV myocardial mass was observed ● Suggested an inhibitory effect of GT/GTE on the progression of cardiac amyloidosis	[107]

Table 1. Natural Product Inhibitor *in vivo* Efficacy: Animal Studies and Clinical Trials.

Enhanced Delivery for *in vivo* Efficacy

A significant number of natural compound inhibitors, such as curcumin, resveratrol, and EGCG, are highly lipophilic [140], which is not ideal for drug delivery. These compounds have a low bioavailability in the plasma, which further limits their availability in the brain. For example, in one of the three clinical trials testing efficacy of curcumin [139], the authors were unable to demonstrate clinical or biochemical evidence of efficacy of curcumin in AD, and preliminary data suggested limited bioavailability (undetectable in CSF and low in plasma at 7.32 ng/mL). In order to address low bioavailability issues, large quantities of the compounds must be administered in order to reach desired therapeutic effects. The large dose size of these compounds could lead to acute toxicity or low patient compliance [141].

Nanoparticle-based drug delivery approach has gained pace in recent years for both small molecules such as natural products as well as biomolecules such as peptides [140, 142]. Nanoparticles can improve the effectiveness of natural compounds in disease treatment and prevention by increasing their bioavailability, including passing the BBB. In a recent study, the superior protective efficacy of resveratrol-loaded polysorbate 80-coated poly(lactide) nanoparticles compared to native resveratrol in a 1-methyl-4-phenyl-1,2,3,6-tetrahydropyridine induced Parkinson's Disease (PD) animal model was demonstrated, thus suggesting the advantage of nanoparticles over native drug in neuroprotection [143]. Another study used lipid-based nanoparticles (curcumin and piperine coloaded glyceryl monooleate nanoparticles). *In vivo* studies revealed that formulated dual drug (curcumin and piperine) loaded nanoparticles were able to cross the BBB, which rescued rotenone-induced motor coordination impairment, and restrained dopaminergic neuronal degeneration in a PD mouse model [144].

We and others recently reviewed and summarized multiple examples of nanoparticle formulations that increased the bioavailability (drug concentration in plasma) of selected natural compounds [140, 145]. For example, poor bioavailability is a major limitation to the therapeutic utility of curcumin in clinical trials[146-147]. Shen et al compared the attenuation of morphine tolerance in mice induced by curcumin encapsulated in nanoparticles of PLGA and in nanoparticles of poly(ethylene glycol)-*b*-poly(lactic acid) (PEG-*b*-PLA)[147]. The mice that were given the curcumin-PLGA nanoparticles orally exhibited significantly greater attenuation of morphine tolerance than those mice given the curcumin-PEG-*b*-PLA nanoparticles, presumably due to greater absorption of the curcumin when formulated with PLGA. The mechanism behind PLGA nanoparticles increasing the bioavailability of curcumin has been investigated. Xie et al showed data suggesting that the increase in bioavailability of curcumin was due to the inhibition of P-glycoprotein (P-gp)-mediated efflux. They concluded that the PLGA nanoparticles inhibit P-gp, which allows increased drug permeability and bioavailability [148]. Elucidation of the mechanisms of nanoparticle-based natural compound drug delivery will be important in further development of this promising technology. Moreover, these studies demonstrate the significant potential of nanoparticle-mediated drug delivery.

Liposomal encapsulation has also been used to improve bioavailability of hydrophobic compounds. Liposomes can better solubilize hydrophobic compounds and may also alter their pharmacokinetic properties. Multiple studies have been reported to use enhance the delivery of curcumin with liposome formulations [145]. In a study of rat oral administration of liposome-encapsulated curcumin (LEC), not only high bioavailability of curcumin but also a faster rate and better absorption of curcumin were observed as compared with other curcumin forms [149]. Oral LEC gave higher pharmacokinetic C(max) and shorter T(max) values, as well as a higher value

for the area under the blood concentration-time curve (AUC), at the entire time points. In another case, a new type of liposome-propylene glycol liposomes (PGL) were engineered to facilitate the intracellular delivery of curcumin. From *in vitro* cell-based experiments, PGL showed the highest uptake of curcumin compared with that of conventional liposomes and free curcumin solution [150].

Another approach for increasing solubility and bioavailability of poorly soluble natural compounds and drugs is to form amorphous solid dispersions (ASDs) of the therapeutic compound with a polymer [151]. Most drugs and natural compounds tend to crystallize, which is a barrier to dissolution at physiological conditions. Those natural compounds that are also highly hydrophobic exhibit especially poor bioavailability due to the combination of hydrophobicity and crystallinity. ASDs are solid solutions of the therapeutic in an amorphous polymer carrier in which attractive interactions prevent crystallization. It is important to choose the polymer for biocompatibility and controlled release of the drug under physiological conditions and also for good storage stability. In particular, polysaccharides have recently been demonstrated to form ASDs that significantly enhance the solubility of natural compounds including ellagic acid, quercetin, curcumin, naringenin, and resveratrol [152-154]. These studies suggest that ASDs in nanoparticle form could potentially be very useful in improving bioavailability through improved solubility and transport across physiological barriers.

Even though nanoparticles have great potential to considerably improve the bioavailability of natural compounds and there has recently been significant progress in the development of such formulation, very few nanoparticle/natural compound drugs are currently being tested in clinical trials. More work needs to be performed to optimize these drug delivery

systems and to better understand the mechanisms underlining the enhanced nanoparticle delivery.

Issues and Perspectives

Natural product inhibitors are not without issues. These compounds examined thus far have relatively moderate inhibition potencies. Medicinal chemistry-based optimization steps (such as analogue synthesis and structure-function activity relationship characterizations) are often necessary. Another common issue is their solubility and bioavailability that has been addressed in the previous Section.

There are a significant number of *in vivo* animal studies, but these studies focused on phenolic compounds and flavonoids that have similar physicochemical properties. Only a few *in vivo* studies test compounds that have significantly different chemical structures (hopeahainol A, rifampicin, and scyllo-inositol (Table 1)). Such limited diversity may hinder discovery of inhibitors that have novel structural scaffolds. To identify novel inhibitors, large library screens with diverse classes of compounds may be required, which in turn needs a high throughput platform. Lee and colleagues have implemented quantitative high throughput (qHTP) screening of approximately 292,000 compounds (not natural product focused) to identify drug-like inhibitors of tau assembly [155]. The Hecht group developed an Aβ-GFP fusion strategy and screened a synthetic triazine library containing ~1000 compounds [68]. Our group also developed a semi-high throughput platform using fluorescence based 384-well plate format, which can be readily expanded to 1596-well plate to achieve high throughput for large library screens, such as screening an NIH Clinical Collection library as part of our repurposing efforts to identify new inhibitors against multiple amyloidogenic proteins including Aβ, amylin, tau, and α-synuclein

(data not shown). These examples indicate that technology is available to perform qHTP screens to identify novel natural product inhibitors from large natural product diversity libraries.

Besides natural product inhibitors, there are numerous non-natural product based inhibitors, including synthetic compounds, peptide mimics, and antibodies. In those cases, protein amyloid inhibition mechanisms are likely to be different, especially for peptide-based inhibitors and antibodies. These topics are beyond the scope of this review.

Fully understanding the mechanisms of inhibition is critical. Currently, a significant gap in knowledge remains in our understanding of the biochemical and pharmacological mechanisms of amyloid inhibition, such as differences in protein remodeling with different natural product inhibitors (see Section 3.2.5). One major reason for our incomplete mechanistic understanding is that many of these amyloidogenic protein targets are partially unfolded or intrinsically disordered, which limits high-resolution structural characterization of the protein-inhibitor interaction. However, recent developments in high-resolution mass spectrometry may provide a powerful tool to rapidly characterize protein-inhibitor covalent compounds. Furthermore, expanding crystal structural information of fragments of amyloidogenic proteins and/or fragments in complex with inhibitors will yield significant insights into inhibition mechanisms as well as provide a basis for structure-based inhibitor design [72, 156].

It is clear that similar types of non-covalent and in some cases covalent interactions can facilitate anti-amyloid activities of numerous inhibitors. However, protein amyloid specificity may play an important role as well. For example, curcumin accelerates α-synuclein amyloid formation into less toxic species [96], whereas it delays and inhibits amylin amyloid formation [90]. Additionally, in many cases EGCG redirects amyloid formation from multiple different protein amyloid systems into off pathway non-toxic species, a common feature for many amyloid

inhibitors. However, the observed anti-amyloid activities of EGCG can vary markedly according to the protein it interacts with: non-covalent mechanisms are only required for the activity of EGCG against amylin amyloid formation [79], whereas covalent interactions are essential for anti-amyloid activity of EGCG against $(PAP)_{248-286}$ amyloid formation [82]. In this context, studies are needed to elucidate the chemical mechanisms by which specific molecular scaffolds inhibit specific amyloid proteins.

Due to bottlenecks in the therapeutic development process, developing a brand-new drug takes an enormous amount of time, money and effort. Therefore, it may be worthwhile to consider the concept of drug repurposing as a strategy to decrease costs and improve success rates: many drugs approved for other uses already have been tested in humans, so detailed information is available on their pharmacology, formulation, potential toxicity and side effects.

References

1. Knowles, T. P. J.; Vendruscolo, M.; Dobson, C. M., The amyloid state and its association with protein misfolding diseases. *Nat Rev Mol Cell Biol* **2014,** *15* (6), 384-396.
2. Chiti, F.; Dobson, C. M., Protein misfolding, functional amyloid, and human disease. *Annual review of biochemistry* **2006,** *75*, 333-66.
3. Eisenberg, D.; Jucker, M., The amyloid state of proteins in human diseases. *Cell* **2012,** *148* (6), 1188-1203.
4. Lambert, M. P.; Barlow, A. K.; Chromy, B. A.; Edwards, C.; Freed, R.; Liosatos, M.; Morgan, T. E.; Rozovsky, I.; Trommer, B.; Viola, K. L.; Wals, P.; Zhang, C.; Finch, C. E.; Krafft, G. A.; Klein, W. L., Diffusible, nonfibrillar ligands derived from Abeta1-42 are potent central nervous system neurotoxins. *Proceedings of the National Academy of Sciences of the United States of America* **1998,** *95* (11), 6448-53.
5. Shankar, G. M.; Li, S.; Mehta, T. H.; Garcia-Munoz, A.; Shepardson, N. E.; Smith, I.; Brett, F. M.; Farrell, M. A.; Rowan, M. J.; Lemere, C. A.; Regan, C. M.; Walsh, D. M.; Sabatini, B. L.; Selkoe, D. J., Amyloid-beta protein dimers isolated directly from Alzheimer's brains impair synaptic plasticity and memory. *Nature medicine* **2008,** *14* (8), 837-42.
6. Kayed, R.; Pensalfini, A.; Margol, L.; Sokolov, Y.; Sarsoza, F.; Head, E.; Hall, J.; Glabe, C., Annular protofibrils are a structurally and functionally distinct type of amyloid oligomer. *The Journal of biological chemistry* **2009,** *284* (7), 4230-7.
7. Kayed, R.; Head, E.; Thompson, J. L.; McIntire, T. M.; Milton, S. C.; Cotman, C. W.; Glabe, C. G., Common Structure of Soluble Amyloid Oligomers Implies Common Mechanism of Pathogenesis. *Science* **2003,** *300* (5618), 486-489.
8. Stroud, J. C.; Liu, C.; Teng, P. K.; Eisenberg, D., Toxic fibrillar oligomers of amyloid-β have cross-β structure. *Proceedings of the National Academy of Sciences of the United States of America* **2012,** *109* (20), 7717-7722.
9. Laganowsky, A.; Liu, C.; Sawaya, M. R.; Whitelegge, J. P.; Park, J.; Zhao, M.; Pensalfini, A.; Soriaga, A. B.; Landau, M.; Teng, P. K.; Cascio, D.; Glabe, C.; Eisenberg, D., Atomic view of a toxic amyloid small oligomer. *Science* **2012,** *335* (6073), 1228-31.
10. Stefani, M.; Dobson, C. M., Protein aggregation and aggregate toxicity: new insights into protein folding, misfolding diseases and biological evolution. *Journal of molecular medicine (Berlin, Germany)* **2003,** *81* (11), 678-99.
11. Rivera, J. F.; Costes, S.; Gurlo, T.; Glabe, C. G.; Butler, P. C., Autophagy defends pancreatic beta cells from human islet amyloid polypeptide-induced toxicity. *The Journal of clinical investigation* **2014,** *124* (8), 3489-500.
12. Demuro, A.; Mina, E.; Kayed, R.; Milton, S. C.; Parker, I.; Glabe, C. G., Calcium dysregulation and membrane disruption as a ubiquitous neurotoxic mechanism of soluble amyloid oligomers. *The Journal of biological chemistry* **2005,** *280* (17), 17294-300.
13. Stroo, E.; Koopman, M.; Nollen, E. A. A.; Mata-Cabana, A., Cellular Regulation of Amyloid Formation in Aging and Disease. *Frontiers in Neuroscience* **2017,** *11* (64).
14. Yang, Y.; Petkova, A.; Huang, K.; Xu, B.; Hua, Q. X.; Ye, I. J.; Chu, Y. C.; Hu, S. Q.; Phillips, N. B.; Whittaker, J.; Ismail-Beigi, F.; Mackin, R. B.; Katsoyannis, P. G.; Tycko, R.; Weiss, M. A., An Achilles' heel in an amyloidogenic protein and its repair: insulin fibrillation and therapeutic design. *The Journal of biological chemistry* **2010,** *285* (14), 10806-21.
15. Westermark, P.; Andersson, A.; Westermark, G. T., Islet amyloid polypeptide, islet amyloid, and diabetes mellitus. *Physiological reviews* **2011,** *91* (3), 795-826.

16. Cao, P.; Abedini, A.; Raleigh, D. P., Aggregation of islet amyloid polypeptide: from physical chemistry to cell biology. *Current opinion in structural biology* **2013,** *23* (1), 82-89.
17. Wiltzius, J. J.; Sievers, S. A.; Sawaya, M. R.; Cascio, D.; Popov, D.; Riekel, C.; Eisenberg, D., Atomic structure of the cross-beta spine of islet amyloid polypeptide (amylin). *Protein science : a publication of the Protein Society* **2008,** *17* (9), 1467-74.
18. Guardado-Mendoza, R.; Davalli, A. M.; Chavez, A. O.; Hubbard, G. B.; Dick, E. J.; Majluf-Cruz, A.; Tene-Perez, C. E.; Goldschmidt, L.; Hart, J.; Perego, C.; Comuzzie, A. G.; Tejero, M. E.; Finzi, G.; Placidi, C.; La Rosa, S.; Capella, C.; Halff, G.; Gastaldelli, A.; DeFronzo, R. A.; Folli, F., Pancreatic islet amyloidosis, β-cell apoptosis, and α-cell proliferation are determinants of islet remodeling in type-2 diabetic baboons. *Proceedings of the National Academy of Sciences* **2009,** *106* (33), 13992-13997.
19. Westermark, P.; Andersson, A.; Westermark, G. T., *Islet Amyloid Polypeptide, Islet Amyloid, and Diabetes Mellitus*. 2011; Vol. 91, p 795-826.
20. Last, N. B.; Rhoades, E.; Miranker, A. D., Islet amyloid polypeptide demonstrates a persistent capacity to disrupt membrane integrity. *Proceedings of the National Academy of Sciences of the United States of America* **2011,** *108* (23), 9460-5.
21. Abedini, A.; Schmidt, A. M., Mechanisms of islet amyloidosis toxicity in type 2 diabetes. *FEBS letters* **2013,** *587* (8), 1119-27.
22. Despa, S.; Margulies, K. B.; Chen, L.; Knowlton, A. A.; Havel, P. J.; Taegtmeyer, H.; Bers, D. M.; Despa, F., Hyperamylinemia contributes to cardiac dysfunction in obesity and diabetes: a study in humans and rats. *Circulation research* **2012,** *110* (4), 598-608.
23. Despa, S.; Sharma, S.; Harris, T. R.; Dong, H.; Li, N.; Chiamvimonvat, N.; Taegtmeyer, H.; Margulies, K. B.; Hammock, B. D.; Despa, F., Cardioprotection by controlling hyperamylinemia in a "humanized" diabetic rat model. *Journal of the American Heart Association* **2014,** *3* (4).
24. Jackson, K.; Barisone, G. A.; Diaz, E.; Jin, L. W.; DeCarli, C.; Despa, F., Amylin deposition in the brain: A second amyloid in Alzheimer disease? *Annals of neurology* **2013,** *74* (4), 517-26.
25. Oskarsson, M. E.; Paulsson, J. F.; Schultz, S. W.; Ingelsson, M.; Westermark, P.; Westermark, G. T., In Vivo Seeding and Cross-Seeding of Localized Amyloidosis: A Molecular Link between Type 2 Diabetes and Alzheimer Disease. *The American journal of pathology* **2015,** *185* (3), 834-46.
26. Guan, J.; Zhao, H. L.; Sui, Y.; He, L.; Lee, H. M.; Lai, F. M.; Tong, P. C.; Chan, J. C., Histopathological correlations of islet amyloidosis with apolipoprotein E polymorphisms in type 2 diabetic Chinese patients. *Pancreas* **2013,** *42* (7), 1129-37.
27. Glabe, C. G.; Kayed, R., Common structure and toxic function of amyloid oligomers implies a common mechanism of pathogenesis. *Neurology* **2006,** *66* (2 Suppl 1), S74-8.
28. Brender, J. R.; Salamekh, S.; Ramamoorthy, A., Membrane disruption and early events in the aggregation of the diabetes related peptide IAPP from a molecular perspective. *Accounts of chemical research* **2012,** *45* (3), 454-62.
29. Chi, N. F.; Chien, L. N.; Ku, H. L.; Hu, C. J.; Chiou, H. Y., Alzheimer disease and risk of stroke: a population-based cohort study. *Neurology* **2013,** *80* (8), 705-11.
30. De Meyer, G. R.; De Cleen, D. M.; Cooper, S.; Knaapen, M. W.; Jans, D. M.; Martinet, W.; Herman, A. G.; Bult, H.; Kockx, M. M., Platelet phagocytosis and processing of beta-amyloid precursor protein as a mechanism of macrophage activation in atherosclerosis. *Circulation research* **2002,** *90* (11), 1197-204.

31. Lee, P. H.; Bang, O. Y.; Hwang, E. M.; Lee, J. S.; Joo, U. S.; Mook-Jung, I.; Huh, K., Circulating beta amyloid protein is elevated in patients with acute ischemic stroke. *Journal of neural transmission (Vienna, Austria : 1996)* **2005,** *112* (10), 1371-9.
32. Yan, L. M.; Tatarek-Nossol, M.; Velkova, A.; Kazantzis, A.; Kapurniotu, A., Design of a mimic of nonamyloidogenic and bioactive human islet amyloid polypeptide (IAPP) as nanomolar affinity inhibitor of IAPP cytotoxic fibrillogenesis. *Proceedings of the National Academy of Sciences of the United States of America* **2006,** *103* (7), 2046-51.
33. Yan, L. M.; Velkova, A.; Tatarek-Nossol, M.; Andreetto, E.; Kapurniotu, A., IAPP mimic blocks Abeta cytotoxic self-assembly: cross-suppression of amyloid toxicity of Abeta and IAPP suggests a molecular link between Alzheimer's disease and type II diabetes. *Angewandte Chemie (International ed. in English)* **2007,** *46* (8), 1246-52.
34. Yan, L. M.; Velkova, A.; Tatarek-Nossol, M.; Rammes, G.; Sibaev, A.; Andreetto, E.; Kracklauer, M.; Bakou, M.; Malideli, E.; Goke, B.; Schirra, J.; Storr, M.; Kapurniotu, A., Selectively N-methylated soluble IAPP mimics as potent IAPP receptor agonists and nanomolar inhibitors of cytotoxic self-assembly of both IAPP and Abeta40. *Angewandte Chemie (International ed. in English)* **2013,** *52* (39), 10378-83.
35. Jackrel, M. E.; Shorter, J., Potentiated Hsp104 variants suppress toxicity of diverse neurodegenerative disease-linked proteins. *Disease Models & Mechanisms* **2014,** *7* (10), 1175-1184.
36. Sevigny, J.; Chiao, P.; Bussiere, T.; Weinreb, P. H.; Williams, L.; Maier, M.; Dunstan, R.; Salloway, S.; Chen, T.; Ling, Y.; O'Gorman, J.; Qian, F.; Arastu, M.; Li, M.; Chollate, S.; Brennan, M. S.; Quintero-Monzon, O.; Scannevin, R. H.; Arnold, H. M.; Engber, T.; Rhodes, K.; Ferrero, J.; Hang, Y.; Mikulskis, A.; Grimm, J.; Hock, C.; Nitsch, R. M.; Sandrock, A., The antibody aducanumab reduces Abeta plaques in Alzheimer's disease. *Nature* **2016,** *537* (7618), 50-6.
37. Morgan, D., The role of microglia in antibody-mediated clearance of amyloid-beta from the brain. *CNS & neurological disorders drug targets* **2009,** *8* (1), 7-15.
38. Rahimi, F.; Murakami, K.; Summers, J. L.; Chen, C.-H. B.; Bitan, G., RNA Aptamers Generated against Oligomeric Aβ40 Recognize Common Amyloid Aptatopes with Low Specificity but High Sensitivity. *PloS one* **2009,** *4* (11), e7694.
39. Fukasawa, K.; Higashimoto, Y.; Ando, Y.; Motomiya, Y., Selection of DNA Aptamer That Blocks the Fibrillogenesis of a Proteolytic Amyloidogenic Fragment of beta2 m. *Therapeutic apheresis and dialysis : official peer-reviewed journal of the International Society for Apheresis, the Japanese Society for Apheresis, the Japanese Society for Dialysis Therapy* **2017**.
40. Knight, J. D.; Hebda, J. A.; Miranker, A. D., Conserved and cooperative assembly of membrane-bound alpha-helical states of islet amyloid polypeptide. *Biochemistry* **2006,** *45* (31), 9496-508.
41. Williamson, J. A.; Loria, J. P.; Miranker, A. D., Helix stabilization precedes aqueous and bilayer-catalyzed fiber formation in islet amyloid polypeptide. *Journal of molecular biology* **2009,** *393* (2), 383-96.
42. Wang, H.; Cao, P.; Raleigh, D. P., Amyloid formation in heterogeneous environments: islet amyloid polypeptide glycosaminoglycan interactions. *Journal of molecular biology* **2013,** *425* (3), 492-505.
43. Oskarsson, M. E.; Singh, K.; Wang, J.; Vlodavsky, I.; Li, J.-p.; Westermark, G. T., Heparan Sulfate Proteoglycans Are Important for Islet Amyloid Formation and Islet Amyloid

Polypeptide-induced Apoptosis. *The Journal of biological chemistry* **2015,** *290* (24), 15121-15132.
44. Soto, C.; Estrada, L., Amyloid Inhibitors and β-Sheet Breakers. In *Alzheimer's Disease: Cellular and Molecular Aspects of Amyloid β*, Harris, J. R.; Fahrenholz, F., Eds. Springer US: Boston, MA, 2005; pp 351-364.
45. Attar, A.; Bitan, G., Disrupting self-assembly and toxicity of amyloidogenic protein oligomers by "molecular tweezers" - from the test tube to animal models. *Current pharmaceutical design* **2014,** *20* (15), 2469-83.
46. Landau, M.; Sawaya, M. R.; Faull, K. F.; Laganowsky, A.; Jiang, L.; Sievers, S. A.; Liu, J.; Barrio, J. R.; Eisenberg, D., Towards a pharmacophore for amyloid. *PLoS biology* **2011,** *9* (6), e1001080.
47. Velander, P.; Wu, L.; Henderson, F.; Zhang, S.; Bevan, D. R.; Xu, B., Natural Product-Based Amyloid Inhibitors. *Biochemical pharmacology* **2017**.
48. Stefani, M.; Rigacci, S., Protein Folding and Aggregation into Amyloid: The Interference by Natural Phenolic Compounds. *International journal of molecular sciences* **2013,** *14* (6), 12411-12457.
49. Savelieff, M. G.; DeToma, A. S.; Derrick, J. S.; Lim, M. H., The ongoing search for small molecules to study metal-associated amyloid-beta species in Alzheimer's disease. *Accounts of chemical research* **2014,** *47* (8), 2475-82.
50. Korshavn, K. J.; Jang, M.; Kwak, Y. J.; Kochi, A.; Vertuani, S.; Bhunia, A.; Manfredini, S.; Ramamoorthy, A.; Lim, M. H., Reactivity of Metal-Free and Metal-Associated Amyloid-beta with Glycosylated Polyphenols and Their Esterified Derivatives. *Sci Rep* **2015,** *5*, 17842.
51. Mishra, S.; Palanivelu, K., The effect of curcumin (turmeric) on Alzheimer's disease: An overview. *Annals of Indian Academy of Neurology* **2008,** *11* (1), 13-19.
52. Rigacci, S., Olive Oil Phenols as Promising Multi-targeting Agents Against Alzheimer's Disease. *Advances in experimental medicine and biology* **2015,** *863*, 1-20.
53. Yamada, M.; Ono, K.; Hamaguchi, T.; Noguchi-Shinohara, M., Natural Phenolic Compounds as Therapeutic and Preventive Agents for Cerebral Amyloidosis. *Advances in experimental medicine and biology* **2015,** *863*, 79-94.
54. Moore, K. S.; Wehrli, S.; Roder, H.; Rogers, M.; Forrest, J. N., Jr.; McCrimmon, D.; Zasloff, M., Squalamine: an aminosterol antibiotic from the shark. *Proceedings of the National Academy of Sciences of the United States of America* **1993,** *90* (4), 1354-8.
55. Zasloff, M.; Adams, A. P.; Beckerman, B.; Campbell, A.; Han, Z.; Luijten, E.; Meza, I.; Julander, J.; Mishra, A.; Qu, W.; Taylor, J. M.; Weaver, S. C.; Wong, G. C. L., Squalamine as a broad-spectrum systemic antiviral agent with therapeutic potential. *Proceedings of the National Academy of Sciences of the United States of America* **2011,** *108* (38), 15978-15983.
56. Takasaki, J.; Ono, K.; Yoshiike, Y.; Hirohata, M.; Ikeda, T.; Morinaga, A.; Takashima, A.; Yamada, M., Vitamin A has anti-oligomerization effects on amyloid-beta in vitro. *Journal of Alzheimer's disease : JAD* **2011,** *27* (2), 271-80.
57. D'Avola, D.; Lopez-Franco, E.; Sangro, B.; Paneda, A.; Grossios, N.; Gil-Farina, I.; Benito, A.; Twisk, J.; Paz, M.; Ruiz, J.; Schmidt, M.; Petry, H.; Harper, P.; de Salamanca, R. E.; Fontanellas, A.; Prieto, J.; Gonzalez-Aseguinolaza, G., Phase I open label liver-directed gene therapy clinical trial for acute intermittent porphyria. *Journal of hepatology* **2016,** *65* (4), 776-83.
58. Eisele, Y. S.; Monteiro, C.; Fearns, C.; Encalada, S. E.; Wiseman, R. L.; Powers, E. T.; Kelly, J. W., Targeting protein aggregation for the treatment of degenerative diseases. *Nature reviews. Drug discovery* **2015,** *14* (11), 759-80.

59. Scarmeas, N.; Stern, Y.; Mayeux, R.; Luchsinger, J. A., Mediterranean diet, Alzheimer disease, and vascular mediation. *Archives of neurology* **2006,** *63* (12), 1709-17.
60. Scarmeas, N.; Luchsinger, J. A.; Schupf, N.; Brickman, A. M.; Cosentino, S.; Tang, M. X.; Stern, Y., Physical activity, diet, and risk of Alzheimer disease. *Jama* **2009,** *302* (6), 627-37.
61. Luchsinger, J. A.; Mayeux, R., Dietary factors and Alzheimer's disease. *The Lancet. Neurology* **2004,** *3* (10), 579-87.
62. Arntzen, K. A.; Schirmer, H.; Wilsgaard, T.; Mathiesen, E. B., Moderate wine consumption is associated with better cognitive test results: a 7 year follow up of 5033 subjects in the Tromso Study. *Acta neurologica Scandinavica. Supplementum* **2010,** (190), 23-9.
63. Ardah, M. T.; Paleologou, K. E.; Lv, G.; Menon, S. A.; Abul Khair, S. B.; Lu, J. H.; Safieh-Garabedian, B.; Al-Hayani, A. A.; Eliezer, D.; Li, M.; El-Agnaf, O. M., Ginsenoside Rb1 inhibits fibrillation and toxicity of alpha-synuclein and disaggregates preformed fibrils. *Neurobiology of disease* **2015,** *74*, 89-101.
64. Rigacci, S.; Guidotti, V.; Bucciantini, M.; Parri, M.; Nediani, C.; Cerbai, E.; Stefani, M.; Berti, A., Oleuropein aglycon prevents cytotoxic amyloid aggregation of human amylin. *The Journal of Nutritional Biochemistry* **2010,** *21* (8), 726-735.
65. Ono, K.; Yoshiike, Y.; Takashima, A.; Hasegawa, K.; Naiki, H.; Yamada, M., Vitamin A exhibits potent antiamyloidogenic and fibril-destabilizing effects in vitro. *Experimental neurology* **2004,** *189* (2), 380-92.
66. Velander, P.; Wu, L.; Ray, W. K.; Helm, R. F.; Xu, B., Amylin Amyloid Inhibition by Flavonoid Baicalein: Key Roles of Its Vicinal Dihydroxyl Groups of the Catechol Moiety. *Biochemistry* **2016**.
67. Chen, J.; Armstrong, A. H.; Koehler, A. N.; Hecht, M. H., Small molecule microarrays enable the discovery of compounds that bind the Alzheimer's Abeta peptide and reduce its cytotoxicity. *Journal of the American Chemical Society* **2010,** *132* (47), 17015-22.
68. Kim, W.; Kim, Y.; Min, J.; Kim, D. J.; Chang, Y. T.; Hecht, M. H., A high-throughput screen for compounds that inhibit aggregation of the Alzheimer's peptide. *ACS chemical biology* **2006,** *1* (7), 461-9.
69. Nelson, R.; Sawaya, M. R.; Balbirnie, M.; Madsen, A. O.; Riekel, C.; Grothe, R.; Eisenberg, D., Structure of the cross-[beta] spine of amyloid-like fibrils. *Nature* **2005,** *435* (7043), 773-778.
70. Berhanu, W. M.; Masunov, A. E., Atomistic mechanism of polyphenol amyloid aggregation inhibitors: molecular dynamics study of Curcumin, Exifone, and Myricetin interaction with the segment of tau peptide oligomer. *Journal of biomolecular structure & dynamics* **2015,** *33* (7), 1399-411.
71. Rao, P. P.; Mohamed, T.; Teckwani, K.; Tin, G., Curcumin Binding to Beta Amyloid: A Computational Study. *Chemical biology & drug design* **2015,** *86* (4), 813-20.
72. Jiang, L.; Liu, C.; Leibly, D.; Landau, M.; Zhao, M.; Hughes, M. P.; Eisenberg, D. S., Structure-based discovery of fiber-binding compounds that reduce the cytotoxicity of amyloid beta. *eLife* **2013,** *2*, e00857.
73. Lemkul, J. A.; Bevan, D. R., Morin inhibits the early stages of amyloid beta-peptide aggregation by altering tertiary and quaternary interactions to produce "off-pathway" structures. *Biochemistry* **2012,** *51* (30), 5990-6009.
74. Lemkul, J. A.; Bevan, D. R., The role of molecular simulations in the development of inhibitors of amyloid beta-peptide aggregation for the treatment of Alzheimer's disease. *ACS Chem Neurosci* **2012,** *3* (11), 845-56.

75. Sato, M.; Murakami, K.; Uno, M.; Nakagawa, Y.; Katayama, S.; Akagi, K.; Masuda, Y.; Takegoshi, K.; Irie, K., Site-specific inhibitory mechanism for amyloid beta42 aggregation by catechol-type flavonoids targeting the Lys residues. *The Journal of biological chemistry* **2013,** *288* (32), 23212-24.
76. Zhu, M.; Rajamani, S.; Kaylor, J.; Han, S.; Zhou, F.; Fink, A. L., The flavonoid baicalein inhibits fibrillation of alpha-synuclein and disaggregates existing fibrils. *The Journal of biological chemistry* **2004,** *279* (26), 26846-57.
77. Palhano, F. L.; Lee, J.; Grimster, N. P.; Kelly, J. W., Toward the Molecular Mechanism(s) by Which EGCG Treatment Remodels Mature Amyloid Fibrils. *Journal of the American Chemical Society* **2013,** *135* (20), 7503-7510.
78. Ishii, T.; Mori, T.; Tanaka, T.; Mizuno, D.; Yamaji, R.; Kumazawa, S.; Nakayama, T.; Akagawa, M., Covalent modification of proteins by green tea polyphenol (-)-epigallocatechin-3-gallate through autoxidation. *Free radical biology & medicine* **2008,** *45* (10), 1384-94.
79. Cao, P.; Raleigh, D. P., Analysis of the inhibition and remodeling of islet amyloid polypeptide amyloid fibers by flavanols. *Biochemistry* **2012,** *51* (13), 2670-83.
80. Tu, L. H.; Young, L. M.; Wong, A. G.; Ashcroft, A. E.; Radford, S. E.; Raleigh, D. P., Mutational analysis of the ability of resveratrol to inhibit amyloid formation by islet amyloid polypeptide: critical evaluation of the importance of aromatic-inhibitor and histidine-inhibitor interactions. *Biochemistry* **2015,** *54* (3), 666-76.
81. Cheng, B.; Gong, H.; Xiao, H.; Petersen, R. B.; Zheng, L.; Huang, K., Inhibiting toxic aggregation of amyloidogenic proteins: a therapeutic strategy for protein misfolding diseases. *Biochimica et biophysica acta* **2013,** *1830* (10), 4860-71.
82. Popovych, N.; Brender, J. R.; Soong, R.; Vivekanandan, S.; Hartman, K.; Basrur, V.; Macdonald, P. M.; Ramamoorthy, A., Site specific interaction of the polyphenol EGCG with the SEVI amyloid precursor peptide PAP(248-286). *The journal of physical chemistry. B* **2012,** *116* (11), 3650-8.
83. Meng, X.; Munishkina, L. A.; Fink, A. L.; Uversky, V. N., Molecular mechanisms underlying the flavonoid-induced inhibition of alpha-synuclein fibrillation. *Biochemistry* **2009,** *48* (34), 8206-24.
84. Hong, D. P.; Fink, A. L.; Uversky, V. N., Structural characteristics of alpha-synuclein oligomers stabilized by the flavonoid baicalein. *Journal of molecular biology* **2008,** *383* (1), 214-23.
85. George, R. C.; Lew, J.; Graves, D. J., Interaction of cinnamaldehyde and epicatechin with tau: implications of beneficial effects in modulating Alzheimer's disease pathogenesis. *Journal of Alzheimer's disease : JAD* **2013,** *36* (1), 21-40.
86. Li, W.; Sperry, J. B.; Crowe, A.; Trojanowski, J. Q.; Smith, A. B., 3rd; Lee, V. M., Inhibition of tau fibrillization by oleocanthal via reaction with the amino groups of tau. *Journal of neurochemistry* **2009,** *110* (4), 1339-51.
87. Ehrnhoefer, D. E.; Bieschke, J.; Boeddrich, A.; Herbst, M.; Masino, L.; Lurz, R.; Engemann, S.; Pastore, A.; Wanker, E. E., EGCG redirects amyloidogenic polypeptides into unstructured, off-pathway oligomers. *Nature structural & molecular biology* **2008,** *15* (6), 558-66.
88. Thapa, A.; Jett, S. D.; Chi, E. Y., Curcumin Attenuates Amyloid-beta Aggregate Toxicity and Modulates Amyloid-beta Aggregation Pathway. *ACS Chem Neurosci* **2016,** *7* (1), 56-68.

89. Jha, N. N.; Ghosh, D.; Das, S.; Anoop, A.; Jacob, R. S.; Singh, P. K.; Ayyagari, N.; Namboothiri, I. N.; Maji, S. K., Effect of curcumin analogs onalpha-synuclein aggregation and cytotoxicity. *Scientific reports* **2016,** *6*, 28511.
90. Liu, G.; Gaines, J. C.; Robbins, K. J.; Lazo, N. D., Kinetic profile of amyloid formation in the presence of an aromatic inhibitor by nuclear magnetic resonance. *ACS medicinal chemistry letters* **2012,** *3* (10), 856-9.
91. Nelson, K. M.; Dahlin, J. L.; Bisson, J.; Graham, J.; Pauli, G. F.; Walters, M. A., The Essential Medicinal Chemistry of Curcumin. *Journal of medicinal chemistry* **2017,** *60* (5), 1620-1637.
92. Guerrero-Muñoz, M. J.; Castillo-Carranza, D. L.; Kayed, R., Therapeutic approaches against common structural features of toxic oligomers shared by multiple amyloidogenic proteins. *Biochemical pharmacology* **2014,** *88* (4), 468-478.
93. Nedumpully-Govindan, P.; Kakinen, A.; Pilkington, E. H.; Davis, T. P.; Chun Ke, P.; Ding, F., Stabilizing Off-pathway Oligomers by Polyphenol Nanoassemblies for IAPP Aggregation Inhibition. *Scientific reports* **2016,** *6*, 19463.
94. Ono, K.; Hasegawa, K.; Naiki, H.; Yamada, M., Curcumin has potent anti-amyloidogenic effects for Alzheimer's beta-amyloid fibrils in vitro. *Journal of neuroscience research* **2004,** *75* (6), 742-50.
95. Yang, F.; Lim, G. P.; Begum, A. N.; Ubeda, O. J.; Simmons, M. R.; Ambegaokar, S. S.; Chen, P. P.; Kayed, R.; Glabe, C. G.; Frautschy, S. A.; Cole, G. M., Curcumin inhibits formation of amyloid beta oligomers and fibrils, binds plaques, and reduces amyloid in vivo. *The Journal of biological chemistry* **2005,** *280* (7), 5892-901.
96. Singh, P. K.; Kotia, V.; Ghosh, D.; Mohite, G. M.; Kumar, A.; Maji, S. K., Curcumin Modulates α-Synuclein Aggregation and Toxicity. *ACS Chemical Neuroscience* **2013,** *4* (3), 393-407.
97. Abedini, A.; Raleigh, D. P., A critical assessment of the role of helical intermediates in amyloid formation by natively unfolded proteins and polypeptides. *Protein engineering, design & selection : PEDS* **2009,** *22* (8), 453-9.
98. Hebda, J. A.; Saraogi, I.; Magzoub, M.; Hamilton, A. D.; Miranker, A. D., A peptidomimetic approach to targeting pre-amyloidogenic states in type II diabetes. *Chemistry & biology* **2009,** *16* (9), 943-50.
99. Saraogi, I.; Hebda, J. A.; Becerril, J.; Estroff, L. A.; Miranker, A. D.; Hamilton, A. D., Synthetic α-Helix Mimetics as Agonists and Antagonists of IAPP Amyloid Formation. *Angewandte Chemie (International ed. in English)* **2010,** *49* (4), 736-739.
100. Porat, Y.; Abramowitz, A.; Gazit, E., Inhibition of amyloid fibril formation by polyphenols: structural similarity and aromatic interactions as a common inhibition mechanism. *Chemical biology & drug design* **2006,** *67* (1), 27-37.
101. Gazit, E., A possible role for pi-stacking in the self-assembly of amyloid fibrils. *FASEB journal : official publication of the Federation of American Societies for Experimental Biology* **2002,** *16* (1), 77-83.
102. Bieschke, J.; Russ, J.; Friedrich, R. P.; Ehrnhoefer, D. E.; Wobst, H.; Neugebauer, K.; Wanker, E. E., EGCG remodels mature α-synuclein and amyloid-β fibrils and reduces cellular toxicity. *Proceedings of the National Academy of Sciences of the United States of America* **2010,** *107* (17), 7710-7715.

103. Lopez del Amo, J. M.; Fink, U.; Dasari, M.; Grelle, G.; Wanker, E. E.; Bieschke, J.; Reif, B., Structural properties of EGCG-induced, nontoxic Alzheimer's disease Abeta oligomers. *Journal of molecular biology* **2012,** *421* (4-5), 517-24.
104. Engel, M. F.; vandenAkker, C. C.; Schleeger, M.; Velikov, K. P.; Koenderink, G. H.; Bonn, M., The polyphenol EGCG inhibits amyloid formation less efficiently at phospholipid interfaces than in bulk solution. *Journal of the American Chemical Society* **2012,** *134* (36), 14781-8.
105. Hyung, S. J.; DeToma, A. S.; Brender, J. R.; Lee, S.; Vivekanandan, S.; Kochi, A.; Choi, J. S.; Ramamoorthy, A.; Ruotolo, B. T.; Lim, M. H., Insights into antiamyloidogenic properties of the green tea extract (-)-epigallocatechin-3-gallate toward metal-associated amyloid-beta species. *Proceedings of the National Academy of Sciences of the United States of America* **2013,** *110* (10), 3743-8.
106. Liu, F. F.; Dong, X. Y.; He, L.; Middelberg, A. P.; Sun, Y., Molecular insight into conformational transition of amyloid beta-peptide 42 inhibited by (-)-epigallocatechin-3-gallate probed by molecular simulations. *The journal of physical chemistry. B* **2011,** *115* (41), 11879-87.
107. Mo, Y.; Lei, J.; Sun, Y.; Zhang, Q.; Wei, G., Conformational Ensemble of hIAPP Dimer: Insight into the Molecular Mechanism by which a Green Tea Extract inhibits hIAPP Aggregation. *Scientific reports* **2016,** *6*, 33076.
108. Mazzulli, J. R.; Burbulla, L. F.; Krainc, D.; Ischiropoulos, H., Detection of Free and Protein-Bound ortho-Quinones by Near-Infrared Fluorescence. *Analytical chemistry* **2016,** *88* (4), 2399-405.
109. Li, J.; Zhu, M.; Manning-Bog, A. B.; Di Monte, D. A.; Fink, A. L., Dopamine and L-dopa disaggregate amyloid fibrils: implications for Parkinson's and Alzheimer's disease. *FASEB journal : official publication of the Federation of American Societies for Experimental Biology* **2004,** *18* (9), 962-4.
110. Conway, K. A.; Rochet, J.-C.; Bieganski, R. M.; Lansbury, P. T., Kinetic Stabilization of the α-Synuclein Protofibril by a Dopamine-α-Synuclein Adduct. *Science* **2001,** *294* (5545), 1346-1349.
111. Ramshini, H.; Ebrahim-Habibi, A.; Aryanejad, S.; Rad, A., Effect of Cinnamomum Verum Extract on the Amyloid Formation of Hen Egg-white Lysozyme and Study of its Possible Role in Alzheimer's Disease. *Basic Clin Neurosci* **2015,** *6* (1), 29-37.
112. Peterson, D. W.; George, R. C.; Scaramozzino, F.; LaPointe, N. E.; Anderson, R. A.; Graves, D. J.; Lew, J., Cinnamon extract inhibits tau aggregation associated with Alzheimer's disease in vitro. *Journal of Alzheimer's disease : JAD* **2009,** *17* (3), 585-97.
113. Plascencia-Villa, G.; Ponce, A.; Collingwood, J. F.; Arellano-Jimenez, M. J.; Zhu, X.; Rogers, J. T.; Betancourt, I.; Jose-Yacaman, M.; Perry, G., High-resolution analytical imaging and electron holography of magnetite particles in amyloid cores of Alzheimer's disease. *Scientific reports* **2016,** *6*, 24873.
114. Tiiman, A.; Luo, J.; Wallin, C.; Olsson, L.; Lindgren, J.; Jarvet, J.; Per, R.; Sholts, S. B.; Rahimipour, S.; Abrahams, J. P.; Karlstrom, A. E.; Graslund, A.; Warmlander, S. K., Specific Binding of Cu(II) Ions to Amyloid-Beta Peptides Bound to Aggregation-Inhibiting Molecules or SDS Micelles Creates Complexes that Generate Radical Oxygen Species. *Journal of Alzheimer's disease : JAD* **2016,** *54* (3), 971-982.
115. Tougu, V.; Tiiman, A.; Palumaa, P., Interactions of Zn(II) and Cu(II) ions with Alzheimer's amyloid-beta peptide. Metal ion binding, contribution to fibrillization and toxicity. *Metallomics : integrated biometal science* **2011,** *3* (3), 250-61.

116. Lovell, M. A.; Robertson, J. D.; Teesdale, W. J.; Campbell, J. L.; Markesbery, W. R., Copper, iron and zinc in Alzheimer's disease senile plaques. *Journal of the neurological sciences* **1998,** *158* (1), 47-52.
117. Mold, M.; Ouro-Gnao, L.; Wieckowski, B. M.; Exley, C., Copper prevents amyloid-beta(1-42) from forming amyloid fibrils under near-physiological conditions in vitro. *Sci Rep* **2013,** *3*, 1256.
118. Atwood, C. S.; Moir, R. D.; Huang, X.; Scarpa, R. C.; Bacarra, N. M.; Romano, D. M.; Hartshorn, M. A.; Tanzi, R. E.; Bush, A. I., Dramatic aggregation of Alzheimer abeta by Cu(II) is induced by conditions representing physiological acidosis. *The Journal of biological chemistry* **1998,** *273* (21), 12817-26.
119. Myhre, O.; Utkilen, H.; Duale, N.; Brunborg, G.; Hofer, T., Metal Dyshomeostasis and Inflammation in Alzheimer's and Parkinson's Diseases: Possible Impact of Environmental Exposures. *Oxidative Medicine and Cellular Longevity* **2013,** *2013*, 726954.
120. Xu, Z. X.; Zhang, Q.; Ma, G. L.; Chen, C. H.; He, Y. M.; Xu, L. H.; Zhang, Y.; Zhou, G. R.; Li, Z. H.; Yang, H. J.; Zhou, P., Influence of Aluminium and EGCG on Fibrillation and Aggregation of Human Islet Amyloid Polypeptide. *J Diabetes Res* **2016,** *2016*, 1867059.
121. Baum, L.; Ng, A., Curcumin interaction with copper and iron suggests one possible mechanism of action in Alzheimer's disease animal models. *Journal of Alzheimer's disease : JAD* **2004,** *6* (4), 367-77; discussion 443-9.
122. Kochi, A.; Lee, H. J.; Vithanarachchi, S. M.; Padmini, V.; Allen, M. J.; Lim, M. H., Inhibitory Activity Of Curcumin Derivatives Towards Metal-free And Metal-induced Amyloid-beta Aggregation. *Current Alzheimer research* **2015,** *12* (5), 415-23.
123. Picciano, A. L.; Vaden, T. D., Complexation between Cu(II) and curcumin in the presence of two different segments of amyloid beta. *Biophysical chemistry* **2013,** *184*, 62-7.
124. Zhao, X.-Z.; Jiang, T.; Wang, L.; Yang, H.; Zhang, S.; Zhou, P., Interaction of curcumin with Zn(II) and Cu(II) ions based on experiment and theoretical calculation. *Journal of Molecular Structure* **2010,** *984* (1–3), 316-325.
125. Liu, K.; Gandhi, R.; Chen, J.; Zhang, S., Bivalent ligands targeting multiple pathological factors involved in Alzheimer's disease. *ACS medicinal chemistry letters* **2012,** *3* (11), 942-946.
126. Kurisu, M.; Miyamae, Y.; Murakami, K.; Han, J.; Isoda, H.; Irie, K.; Shigemori, H., Inhibition of Amyloid β Aggregation by Acteoside, a Phenylethanoid Glycoside. *Bioscience, Biotechnology, and Biochemistry* **2013,** *77* (6), 1329-1332.
127. Ladiwala, A. R.; Lin, J. C.; Bale, S. S.; Marcelino-Cruz, A. M.; Bhattacharya, M.; Dordick, J. S.; Tessier, P. M., Resveratrol selectively remodels soluble oligomers and fibrils of amyloid Abeta into off-pathway conformers. *The Journal of biological chemistry* **2010,** *285* (31), 24228-37.
128. Ladiwala, A. R.; Dordick, J. S.; Tessier, P. M., Aromatic small molecules remodel toxic soluble oligomers of amyloid beta through three independent pathways. *The Journal of biological chemistry* **2011,** *286* (5), 3209-18.
129. Andrich, K.; Hegenbart, U.; Kimmich, C.; Kedia, N.; Bergen, H. R., 3rd; Schonland, S.; Wanker, E. E.; Bieschke, J., Aggregation of Full Length Immunoglobulin Light Chains from AL Amyloidosis Patients Is Remodeled by Epigallocatechin-3-gallate. *The Journal of biological chemistry* **2016**.
130. Glabe, C. G., Structural classification of toxic amyloid oligomers. *The Journal of biological chemistry* **2008,** *283* (44), 29639-43.

131. Taniguchi, S.; Suzuki, N.; Masuda, M.; Hisanaga, S.; Iwatsubo, T.; Goedert, M.; Hasegawa, M., Inhibition of heparin-induced tau filament formation by phenothiazines, polyphenols, and porphyrins. *The Journal of biological chemistry* **2005,** *280* (9), 7614-23.
132. Umeda, T.; Ono, K.; Sakai, A.; Yamashita, M.; Mizuguchi, M.; Klein, W. L.; Yamada, M.; Mori, H.; Tomiyama, T., Rifampicin is a candidate preventive medicine against amyloid-beta and tau oligomers. *Brain : a journal of neurology* **2016,** *139* (Pt 5), 1568-86.
133. McLaurin, J.; Kierstead, M. E.; Brown, M. E.; Hawkes, C. A.; Lambermon, M. H.; Phinney, A. L.; Darabie, A. A.; Cousins, J. E.; French, J. E.; Lan, M. F.; Chen, F.; Wong, S. S.; Mount, H. T.; Fraser, P. E.; Westaway, D.; St George-Hyslop, P., Cyclohexanehexol inhibitors of Abeta aggregation prevent and reverse Alzheimer phenotype in a mouse model. *Nature medicine* **2006,** *12* (7), 801-8.
134. Weinreb, O.; Mandel, S.; Youdim, M. B.; Amit, T., Targeting dysregulation of brain iron homeostasis in Parkinson's disease by iron chelators. *Free radical biology & medicine* **2013,** *62*, 52-64.
135. Kristen, A. V.; Lehrke, S.; Buss, S.; Mereles, D.; Steen, H.; Ehlermann, P.; Hardt, S.; Giannitsis, E.; Schreiner, R.; Haberkorn, U.; Schnabel, P. A.; Linke, R. P.; Rocken, C.; Wanker, E. E.; Dengler, T. J.; Altland, K.; Katus, H. A., Green tea halts progression of cardiac transthyretin amyloidosis: an observational report. *Clinical research in cardiology : official journal of the German Cardiac Society* **2012,** *101* (10), 805-13.
136. Diomede, L.; Rigacci, S.; Romeo, M.; Stefani, M.; Salmona, M., Oleuropein aglycone protects transgenic C. elegans strains expressing Abeta42 by reducing plaque load and motor deficit. *PloS one* **2013,** *8* (3), e58893.
137. Regitz, C.; Dussling, L. M.; Wenzel, U., Amyloid-beta (Abeta(1)(-)(4)(2))-induced paralysis in Caenorhabditis elegans is inhibited by the polyphenol quercetin through activation of protein degradation pathways. *Molecular nutrition & food research* **2014,** *58* (10), 1931-40.
138. Karuppagounder, S. S.; Pinto, J. T.; Xu, H.; Chen, H. L.; Beal, M. F.; Gibson, G. E., Dietary supplementation with resveratrol reduces plaque pathology in a transgenic model of Alzheimer's disease. *Neurochemistry international* **2009,** *54* (2), 111-8.
139. Ringman, J. M.; Frautschy, S. A.; Teng, E.; Begum, A. N.; Bardens, J.; Beigi, M.; Gylys, K. H.; Badmaev, V.; Heath, D. D.; Apostolova, L. G.; Porter, V.; Vanek, Z.; Marshall, G. A.; Hellemann, G.; Sugar, C.; Masterman, D. L.; Montine, T. J.; Cummings, J. L.; Cole, G. M., Oral curcumin for Alzheimer's disease: tolerability and efficacy in a 24-week randomized, double blind, placebo-controlled study. *Alzheimer's research & therapy* **2012,** *4* (5), 43.
140. Watkins, R.; Wu, L.; Zhang, C.; Davis, R. M.; Xu, B., Natural product-based nanomedicine: recent advances and issues. *International journal of nanomedicine* **2015,** *10*, 6055-74.
141. Muqbil, I.; Masood, A.; Sarkar, F. H.; Mohammad, R. M.; Azmi, A. S., Progress in nanotechnology based approaches to enhance the potential of chemopreventive agents. *Cancers* **2011,** *3* (1), 428-45.
142. Zhang, L.; Qiu, W.; Crooke, S.; Li, Y.; Abid, A.; Xu, B.; Finn, M. G.; Lin, F., Development of Autologous C5 Vaccine Nanoparticles to Reduce Intravascular Hemolysis in Vivo. *ACS chemical biology* **2017,** *12* (2), 539-547.
143. da Rocha Lindner, G.; Bonfanti Santos, D.; Colle, D.; Gasnhar Moreira, E. L.; Daniel Prediger, R.; Farina, M.; Khalil, N. M.; Mara Mainardes, R., Improved neuroprotective effects of resveratrol-loaded polysorbate 80-coated poly(lactide) nanoparticles in MPTP-induced Parkinsonism. *Nanomedicine (London, England)* **2015,** *10* (7), 1127-38.

144. Kundu, P.; Das, M.; Tripathy, K.; Sahoo, S. K., Delivery of Dual Drug Loaded Lipid Based Nanoparticles across the Blood-Brain Barrier Impart Enhanced Neuroprotection in a Rotenone Induced Mouse Model of Parkinson's Disease. *ACS Chem Neurosci* **2016,** *7* (12), 1658-1670.
145. Prasad, S.; Tyagi, A. K.; Aggarwal, B. B., Recent developments in delivery, bioavailability, absorption and metabolism of curcumin: the golden pigment from golden spice. *Cancer research and treatment : official journal of Korean Cancer Association* **2014,** *46* (1), 2-18.
146. Gupta, S. C.; Patchva, S.; Aggarwal, B. B., Therapeutic roles of curcumin: lessons learned from clinical trials. *The AAPS journal* **2013,** *15* (1), 195-218.
147. Shen, H.; Hu, X.; Szymusiak, M.; Wang, Z. J.; Liu, Y., Orally administered nanocurcumin to attenuate morphine tolerance: comparison between negatively charged PLGA and partially and fully PEGylated nanoparticles. *Molecular pharmaceutics* **2013,** *10* (12), 4546-51.
148. Xie, X.; Tao, Q.; Zou, Y.; Zhang, F.; Guo, M.; Wang, Y.; Wang, H.; Zhou, Q.; Yu, S., PLGA nanoparticles improve the oral bioavailability of curcumin in rats: characterizations and mechanisms. *Journal of agricultural and food chemistry* **2011,** *59* (17), 9280-9.
149. Takahashi, M.; Uechi, S.; Takara, K.; Asikin, Y.; Wada, K., Evaluation of an oral carrier system in rats: bioavailability and antioxidant properties of liposome-encapsulated curcumin. *Journal of agricultural and food chemistry* **2009,** *57* (19), 9141-6.
150. Zhang, L.; Lu, C. T.; Li, W. F.; Cheng, J. G.; Tian, X. Q.; Zhao, Y. Z.; Li, X.; Lv, H. F.; Li, X. K., Physical characterization and cellular uptake of propylene glycol liposomes in vitro. *Drug development and industrial pharmacy* **2012,** *38* (3), 365-71.
151. Lee, T. W.; Boersen, N. A.; Yang, G.; Hui, H. W., Evaluation of different screening methods to understand the dissolution behaviors of amorphous solid dispersions. *Drug development and industrial pharmacy* **2014,** *40* (8), 1072-83.
152. Li, B.; Konecke, S.; Wegiel, L. A.; Taylor, L. S.; Edgar, K. J., Both solubility and chemical stability of curcumin are enhanced by solid dispersion in cellulose derivative matrices. *Carbohydrate polymers* **2013,** *98* (1), 1108-16.
153. Li, B.; Harich, K.; Wegiel, L.; Taylor, L. S.; Edgar, K. J., Stability and solubility enhancement of ellagic acid in cellulose ester solid dispersions. *Carbohydrate polymers* **2013,** *92* (2), 1443-50.
154. Li, B.; Konecke, S.; Harich, K.; Wegiel, L.; Taylor, L. S.; Edgar, K. J., Solid dispersion of quercetin in cellulose derivative matrices influences both solubility and stability. *Carbohydrate polymers* **2013,** *92* (2), 2033-40.
155. Crowe, A.; Huang, W.; Ballatore, C.; Johnson, R. L.; Hogan, A. M.; Huang, R.; Wichterman, J.; McCoy, J.; Huryn, D.; Auld, D. S.; Smith, A. B., 3rd; Inglese, J.; Trojanowski, J. Q.; Austin, C. P.; Brunden, K. R.; Lee, V. M., Identification of aminothienopyridazine inhibitors of tau assembly by quantitative high-throughput screening. *Biochemistry* **2009,** *48* (32), 7732-45.
156. Krotee, P.; Rodriguez, J. A.; Sawaya, M. R.; Cascio, D.; Reyes, F. E.; Shi, D.; Hattne, J.; Nannenga, B. L.; Oskarsson, M. E.; Philipp, S.; Griner, S.; Jiang, L.; Glabe, C. G.; Westermark, G. T.; Gonen, T.; Eisenberg, D. S., Atomic structures of fibrillar segments of hIAPP suggest tightly mated beta-sheets are important for cytotoxicity. *eLife* **2017,** *6*.

Chapter 2: Amylin Amyloid Inhibition by Flavonoid Baicalein: Key Roles of its Vicinal Dihydroxyl Groups of the Catechol Moiety

This chapter is adapted from:

Paul Velander, Ling Wu, Keith Ray, Richard Helm, Bin Xu (2016) *Biochemistry. 55*, 4255-4258.

I acknowledge pleasant and fruitful collaboration with Dr**.** Ling Wu, who developed, performed and analyzed all data sets pertaining to the cell viability assays, and with Drs. Keith Ray and Richard Helm, who developed, executed and analyzed all data sets pertaining to Mass spectrometry assays.

Abstract

Amyloid formation of the 37-residue amylin is involved in the pathogenesis of type 2 diabetes and potentially, diabetes-induced neurological deficits. Numerous flavonoids exhibit inhibitory effects against amylin amyloidosis, but the mechanisms of inhibition remain not fully understood. Screening a library of natural compounds uncovered a potent lead compound, the flavone baicalein. Baicalein inhibits amylin amyloid formation and reduces amylin-induced cytotoxicity. Analog analyses demonstrated, for the first time, key roles of the vicinal hydroxyl groups on the A-ring. We provide mass spectrometric evidence that incubating baicalein and amylin leads to their conjugation, consistent with a Schiff base mechanism.

Introduction

Amylin, also called islet amyloid polypeptide, is a hormone co-expressed and co-secreted with insulin by pancreatic β-cells. Amylin is one of the most amyloidogenic proteins known[1]. Obese and insulin-resistant type 2 diabetes (T2D) patients have increased blood concentrations of amylin due to the compensatory effect of increased insulin secretion. This hyperamylinemic state is associated with the high propensity of human amylin to form amyloids. Toxic amyloid significantly contributes to β-cell death. Indeed, individuals with T2D manifest increased β-cell apoptosis and reduced β-cell mass. Therefore, amylin fibrillation and its deposition in the pancreas are hallmark features of T2D[2]. Recent work has shown that hyperamylinemia also induces toxicity in other organs, including the brain[3]. Clinical studies reported that amylin plaques were observed in the brain of diabetic patients, but not in those of healthy controls, suggesting that amylin may be a new amyloid in the brain[3-5].

Both T2D and Alzheimer's disease are protein amyloidosis diseases, of which currently there are no known cures[6-7]. New therapeutic strategies are urgently needed to decrease the burden of morbidity from these diseases. However, identifying therapeutic inhibitors is difficult, because many protein targets of amyloid assembly are partially folded or intrinsically disordered, which rules out structure-based design. Natural product based amyloid inhibitors have been reported. One proposed amyloidosis disease-modifying therapeutic strategy is amyloid remodeling[7]. For example, EGCG is currently under preclinical trials for different amyloidogenic proteins and a clinical study reported the beneficial effects of green tea and green tea extracts (EGCG is the most abundant catechin in green tea) on the progression of transthyretin cardiac amyloidosis[8]. Several flavanols, EGCG included, have been identified as amylin amyloid inhibitors or remodeling agents[9,10]. However, the mechanisms of how these flavonoids and

polyphenols inhibit amyloid formation and amyloid-induced cytotoxicity are not well understood.

Results/Discussion

We took the approach of screening a library of natural compounds (mostly flavonoids and polyphenols) that are known to have anti-diabetes, anti-inflammation, and neuro-protective functions in Alternative and Complementary Medicine and performed a screening based on thioflavin T (ThT) fluorescence in a 384-well high throughput format. Several strong inhibitors (including EGCG and morin as positive controls) were identified and confirmed. Among those hits, one of the highest-ranking compounds was the flavonoid baicalein (Figure 1A). Baicalein has been reported to have anti-diabetes and anti-inflammatory functions[11,12]. It is also known to be an enzymatic inhibitor against human hypoxygenases [13]. Relevant to protein amyloid, baicalein was reported to reduce the production of β-amyloid by increasing APP processing[14]. It has been shown to inhibit fibrillation of α-synuclein[15].

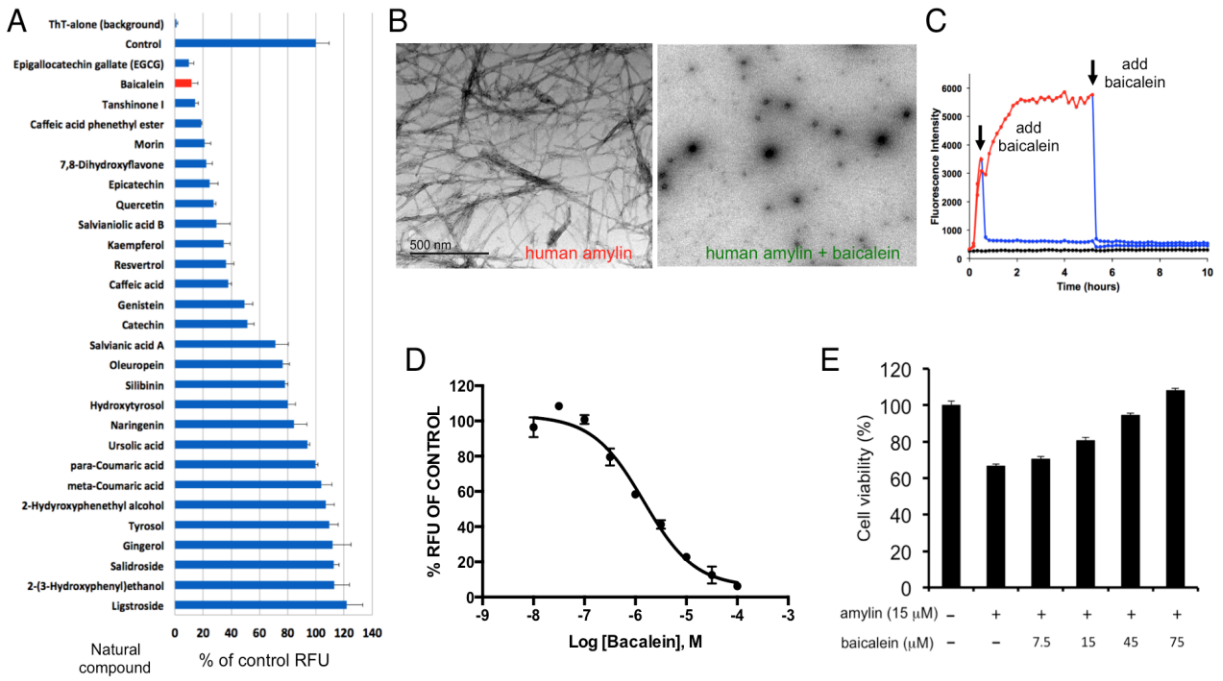

Figure 1. Identification and characterization of flavonoid baicalein in amylin amyloid inhibition. (A) Identification of baicalein (in red) as a potent amylin amyloid inhibitor using a high throughput ThT fluorescence assay. The sample of amylin peptide plus ThT is used as control. All the rest samples were amylin, ThT, and specified compound (molar ratio of amylin: compound is estimated to be 1:3). (B) TEM images of human amylin amyloid and its treatment with baicalein (estimated 1:10 peptide: drug molar ratio). (C) ThT fluorescence assay shows amyloid formation (red traces) and baicalein spiking at designated time points (arrowed) and the resulting rapid disaggregation of the amyloid (blue traces). (D) Amylin-ThT fluorescence inhibition assay with different doses of baicalein. Fluorescence intensity without the drug is used as 100%. (E) Neutralization of amylin-induced cytotoxicity by baicalein in INS-1 β-cells. Amylin concentration was estimated to be 5 μM and molar ratio of amylin to compound is 1:3.

To validate our finding of baicalein as a potent amylin amyloid inhibitor, we performed multiple secondary assays. These orthogonal assays are necessary, partly due to the reported limitations of ThT fluorescence assays in defining amyloidogenicity in some cases[16]. We used transmission electron microscopy to compare fibril formation with and without baicalein treatment. Baicalein treatment (at an estimated molar ratio of 10:1 to amylin) significantly inhibits amylin fibrillation (Figure 1B). Consistently, rapid disaggregation of existing amyloid was observed when we spiked baicalein to the pre-formed amylin amyloid in a ThT fluorescence kinetic assay (Figure 1C). We also performed baicalein dose-dependence analyses and determined that the apparent IC_{50} is estimated to be 1 μM at the condition of 10 μM amylin in 1x DPBS buffer (Figure 1D). Our cell-based functional assay results demonstrated that human amylin has significant cytotoxicity against pancreatic INS-1 β-cells and neuronal line Neuro2A cells (Figure S2). To further test if baicalein can reduce amylin-induced cytotoxicity in cell-based assays, we performed cell viability experiments with different doses of baicalein in the presence of amylin. Baicalein "neutralizes" amylin-induced cytotoxicity in INS-1 beta-cells in a dose-dependent fashion (Figure 1E). Baicalein itself has no effect on cell viability (Figure S3).

To pinpoint which chemical functional groups are important for baicalein's inhibitory functions, we did a systematic structure activity relationship analysis. Many flavonoids and polyphenolic compounds carry catechol structural moieties. From our screen results, we found that majority of the top hits showing amyloid inhibitory effects were catechol-containing compounds (Figures 1A & S1). We therefore hypothesized that the catechol groups or the hydroxyl groups in the catechol (or catechol-like) groups

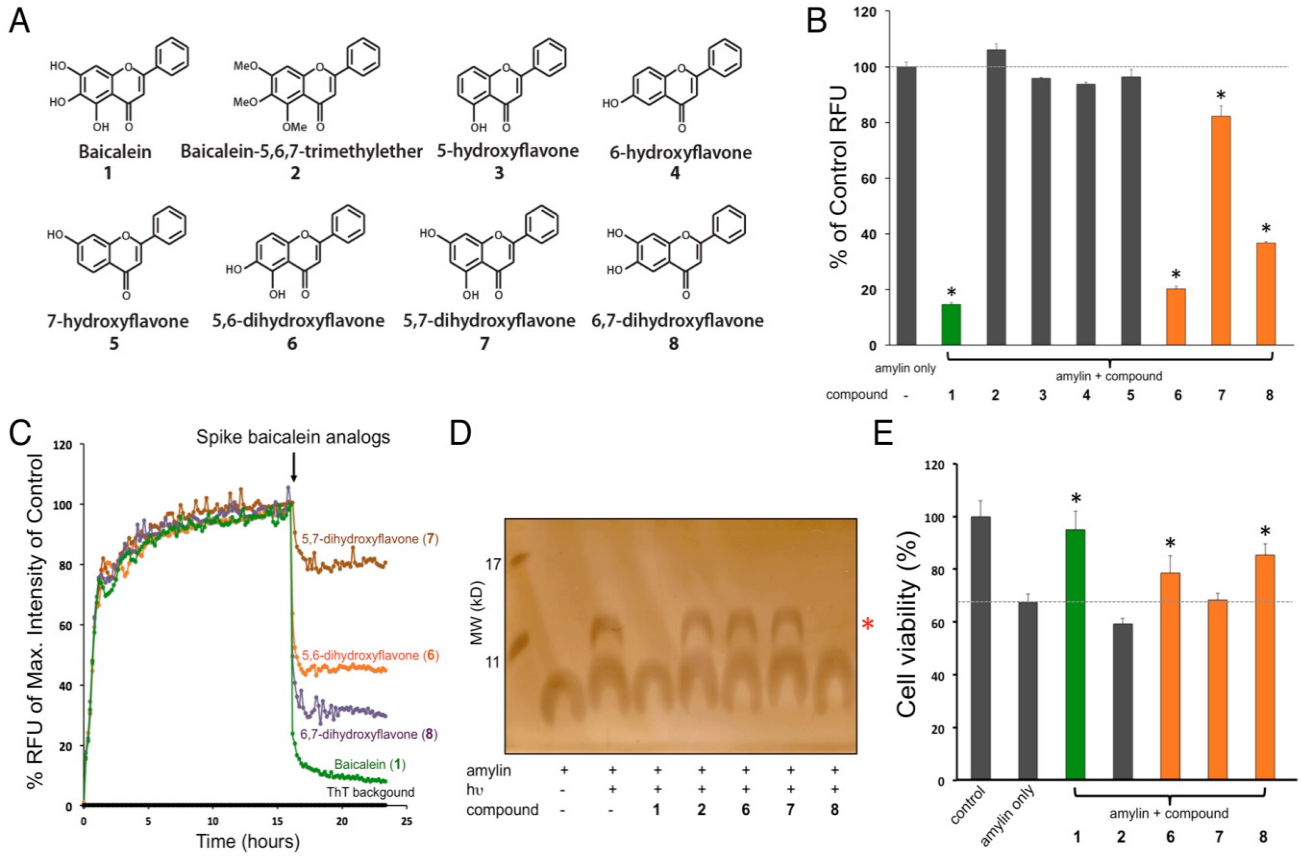

Figure 2. Structural activity relationship analyses of baicalein and its analogs. (A) Chemical structures of baicalein and selected baicalein analogs are shown. (B) ThT fluorescence assay was used to quantify inhibition of amylin amyloid formation by baicalein and its analogs. Compounds with significant amyloid inhibition are shown with asterisk symbols. (C) ThT fluorescence-based assay shows amyloid formation (traces before the black arrow) and baicalein analog spiking at specified time point (black arrowed) and the resulting complete, partial, or no disaggregation of the amyloid. Bold numbers in the parentheses correspond to the analogs in panel A. (D) Photo-induced cross-linking of unmodified protein (PICUP) analysis of amylin oligomer formation with and without treatment of designated baicalein analogs. Cross-linked dimer position is marked with the red asterisk symbol. *(continued next page)*

(E) Neutralization of amylin-induced cytotoxicity by baicalein analogs in INS-1 β-cells. Amylin concentration was 5 μM and the molar ratio of amylin to compound is 1:3 in the treatments. Analogs that significantly reduce amylin amyloid cytotoxicity are shown with asterisk symbols.

play important roles in inhibition. To dissect the roles of the three hydroxyl groups on baicalein A-ring, we systematically compared the functions of baicalein and its analogs that are varied at these hydroxyl positions (positions 5, 6, and 7 in the A ring; Figure 2A). Analogs include single hydroxyl groups in these positions (compounds **3**, **4**, and **5**), dual hydroxyl groups in these positions (compounds **6**, **7**, and **8**), and methoxy groups replacing hydroxyl groups in these positions (compound **2**). From the ThT fluorescence assay, we found that all analogs with single hydroxyl groups in these three positions were inactive, suggesting that more than one hydroxyl group is required for inhibition. Replacing all hydroxyl groups with methoxy groups also yielded an inactive compound, suggesting the hydroxyl groups may be involved in interaction with amylin. We observed that 5,6-dihydroxyflavone (5,6-DHF) and 6,7-dihydroxyflavone (6,7-DHF) retained most of baicalein's inhibitory activity, but 5,7-dihydroxyflavone (5,7-DHF) lost most of its activity (Figure 2B). We further tested the functions of selected baicalein analogs by spiking them into solutions containing pre-formed amylin amyloid (Figure 2C). Both 5,6-DHF and 6,7-DHF showed significant amyloid inhibition functions. Oligomer formation is the intermediate step in forming mature fibrils and oligomers are thought to be more cytotoxic than fibrils (2). We found 6,7-DHF strongly disrupted oligomer (dimer) formation in an *in vitro* PICUP assay (Figure 2D). Possibly due to the low solubility of 5,6-DHF in the PICUP assay condition, it is unclear if 5,6-DHF inhibits dimer formation. Most importantly, cell-based assays demonstrated significant neutralization functions of 5,6-DHF and 6,7-DHF, but little activity for 5,7-DHF, and no activity for baicalein-5,6,7-methoxyflavone (Figure 2E). Additional collaborating evidence comes from 7,8-dihydroxyflavone: it also displayed strong inhibitory effects (Figure 1A) and reduced amylin amyloid-induced cytotoxicity (data not shown). Together, these multiple lines of data demonstrated, for the first time to our knowledge, the key functional roles of the vicinal

hydroxyl groups in the baicalein A-ring.

To probe the interaction between baicalein and amylin, we performed mass spectrometric analyses of their incubation mixtures. Our liquid chromatography-mass spectrometry (LC-MS) results demonstrated the formation of baicalein-amylin covalent adduct(s) (Figures 3A, 3B, & S4). The mass spectrometric data of the adduct(s) were consistent with a Schiff base mechanism with *o*-quinone as an intermediate (Figure 3C). Schiff base conjugation is either through Lys^{1} and/or Arg^{11} residues. Similar conjugation reactions were reported in the case of α-synuclein aggregation inhibition by baicalein and in the case of inhibition of Aβ42 aggregation by taxifolin, also a catechol-type flavonoid (15,17). We propose catechol-like flavonoids, such as baicalein, can be autoxidized to quinone intermediates and *o*-quinones will conjugate with amines in the peptide via a Schiff base mechanism (Figure 3C). The proposed mechanism explains why the vicinal hydroxyl groups (but not 5,7-DHF) are so critical, because they can readily transition into *o*-quinone intermediates to form adducts with the peptide. Our results, however, do not rule out potential non-covalent interactions between these natural compounds and amylin as additional mechanisms of inhibition. Non-covalent interactions (such as hydrophobic interactions) between inhibitory natural compounds and amyloidogenic proteins have been suggested in the literature (18,19).

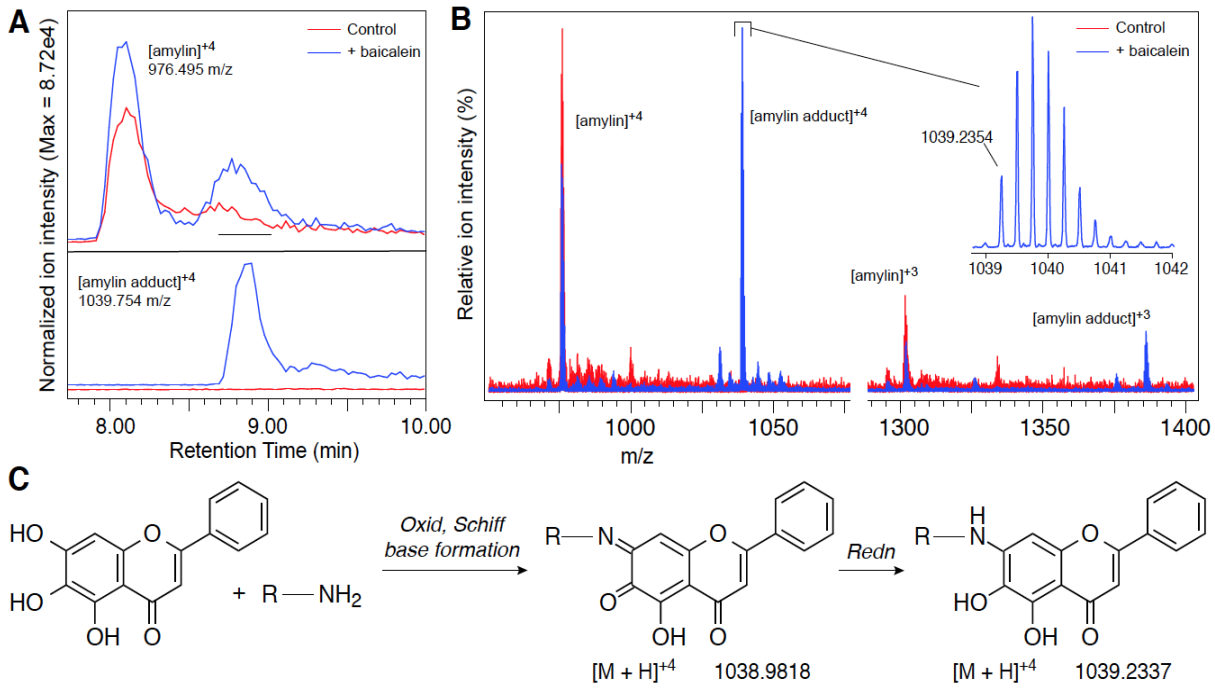

Figure 3. Mass spectrometric evidence of baicalein-amylin conjugation and a proposed mechanism for the conjugation. (A) Liquid chromatography-mass spectrometry analysis of amylin in the presence and absence of baicalein showing the elution time for amylin and its adduct. Amylin (15 μM) in 1X Dulbecco's phosphate buffer containing 2.25% DMSO (v/v) was incubated for 4 days in the presence and absence of baicalein at a molar ratio of 1:10 (amylin: compound). The upper panel shows the extracted ion chromatograms for the m/z of the most intense ion of unmodified amylin and the lower panel shows the m/z for a product with mass corresponding to a Schiff base adduct of baicalein-amylin conjugate. Human amylin has an average mass of 3903.3 Dalton. (B) Mass spectrometric m/z profile of baicalein-amylin reaction product indicated by the black bar in (A). The regions shown correspond to the $[M + 3H]^{+3}$ and $[M + 4H]^{+4}$ for both unreacted and conjugated compounds. The inset shows the isotope distribution for the baicalein-amylin adduct, which best matches a reduced structure. (C) Proposed mechanisms for the conjugation of catechol-containing compounds to amylin along with their theoretical monoisotopic masses.

Conclusions

In summary, our work identifies baicalein as a potent inhibitor against amylin amyloid. Using an analytical approach, we compared a list of selected baicalein analogs. We identified that the vicinal hydroxyl groups in the catechol-like structural moiety in baicalein played vital roles in amyloid inhibition. We provided mass spectrometric evidence that baicalein interacts with amylin to form covalent adduct(s) as a potential mechanism of amyloid inhibition. Whether such covalent modification of an amyloidogenic protein or alternative non-covalent interactions is the main driving force of inhibition merits further investigation.

Material and Methods

Peptides and Other Reagents. Synthetic human amylin was purchased from AnaSpec (Fremont, CA), GenScript Inc. (Piscataway, NJ), or EMD Millipore (Billerica, MA). Amylin stocks were quantified by Pierce BCA protein assay kit (Thermo Fisher Scientific (Waltham, MA). Dimethyl sulfoxide (DMSO) was purchased from Fisher Scientific (Pittsburg, PA). Hexafluoro isopropanol (HFIP) and thioflavin T (ThT) were purchased from Sigma Aldrich (St. Louis, MO). Baicalein and its analogs were purchased from Indofine Chemical Company (Hillsborough, NJ). Additional natural compounds were purchased from Sigma Aldrich and Cayman Chemical Company (Ann Arbor, MI). Dulbecco's phosphate buffer saline (DBPS) was purchased from Lonza, (Walkersville, MD). 200 mesh Formvar-carbon coated copper grids were purchased from Electron Microscopy Sciences (Hatfield, PA). All solvents used for liquid chromatography-mass spectrometry were LC-MS grade.

Peptide and Natural Compound Preparation. 0.5 mg lyophilized human amylin powder was initially dissolved in 100% HFIP at a final concentration of 1-2 mM. After 2 hours of incubation at room temperature, the solution was lyophilized and re-dissolved in 100% DMSO to a final concentration of 1-2 mM. The additional lyophilizing step is employed to eliminate traces of organic solvents present in the synthetic peptide. The latter may affect amylin aggregation. Aliquots were either lyophilized again prior to use for cell-based assays or dissolved directly into DPBS, 10 mM phosphate buffer pH 7.4 or 20 mM Tris-HCl pH 7.4 for all *in vitro* assays. All remaining 1-2 mM stocks in 100% DMSO were stored at -80 °C until later use. Natural compounds and ThT (Sigma Aldrich) were dissolved in DMSO (10 mM) and distilled water (1 mM), respectively. These stocks were stored at -20 °C until later use. Residual DMSO present in the final concentrations used for all *in vitro* assays ranged from 0-5.4%. We determined that

these DMSO concentrations had negligible effects on amylin amyloid formation as reflected by ThT fluorescence, TEM, or PICUS assays.

Thioflavin T Fluorescence Assay. Fluorescence experiments were performed using a SpectraMax M5 plate reader. All kinetic reads were taken at 25 °C in low-binding all black clear bottom Greiner 96 (or 384-well) plates covered with optically clear films and shook for 10 seconds prior to each reading. ThT fluorescence was measured with excitation wavelength at 444 nm and emission wavelength at 482 nm. Each kinetic assay consisted of final concentrations of 5-30 μM amylin and optimal concentrations of ThT (typical molar ratio of amylin: ThT is 3:1). The apparent inhibition constant (IC_{50}) values for dose response curves were estimated by multi-parameter logistic nonlinear regression analysis. All experiments were repeated at least three times.

Transmission Electron Microscopy (TEM). 15-30 μM amylin (20 mM Tris-HCl, 2 % DMSO, pH 7.4) in the presence of a natural compound or vehicle control were incubated for ≥48 hours at 37 °C with agitation (optimum signal at 60-72 hours). Prior to imaging analyses, 3 μL of sample were blotted on a 200-mesh formvar-carbon coated grid for 5 minutes, and stained with uranyl acetate (1%). Both the sample and the stain solutions were wicked dry (sample dried before addition of stain) by filter paper. Prior to taking representative images (obtained by a JEOL 1400 operated at 120 kV, a qualitative assessment of the number of fibrils or oligomers observed were made by scanning each grid quadrant for deposited material. The range of final DMSO concentration (0-3.3%) that we used had negligible effects on fiber formation.

Photo Induced Crosslinking of Unmodified Proteins (PICUP). Amylin aliquots from a master mix in 10 mM phosphate buffer, pH 7.4 were added separately to 0.6 ml eppendorf tubes

containing small molecule inhibitors or DMSO vehicle loaded controls. Crosslinking for each tube was subsequently initiated by adding tris(bipyridyl)Ru(II) complex (RuBpy) and ammonium persulfate (APS) (Amylin: RuBpy: APS ratios were fixed at 1:2:20, respectively), followed by exposure to visible light, emitted from a 150-Watt incandescent light bulb, from 5 cm and for a duration of 5 seconds. The reaction was quenched by addition of SDS sample buffer. PICUP was visualized by SDS-PAGE (16% acrylamide gels containing 6 M urea), followed by silver staining. Final concentrations for all PICUP reactions included 30 μM amylin, with addition of 150 μM of inhibitors. All samples, treated and untreated with specified compounds, contained equal percentage of DMSO for normalization. DMSO content in the reaction, ranging between 0-5.4%, had negligible effects on the results.

Cell Culture and Cell Viability Assays. Cell culture: rat pancreatic INS-1 cells and mouse neuroblastoma Neuro-2A cells are cultured per vendor's instructions. An MTT-based cell viability assay was used. The INS-1 cells or Neuro-2A cells were seeded in 96-well plate at a density of $4x10^4$ cells/well. After 24 hours incubation, cells are treated with either human amylin, with or without specified natural compounds. Following another 24 hours incubation, 0.9 mM MTT is added to each well. The reduced insoluble MTT formazan product is then dissolved in SDS-HCl lysis buffer (5 mM HCl, 5% SDS) at 37 °C. Cell viability is determined by measurement of absorbance change at 570 nm using a spectrometric plate reader. Peptides dissolving buffer treated cells were used as positive control and taken as 100%, and 0.5% Triton X-100 treated cells at the start of the incubation period with test peptides are used as negative control and taken as 0%.

MALDI-TOF/TOF Mass Spectrometry. Analyses were performed on an ABSciex 4800 MALDI-TOF/TOF operating in linear positive ion mode using α-cyano-4-hydroxycinnamic acid (4

mg/ml in 50:50 water: acetonitrile supplemented with 0.1% (v/v) trifluoracetic acid and 10 mM ammonium chloride) as the matrix.

Liquid Chromatography-Mass Spectrometry. Amylin (15 μM) in 1X Dulbecco's phosphate buffer containing 2.25% DMSO (v/v) was incubated for 4 days in the presence and absence of baicalein at a molar ratio of 1:10 (amylin: compound). Peptide solutions were separated using an Acquity UPLC I-class system (Waters, Milford, MA). Mobile phases were 0.1% (v/v) formic acid in water (solvent A) and 0.1% (v/v) formic acid in acetonitrile (solvent B). The separation was performed using a CSH130 C_{18} 1.7 μm, 1.0 x 150 mm column (Waters, Milford, MA) at 50 μL/min using and a 13-minute gradient from 3-90% solvent B with the column temperature maintained at 45°C. Analysis utilized a Synapt G2-S mass spectrometer (Waters, Milford, MA) operated in continuum positive ion "resolution" MS mode using an $HDMS^E$ acquisition method (high-definition mass spectrometry with alternating scans utilizing low and elevated collision energies with ion mobility separation (IMS) of peptides prior to fragmentation). Both low energy (4 V and 2 V in the trap and transfer region, respectively) and elevated energy (4 V in the trap and ramped from 20 to 50 V in the transfer region) scans were 1.2 seconds each covering the m/z range of 50 to 1800. For ion mobility separation, the IMS and transfer wave velocities were 600 and 1200 m/sec, respectively. Wave height within the ion mobility cell was ramped from 10 to 40 V. For lock-mass correction, a 1.2 second low energy scan was acquired every 30 seconds of a 100 fmol/μL [Glu1]-fibrinopeptide B (Waters, Milford, MA) solution (50:50 acetonitrile: water supplemented with 0.1% (v/v) formic acid) infused at 10 μL/min introduced into the mass spectrometer via a different source also utilizing a capillary voltage of 3 kV.

Statistical Analyses. All data are presented as the mean ± S.E.M. and the differences were analyzed with an one-way ANOVA analyses for amylin kinetics as implemented within

GraphPad Prism software (version 6.0) or with unpaired Student's *t* test in analyzing the significance in cell viability changes. p values < 0.05 were considered statistically significant.

Supplemental Figures

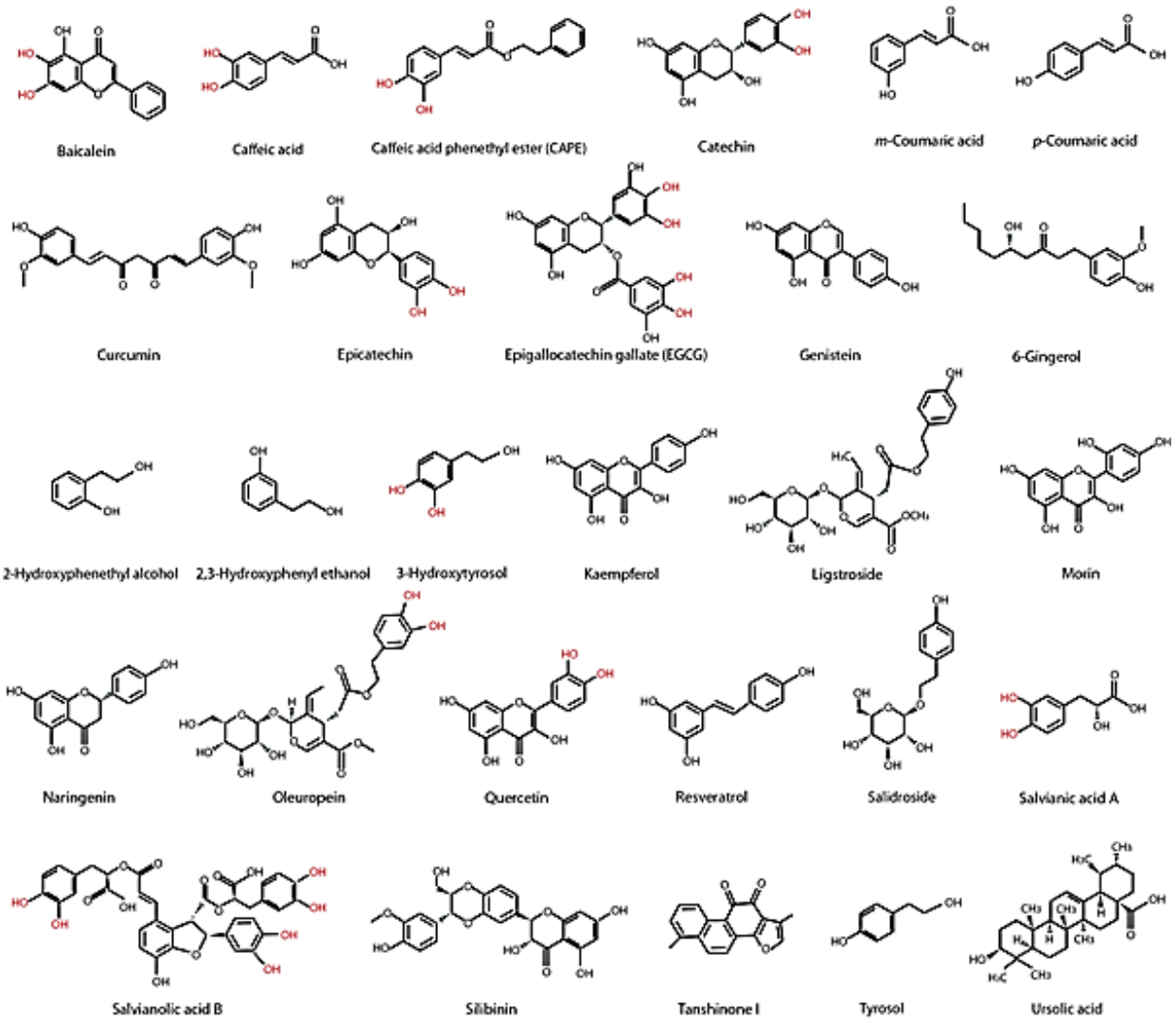

Figure S1. Chemical structures of the targeted set of natural compounds that have been tested in this work (corresponding to compounds listed in Figure 1A). Vicinal dihydroxyl groups of the catechol moieties are highlighted in red.

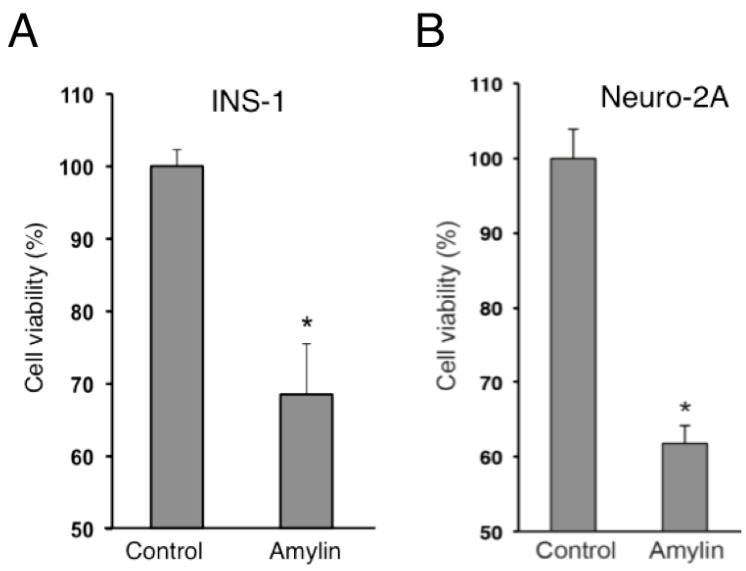

Figure S2. Cytotoxicity assays demonstrated the toxic effects of human amylin against INS-1 pancreatic β-cells (panel A) and Neuro-2A neuronal cells (panel B), each at 5 μM concentration. * Symbols indicate significantly reduced cell viability with amylin treatments in comparison with controls.

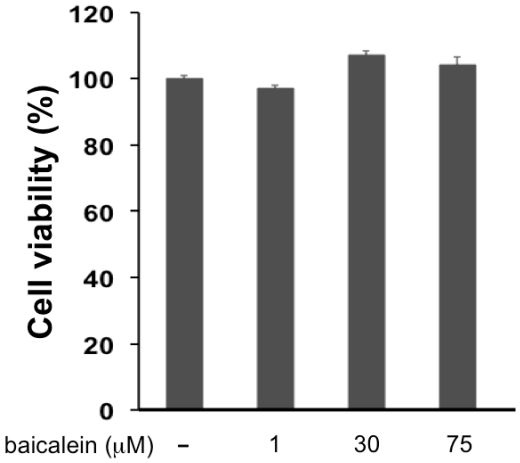

Figure S3. Cell viability assay demonstrates that baicalein itself has no significant effects to INS-1 cell viability at the concentrations from 1-75 μM.

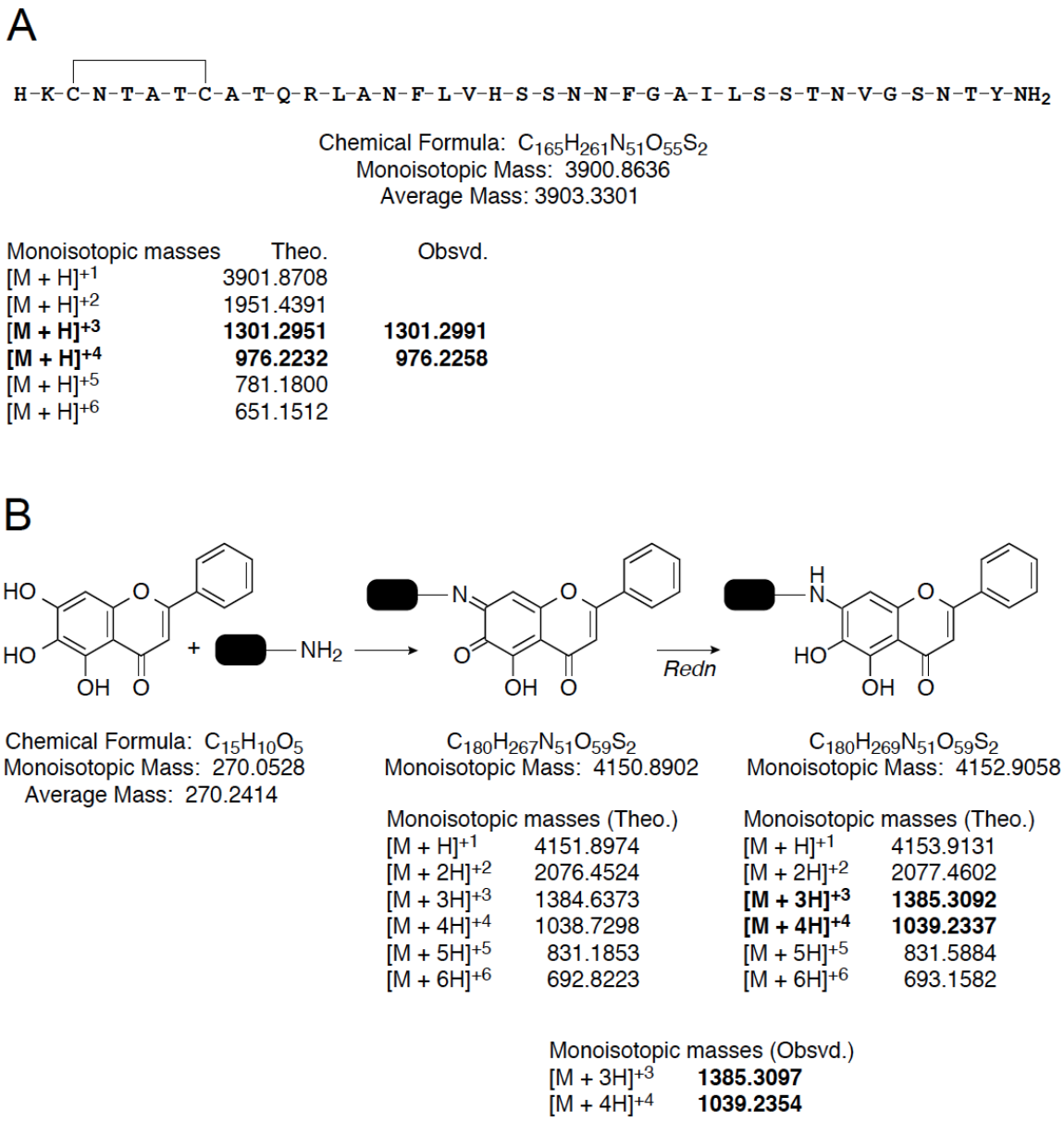

Figure S4. Mass information about the human amylin peptide and baicalein-amylin conjugated products. (A) Amino acid sequence of human amylin is shown. Theoretically calculated and observed monoisotopic masses are shown side by side in comparison. (B) Proposed mechanisms for the conjugation of baicalein to amylin (via oxidative Schiff based formation). Theoretically calculated and experimentally observed monoisotopic masses are shown side by side in comparison. The amylin peptides are schematically shown as filled black blocks.

References

1. Abedini, A., Schmidt, A.M. Mechanisms of islet amyloidosis toxicity in type 2 diabetes**.** *FEBS Lett.* **(2013)** 587, 1119-1127.
2. Westermark, P., Andersson, A., Westermark, G.T. Islet amyloid polypeptide, islet amyloid, and diabetes mellitus **(2011)** *Physiol. Rev.* 91, 795-826.
3. Jackson, K., Barisone, G.A., Diaz, E., Jin, L.W., DeCarli, C., Despa, F. Amylin deposition in the brain: A second amyloid in Alzheimer disease? **(2013)** *Ann. Neurol.* 74, 517-526.
4. Despa, F., DeCarli, C. Amylin: What might be its role in alzheimer's disease and how could this affect therapy **(2013)** *Expert Rev. Proteomics.* 10, 403-405.
5. Fawver, J.N., Ghiwot, Y., Koola, C., Carrera, W., Rodriguez-Rivera, J., Hernandez, C., Dineley, K.T., Kong, Y., Li, J., Jhamandas, J., Perry, G., Murray, I.V. Islet amyloid polypeptide (IAPP): a second amyloid in Alzheimer's disease. **(2014)** *Curr. Alzheimer Res.* 11, 928-940.
6. Arosio, P., Vendruscolo, M., Dobson, C. M., Knowles, T. P. Chemical kinetics for drug discovery to combat protein aggregation diseases. **(2014)** *Trends Pharmacol. Sci.* 35, 127-135.
7. Eisele, Y. S., Monteiro, C., Fearns, C., Encalada, S. E., Wiseman, R. L., Powers, E. T., Kelly, J. W. Targeting protein aggregation for the treatment of degenerative diseases. **(2015)** *Nat. Rev. Drug Discov.* 14, 759-780.
8. Kristen, A. V., Lehrke, S., Buss, S., Mereles, D., Steen, H., Ehlermann, P., Hardt, S., Giannitsis, E., Schreiner, R., Haberkorn, U., Schnabel, P. A., Linke, R. P., Rocken, C., Wanker, E. E., Dengler, T. J., Altland, K., Katus, H. A. Green tea halts progression of cardiac transthyretin amyloidosis: an observational report. **(2012)** *Clin. Res. Cardiol.* 101, 805-813.
9. Meng, F., Abedini, A., Plesner, A., Verchere, C. B., Raleigh, D. P. The flavanol (-)-epigallocatechin 3-gallate inhibits amyloid formation by islet amyloid polypeptide, disaggregates amyloid fibrils, and protects cultured cells against IAPP-induced toxicity. **(2010)** *Biochemistry*. 49, 8127-8133.
10. Cao, P., Raleigh D. P. Analysis of the Inhibition and Remodeling of Islet Amyloid Polypeptide Amyloid Fibers by Flavanols **(2012)** *Biochemistry*. 51, 2670-2683.
11. Fu, Y., Luo, J., Jia, Z., Zhen, W., Zhou, K., Gilbert, E., Liu, D. Baicalein Protects against Type 2 Diabetes via Promoting Islet β-Cell Function in Obese Diabetic Mice. **(2014)** *Int. J. Endocrinol. 2014,* 846742.
12. Hsieh, C. J., Hall, K., Ha, T., Li, C., Krishnaswamy, G., Chi, D. S. Baicalein inhibits IL-1beta- and TNF-alpha-induced inflammatory cytokine production from human mast cells via regulation of the NF-kappaB pathway. **(2007)** *Clin. Mol. Allergy.* 5, 5.
13. Deschamps, J. D., Kenyon, V. A., Holman, T. R. **(2006)** *Bioorg. Med. Chem.* 14, 4295-4301.
14. Zhang, S. Q., Obregon, D., Ehrhart, J., Deng, J., Tian, J., Hou, H., Giunta, B., Sawmiller, D., Tan, J. Baicalein reduces β-amyloid and promotes nonamyloidogenic amyloid precursor protein processing in an Alzheimer's disease transgenic mouse model. **(2013)** *J. Neurosci. Res.* 91, 1239-1246.
15. Zhu, M., Rajamani, S., Kaylor, J., Han, S., Zhou, F., Fink, A. L. The flavonoid baicalein inhibits fibrillation of alpha-synuclein and disaggregates existing fibrils. **(2004)** *J. Biol. Chem.* 279, 26846-26857.
16. Wong, A. G., Wu, C., Hannaberry, E., Watson, M. D., Shea, J. E., Raleigh, D. P. Analysis of the Amyloidogenic Potential of Pufferfish (Takifugu rubripes) Islet Amyloid

Polypeptide Highlights the Limitations of Thioflavin-T Assays and the Difficulties in Defining Amyloidogenicity. **(2016)** *Biochemistry.* 55, 510-518.
17. Sato, M., Murakami, K., Uno, M., Nakagawa, Y., Katayama, S., Akagi, K., Masuda, Y., Takegoshi, K., Irie, K. Site-specific inhibitory mechanism for amyloid β42 aggregation by catechol-type flavonoids targeting the Lys residues. **(2013)** *J. Biol. Chem.* 288, 23212-23224.
18. Tu, L. H., Young, L. M., Wong, A. G., Ashcroft, A. E., Radford, S. E., Raleigh, D. P. Mutational analysis of the ability of resveratrol to inhibit amyloid formation by islet amyloid polypeptide: critical evaluation of the importance of aromatic-inhibitor and histidine-inhibitor interactions. **(2015)** *Biochemistry.* 54, 666-676.
19. Palhano, F. L., Lee, J., Grimster, N. P., Kelly, J. W. Toward the molecular mechanism(s) by which EGCG treatment remodels mature amyloid fibrils. **(2013)** *J. Am. Chem. Soc.* 135, 7503-7510.

Chapter 3: Olive component oleuropein promotes β-cell insulin secretion and protects β-cells from amylin amyloid induced cytotoxicity

This chapter is adapted from:

Ling Wu, Paul Velander, Dongmin Liu, Bin Xu. (2017) *Biochemistry. 56* (38), 5035-5039.

I acknowledge pleasant and fruitful collaboration with Dr. Ling Wu, who developed, executed and analyzed all data pertaining to cell based assays including the novel GSIS activities of oleuropein.

Abstract

Oleuropein, a natural product derived from olive leaves, has reported anti-diabetic functions. However, detailed molecular mechanisms on how it affects β-cell functions remain poorly understood. Here, we present evidence that oleuropein promotes glucose-stimulated insulin secretion (GSIS) in β-cells. The effect is dose-dependent, and it stimulates ERK/MAPK signaling pathway. We further demonstrated that oleuropein inhibits the cytotoxicity induced by amylin amyloids, a hallmark feature of type 2 diabetes. We demonstrated that these dual functions are structure-specific: we identified 3-hydroxytyrosol moiety of oleuropein as the main functional entity responsible for amyloid inhibition, but the novel GSIS function requires the entire structure scaffold of the molecule.

Introduction

Natural products derived from olive fruits, olive oil, and olive leaves have received widespread attention for their potential benefits to prevent several currently prevalent chronic human diseases, including type 2 diabetes (T2D)[1]. Oleuropein is a phenolic compound that is mainly found in olive leaves and fruits. This compound, as well as other olive-derived compounds such as ligstroside, are tyrosol esters of elenolic acid that are further hydroxylated and glycosylated (Figure 1A). Oleuropein has been reported to have beneficial anti-diabetic functions such as reduction of glycemia and enhanced glucose tolerance in diabetic animal models[2-3]. Oleuropein-containing olive leaf extract has been shown to promote insulin sensitivity and glucose tolerance in overweighed humans[4]. However, the mechanisms by which oleuropein contributes to these anti-diabetic functions and whether any structure moiety of oleuropein is responsible for such beneficial effects are not well understood. Oleuropein has also been reported to prevent cytotoxic amyloid aggregation of human amylin, Aβ42, and transthyretin, which links to T2D, neurodegeneration, or cardiovascular diseases[5-7]. However, it is not known if oleuropein's amyloid inhibition properties are structure specific, as very few studies on structure-function relationship have been investigated in this context. A recent study reported that polyphenolic glycosides and aglycones may utilize different pathways to selectively remodel and inactivate toxic Aβ oligomers[8].

Results/Discussion

We identified oleuropein from screening a library of natural compounds (mostly flavonoids and polyphenols) that are known to have anti-diabetic functions in Complementary Medicine based on a thioflavin T (ThT) fluorescence assay[9]. Several strong inhibitors (including EGCG control) were identified and confirmed. Among these hits, one that has been described to have multiple beneficial functions in health was oleuropein, an olive component[2,3,10] (Figure 1A).

Because oleuropein has the potential to activate G-protein-coupled estrogen receptor GPER/GPR30[11,12] we hypothesized that oleuropein may have biological functions similar to genistein because phytoestrogen genistein is a known GPER/GPR30 agonist and can induce significant anti-diabetic effects[13]. One prominent biological function of genistein is its anti-diabetic glucose-stimulated insulin secretion (GSIS). We therefore investigated oleuropein's insulin secretion function in INS-1 β-cells and further validated it with specific signaling pathway analyses.

Oleuropein has also been reported to prevent cytotoxic amyloid aggregation of human amylin[5]. But detailed structure activity dissection of the molecule has not been investigated. Oleuropein has three parts to its structure – 3-hydroxytyrosol (3-HT), elenolic acid (EA), and glucose (Figure 1A). To pinpoint which part(s) of the molecule is responsible for its anti-aggregation effects, we took an analytical approach using structural analogs of oleuropein.

Health benefits of olives and its associated natural products have long been recognized, as seen in the Mediterranean diet, but compound-specific effects and mechanisms related to their biomedical and nutritional values are just beginning to be unraveled in recent years[1,4-6,14,15]. Our mechanistic studies will therefore contribute to the better understanding of those potential "nutraceuticals" for prevention of epidemic aging and metabolic syndromes.

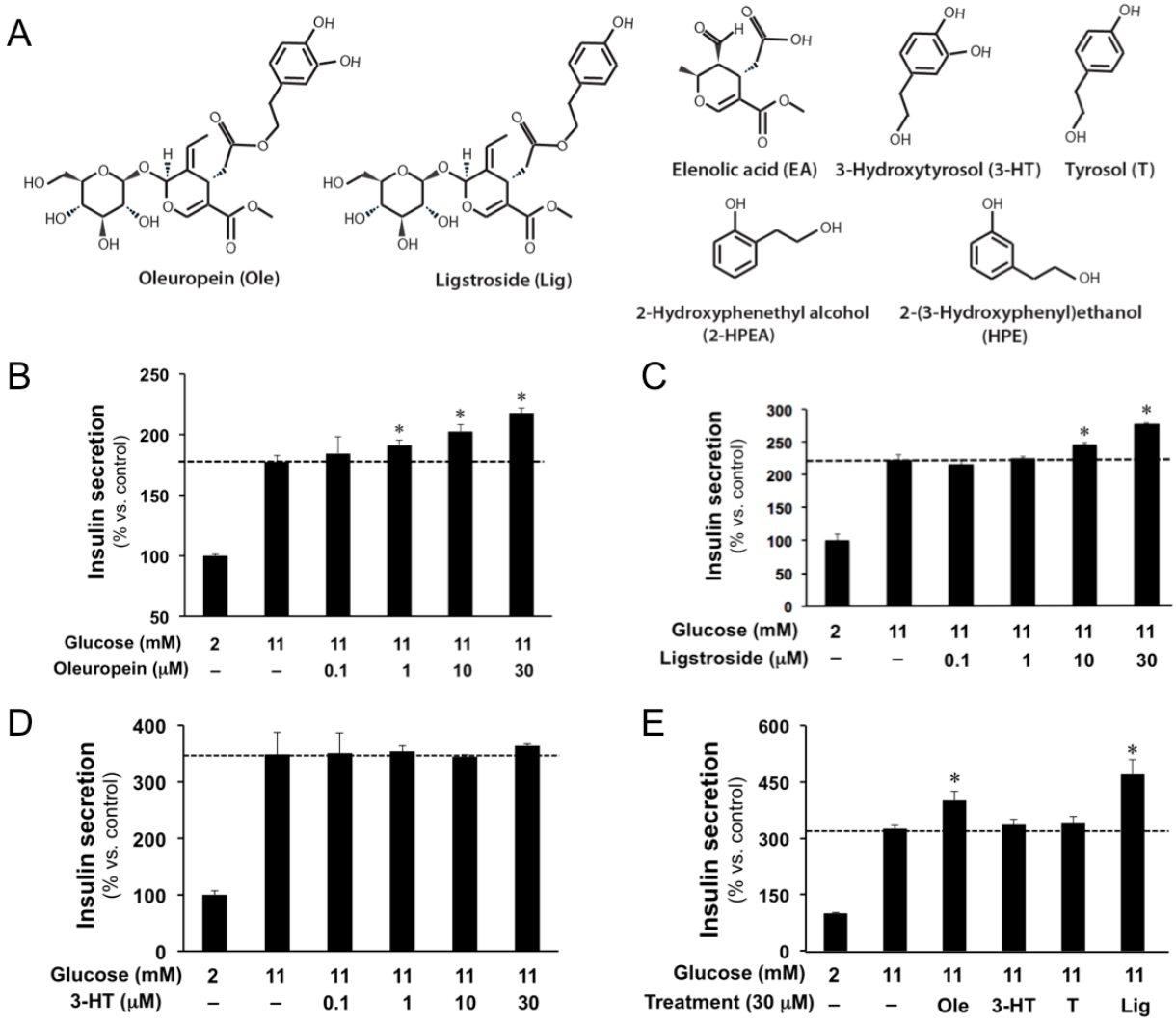

Figure 1. Oleuropein and its analog ligstroside, but not 3-hydroxytyrosol or tyrosol, promote glucose-stimulated insulin secretion in INS-1 β-cells. (A) Chemical structures of oleuropein and its analogs. (B-E) Dose-dependent GSIS effects of oleuropein and its analog, ligstroside, in promoting GSIS in INS-1 β-cells, where 3-hydroxytyrosol serves as a negative control. Effects that are statistically significant with respect to 11 mM glucose controls are indicated with asterisks. Comparative analyses of GSIS effects in INS-1 β-cells with the different compounds are shown in panel E.

To investigate oleuropein and its analogs' potential GSIS function, we tested them in INS-1 β-cells followed by ELISA measurements of secreted insulin concentrations. We observed modest, yet significant elevations of insulin secretion with increasing doses of oleuropein in the treatment starting at low μM ranges. Increases of 10-20% in insulin secretion were observed at the concentration of 30 μM (Figure 1B). The potency of oleuropein is comparable to the natural compound genistein by percent of increase in insulin secretion[13]. In this assay, glucagon-like peptide 1 (GLP-1), a potent GSIS agonist, was used as a positive control (Figure S1). We further tested structural analogs of oleuropein. We found that oleuropein's close analog, ligstroside, retains GSIS function with similar potency to that of oleuropein (Figures 1C & 1E), but 3-HT, a component of oleuropein's structure, and its related analog tyrosol, have no effects on stimulating insulin secretion (Figures 1D & 1E). Elenolic acid, another structural component of oleuropein, showed no GSIS activity (data no shown). These results suggest that the main structure scaffold of oleuropein is required for this novel metabolic effect and 3-hydroxyl group on the 3-HT component is not critical for oleuropein's GSIS function.

To further validate and gain mechanistic insights into oleuropein's GSIS effect, we performed cell-signaling analyses in INS-1 β-cells. Based on the cell signaling activation used by other ligands (such as genistein and GLP-1) that induce GSIS effects in β-cells,[13,16] we used a standard pharmacological inhibitor approach. We tested the involvement of major kinase pathways that are related to metabolism: protein kinase A (PKA), protein kinase C (PKC), ERK/MAPK, PI3 kinase, and the AMP-activated kinase (AMPK)[13,16,17]. The inhibitors we used were KT-5702 (PKA), H-89 (PKA), Ro-318220 (PKC), LY-294002 (PI3K), Compound C

(AMPK), and PD98059 (ERK/MAPK). Except for the ERK/MAPK pathway showing strong activation (Figure 2), we did not observe significant activation by other pathways (data not shown). We not only observed dose-dependent ERK activation by oleuropein (Figure 2A), but also found that oleuropein rapidly stimulated insulin secretion with peaks at 5-10 minutes upon treatment (Figure 2B). Consistently, the inhibition of ERK phosphorylation diminished with an increased dose of ERK/MAPK-specific inhibitor PD98059 (Figure 2C). Oleuropein was shown to induce AMPK phosphorylation (and mTOR inhibition)-related autophagy in SHSY-5Y neuroblastoma cells[19]. When we tested autophagy induction upon oleuropein treatment in INS-1 cells, we found no significant induction of autophagic markers beclin-1 or LC3 proteins (Figure S2). The differences between our results and the literature could arise from the different cell models used.

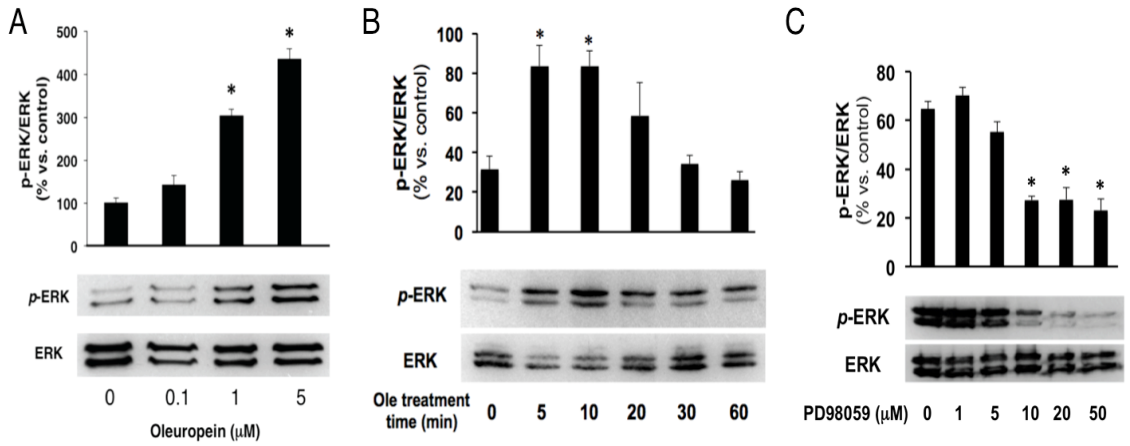

Figure 2. Oleuropein activates ERK/MAPK signaling pathways in INS-1 β-cells. Cells were treated with oleuropein at the indicated concentrations or with the specified durations, and protein extracts were probed by Western blotting. Levels of phosphorylated p-ERK were quantified by densitometry, normalized against total ERK. Effects that are statistically significant with respect to vehicle control or zero-minute treatments are indicated with asterisks. (A) Dose-dependent ERK phosphorylation by oleuropein. Treatment time was 10 minutes. (B) Time dependence of ERK phosphorylation. Concentration of oleuropein in the treatment was 5 μM for both panels B and C. (C) Oleuropein-induced ERK activation is specifically blocked by ERK signaling pathway inhibitor PD98059 in a dose-dependent manner.

The anti-diabetic effects of oleuropein have been attributed in part to its neutralizing effects against the cytotoxic amyloids of a peptide hormone, amylin[5]. This 37-residue peptide co-secretes with insulin from the β-cells. Insulin resistance-associated hyperamylinemia can lead to toxic amylin amyloid deposits in the pancreas, which occurs in up to 90% of T2D patients[20]. To validate oleuropein as an effective amylin amyloid inhibitor identified from our initial natural product library screens[9], we performed multiple secondary assays. These orthogonal assays are necessary, partly because of the reported limitations of ThT fluorescence screen assays in defining amyloidogenicity in some cases[21]. We used transmission electron microscopy (TEM) to validate that oleuropein significantly blocked fibrillation under experimental conditions (Figure 3D). We showed in two orthogonal remodeling assays that oleuropein significantly remodeled pre-formed amylin amyloids such that ThT fluorescence signals were significantly reduced (Figure 3B) or led amyloid into non-toxic, off-pathway aggregates that have broad molecular weight distributions as exemplified by EGCG[17,18] (Figure 3C). During the early phase of amyloid formation, we found oleuropein disrupted oligomer (dimer and trimer) formation in an *in vitro* photo-induced crosslinking of unmodified proteins (PICUP) assay (Figure 3E). Expectedly, oleuropein inhibited amylin amyloid in a dose-dependent manner (Figure 3A) with an estimated IC_{50} of 100 μM (Figure S3B). Oleuropein also induced kinetic delay (longer $t_{1/2}$) in the lag-phase of amyloid formation at high concentrations (Figures 3A and S3A). Lastly and importantly, oleuropein neutralized amylin amyloid induced cytotoxicity against β-cells in a dose-dependent manner (Figures 3F and 3G). Oleuropein itself has no significant effects on cell viability (Figure S5).

To further pinpoint which functional group(s) in oleuropein are important for its amyloid inhibitory effects, we performed an analog-based structure-activity relationship analyses. Our

assays compared and contrasted oleuropein with each of its component and related analogs (Figures 1A and 3). In both ThT-fluorescence and gel-based amyloid remodeling assays, we found oleuropein and 3-HT showed similar remodeling activities, whereas all other compounds, including the oleuropein analog ligstroside, the 3-HT analog tyrosol, and oleuropein components EA and glucose, showed no such activities. TEM results validated that both oleuropein and 3-HT, but not EA or glucose, significantly reduced fibrillation in comparison to vehicle control (Figure 3D and data not shown). Consistently, oleuropein and 3-HT have similar IC_{50} inhibition potencies (Figure S3B). Oligomer formation is the intermediate step in forming mature fibrils, and oligomers are thought to be more cytotoxic than fibrils[20]. Our data suggested that oleuropein and 3-HT inhibit oligomer formation (Figure 3E). Only at much higher concentration (at 20:1 compound: amylin molar ratio), tyrosol, ligstroside, 2-HPEA, and HPE showed moderate dimer break-up functions (at this ratio, EA and glucose remained negative; Figure S4). Importantly, cell-based assays demonstrated significant neutralization functions of oleuropein and 3-HT, but no activities for ligstroside and tyrosol at comparable concentrations (Figure 3G). All compounds alone have no effects on cell viability (Figure S5B). Ligstroside, a close analog of oleuropein that is active in stimulating GSIS effect, has no amyloid inhibitory functions (Figures 3B, 3C, 3E, and 3G). Loss of inhibition activities of tyrosol and ligstroside demonstrated that vicinal dihydroxyl groups of the catechol moieties of 3-HT and oleuropein are required for amyloid inhibition functions, as we showed with other catechol-containing compounds[9]. Together, multiple independent lines of data demonstrated that 3-HT moiety of oleuropein is the main functional entity responsible for its amyloid inhibition.

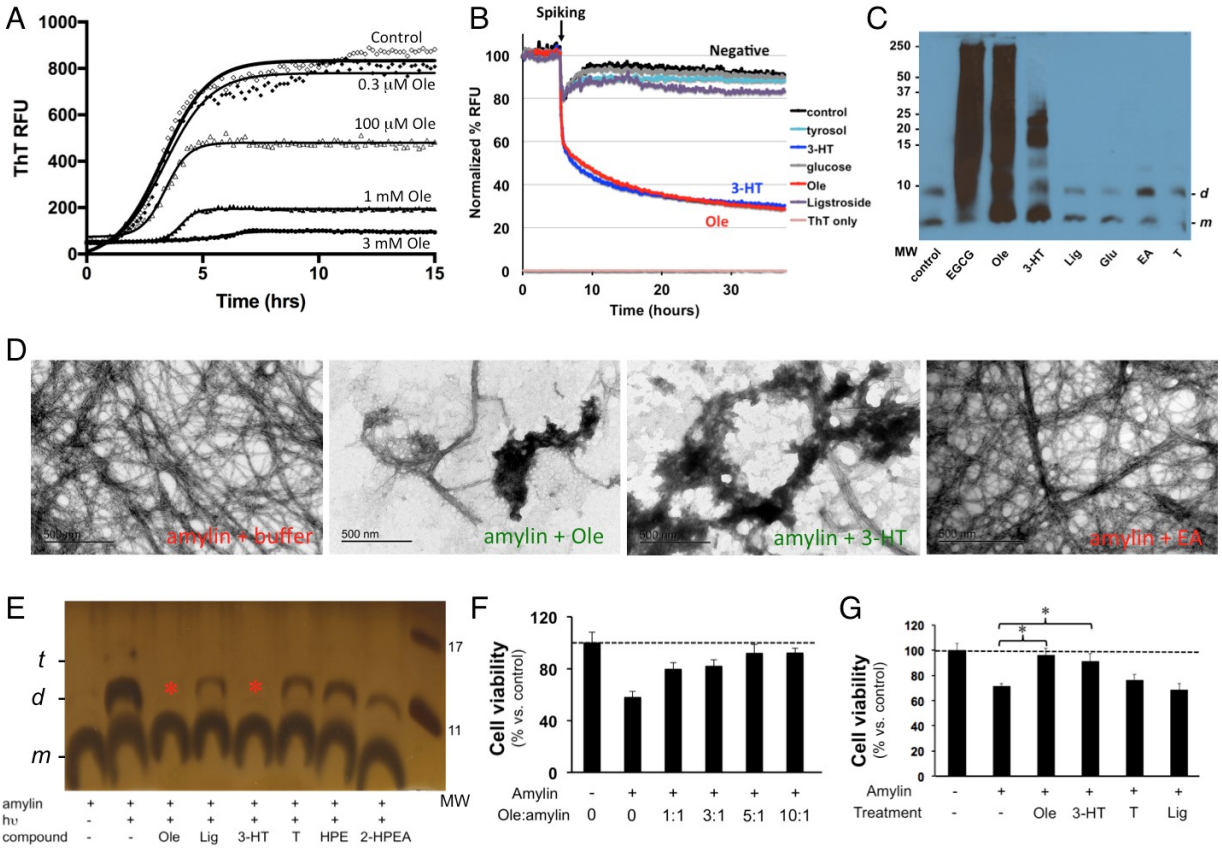

Figure 3. Oleuropein inhibits the formation and the cytotoxicity of amylin amyloid primarily through its component 3-hydroxytyrosol moiety. (A) ThT fluorescence-based assay showing dose-dependent amyloid inhibition by oleuropein. (B,C) ThT fluorescence-based and gel-based amyloid remodeling assays showed oleuropein and 3-HT, but not other analogs, remodeled amylin amyloid. In panel B, vehicle control or specified compounds were spiked into pre-aggregated amyloid samples (arrowed) that already reached plateaus (equivalent to 10-hour point in panel A). Fluorescence signals after spiking were recorded continuously. Compound: amylin molar ratio was 10:1. In panel C, 3 days after spiking, samples were vacuum dried, re-dissolved in 6.5 M urea and subjected to SDS-PAGE and Western blotting with amylin–specific antibody T-4157. EGCG served as a remodeling positive control (17,18). Monomer (m) and dimer (d) sizes are marked. Compound: amylin molar ratio was 20:1. *(continued next page)*

(D) Representative TEM images of amylin amyloid and its treatment with vehicle, oleuropein, 3-HT, or EA. Amylin concentration used was 15 μM and drug: amylin molar ratio was 20:1. (E) Photo-induced crosslinking of unmodified protein (PICUP) analysis of amylin oligomer formation with various oleuropein analog treatments. Absence of the cross-linked dimers is marked with the red asterisks. Amylin concentration used was 10 μM and drug:amylin molar ratio was 10:1. (F,G) Neutralization of amylin-induced cytotoxicity by oleuropein analogs in INS-1 β-cells. The amylin concentration was 5 μM, and the Ole:amylin molar ratios are indicated (panel F). Treatment of Ole and 3-HT, but not T and Lig, have significant effects that protect INS-1 cell viability (asterisks in panel G).

Conclusion

In summary, here we report, for the first time to our knowledge, that oleuropein is a novel natural compound inducing anti-diabetic GSIS function. Our data suggested that its GSIS function requires the entire structural scaffold of oleuropein. In contrast, the 3-HT moiety of oleuropein is responsible for its amyloid inhibition function relevant to its second anti-diabetic function. Our work thus provides insights into the dual anti-diabetic functions of oleuropein. Anti-amyloid effects of oleuropein have been shown in an animal study to effectively counteract the toxicity of a well-studied amyloidogenic peptide, Aβ42[4]. It will be interesting to test the specific effects of oleuropein and its components in counteracting amylin amyloid deposition in the pancreas as well as in positively regulating hyperglycemia in diabetic animal models in the future.

Material and Methods

Chemicals, Peptides and Other Reagents. Synthetic human amylin was purchased from AnaSpec (Fremont, CA) and the peptide quality was further validated by Virginia Tech core facility Mass Spectrometry Incubator. Amylin stocks were quantified by Pierce BCA protein assay kit (Thermo Fisher Scientific, Waltham, MA). Oleuropein (>98% purity; glycated form, Fig. 1A), tyrosol, 2-(3-hydroxyphenyl)ethanol, hexafluoro isopropanol (HFIP), and thioflavin T (ThT) were purchased from Sigma Aldrich (St. Louis, MO). Dimethyl sulfoxide (DMSO) and 2-Hydroxyphenethyl alcohol were purchased from Fisher Scientific (Pittsburgh, PA). 3-Hydroxytyrosol was purchased from Cayman Chemical (Ann Arbor, MI). Ligstroside and elenolic acid were purchased from Toronto Research Chemicals (Toronto, Ontario, Canada). Dulbecco's phosphate buffer saline (DBPS) was purchased from Lonza (Walkersville, MD).

Peptide and Natural Compound Preparation. Typical amylin stock preparation was initiated by dissolving 0.5 mg lyophilized human amylin powder in 100% DMSO at a final concentration of 1-2 mM. After at least 2 hours of incubation at room temperature these solutions were aliquoted and either lyophilized again prior to use for cell-based assays or dissolved directly into DPBS, 10 mM phosphate buffer pH 7.4 or 20 mM Tris-HCl pH 7.4 for all amylin amyloid-related *in vitro* assays. All remaining 1-2 mM stocks in 100% DMSO were stored at -80 °C until later use. In some cases, DMSO amylin stock solutions were made by first dissolving 0.5 mg of lyophilized human amylin powder in 100% HFIP before subsequently being air dried and re-dissolved in DMSO. Oleuropein and its analogs were dissolved in DMSO or ethanol (10 mM) and ThT (Sigma Aldrich) was dissolved in distilled water or relevant buffer (1-4 mM). These stocks were stored at -20 °C until later use. Residual DMSO present in the final concentrations used for all *in*

vitro assays ranged from 0-9.5%. We determined that residual DMSO present in samples (which depending on the assay ranged from 0-9.5%) had negligible effects on amylin aggregation as reflected by ThT fluorescence, transmission electron microscopy, PICUP assay[9], and inhibitor-induced amylin amyloid remodeling assays.

Cell Culture and Glucose-Stimulated Insulin Secretion Analysis. Rat pancreatic INS-1 cells were cultured as previously described[13]. INS-1 cells were cultured in RPMI-1640 medium containing 10% fetal bovine serum and supplemented with 11.1 mM glucose, 1 mM sodium pyruvate, 10 mM HEPES, 50 μM β-mercaptoethanol, 23.8 mM $NaHCO_3$. The medium was changed every other day until the cells became confluent. For insulin secretion analysis, INS-1 cells were plated in 12 wells with 70-80% confluence. The cells were starved in RPMI medium containing 2 mM glucose and 5% FBS overnight and incubated with Krebs-Ringer bicarbonate buffer (KRBB; 129 mM NaCl, 4.8 mM KCl, 1.2 mM $MgSO_4$, 1.2 mM KH_2PO_4, 2.5 mM $CaCl_2$, 5 mM $NaHCO_3$, 0.1% BSA, and 10 mM HEPES, pH 7.4) containing 2.0 mM glucose for 1 hour. Drugs were added to KRBB and incubated for another 1 hour. The supernatants were used for measuring the insulin secretion using rat insulin ELISA kit (Mercodia, Sweden).

Cell Signaling Analysis. INS-1 cells were plated in six-well plates and treated with drugs/ pretreated with inhibitor for 45 min. The treated and untreated cells were harvested, washed with ice-cold PBS (pH 7.4), and lysed with ice-cold lysis buffer (20 mM Tris-HCl, pH 7.5, 0.15 M NaCl, 1 mM EDTA, 1% NP-40, 1% sodium deoxycholate, 2.5 mM sodium phosphate, 1 mM sodium orthovanadate, 1 mM sodium fluoride and proteinase inhibitor) on ice for 1 hour. The lysates were sonicated and protein concentration was determined. Equivalent samples were subjected to SDS-PAGE, then transferred onto PVDF membranes and subsequently incubated

with primary antibodies against phosphorylated phospho-p44/42 Erk1/2 (T202/Y204, rabbit monoclonal, 1:1000; Cell Signaling Technology, Danvers, MA), p44/42 ERK1/2 (L34F12, mouse monoclonal, 1:1000; Cell Signaling Technology, Danvers, MA) in PBS with 0.1% Tween 20 that contained 5% milk overnight at 4 °C, followed by horseradish peroxidase (HRP)-conjugated anti-IgG (1:5000, Jackson ImmunoResearch, West Grove, PA). The immune complexes were visualized via enhanced chemiluminescence (ECL) using an ECL kit (Thermo Scientific, Waltham, MA). The film signals were quantified using Imagelab software (Bio-Rad Laboratories, Hercules, CA). In the analysis of autophagy induction by oleuropein or its analog ligstroside, INS-1 cells were exposed to either compound for 10 minutes with or without pre-treatment of compound C for 30 minutes, a known AMPK inhibitor. Autophagy cellular protein markers, beclin-1 and LC3A/B levels were analyzed by Western blots with specific primary antibodies: rabbit polyclonal anti-beclin-1 antibody (1:3000, Cell Signaling) and rabbit polyclonal anti-LC3A/B antibody (1:1000, Cell Signaling). Mouse anti-GAPDH monoclonal antibody (1:6000, Cell Signaling) was used for protein load normalization.

Cell Viability Assays. An MTT-based cell viability assay was used. The INS-1 β-cells were seeded in 96-well plate at a density of $4x10^4$ cells/well. After 24 hours incubation, cells were treated with human amylin, either with or without specified natural compounds. Following another 24 hours incubation, 0.9 mM MTT was added to each well. The reduced insoluble MTT formazan product was then dissolved in SDS-HCl lysis buffer (5 mM HCl, 5% SDS) at 37 °C. Cell viability was determined by measurement of absorbance change at 570 nm using a spectrometric plate reader. Cells treated with the buffer that was used to dissolve peptides were

used as positive control and taken as 100%, and 0.5% Triton X-100 treated cells at the start of the incubation period with test peptides are used as negative control and taken as 0%.

Thioflavin T Fluorescence Assay. Fluorescence experiments were performed using a SpectraMax M5 plate reader. Kinetic readings were taken at 25 °C in low- or medium-binding all black clear bottom Greiner 96 (or 384-well) plates covered with optically clear films and shaken for 10 seconds prior to each reading. ThT fluorescence was measured with excitation wavelength at 444 nm and emission wavelength at 491 nm. IC-50 experiments were conducted at an amylin concentration of 15 μM that included an amylin: ThT molar ratio of 1:4. All experiments were repeated at least twice. IC_{50} analysis was determined by percent of normalized fluorescence signal in relation to inhibitor concentrations. The $t_{1/2}$ was defined as the time taken to reach half maximum RFU signal (difference between the plateaued maximum RFU and the background RFU signal at the time of 0 hr.).

Transmission Electron Microscopy (TEM). Amylin fibrillation was initiated in 20 mM Tris-HCl, pH 7.4 and a residual amount (0-3.75%) of DMSO or ethanol solvents from vehicle control or testing compounds. Final amylin concentration was 15 μM and the molar ratio of a compound to amylin was 20:1. Samples were typically incubated at 37 °C without agitation for 3-4 days. Prior to imaging analyses, ~2 μls of samples were blotted on a 200-mesh formvar-carbon coated grid for 5 minutes and wicked dry by filter paper (this cycle was repeated twice to enhance signal). Dried samples were then immediately stained with uranyl acetate (1%) for one minute, and again, wicked dry with filter paper before imaging. Prior to taking representative images (obtained from a JEOL 1400 operated at 120 kV, a qualitative assessment of the number of

fibrils or oligomers observed was made by scanning each grid quadrant for deposited material. Residual solvent(s) are expected to have negligible effects on fiber formation. TEM experiments were repeated at least twice.

Inhibitor-induced Amyloid Remodeling Assays. Vehicle control or specified compounds were spiked into pre-aggregated amyloid samples (containing amylin, buffer and ThT) that already reached plateaus as determined by fluorescence readings. Amylin concentrations ranged from 9.4-12.9 μM and the compound: amylin molar ratio was 10:1. Temperature was 25 °C. Thereafter, ThT fluorescence signals were continuously recorded. In the gel-based amyloid remodeling assays, amylin aggregation was initiated in the absence of compounds until the plateau phase was reached as estimated from ThT assay kinetic data (typically > 8 hours). Next, each pre-aggregated sample was spiked with a vehicle control or specified compounds. Amylin concentration was 15 μM and the compound: amylin molar ratio was 20:1. After 3 days, these samples were vacuum dried and re-dissolved in ~6.5 M urea containing 15 mM tris and 1X SDS laemmeli sample buffer, boiled at 95 °C for 5-10 minutes and subjected to SDS-PAGE followed by Western blot analysis with anti-amylin primary antibody (T-4157, 1:5000, Peninsula Laboratories, San Carlos, CA). All ThT fluorescence-based assays and gel-based amyloid remodeling assays were repeated at least twice.

Photo-Induced Crosslinking of Unmodified Proteins (PICUP). Amylin aliquots from a master mix in 10 mM phosphate buffer, pH 7.4 were added separately to 0.6 mL eppendorf tubes containing small molecule inhibitors or DMSO vehicle loaded controls. Crosslinking for each tube was subsequently initiated by adding tris(bipyridyl)Ru(II) complex (RuBpy) and

ammonium persulfate (APS) (Typical Amylin:RuBpy:APS ratios were fixed at 1:2:20, respectively), followed by exposure to visible light, emitted from a 150-Watt incandescent light bulb, from a distance of 5 cm and for a duration of 5 seconds. The reaction was quenched by addition of SDS sample buffer. PICUP was visualized by SDS-PAGE (16% acrylamide gels containing 6 M urea), followed by silver staining. Final concentrations for all PICUP reactions included 20-30 μM amylin, with addition of drug: amylin ranging from 1:1 to 20:1 in molar ratios.

Statistical Analyses. All data are presented as the mean ± S.E.M. and the differences were analyzed with one-way ANOVA analyses for amylin kinetics ($t_{1/2}$) as implemented within GraphPad Prism software (version 6.0) or with Student's *t* test in determining the significance in cell viability changes and ERK phosphorylation. p values < 0.05 were considered statistically significant.

Supplemental Figures

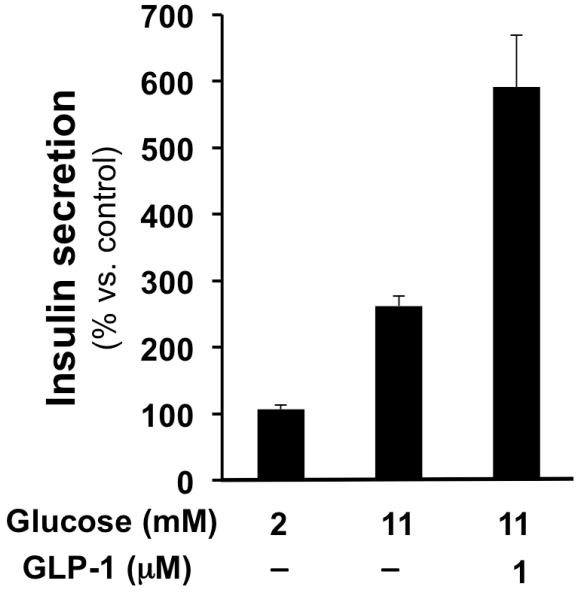

Figure S1. Control experiment demonstrates strong GSIS effect of glucagon like peptide 1 (GLP-1) in INS-1 β-cells. GLP-1 concentration in the treatment was 1 μM.

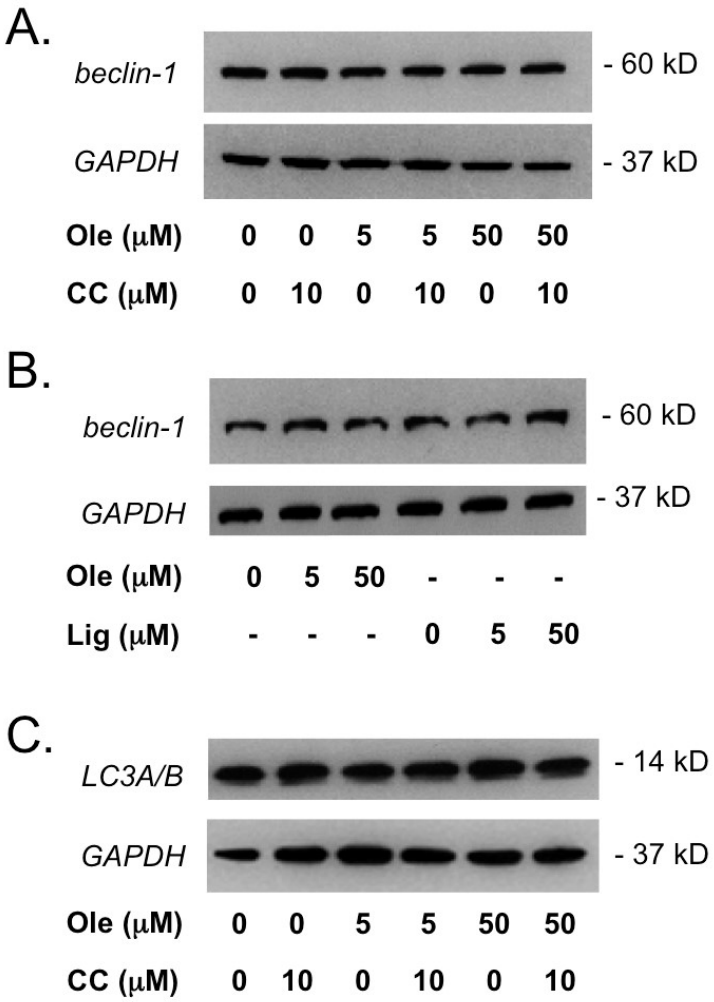

Figure S2. Control experiments demonstrate oleuropein-treated cell autophagy is unmodified in pancreatic INS-1 cells. INS-1 cells were treated with oleuropein (Ole) or its analog ligstroside (Lig) at the indicated concentrations for 10 minutes with or without pre-treatment of 10 μM compound C (CC) for 30 minutes, a known AMPK inhibitor[19]. Autophagy cellular protein markers, beclin-1 (panels A and B) and LC3A/B (panel C) levels were analyzed by Western blots with specific primary antibodies. Corresponding lower panels of cellular GAPDH levels probed by Western blot demonstrated equal protein load for each lane.

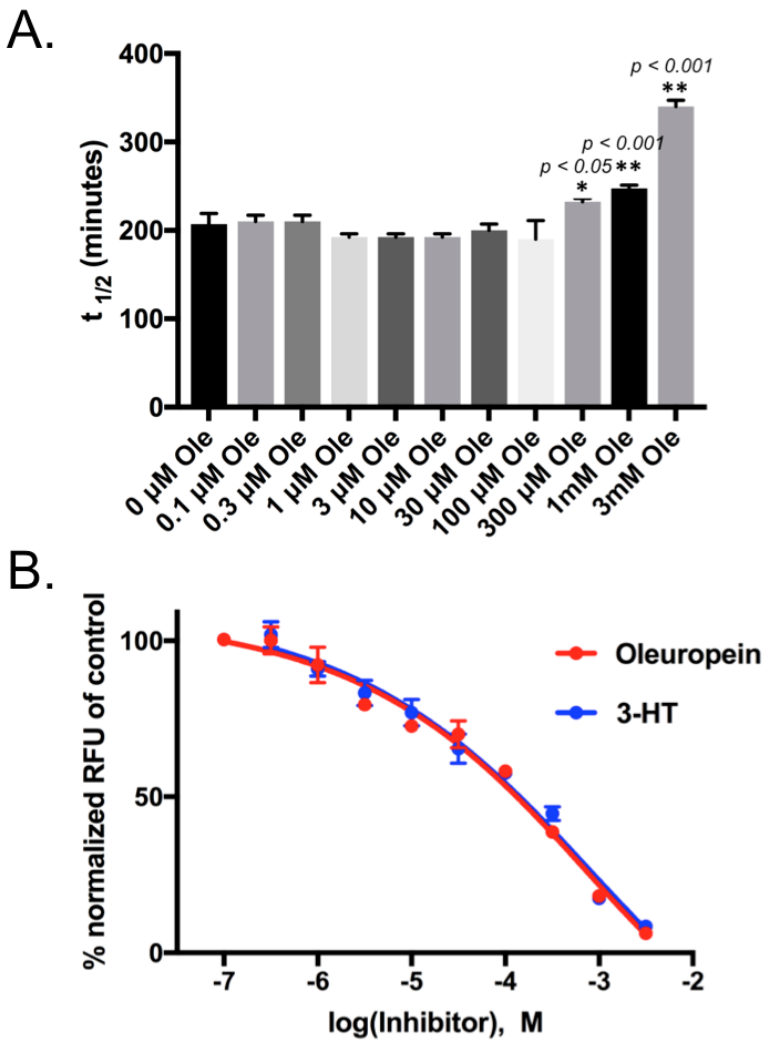

Figure S3. Quantification of oleuropein-induced lag-phase kinetic delay ($t_{1/2}$) in amylin amyloid formation (A) and IC_{50} measurements of oleuropein and 3-HT in inhibiting amylin amyloid formation (B) based ThT fluorescence based assays. Corresponding oleuropein dose-dependent kinetic profiles are shown in Figure 3A. Both oleuropein and 3-HT have an estimated IC_{50} of 100 µM. Amylin concentration in both experiments was 15 µM.

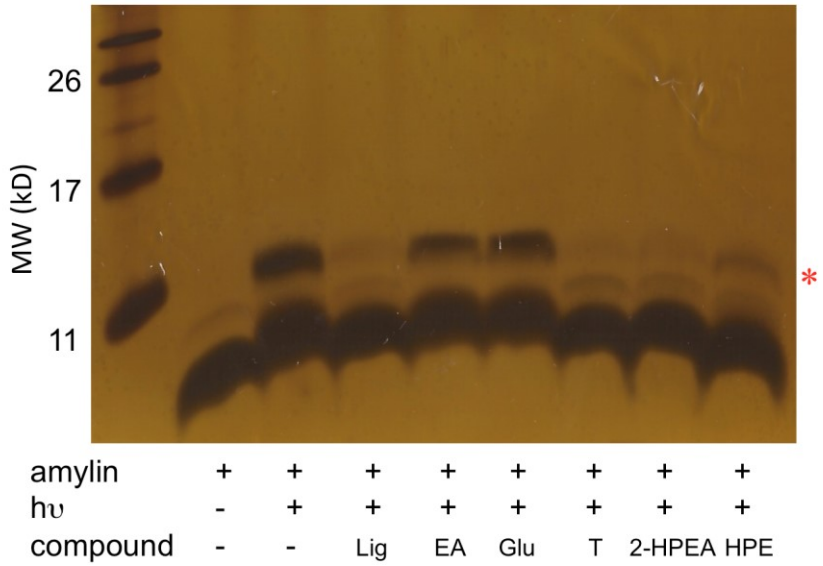

Figure S4. PICUP assay demonstrates that ligstroside (Lig), tyrosol (T), 2-hydroxyphenethyl alcohol (2-HPEA), and 2-(3-hydroxyphenyl)ethanol (HPE), but not elenolic acid (EA) and glucose (Glu), exhibited amylin oligomer (highlighted as red asterisk) inhibition at high concentrations (20:1 drug:amylin molar ratio, at 20uM amylin). Note: the stronger oligomer break-up effects exhibited by OLE and 3HT versus Lig, T, 2-HPEA, and HPE (Figure 3E) was further suggested by a separate PICUP experiment that compared concentration dependent oligomer break-up effects between Ole and 3HT alongside Lig and T (data not shown).

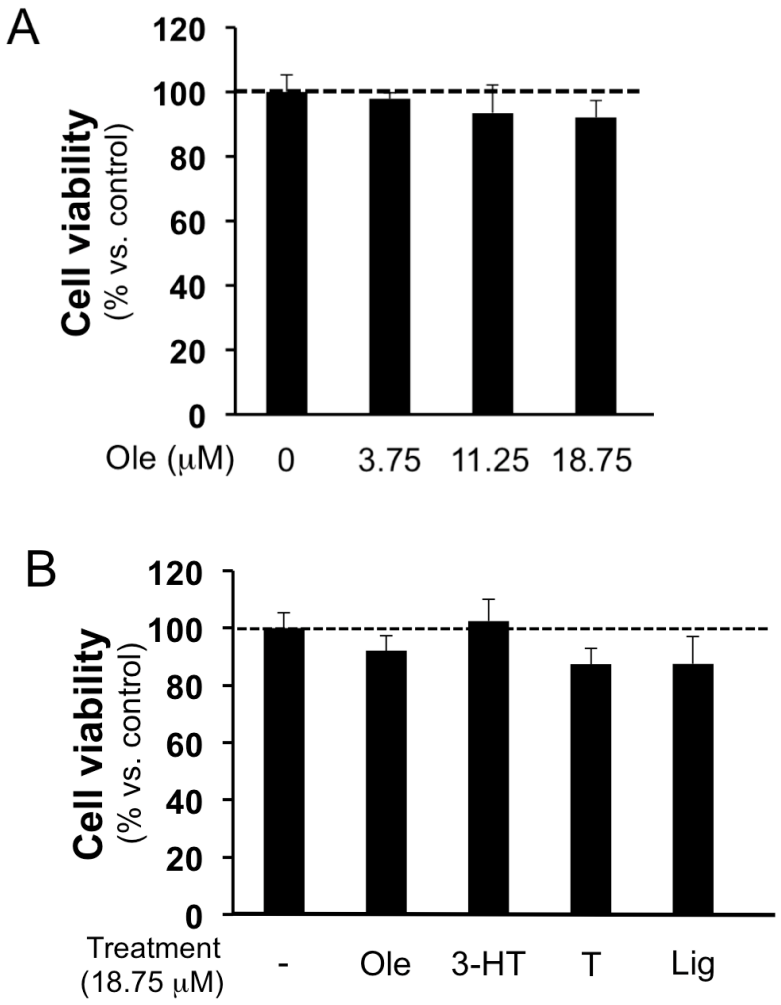

Figure S5. Control experiments demonstrate oleuropein and its analogs themselves have no significant effects on INS-1 cell viability at the specified concentrations. Oleuropein itself has no significant effects to INS-1 cell viability at the concentrations from 0-18.75 μM (A). Oleuropein (Ole), 3-hydroxytyrosol (3-HT), tyrosol (T), and ligstroside (Lig), have no significant effects on INS-1 cell viability at the concentration of 18.75 μM (B).

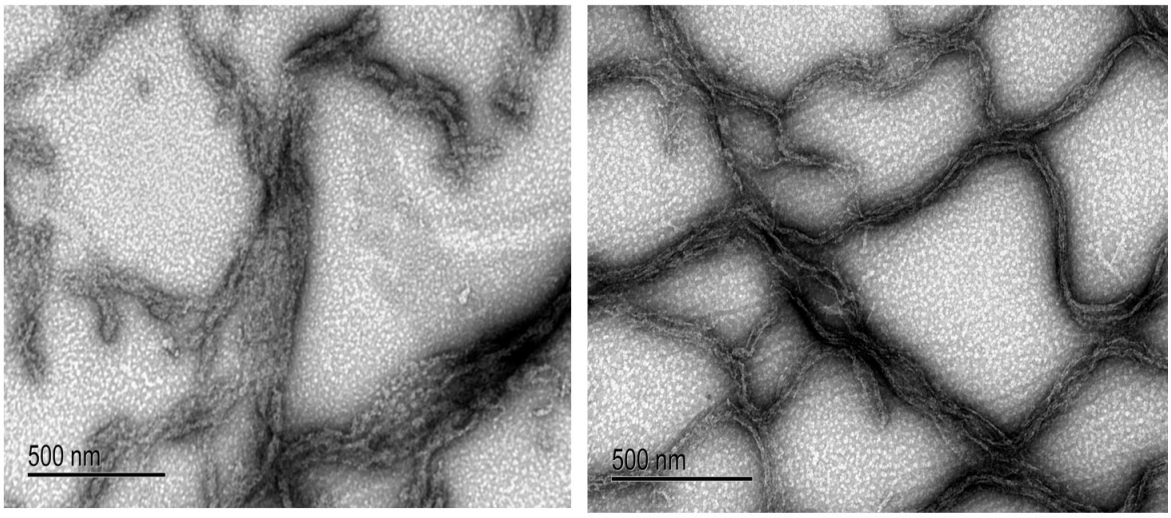

Figure S6. Variations of effects of 3-HT treatments on amylin fibril formation under transmission electron microscopy (TEM). At 20:1 ratio (3-HT:amylin) 3-HT treated amylin samples showed significantly reduced amount of amylin string fibrils in comparison with buffer-treated samples (Figure 3D). We also observed morphology of non-string like, wavy ribbon bundles of aggregates (panels below) after 3-HT treatment. In either case, string-like amylin fibrils were reduced compared to vehicle-treated controls. Furthermore, at high concentrations of treatment (50:1, 3-HT:amylin) 3-HT prevented virtually any fibril deposition in concert with showing lots of dark amorphous aggregate structures(data not shown). Note that in these conditions, vehicle-treated controls (7.5% ethanol, 0.75% DMSO) contained ~ 50:50 mixture of fibrils and dark amorphous aggregates (data not shown).

References

1. Rigacci, S., and Stefani, M. Nutraceutical Properties of Olive Oil Polyphenols. An Itinerary from Cultured Cells through Animal Models to Humans. **(2016)** *Int. J. Mol. Sci. 17*, 843.
2. Jemai, H., El Feki, A., and Sayadi, S. Antidiabetic and Antioxidant Effects of Hydroxytyrosol and Oleuropein from Olive Leaves in Alloxan-Diabetic Rats **(2009)** *J. Agric. Food Chem. 57*, 8798-8804.
3. Murotomi K, Umeno A, Yasunaga M, Shichiri M, Ishida N, Koike T, Matsuo T, Abe H, Yoshida Y, and Nakajima Y. Oleuropein-Rich Diet Attenuates Hyperglycemia and Impaired Glucose Tolerance in Type 2 Diabetes Model Mouse. **(2015)** *J. Agric. Food Chem. 63*, 6715-6722.
4. de Bock, M., Derraik, J. G. B., Brennan, C. M., Biggs, J. B., Morgan, P. E., Hodgkinson, S. C., Hofman, P. L., and Cutfield, W. S. Olive (Olea europaea L.) leaf polyphenols improve insulin sensitivity in middle-aged overweight men: a randomized, placebo-controlled, crossover trial. **(2013)** *PLoS One. 8*, e57622.
5. Rigacci, S., Guidotti, V., Bucciantini, M., Oarri, M., Nediano, C., Cerbai, E., Stefani, M., and Berti, A. Oleuropein aglycon prevents cytotoxic amyloid aggregation of human amylin. **(2010)** *J. Nutr. Biochem. 21*, 726-735.
6. Luccarini, I., Ed Dami, T., Grossi, C., Rigacci, S., Stefani, M., and Casamenti, F. Oleuropein aglycone counteracts Aβ42 toxicity in the rat brain. **(2014)** *Neurosci. Lett. 558*, 67-72.
7. Leri, M., Nosi, D., Natalello, A., Porcari, R., Ramazzotti, M., Chiti, F., Bellotti, V., Doglia, S. M., Stefani, M., and Bucciantini, M. The polyphenol Oleuropein aglycone hinders the growth of toxic transthyretin amyloid assemblies. **(2016)** *J. Nutr. Biochem. 30*, 153-166.
8. Ladiwala, A. R. A., Mora-Pale, M., Lin, J. C., Bale, S. S., Fishman, Z. S., Dordick, J. S., and Tessier, P. M. Polyphenolic glycosides and aglycones utilize opposing pathways to selectively remodel and inactivate toxic oligomers of amyloid β. **(2011)** *ChemBioChem. 12*, 1749-1758.
9. Velander, P., Wu, L., Ray, W. K., Helm, R. F., and Xu B. Amylin Amyloid Inhibition by Flavonoid Baicalein: Key Roles of its Vicinal Dihydroxyl Groups of the Catechol Moiety **(2016)** *Biochemistry. 55*, 4255-4258.
10. Umento, A., Horie, M., Murotomi, K., and Yoshida, Y. **(2016)** *Molecules. 21*, 708.
11. Chimento, A., Casaburi, I., Rosano, C., Avena, P., De Luca, A., Campana, C., Martire, E., Santolla, M. F., Maggiolini, M., Pezzi, V., and Sirianni, R. Oleuropein and hydroxytyrosol activate GPER/ GPR30-dependent pathways leading to apoptosis of ER-negative SKBR3 breast cancer cells. **(2014)** *Mol. Nutr. Food Res. 58*, 478-489.
12. Wang, A., Luo, J., Moore, W., Alkhalidy, H., Wu, L., Zhang, J., Zhen, W., Wang, Y., Clegg, D. J., Xu, B., Cheng, Z., McMillian, R. P., Hulver, M. W., and Liu, D. GPR30 regulates diet-induced adiposity in female mice and adipogenesis in vitro. **(2016)** *Sci. Rep. 6*, 34302.
13. Liu, D., Zhen, W., Yang, Z., Carter, J. D., Si, H., and Reynolds, K. A. Genistein acutely stimulates insulin secretion in pancreatic beta-cells through a cAMP-dependent protein kinase pathway. **(2006)** *Diabetes. 55*, 1043-1050.
14. Watkins, R., Wu, L., Zhang, C., Davis, R. M., Xu, B. Natural product-based nanomedicine: recent advances and issues **(2015)** *Int. J. Nanomed. 10*, 6055-6074.

15. Velander, P., Wu, L., Henderson, F., Zhang, S., Bevan, D. R., and Xu, B. Natural product-based amyloid inhibitors **(2017)** *Biochem. Pharmacol. 139*, 40-55.
16. Drucker, D. J. The biology of incretin hormones. **(2006)** *Cell Metab. 3*, 153-165.
17. Ehrnhoefer, D. E., Bieschke, J., Boeddrich, A., Herbst, M., Masino, L., Lurz, R., Engemann, S., Pastore, A., and Wanker, E. E. EGCG redirects amyloidogenic polypeptides into unstructured, off-pathway oligomers. **(2008)** *Nat. Struct. Mol. Biol. 15*, 558-566.
18. Palhano, F. L., Lee, J., Grimster, N. P., and Kelly, J. W. Toward the molecular mechanism(s) by which EGCG treatment remodels mature amyloid fibrils. **(2013)** *J. Am. Chem. Soc. 135*, 7503-7510.
19. Rigacci, S., Miceli, C., Nediani, C., Berti, A., Cascella, R., Pantano, D., Nardiello, P., Luccarini, I., Casamenti, F., and Stefani, M. Oleuropein aglycone induces autophagy via the AMPK/mTOR signalling pathway: a mechanistic insight. **(2015)** *Oncotarget. 6*, 35344-35357.
20. Westermark, P., Anderson, A., and Westermark, G. T. Islet amyloid polypeptide, islet amyloid, and diabetes mellitus. **(2011)** *Physiol. Rev. 91*, 795-826.
21. Wong, A. G., Wu, C., Hannaberry, E., Watson, M.D., and Raleigh, D. P. Analysis of the Amyloidogenic Potential of Pufferfish (Takifugu rubripes) Islet Amyloid Polypeptide Highlights the Limitations of Thioflavin-T Assays and the Difficulties in Defining Amyloidogenicity. **(2016)** *Biochemistry. 55*, 510-518.

Chapter 4: A Synthetic Rosmarinic Acid Analogue Potently Detoxifies Amylin Amyloid

I acknowledge pleasant and fruitful collaboration with Dr. Ling Wu, who performed all cell-based assays and western blot analyses of sera samples, Drs. Anne Brown and David Bevan who performed and or analyzed all MD simulations, Drs. Shijun Zhang and John Saathoff synthesized RA analogues.

Abstract

Amyloid formation has been implicated in more than a dozen human protein misfolding diseases, yet effective therapeutic small molecules are currently not available. Amylin amyloid and plaque depositions are found in the pancreas of over 90% of type 2 diabetes (T2D) patients in postmortem examinations and have been implicated in the pathogenesis of neurodegeneration and cardiovascular disorders as diabetic complications. Screening of a targeted library of natural compounds used in complementary medicine identified rosmarinic acid (RA), a catechol-containing natural product, as a strong inhibitor against amylin amyloid formation (estimated IC_{50} = 200-300 nM). RA significantly reduces amylin amyloid-induced cytotoxicity. Dissecting the two functional groups of rosmarinic acid, we found each group, caffeic acid and salvianic acid A, contributes in an additive manner to the anti-amyloid activities observed with RA alone. We further synthesized multiple RA analogues. One RA analogue, which replaces the ester link with an amide in the RA molecule, showed significantly enhanced functions in converting toxic amylin amyloid into non-toxic amorphous aggregates. We further showed that in a dose- and time-dependent manner, both RA and the synthetic RA analogue effectively disassociates pre-formed amylin oligomers taken from the sera of transgenic HIP rats. Moreover, both small molecules demonstrated efficacy in reducing pre-formed human amylin oligomers taken from diabetic patient sera.

Introduction

Amyloid formation is associated with a large class of protein misfolding diseases that includes a broad spectrum of neurological, metabolic and aging related diseases such as Alzheimer's disease (AD), Parkinson's disease, prion disease, and type 2 diabetes (T2D). The pathological hallmarks of amyloid disease are structurally conserved intracellular and extracellular insoluble proteinaceous deposits termed amyloid fibrils [1,2,3]. Protein amyloid aggregation proceeds through a nucleation-dependent process wherein monomeric and oligomeric aggregates form "seeds" that initiate an aggregation cascade that results in equilibrium between mature amyloid fibrils and their small precursor aggregates. Over the last two decades, increasing evidence indicates that the primary pathological amyloid species are non-fibrillar precursor aggregates that range from unstructured oligomers to β-sheet rich aggregates termed protofibrils (as small as 20-mers) [1].

Amylin is a 37-residue peptide hormone co-secreted with insulin by pancreatic β-cells. It is one of the most amyloidogenic proteins known[4]. Increased amylin concentrations in the blood have been detected in T2D-related obese and insulin-resistant patients likely due to the compensatory effect of increased insulin secretion[5]. Hyperamylinemia leads to toxic amylin oligomer/amyloid formation and plaque deposition in the pancreas, which are established features of T2D [6,7,8,9]. Growing experimental evidence shows that hyperamylinemia also induces toxicity in peripheral organs, including the heart, kidneys, and the brain [10,11]. Moreover, a "humanized" transgenic diabetic rat model that overexpresses human amylin (HIP rats) provided strong causal evidence that amylin oligomers/amyloid contribute to the heart dysfunction and the AD-mimicking neurobehavioral deficits [12,13,11].

Currently there are no cures for any protein amyloid diseases. Progress toward managing protein misfolding diseases in general has been hampered by the failure to develop any effective disease-modifying drugs. This lack of progress is in part due to our limited understanding of amyloidogenic proteins as well as their interactions with small molecules/inhibitors. Identification of effective amyloid inhibitors is challenging because of intrinsic structural disorder of many protein targets of amyloid assembly.

There are multiple therapeutic strategies to identify disease-modifying agents against amyloid disease (see literature for a recent review[14]). One of the current strategies aimed at identifying therapeutic lead compounds focuses on inhibiting amyloid aggregation by (i) preventing toxic amyloid formation or stabilizing its native form from aggregating and (ii) remodeling or degrading toxic amyloid oligomers and/or insoluble fibrils. For natural product based amyloid inhibitor identification, one source of information comes from epidemiological studies that suggest preventative effects against dementia or diabetes may be associated with the diets containing high intake of flavonoids and polyphenolic compounds[15]. Information from these epidemiological sources as well as information reported by alternative and complementary medicine led to testable hypotheses and experimental efforts that successfully identified numerous natural compound amyloid inhibitors[16,17,18,19,20].

In the present study, we screened a targeted library of natural compounds used in complementary medicine and identified rosmarinic acid (RA), a catechol-containing natural product, as a strong inhibitor. We further investigated the structure-function relationship of RA and as a result uncovered the additive effect of two catechol-containing components of the RA molecule. We further synthesized an RA analogue (RA-amide or RA-A) that significantly enhanced its functions in converting toxic amylin amyloid into non-toxic amorphous aggregates.

Moreover, both RA and the synthetic RA analogue demonstrated the ability to dissociate pre-formed amylin oligomers taken from the sera from transgenic HIP rats as well as from diabetic patients.

Results

Identification of Rosmarinic Acid. Using the ThT fluorescence assay, we rapidly screened a small library of natural compounds (~100 compounds) that are rich in flavonoids and polyphenols and are used in Complementary and Alternative Medicine for their anti-diabetes, anti-inflammatory, or neuroprotective effects. EGCG was used as a positive control (Fig. 1A [21,22,23]). Several other compounds, including morin, salvianolic acid B, resveratrol, caffeic acid, and oleuropein, were confirmed for their inhibitory effects against amylin amyloid [24,25, 26,27,19,20]. RA was one of the highest-ranking inhibitors that blocked amylin amyloid formation. We further validated RA in multiple secondary assays. Using transmission electron microscopic (TEM) analysis, we found that RA converted a large amount (estimated to be 50%) of amyloid fibrils into non-toxic aggregates at the given condition of 10:1 drug:amylin molar ratio (Fig. 1B). The potency is similar to EGCG, a well-known strong inhibitor. Based on the ThT fluorescence assay, we further determined that the IC_{50} for RA is 200-300 nM, slightly stronger than the positive control EGCG (~1 μM) (Fig. 1C). Consistent with the reduced amount of mature fibrils observed in TEM, RA significantly delays amylin amyloid formation, and such kinetic delay ($t_{1/2}$) displays a dose-dependent relationship (Fig. 1D and Fig. S5). In addition, RA demonstrated significant amyloid remodeling functions in orthogonal ThT fluorescence assay and gel-based remodeling assays, similar to EGCG (Fig. 4 [21,28,29]).

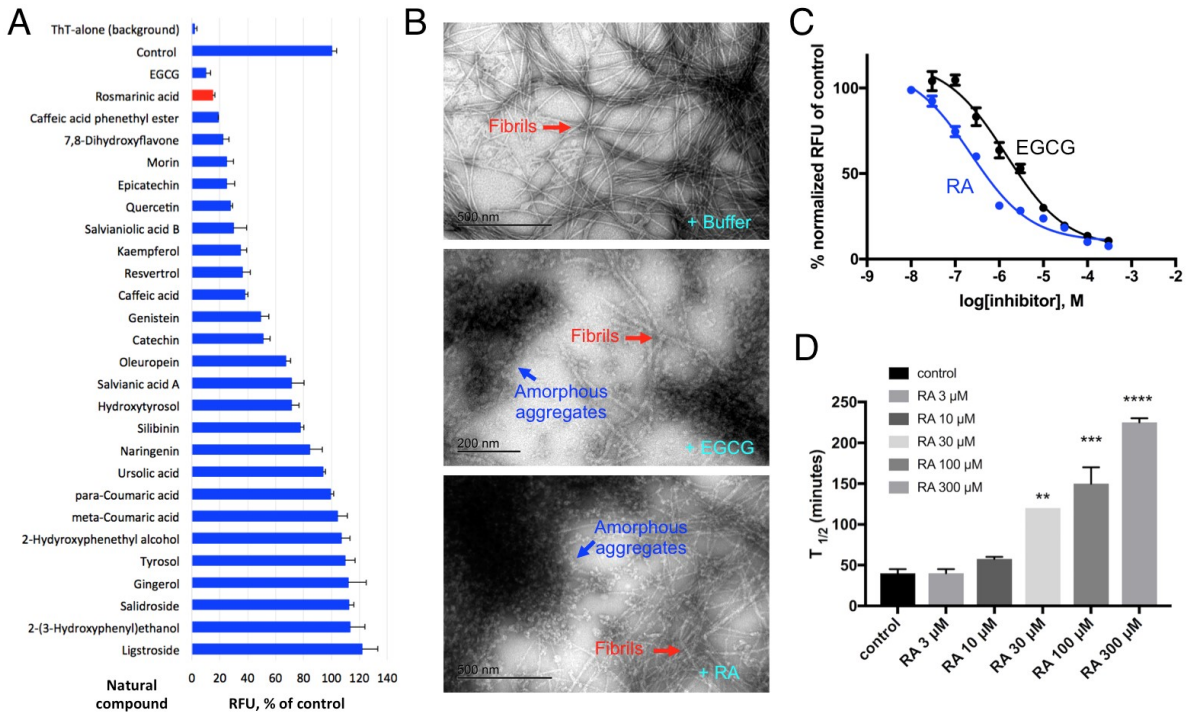

Figure 1. Identification and biochemical and biophysical characterizations of RA as a strong amylin amyloid inhibitor. (A) Identification of rosmarinic acid as strong amylin amyloid inhibitor using a ThT fluorescence based screening assay. (B) TEM images of human amylin amyloid and its treatment with and without inhibitor treatment (1:20 amylin: drug molar ratio). Mature fibrils and amorphous aggregates are indicated by the red and blue arrows respectively. Buffer treatment sample served as control (100% mature fibril). RA treatment resulted in samples containing about 50% mature fibrils and 50% amorphous aggregates, which compared similarly to the anti-amyloid effects of EGCG, a known strong amylin amyloid inhibitor. (C) Amylin-ThT fluorescence-based inhibition assay. RA is estimated to have an IC_{50} between 200-300 nM. IC_{50} curve for a known control EGCG is also shown (1 μM). (D) Dose-dependence of $t_{1/2}$ of amylin amyloid formation in amylin-ThT fluorescence based assays. Concentration of amylin was 10 μM. With increased concentration of RA treatment, $t_{1/2}$ becomes significantly delayed (arrows in Figure S5).

Additive Effects of Rosmarinic Acid. Based on our recent studies on catechol-containing compounds, we discovered that the catechol group is a key functional moiety in inhibiting amyloid formation and related cytotoxicity [19,20] (Velander et al, unpublished manuscript, 2017). Because RA consists of two catechol-containing components, caffeic acid (CA) and salvianic acid A (SAA) that are linked by an ester bond, we hypothesized that each component, CA and SAA, should be amyloid inhibitors as well and that they would display additive anti-amyloid effects similar to that observed with RA alone. To test this hypothesis, we first performed ThT fluorescence assays (Fig. 2A and Fig 2B). CA and SAA each showed significant amyloid inhibition activities, but less than that of RA. However, a 1:1 molar ratio mixture of CA:SAA showed a level of inhibition like that of RA. We also determined the IC_{50} for RA, CA and SAA to be 200-300 nM, 7.2 μM, and 90 μM, respectively (Fig. 2B). This additive effect was also manifested in amylin amyloid induced cytotoxicity assays. At the inhibitor: amylin ratio of 3:1 (amylin concentration was 15 μM), RA fully neutralized amylin-induced neurotoxicity while CA and SAA partially rescued the cell viability (Fig. 2C).

In parallel with biochemical and cell biology experiments, we performed molecular dynamics (MD) simulation studies. Simulations were done using fragments of amylin consisting of residues 20-29, which are important in the formation of amyloid in full length amylin. These fragments have been shown to form distinct β-sheet structures during MD simulation. Simulations were done using three human amylin (20-29) fragments in the absence of any inhibitor, in the presence of RA, and in the presence of CA (Fig. 2D). Significantly less β−sheet structure was observed in the presence of RA, and the amount of β-sheet structure was also reduced in the presence of CA (Tables S1 and S2). Analysis of inter-peptide interactions also revealed a reduction in the presence of RA and less so in the presence of CA as expected (Fig. 2D).

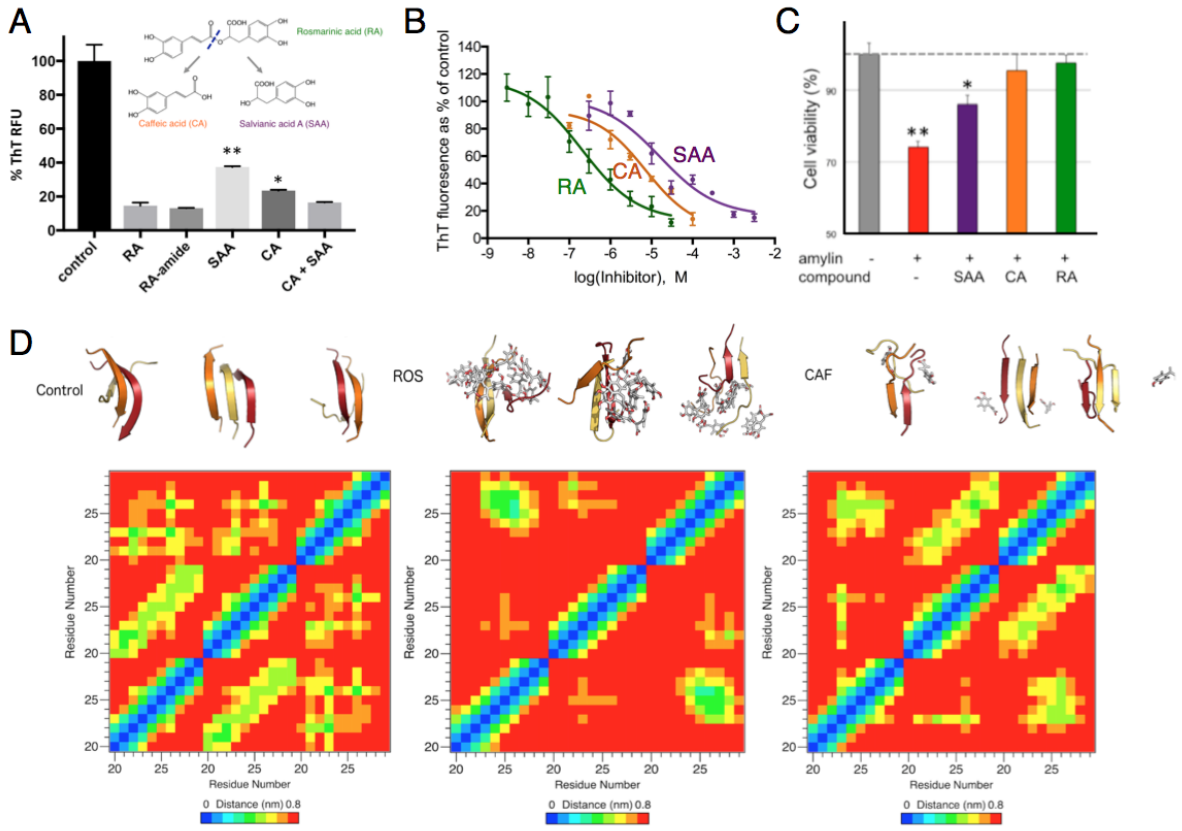

Figure 2. Additive effects of rosmarinic acid components in amylin amyloid inhibition. (A) ThT fluorescence based amyloid inhibition assay by RA and its hydrolytic components CA and SAA. Inhibition from 1:1 molar ratio of mixture of CA and SAA is comparable RA alone. (B) Amylin-ThT fluorescence based inhibition assay. IC_{50} is estimated to be 200-300 nM for RA, 7.2 μM for CA, and 90 μM for SAA. (C) Neutralization of amylin-induced neurotoxicity by RA, CA, and SAA in Neuro2A cells. Amylin concentration was 15 μM and the ratio of the inhibitor: amylin is 3:1. (D) MD simulation studies showing the effects of RA and CA on amylin fragment oligomerization. Dominant morphologies of $amylin_{20\text{-}29}$ trimer formation with and without the presence of RA and CA (at a 5:1 molar ratio of compound to amylin). Individual $amylin_{20\text{-}29}$ peptide fragments are shown in cartoon and colored red (peptide 1), orange (peptide 2) and yellow (peptide 3). RA and CA are shown as grey sticks, colored by element. *(continued below)*

For clarity, only CA molecules within 1.0 nm of the amylin$_{20\text{-}29}$ trimer are shown. Significantly less β-structure is observed in the presence of RA, and reduction in β-structure is observed in the case of CA. Residue-residue interaction plots for corresponding drug treatment are shown as "heat" maps in the lower panels. X- and Y-axis labels are in peptide fragment length (residues 20-29), with each repeating number (e.g., 20) being a separate peptide.

A Synthetic Rosmarinic Acid Analogue. To further optimize the inhibitory effects of RA, we synthesized multiple RA analogs that changed various functional groups. We found that one analog (RA-amide; Fig. 3A) significantly improved anti-amyloid activities in comparison with RA, even though both inhibitors showed similar 200-300 nM IC50 based on ThT fluorescence based inhibition assays (Fig. 3B): (i) RA-amide nearly completely prevented amylin amyloid deposition while RA only prevented amyloid fibril deposition about 50% of the time (Fig. 3C); (ii) RA-amide displayed significantly stronger potency in neutralizing amylin amyloid induced cytotoxicity in comparison with RA of the same concentration in both INS-1 cells and Neuro2A cells (Fig. 3E).

Like EGCG, we also discovered that both RA and RA-amide remodel freshly dissolved or preformed amylin amyloid into non-toxic aggregates, via presumably off-pathway channels(Figs. 4C,D;S6). Moreover distinct biochemical differences between RA and RA-amide remodeled aggregates were noted: RA-amide induced amyloid remodeling was more resistant to blockage by reducing reagent TCEP (higher concentration of TCEP was needed as compared to the case for RA; Fig. 3D); Additionally, RA-amide as well as EGCG remodeled aggregates are more soluble in non-denaturing Tris-buffer. In contrast, there are no discernable differences among RA, RA-amide and EGCG treatments when the amyloids were dissolved in 6.5 M urea denaturing conditions (Fig. S6). It is important to note that the differences observed in remodeled aggregate stability or solubility between RA and RA-amide does not imply differential or even advantageous anti-amyloid potency. Indeed, future work is required to determine if these differences or even remodeling phenomena in general, are linked in any way to the ability of RA-amide to exert greater cell rescue effects against amylin amyloid induced cytotoxicity compared to RA.

We next used the ThT assay in concert with a "two fractions" gel-based remodeling assay to (i) investigate the remodeling capacity of RA, its metabolites CA and SAA, as well as RA-amide at different stages of amyloid formation and (ii) assess if potential remodeling activity against pre-formed mature amyloid fibrils can result in their dissolution. A sharp drop in ThT signal was seen when preformed amylin amyloids were treated with RA, RA-amide, CA, SAA or a combination of CA and SAA at a 1:1 molar ratio that was equimolar to the final concentration employed for single compound treated amylin samples (Fig 4A). The amyloid remodeling potency depicted by these data is consistent with the anti-amyloid additive effects demonstrated by CA and SAA in Figs 2A and 2B. The same general steep drop in ThT fluorescence was seen when RA, RA-amide and positive control EGCG (previously indicated to disaggregate pre-formed amylin fibrils[30]) when spiked in at times before amyloid was formed (t=0), at the plateau phase of amyloid formation (t=17 hours) and finally after mature fibrils were formed (based on our TEM conditions, t=3 days) (Fig 4B). In some cases, this rapid drop in ThT fluorescence has been shown to reflect disaggregation of mature amyloid fibrils[30]. In other cases, this drop-in signal reflects an altered stability and seeding capacity of the remodeled fibril masses but not their solubility[29]. We used the gel remodeling assay to further clarify the meaning behind our observed ThT data and to determine if either RA or RA-A can dissolve mature amyloid fibrils as has been noted for EGCG[30]. Herein we spiked RA, RA-A, and EGCG with either freshly dissolved unaggregated amylin or with preformed mature amyloid fibrils, and after three days analyzed the insoluble and soluble fractions from both conditions via western blot analysis (Figs 4C and 4D). As expected for *bona fide* amyloid inhibitors, all compounds maintained a significant amount of peptide mass within the soluble fraction when spiked into solutions initially containing freshly dissolved unaggregated amylin (i.e., a significant amount of

insoluble amyloid formation was prevented). Moreover RA, RA-A and EGCG all induced amyloid remodeling towards denaturant resistant aggregates regardless if compounds were spiked into solutions that initially contain unaggregated amylin or solutions that contained preformed mature amylin fibrils. However, no compound was able to dissolve pre-formed amyloid fibrils, as reflected by the absence of any detectable amylin mass in the soluble fraction of amylin fibril samples treated with the compounds (Fig 4D). Further elucidating the mechanisms of remodeling and related changes of physical species and molecular interactions remain to be an interesting subject for further investigation (the work presented in Chapter 5 focuses on this subject).

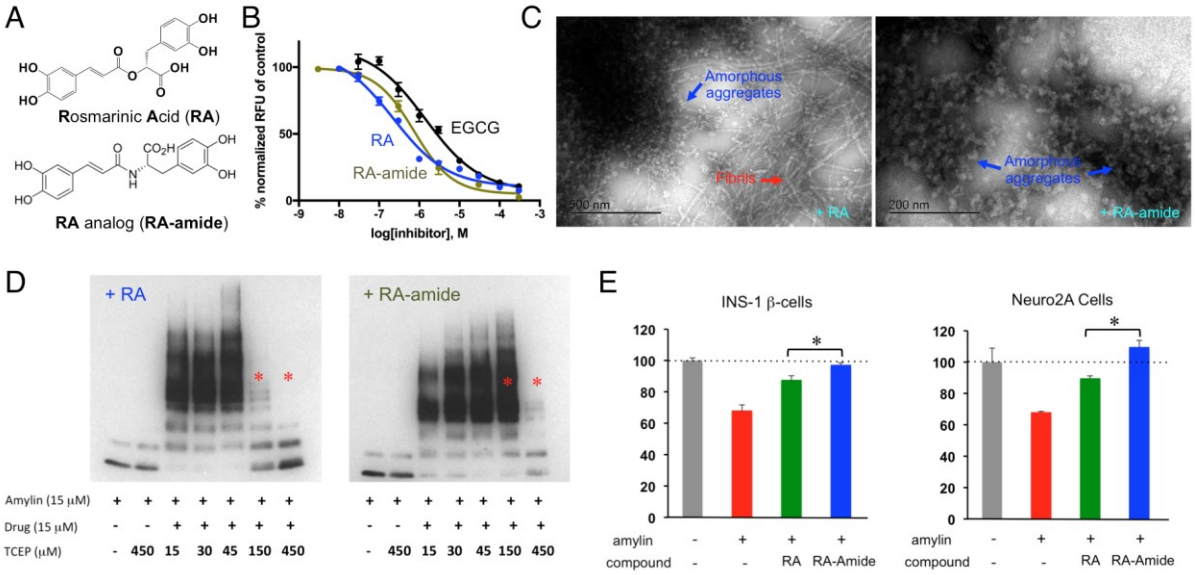

Figure 3. RA-amide displays improved amylin amyloid inhibition activity in multiple biochemical, biophysical and cell biology assays. (A) Chemical structures of RA and RA-amide are shown. (B) Amylin-ThT fluorescence based inhibition assay. Both RA and RA-amide are estimated to have an IC_{50} between 200-300 nM. IC_{50} (1 μM) for positive control, EGCG, is also shown. (C) TEM images of human amylin amyloid and its treatment with and without inhibitor treatment (1:10 amylin: drug molar ratio). Mature fibrils and non-toxic, amorphous aggregates are indicated by the red and blue arrows respectively. One out of two replicates indicate that RA treatment resulted in an estimated 50% of mature fibrils and 50% of amorphous aggregates whereas RA-amide treatment resulted in significantly higher, near 100% amorphous aggregates. However, a second replicate of the TEM experiment indicated only negligible differences between the amyloid inhibition demonstration by RA and RA-A (D) Reducing reagent TCEP blocks RA or RA-amide induced amyloid remodeling in a dose-dependent fashion. A ratio of 1:1 amylin: drug was used. Highlighted (red asterisks) show the differential effects by RA and RA-amide (RA-amide being a more potent remodeling reagent). (E) Neutralization of amylin amyloid-induced cytotoxicity by RA and RA-amide in INS-1 cells and Neuro2A cells. Amylin concentration was 3.75 μM and the ratio of inhibitor: amylin is 5:1.

***Ex vivo* Efficacies of RA and RA-amide.** Because rodent amylin is not amyloidogenic, a "humanized" diabetic rat model has been established where it over-expresses human amylin for mechanistic and translational applications[31]. As a step towards testing *in vivo* efficacy of RA and RA-amide, we obtained the sera samples from HIP rats that have been demonstrated to have amylin oligomers in the plasma samples[11]. Both RA and RA-amide effectively reduced amylin oligomers in the sera from HIP rats based on the oligomer sizes of 14-mers, 20-mers, and 22-mers detected by Western blotting with amylin specific antibody T-4157 (Fig 5A). We demonstrated that RA and RA-amide were effective to significantly reduce amylin oligomers in a dose-dependent fashion. We also showed that both RA and RA-amide can effectively reduce amylin oligomers (14-mers) in the sera from diabetic patients at an initial treatment concentration of 0.5 mM (Fig. 5B). We showed that reduction of amylin oligomers from diabetic patients was time-dependent. The sizes of respective oligomers were estimated without considering potential posttranslational modifications of human amylin *in vivo*. In sera from both HIP rats and diabetic patients, RA and RA-amide were effective at disrupting pre-formed amylin oligomers at concentration ranges of 0.1-0.5 mM. We speculate that effective concentrations to disrupt toxic amylin oligomers can be significantly lower if the incubation times were extended to mimic *in vivo* treatment time frames, which are typically 2-3-month durations).

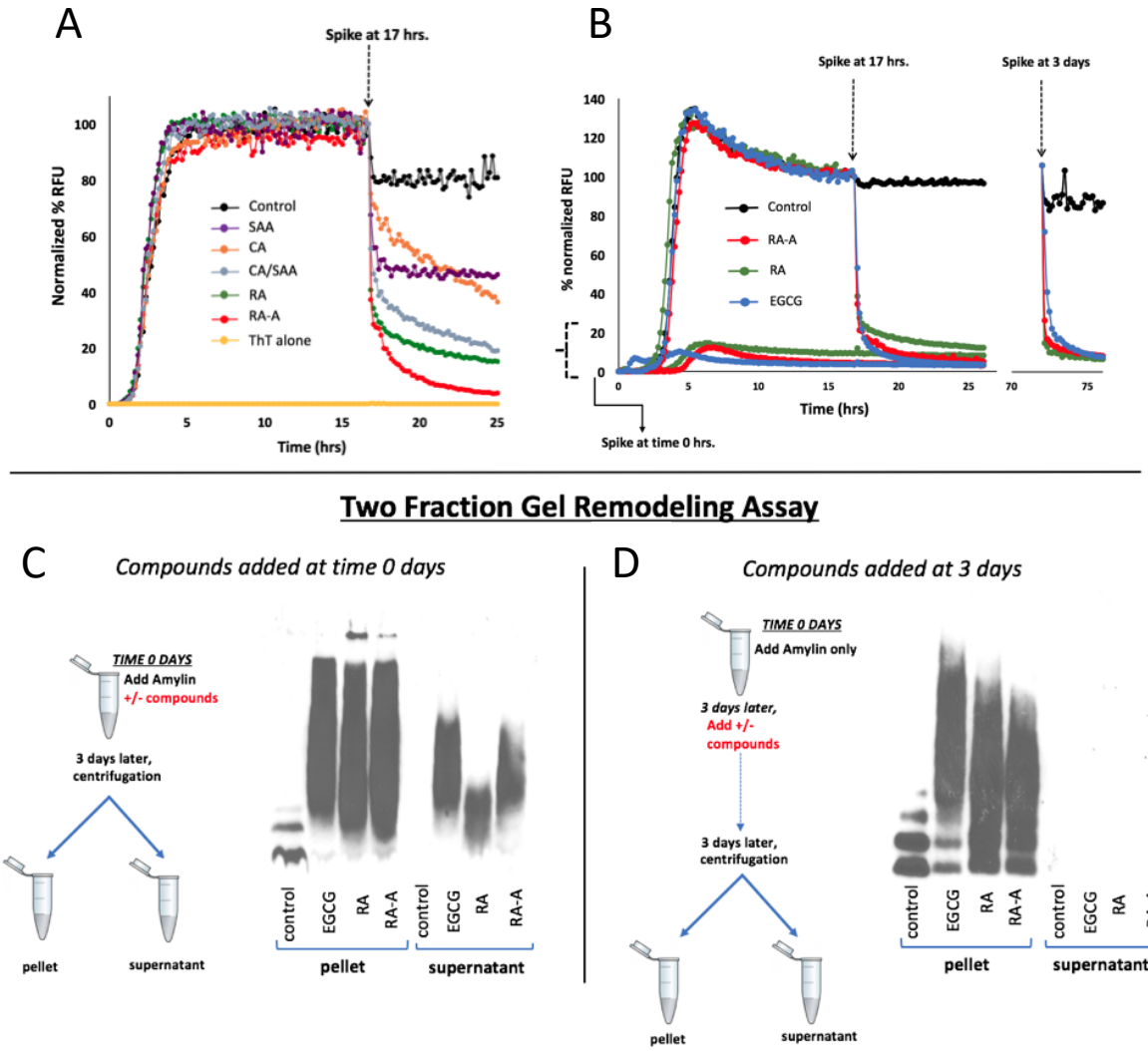

Figure 4. Amylin amyloid remodeling induced by ThT fluorescence and an orthogonal gel-based assay. (A) ThT fluorescence-based assay showed remodeling after spiking pre-formed amylin amyloid with either RA, CA, SAA, CA+SAA, and RA-amide (compounds were spiked in at the plateau phase, t=17 hrs., at 10:1 compound: amylin molar ratio). Likewise, at 10:1 molar ratio, similar activity was observed for RA, RA-A and EGCG when spiked in before amyloid had formed (time=0), or after amyloid formed (t=17 hours or t=72 hours) (C) Two fraction amyloid remodeling assay revealed that when added to freshly dissolved unaggregated amylin RA, RA-A and EGCG exerted remodeling activity concomitant with preventing insoluble amyloid formation by maintaining a significant amount of peptide *(continued below)*

mass within the supernatant, whereas all detectable peptide mass of the vehicle treated sample (presumably insoluble amyloid) was maintained within the pellet. (D) Two fraction amyloid remodeling assay for compounds spiked into preformed amyloid fibrils (t=3 days), demonstrated that RA, RA-A and EGCG induce denaturant resistant aggregate formation against pre-formed amyloid fibrils, whereas buffer treated amyloid fibrils dissociated to a distribution of monomer to trimer. However, these remodeling activities do not enable any compound to re-dissolve preformed insoluble amyloid mass. Quenching amyloid aggregation for both gel based remodeling assay conditions was achieved under denaturing conditions (i.e., samples were boiled for 5 minutes in solutions containing a final concentration of 6.5 M urea in 1X SDS-reducing sample buffer). Finally, all samples were separated by SDS-PAGE and probed by an antibody specific for human amylin (T-4157).

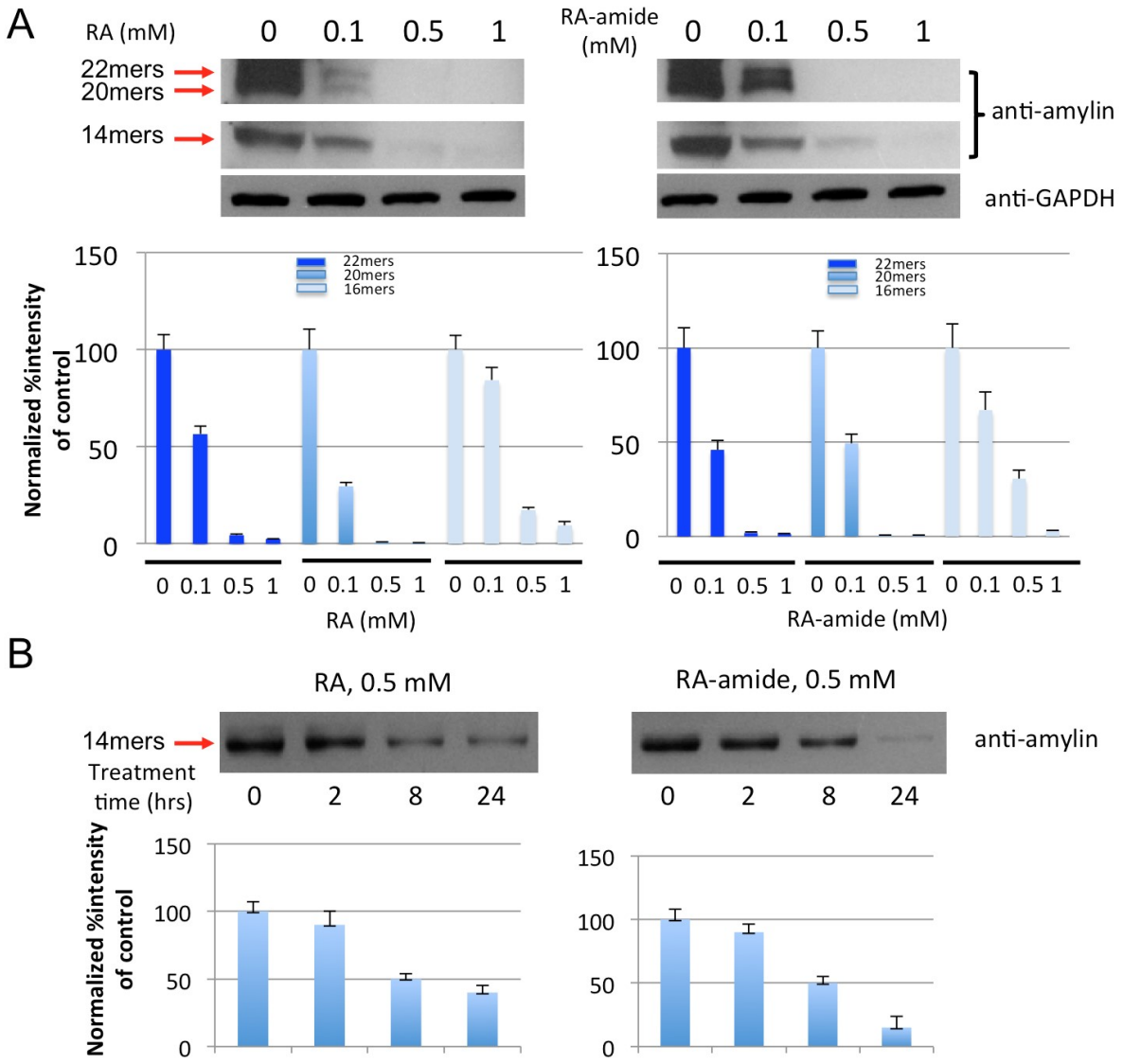

Figure 5. *Ex vivo* experiments demonstrate RA and RA-amide significantly reduced human amylin oligomers in the sera from HIP rat animal model and diabetic patients. HIP rat is an established diabetic rat model that overexpresses human amylin. (A) Western blot analyses of HIP rat sera treated with increased concentrations of RA or RA-amide as indicated. Samples were incubated with RA or RA-amide at indicated concentrations for 3 hours at 37 °C. Equal amounts of sera were loaded in each well as demonstrated by equal intensities of Western blot bands of GAPDH. Lanes labeled as 0 mM are the no treatment *(continued below)*

negative controls. Anti-human amylin blots were probed with amylin specific antibody (T-4157). Human amylin oligomers, 14-mer, 20-mer and 22-mer (estimated sizes) are indicated. Quantification of the Western blot results in Panel A by densitometry are shown in the lower panels in A. (B) Western blot analyses of diabetic patient sera treated with 0.5 mM of RA or RA-amide as indicated over a time course of 0, 2, 8, and 24 hours. Equal amounts of sera were loaded in each well as in A. Anti-human amylin blots were probed with amylin specific antibody (T-4157). Estimated size of the human amylin oligomer is indicated. Western blot results in Panel B were quantified by densitometry, shown in the lower panels in B.

Discussion

Botanical RA was identified from our library screening for amylin amyloid inhibition. The library is a collection of natural compounds that are known to have anti-diabetes and anti-inflammatory effects, but the mechanisms of action are poorly understood. RA has been tested as an inhibitor for Aβ amyloid in the past and showed *in vivo* efficacy in reducing Aβ plaques in the brain of an AD mouse model[32], which provides useful guidance on treatment doses and delivery route for our planned *in vivo* HIP rats studies (experiments are under way). On the other hand, our synthetic RA analogue, RA-amide, is a novel and more potent inhibitor in comparison with RA in multiple *in vitro* and cell-based assays (we have filed an US Provisional patent for this synthetic compound). Predictably, RA-amide will be an exciting new tool in aiding us to validate the novel molecular link of amylin between T2D and its complication of neurodegeneration.

What is the nature of amyloid inhibition by small molecules? Are they non-covalent, covalent or both? We propose that the catechol functional groups in RA and RA-amide can be autoxidized to *o*-quinone intermediates, which then react with amylin(see chapter 2)[33]. Quinones may be readily conjugated with the amine groups in Lys^{1} and/or Arg^{11} in human amylin and form Schiff base or Michael addition conjugates. If this covalent bond formation is indeed part of the inhibitory mechanisms, it will be interesting to isolate amylin-RA and/or amylin-RA-amide adduct(s) and map the adduct formation site(s) on the peptide and determine the type of conjugation reaction (Schiff base or Michael addition) using mass spectrometry. To extend the investigation of amylin-inhibitor conjugations further, it will be interesting and highly significant to detect amylin-RA and/or amylin-RA-amide conjugates from *in vivo* sera from HIP rats.

Using EGCG as a benchmark, we postulate that both RA and RA-amide will "remodel" human amylin oligomers and lead them to form non-toxic amorphous aggregates, which have the characteristic broad "smears" in SDS-PAGE experiments. We will correlate these biochemical observations with sample cytotoxicity by dot blotting analyses using oligomer-specific antibodies[34,35].

The concept of amylin as a specific molecular link between T2D and neurologic deficits, originally proposed by Despa and colleagues, is relatively new[11,36]. Validating this hypothesis will be highly significant, as it identifies a specific molecular link (and a novel therapeutic target) between diabetes and neurodegeneration, which supports the observation that obese/diabetic individuals are more prone to dementia/AD.

There is an urgent need for pathophysiological, diagnostic and therapeutic studies oriented specifically toward neuropathy in diabetic patients to better understand the factors that initiate and progress diabetic neuropathy and to develop more effective treatments. Showing that amylin oligomer/amyloid species, the entities that contribute to the development of T2D, are causally linked to neuro-dysfunction in T2D patients can greatly increase our ability to predict the onset of neuro-dysfunction in T2D. Moreover, if amylin accumulation in the brain is indeed important to trigger cerebral dysfunction, it will potentially be a new therapeutic target for T2D patients.

Materials and Methods

Peptides and Chemicals. Synthetic amidated human amylin was purchased from Genscript Inc. (Piscataway, NJ). Hexafluoro isopropanol (HFIP) and thioflavin T (ThT) were purchased from Sigma Aldrich (St. Louis, MO). Rosmarinic acid, caffeic acid, and salvianic acid A were purchased from Toronto Research Chemicals (North York, ON, Canada), Fisher Scientific Inc. (Hampton, NH), and Sigma-Aldrich Corp. (St. Louis, MO), respectively. Dulbecco's phosphate buffer saline (DBPS), pH 7.4 was purchased from Lonza (Walkersville, MD). Black 96 well non-stick-clear-bottom plates and optically clear sealing film were purchased from Greiner Bio-one (Germany) and Hampton Research (Aliso Viejo, CA). The 150-300 mesh formvar-carbon coated copper grids and uranyl acetate replacement solution (UAR) were purchased from Electron Microscopy Sciences (Hatfeild, PA).

Peptide preparation. A sample of 1- 0.5 milligrams of lyophilized amylin powder was initially dissolved in 100% HFIP at a final concentration of 1-2 mM. After HFIP dissolution, the peptide was vacuum dried again and re-dissolved with 100% DMSO to final concentration of 1-2mM. Aliquots were either lyophilized again prior to use in cell-based assays or dissolved directly into DPBS, 10 mM phosphate buffer pH 7.4 or 20 mM Tris-HCl pH 7.4 for all amylin amyloid-related *in vitro* assays. All remaining 1-2 mM stocks in 100% DMSO were stored at -80 °C until later use. The lyophilized powder from all compounds and ThT (Sigma-Aldrich Corp, St Louis, MO) were dissolved in DMSO (10 mM) and distilled water or relevant buffer (1-4 mM). These stocks were stored at -20 °C until later use. We determined that any residual DMSO present during amylin amyloid activity assays, (i.e. ThT fluorescence, TEM, PICUP, and inhibitor-induced amylin amyloid remodeling assays) had negligible effects on amyloid aggregation.

RA-amide Synthesis and Validation. 3,4-dihydroxyphenyl-alanine (DOPA) methyl ester was synthesized via Fischer esterification from a mixture of racemic DOPA in the presence of thionyl chloride and methanol (Wells et al, 2001). Coupling of this ester with caffeic acid in the presence of hydroxybenzotriazole hydrate (HOBt) and *N,N'*-dicyclohexylcarbodiimide (DCC; Lee et al, 2007) followed by hydrolysis with HCl gave compound target compound[37].

Step I:

^{1}H NMR (400 MHz, DMSO-*d*$_6$) δ 2.95 (2H, m, CH_2), 3.69 (3H, s, CH_3), 4.12 (1H, t, *J* = 6.40 Hz, CH), 6.44 (1H, dd, *J* = 8.03 Hz, *J* = 2.01 Hz, aromatic), 6.59 (1H, d, *J* = 2.01 Hz, aromatic), 6.67 (1H, d, *J* = 7.78 Hz, aromatic), 8.52 (2H, broad, NH_2), 8.93 (2H, d, *J* = 13.55 Hz, OH).

^{13}C NMR (400 MHz, DMSO-*d*$_6$) δ 35.3, 52.5, 53.4, 115.7, 116.7, 120.1, 124.8, 144.6, 145.3, 169.4.

Step II:

^{1}H NMR (400 MHz, DMSO-*d*$_6$) δ 2.81 (2H, m, CH_2), 3.60 (3H, s, CH_3), 4.47 (1H, m, CH), 6.39 (1H, d, *J* = 15.8 Hz, CH), 6.44 (1H, dd, *J* = 8.03, *J* = 2.26 Hz, aromatic), 6.59 (1H, d, *J* = 2.26 Hz, aromatic), 6.61 (1H, d, *J* = 8.10 Hz, aromatic), 6.72 (1H, d, *J* = 8.03 Hz, aromatic), 6.81 (1H, dd, *J* = 8.16, *J* = 2.13 Hz, aromatic), 6.92 (1H, d, *J* = 2.01 Hz, aromatic), 7.20 (1H, d, *J* = 15.81 Hz, CH), 8.30 (1H, d, *J* = 8.03 Hz, NH).

^{13}C NMR (400 MHz, DMSO-*d*$_6$) δ 36.4, 51.6, 54.0, 114.1, 115.5, 115.9, 116.5, 117.5, 119.6, 120.3, 125.9, 127.7, 139.9, 144.1, 145.1, 145.8, 147.9, 165.4, 172.6.

Step III:

^{1}H NMR (400 MHz, DMSO-*d*$_6$) δ 2.81 (2H, m, CH_2) 4.40 (1H, m, CH) 6.43 (1H, d, *J* = 15.6 Hz, CH) 6.47 (1H, d, *J* = 1.25 Hz, aromatic) 6.59 (1H, d, *J* = 8.03 Hz, aromatic) 6.62 (1H, d, *J* = 1.51 Hz, aromatic) 6.73 (1H, d, *J* = 8.28 Hz, aromatic) 6.82 (1H, dd, *J* = 8.16, *J* = 2.13 Hz, aromatic)

6.94 (1H, d, *J* = 1.80 Hz, aromatic) 7.18 (1H, d, *J* = 15.81 Hz, CH) 8.05 (1H, d, *J* = 7.78 Hz, NH).

^{13}C NMR (400 MHz, DMSO-d_6) δ 36.6, 54.4, 113.9, 115.2, 115.8, 116.5, 118.4, 119.8, 120.3, 126.3, 128.8, 139.3, 143.7, 144.8, 145.5, 147.4, 165.1, 173.7.

Based on high-resolution mass spectrometry (ESI), target compound $C_{18}H_{17}NO_7$ has molecular mass (M+H) of 358.09 daltons. Calculated molecular mass (M+H) is 359.10.

Cell Culture. Rat pancreatic INS-1 cells and mouse neuroblastoma Neuro-2A cells were generously provided by Profs. Dongmin Liu and Deborah Good (Virginia Tech), respectively. The SH-SY5Y cells were purchased from ATCC (#CRL-2266). Vascular Smooth Muscle Cells (VSMCs) were primary cells isolated from mouse aorta using the treatment of type I, II collagenases and type III elastase. INS-1, Neuro2A, SHSY-5Y were cultured per vendor instructions. Briefly, INS-1 cells were cultured in RPMI-1640 medium containing 10% fetal bovine serum and supplemented with 11.1 mM glucose, 1 mM sodium pyruvate, 10 mM HEPES, 50 μM β-mercaptoethanol, 23.8 mM $NaHCO_3$. The medium was changed every other day until the cells became confluent. Neuro2A cells were cultured in DMEM medium containing 1% non-essential amino acids, 1% L-glutamate and 10% FBS. SH-SY5Y cells were cultured in EMEM with 1% non-essential amino acids and 10% FBS. VSMCs were growing in DMEM containing 20% FBS.

Cytotoxicity Assay and Inhibitor Activity Quantification. An MTT-based cell viability assay was used. The INS-1 cells, Neuro-2A, SH-SY5Y cells were seeded in 96-well plate at a density of $4x10^4$ cells/well. After 24 hours incubation, cells are treated with either human amylin (3.75

μM) with or without specified natural compounds. Following another 24 hours incubation, 0.9 mM MTT was added to each well. The reduced insoluble MTT formazan product was then dissolved in SDS-HCl lysis buffer (5 mM HCl, 5% SDS) at 37 °C. Cell viability was determined by measurement of absorbance change at 570 nm using a spectrometric plate reader. Peptides dissolving buffer treated cells were used as positive control and taken as 100%, and 0.5% Triton X-100 treated cells at the start of the incubation period with test peptides were used as negative control and taken as 0%.

Thioflavin-T Fluorescence Assay. Fluorescence experiments were performed using a SpectraMax M5 plate reader (Molecular Devices, Sunnyvale, CA). All kinetic reads were taken at 25 °C in non-binding all black clear bottom Greiner 96-well plates covered with optically clear films and stirred for 10 seconds prior to each reading. ThT fluorescence was measured at 444 nm and 491 nm as excitation and emission wavelengths, respectively. Each kinetic assay consisted of final concentrations of 30 μM amylin and 10 μM. ThT inhibition constant (IC_{50}) values for dose response curves were estimated by multi-parameter logistic nonlinear regression analysis using GraphPad Prism software (version 6.0). All experiments were repeated three times using peptide stock solutions from the same lot.

Transmission Electron Microscopy (TEM). TEM images were obtained by a JEOL 1400 microscope operating at 120 kV. A sample containing 30 μM amylin (20 mM Tris-HCl, 2 % DMSO, pH 7.4) in the presence of drug or vehicle control was incubated for ≥48 hours at 37 °C with agitation. Prior to imaging, 10 μL of sample were blotted on a 200 mesh formvar-carbon coated grid for 5 minutes, and stained with uranyl acetate (1%). Both sample and stain solutions

were wicked dry (sample dried before addition of stain) by filter paper. Qualitative assessments of the amounts of fibrils or oligomers observed were made by taking representative images following a careful survey of each grid.

Statistical Analysis for *in vitro* data sets. Data presented as the mean ± S.E.M and the differences were analyzed with a one-way analysis of variance followed by Holm-Sidak's multiple comparisons (amylin kinetics) or unpaired Student's *t* test (cell based data). These tests were implemented within GraphPad Prism software (version 6.0). p values < 0.05 were considered significant.

MD Simulations. To simulate trimer formation of amylin in a reasonable time scale using MD simulations, the principal amyloidogenic region (residues 20-29) was extracted from an equilibrated MD structure of full length (residues 1-37) human amylin. Initial coordinates for full-length amylin were used from PDB access code 2L86 [42]. This PDB structure was chosen to best represent biologically active, monomeric amylin given the presence of the disulfide bound between Cys2-Cys7 and C-terminal amidation. However, 2L86 was solved in an SDS micelle environment, and to better mimic experimental procedures, we sought to use a structure of amylin that mimicked solution conditions (water and 150 mM NaCl). Simulations of full-length amylin were constructed by placing the structure of 2L86 in a cubic box with a minimum solute-box distance of 1.0 nm. The SPC water model[43] was used to solvate the box, and Na+ and Cl- ions were added to reach a final concentration of 0.150 mM NaCl and maintain a net neutral system. All simulations were done using the GROMACS software package, version 4.6.0 [44,45] and the GROMOS53a6 force field [46]. Energy minimization was performed using the steepest

descent method, with all protein heavy atoms being restrained during equilibration and later released during MD simulation. Equilibration was performed in two sequential steps, NVT and NPT. Three replicates starting with different random starting velocities in NVT were performed. NVT was performed for 100 ps and maintained at 310 K using the Berendsen weak coupling method [47]. Following NVT, NPT dynamics using a Nosé-Hoover thermostat [48,54] and a Parrinello-Rahman barostat [4,53]) to maintain temperature (310 K), and pressure (1 bar) was performed for 100 ps. Following equilibration, MD simulations were run using three-dimensional periodic boundary conditions with short-range cutoffs of 1.4 nm being applied to all nonbonded interactions. Long-range interactions were calculated using the smooth particle mesh Ewald (PME method) [50,51] using cubic interpolation and Fourier grid spacing of 0.16 nm. Bond lengths were constrained by P-LINCS [52], which enabled an integration time step of 0.2 fs. Simulations were run until the criteria of convergence was met, which consisted of stabilization of 100 ns for both backbone root-mean-square deviation (RMSD) and protein secondary structure, as determined by DSSP algorithm[38]. RMSD clustering using the method of Daura et al[39] was used to produce a representative structure of the last 100 ns of each replicate. The center structure of the replicate cluster structure, whose average secondary structure was closest to the set average, was chosen as the template for simulations of trimer formation of amylin$_{(20-29)}$.

Trimer Formation Residues 20-29 of amylin were extracted from the representative structure generated by MD simulations of full-length amylin in water and 0.150 mM NaCl. Acetyl and amide groups were added to cap the ends of the ten-residue fragment to negate spurious effects from having charges at the termini. The sequence of amylin$_{(20-29)}$ fragment is as follows: Ace-Ser-Asn-Asn-Phe-Gly-Ala-Ile-Leu-Ser-Ser-NH2. Three amylin$_{(20-29)}$ fragments were randomly

placed at least 2.0 nm away from each other in a cubic box with dimensions of 11 x 11x 11 nm, with a solute-box distance of 1.0 nm. For control simulations, no small molecules (SM) were added to the system. For simulations with rosmarinic acid or caffeic acid, five molecules were randomly placed in the system at least 2.0 nm away from amylin $_{(20\text{-}29)}$ fragments and other SMs. Topologies for rosmarinic acid and caffeic acid were generated using the PRODRG2 server[40] and refined by using charges and atom types found in functional groups within the GROMOS53a6 force field. For the ester functional group, parameters were taken from Horta et al.[41] and modified to account for the double bond in the "R" position. The charges assigned to each atom can be found in Table S1. Rosmarinic acid and caffeic acid were both deprotonated to mimic protonation state at pH 7.4 (net charge -1). The following systems were generated and are identified in the following way: Control – 3 amylin$_{(20\text{-}29)}$ fragments and no SMs, ROS – 3 amylin$_{(20\text{-}29)}$ fragments and five molecules of RA, and CA -- 3 amylin$_{(20\text{-}29)}$ fragments and five molecules of caffeic acid. These systems were then equilibrated and run in MD simulations in the same way as full-length amylin. Simulations were run to 600 ns, which was found to be an adequate amount of time for trimer formation and β-strand structure to remain stabilized in the control simulations. Backbone RMSD and secondary structure analysis were also used to determine convergence. Analysis was performed using programs in the GROMACS package and over the last 100 ns of simulation time (e.g., 500-600 ns). RMSD clustering with a cutoff of 0.2 nm was used to generate the structures shown in Figure 1. PyMOL was used for molecular visualization and any statistical analysis was done using a two-tailed *t*-test, with significance determined if $p < 0.05$.

Supplemental Tables and Figures

Table S1. Average secondary structure (shown in %) of trimer fragment formation (residues 20 – 29) of amylin with or without the presence of small molecules (SMs).[a]

System	Coil	β-strand	α-helix
WT	42 ± 11	58 ± 11	0 ± 0
RA	73 ± 13	28 ± 13	0 ± 0
CA	63 ± 17	37 ± 17	0 ± 0

[a] Percentages represent averages of 3 replicates over the final 100 ns of simulation time, with associated standard deviations.

Table S2. Average hydrogen bond presence between amylin fragments (20-29), amylin fragments and SMs, and between SMs. [a,b]

System	Protein-Protein	Protein-SM	SM-SM
WT	19 ± 3	n/a	n/a
RA	12 ± 3	13 ± 4	3 ± 1
CA	15 ± 2	4 ± 4	0.1 ± 0.1

[a] Averages of 3 replicates over the final 100 ns of simulation time, with associated standard deviations.

[b] n/a represents not applicable to the system tested.

Table S3. Average total SASA (nm^2) of amylin fragments (20-29) and SMs. [a,b]

System	Protein	SM
WT	24 ± 1	n/a
RA	29 ± 2	19 ± 1.6
CA	26 ± 1	14.7 ± 0.1

[a] Averages of 3 replicates over the final 100 ns of simulation time, with associated standard deviations.

[b] n/a represents not applicable to the system tested.

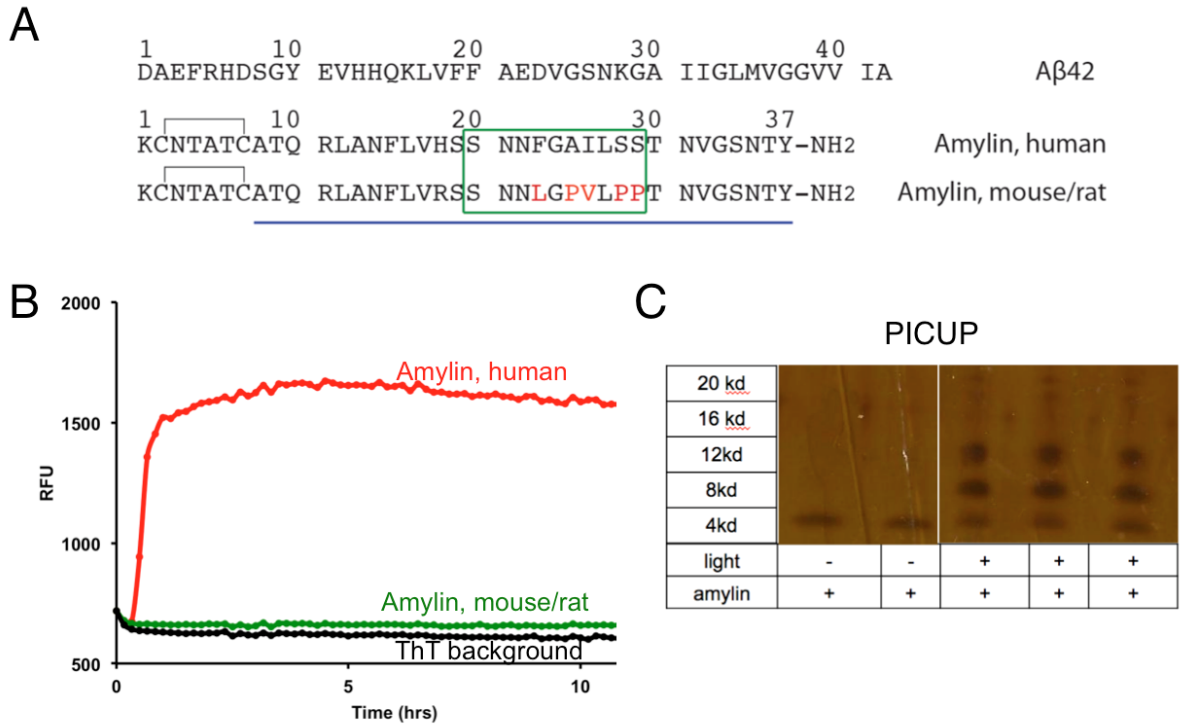

Figure S1. Amylin and Aβ42 sequences, ThT, and PICUP assays. (A) Amino acid sequences of human and rodent amylin and amyloid β peptide (Aβ) are shown. The green box indicates a key region in amylin sequence (20-29) determining human amylin amyloid formation. (B) ThT fluorescence assay showing human amylin amyloid formation, but not non-amyloidogenic rodent amylin. (C) Proof-of-principle *in vitro* photoinduced cross-linking of unmodified proteins (PICUP) assay that identifies stable amylin oligomers. The assay was analyzed with SDS-PAGE followed by silver staining.

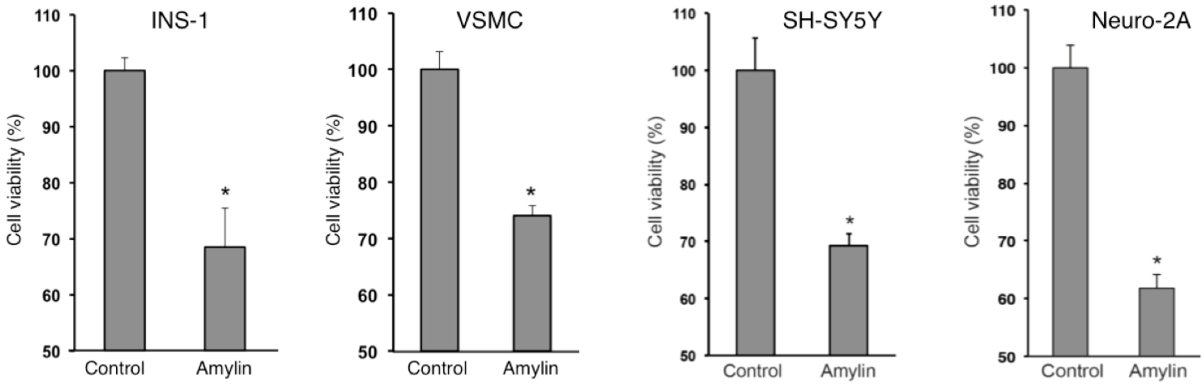

Figure S2. Cytotoxicity assays demonstrate the toxic effects of amylin against multiple relevant cell lines: pancreatic β-cells INS-1, mouse vascular smooth muscle cells, human SH-SY5Y neuronal cells, and mouse Neuro-2A cells, each at 5 μM concentration.

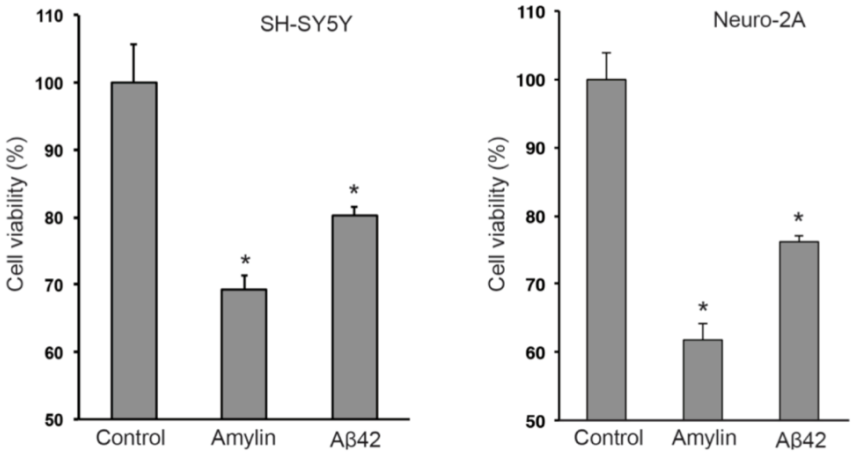

Figure S3. Neurotoxicity assays demonstrate the toxic effects of amylin and control amyloid β-peptide Aβ42, each at 10 μM for SH-SY5Y treatment or 15 μM for Neuro2A treatment.

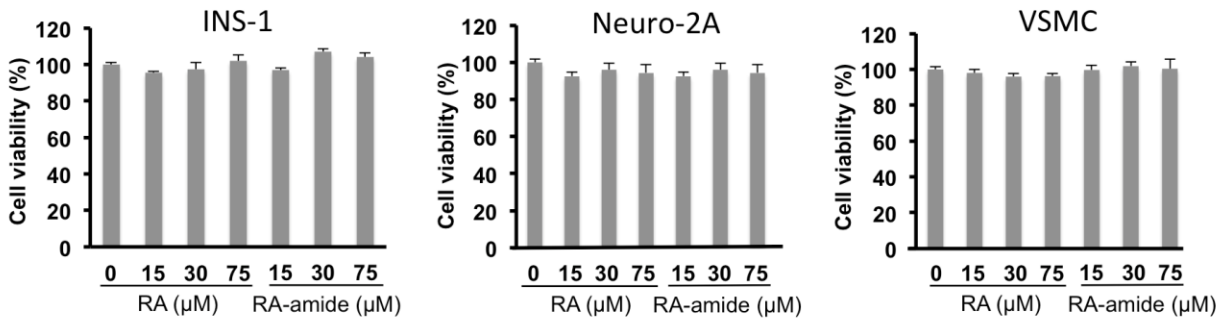

Figure S4. Control experiments demonstrate that RA and RA-amide have no effects on cell viability at the specified concentrations in INS-1, Neuro2A, and VSMC cell lines.

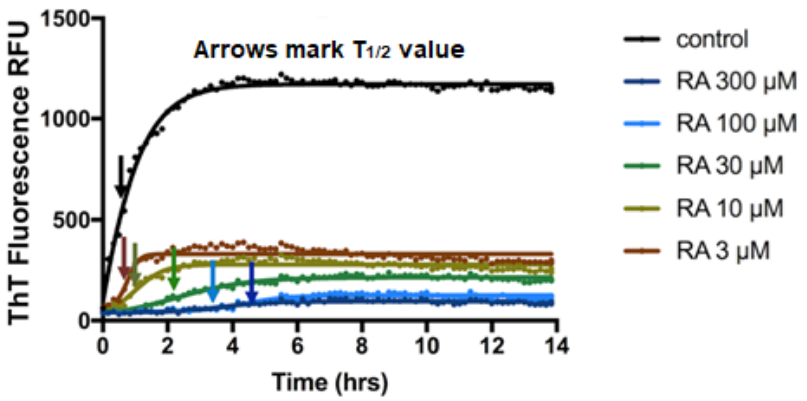

Figure S5. Measurement of $t_{1/2}$ of amylin amyloid formation by amylin-ThT fluorescence based assays. Concentration of amylin was 10 μM. With increased concentration of RA treatment, $t_{1/2}$ becomes significantly delayed (arrows).

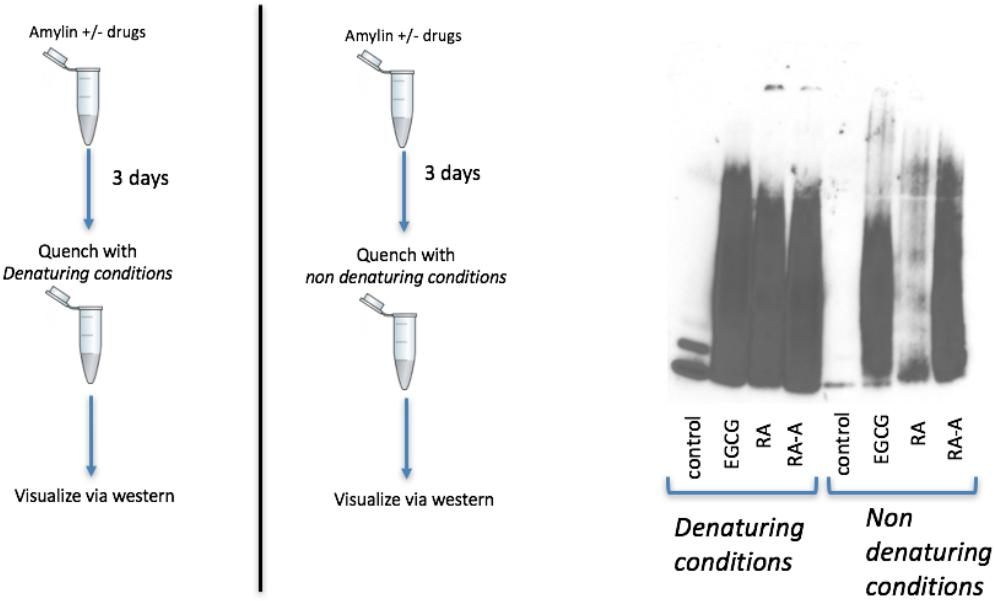

Figure S6 Single Fraction remodeling assays indicate RA remodeled aggregates are less soluble than EGCG or RA-A remodeled aggregates. Under denaturing conditions (defined by aggregating samples being quenched in 6.5 M Urea containing 1X SDS sample buffer and then boiled for 5-10 minutes), EGCG, RA and RA-A induced formation of a broad distribution of denaturant resistant amylin aggregates while only monomer and dimer bands of amylin were seen in untreated samples. In contrast, remodeled aggregates visualized under non-denaturing conditions (defined as aggregating samples that were quenched with 1X Sample buffer in the absence of SDS or heat treatment) show that RA induced remodeled aggregates are less soluble than RA-amide and EGCG stabilized aggregates. Both Single fraction assays were visualized by SDS-PAGE followed by western blot analysis via human amylin antibody (T-4157). Repeat experiments indicated that similar results were observed for samples that were quenched under non-denaturing conditions (as described above) regardless if they were exposed to SDS during PAGE or western blot transfer.

References

1. Chiti, F.; Dobson, C. M., Protein misfolding, functional amyloid, and human disease. *Annual review of biochemistry* **2006,** *75*, 333-66.
2. Knowles, T. P. J.; Vendruscolo, M.; Dobson, C. M., The amyloid state and its association with protein misfolding diseases. *Nat Rev Mol Cell Biol* **2014,** *15* (6), 384-396.
3. Krotee, P.; Rodriguez, J. A.; Sawaya, M. R.; Cascio, D.; Reyes, F. E.; Shi, D.; Hattne, J.; Nannenga, B. L.; Oskarsson, M. E.; Philipp, S.; Griner, S.; Jiang, L.; Glabe, C. G.; Westermark, G. T.; Gonen, T.; Eisenberg, D. S., Atomic structures of fibrillar segments of hIAPP suggest tightly mated beta-sheets are important for cytotoxicity. *eLife* **2017,** *6*.
4. Abedini, A.; Schmidt, A. M., Mechanisms of islet amyloidosis toxicity in type 2 diabetes. *FEBS letters* **2013,** *587* (8), 1119-27.
5. Enoki, S.; Mitsukawa, T.; Takemura, J.; Nakazato, M.; Aburaya, J.; Toshimori, H.; Matsukara, S., Plasma islet amyloid polypeptide levels in obesity, impaired glucose tolerance and non-insulin-dependent diabetes mellitus. *Diabetes Research and Clinical Practice* **1992,** *15* (1), 97-102.
6. Westermark, P., Quantitative studies on amyloid in the islets of Langerhans. *Upsala journal of medical sciences* **1972,** *77* (2), 91-4.
7. Verchere, C. B.; D'Alessio, D. A.; Palmiter, R. D.; Weir, G. C.; Bonner-Weir, S.; Baskin, D. G.; Kahn, S. E., Islet amyloid formation associated with hyperglycemia in transgenic mice with pancreatic beta cell expression of human islet amyloid polypeptide. *Proceedings of the National Academy of Sciences of the United States of America* **1996,** *93* (8), 3492-6.
8. Hoppener, J. W.; Ahren, B.; Lips, C. J., Islet amyloid and type 2 diabetes mellitus. *N Engl J Med* **2000,** *343* (6), 411-9.
9. Westermark, P.; Andersson, A.; Westermark, G. T., Islet amyloid polypeptide, islet amyloid, and diabetes mellitus. *Physiological reviews* **2011,** *91* (3), 795-826.
10. Jackson, K.; Barisone, G. A.; Diaz, E.; Jin, L. W.; DeCarli, C.; Despa, F., Amylin deposition in the brain: A second amyloid in Alzheimer disease? *Annals of neurology* **2013,** *74* (4), 517-26.
11. Srodulski, S.; Sharma, S.; Bachstetter, A. B.; Brelsfoard, J. M.; Pascual, C.; Xie, X. S.; Saatman, K. E.; Van Eldik, L. J.; Despa, F., Neuroinflammation and neurologic deficits in diabetes linked to brain accumulation of amylin. *Molecular neurodegeneration* **2014,** *9*, 30.
12. Despa, S.; Margulies, K. B.; Chen, L.; Knowlton, A. A.; Havel, P. J.; Taegtmeyer, H.; Bers, D. M.; Despa, F., Hyperamylinemia contributes to cardiac dysfunction in obesity and diabetes: a study in humans and rats. *Circulation research* **2012,** *110* (4), 598-608.
13. Despa, S.; Sharma, S.; Harris, T. R.; Dong, H.; Li, N.; Chiamvimonvat, N.; Taegtmeyer, H.; Margulies, K. B.; Hammock, B. D.; Despa, F., Cardioprotection by controlling hyperamylinemia in a "humanized" diabetic rat model. *Journal of the American Heart Association* **2014,** *3* (4).
14. Eisele, Y. S.; Monteiro, C.; Fearns, C.; Encalada, S. E.; Wiseman, R. L.; Powers, E. T.; Kelly, J. W., Targeting protein aggregation for the treatment of degenerative diseases. *Nature reviews. Drug discovery* **2015,** *14* (11), 759-80.
15. Yamada, M.; Ono, K.; Hamaguchi, T.; Noguchi-Shinohara, M., Natural Phenolic Compounds as Therapeutic and Preventive Agents for Cerebral Amyloidosis. *Advances in experimental medicine and biology* **2015,** *863*, 79-94.

16. Ono, K.; Hasegawa, K.; Naiki, H.; Yamada, M., Curcumin has potent anti-amyloidogenic effects for Alzheimer's beta-amyloid fibrils in vitro. *Journal of neuroscience research* **2004,** *75* (6), 742-50.
17. Rigacci, S.; Guidotti, V.; Bucciantini, M.; Parri, M.; Nediani, C.; Cerbai, E.; Stefani, M.; Berti, A., Oleuropein aglycon prevents cytotoxic amyloid aggregation of human amylin. *The Journal of Nutritional Biochemistry* **2010,** *21* (8), 726-735.
18. Ardah, M. T.; Paleologou, K. E.; Lv, G.; Menon, S. A.; Abul Khair, S. B.; Lu, J. H.; Safieh-Garabedian, B.; Al-Hayani, A. A.; Eliezer, D.; Li, M.; El-Agnaf, O. M., Ginsenoside Rb1 inhibits fibrillation and toxicity of alpha-synuclein and disaggregates preformed fibrils. *Neurobiology of disease* **2015,** *74*, 89-101.
19. Velander, P.; Wu, L.; Ray, W. K.; Helm, R. F.; Xu, B., Amylin Amyloid Inhibition by Flavonoid Baicalein: Key Roles of Its Vicinal Dihydroxyl Groups of the Catechol Moiety. *Biochemistry* **2016**.
20. Wu, L.; Velander, P.; Liu, D.; Xu, B., Olive Component Oleuropein Promotes beta-Cell Insulin Secretion and Protects beta-Cells from Amylin Amyloid-Induced Cytotoxicity. *Biochemistry* **2017,** *56* (38), 5035-5039.
21. Ehrnhoefer, D. E.; Bieschke, J.; Boeddrich, A.; Herbst, M.; Masino, L.; Lurz, R.; Engemann, S.; Pastore, A.; Wanker, E. E., EGCG redirects amyloidogenic polypeptides into unstructured, off-pathway oligomers. *Nature structural & molecular biology* **2008,** *15* (6), 558-66.
22. Meng, F.; Raleigh, D. P.; Abedini, A., Combination of kinetically selected inhibitors in trans leads to highly effective inhibition of amyloid formation. *Journal of the American Chemical Society* **2010,** *132* (41), 14340-2.
23. Pithadia, A. S.; Bhunia, A.; Sribalan, R.; Padmini, V.; Fierke, C. A.; Ramamoorthy, A., Influence of a curcumin derivative on hIAPP aggregation in the absence and presence of lipid membranes. *Chemical communications (Cambridge, England)* **2016,** *52* (5), 942-5.
24. Cheng, B.; Liu, X.; Gong, H.; Huang, L.; Chen, H.; Zhang, X.; Li, C.; Yang, M.; Ma, B.; Jiao, L.; Zheng, L.; Huang, K., Coffee components inhibit amyloid formation of human islet amyloid polypeptide in vitro: possible link between coffee consumption and diabetes mellitus. *Journal of agricultural and food chemistry* **2011,** *59* (24), 13147-55.
25. Noor, H.; Cao, P.; Raleigh, D. P., Morin hydrate inhibits amyloid formation by islet amyloid polypeptide and disaggregates amyloid fibers. *Protein science : a publication of the Protein Society* **2012,** *21* (3), 373-82.
26. Cheng, B.; Gong, H.; Li, X.; Sun, Y.; Chen, H.; Zhang, X.; Wu, Q.; Zheng, L.; Huang, K., Salvianolic acid B inhibits the amyloid formation of human islet amyloid polypeptide and protects pancreatic beta-cells against cytotoxicity. *Proteins* **2013,** *81* (4), 613-21.
27. Tu, L. H.; Young, L. M.; Wong, A. G.; Ashcroft, A. E.; Radford, S. E.; Raleigh, D. P., Mutational analysis of the ability of resveratrol to inhibit amyloid formation by islet amyloid polypeptide: critical evaluation of the importance of aromatic-inhibitor and histidine-inhibitor interactions. *Biochemistry* **2015,** *54* (3), 666-76.
28. Bieschke, J.; Russ, J.; Friedrich, R. P.; Ehrnhoefer, D. E.; Wobst, H.; Neugebauer, K.; Wanker, E. E., EGCG remodels mature α-synuclein and amyloid-β fibrils and reduces cellular toxicity. *Proceedings of the National Academy of Sciences of the United States of America* **2010,** *107* (17), 7710-7715.

29. Palhano, F. L.; Lee, J.; Grimster, N. P.; Kelly, J. W., Toward the Molecular Mechanism(s) by Which EGCG Treatment Remodels Mature Amyloid Fibrils. *Journal of the American Chemical Society* **2013,** *135* (20), 7503-7510.
30. Meng, F.; Abedini, A.; Plesner, A.; Verchere, C. B.; Raleigh, D. P., The flavanol (-)-epigallocatechin 3-gallate inhibits amyloid formation by islet amyloid polypeptide, disaggregates amyloid fibrils, and protects cultured cells against IAPP-induced toxicity. *Biochemistry* **2010,** *49* (37), 8127-33.
31. Butler, A. E.; Jang, J.; Gurlo, T.; Carty, M. D.; Soeller, W. C.; Butler, P. C., Diabetes due to a progressive defect in beta-cell mass in rats transgenic for human islet amyloid polypeptide (HIP Rat): a new model for type 2 diabetes. *Diabetes* **2004,** *53* (6), 1509-16.
32. Hamaguchi, T.; Ono, K.; Murase, A.; Yamada, M., Phenolic Compounds Prevent Alzheimer's Pathology through Different Effects on the Amyloid-β Aggregation Pathway. *The American journal of pathology* **2009,** *175* (6), 2557-2565.
33. Sato, M.; Murakami, K.; Uno, M.; Nakagawa, Y.; Katayama, S.; Akagi, K.; Masuda, Y.; Takegoshi, K.; Irie, K., Site-specific inhibitory mechanism for amyloid beta42 aggregation by catechol-type flavonoids targeting the Lys residues. *The Journal of biological chemistry* **2013,** *288* (32), 23212-24.
34. Kayed, R.; Glabe, C. G., Conformation-Dependent Anti-Amyloid Oligomer Antibodies. In *Methods in enzymology*, Indu, K.; Ronald, W., Eds. Academic Press: 2006; Vol. Volume 413, pp 326-344.
35. Glabe, C. G., Structural classification of toxic amyloid oligomers. *The Journal of biological chemistry* **2008,** *283* (44), 29639-43.
36. Liu, P.; Reed, Miranda N.; Kotilinek, Linda A.; Grant, Marianne K. O.; Forster, Colleen L.; Qiang, W.; Shapiro, Samantha L.; Reichl, John H.; Chiang, Angie C. A.; Jankowsky, Joanna L.; Wilmot, Carrie M.; Cleary, James P.; Zahs, Kathleen R.; Ashe, Karen H., Quaternary Structure Defines a Large Class of Amyloid-β Oligomers Neutralized by Sequestration. *Cell reports 11* (11), 1760-1771.
37. Park, K.; Hoffmeister, B.; Han, D. K.; Hasty, K., Therapeutic ultrasound effects on interleukin-1beta stimulated cartilage construct in vitro. *Ultrasound Med Biol* **2007,** *33* (2), 286-95.
38. Kabsch, W.; Sander, C., Dictionary of protein secondary structure: pattern recognition of hydrogen-bonded and geometrical features. *Biopolymers* **1983,** *22* (12), 2577-637.
39. Daura, X.; van Gunsteren, W. F.; Mark, A. E., Folding-unfolding thermodynamics of a beta-heptapeptide from equilibrium simulations. *Proteins* **1999,** *34* (3), 269-80.
40. Schuttelkopf, A. W.; van Aalten, D. M., PRODRG: a tool for high-throughput crystallography of protein-ligand complexes. *Acta Crystallogr D Biol Crystallogr* **2004,** *60* (Pt 8), 1355-63.
41. Horta, B. A.; Fuchs, P. F.; van Gunsteren, W. F.; Hunenberger, P. H., New Interaction Parameters for Oxygen Compounds in the GROMOS Force Field: Improved Pure-Liquid and Solvation Properties for Alcohols, Ethers, Aldehydes, Ketones, Carboxylic Acids, and Esters. *J Chem Theory Comput* **2011,** *7* (4), 1016-31.
42. Ravi Prakash Reddy Nanga, Jeffrey R. Brender, Subramanian Vivekanandan, Ayyalusamy Ramamoorthy. Structure and Membrane Orientation of IAPP in its Natively Amidated Form at Physiological pH in a Membrane Environment. *Biochim Biophys Acta.* **2011,** *1808(10): 2337–2342.*

43. H.J.C.Berendsen, J.P.M.Postma, W.F.van Gunsteren and J. Hermans Interaction Models for Water in Relation to Protein Hydration. *Nature **1981*** 11(1):331-342
44. Hess B, Kutzner C, Van der Spoel D, Lindahi E. GROMACS 4: Algorithms for Highly Efficient, Load-Balanced, and Scalable Molecular Simulation. *J. Chem Theory Comput.* **2008**, 4(3):435-47
45. Pronk S, Páll S, Schulz R, Larsson P, Bjelkmar P, Apostolov R, Shirts MR, Smith JC, Kasson PM, van der Spoel D, Hess B, Lindahl E. GROMACS 4.5: a high-throughput and highly parallel open source molecular simulation toolkit. *Bioinformatics. **2013*** Apr 1;29(7):845-54
46. Soares TA, Daura X, Oostenbrink C, Smith LJ, van Gunsteren WF. Validation of the GROMOS force-field parameter set 45Alpha3 against nuclear magnetic resonance data of hen egg lysozyme. *J Biomol NMR*. ***2004*** 30(4):407-22.
47. H. J. C. Berendsen, J. P. M. Postma, W. F. van Gunsteren, A. DiNola, J. R. Haak. Molecular dynamics with coupling to an external bath. *Journal of Chemical Physics* **1984**, 81, 3684.
48. William G. Hoover. Canonical dynamics: Equilibrium phase-space distributions. *Phys. Rev. A* **1985,** 31, 1695.
49. Parrinello, M.; Rahman, A. Polymorphic transitions in single crystals: A new molecular dynamics method. *Journal of Applied Physics.* **1981,** 52(12) 7182-7190.
50. Ulrich Essmann, Lalith Perera, and Max L. Berkowitz.A smooth particle mesh Ewald method. *J Chem Phys*. **1995**, 103 (19) 8577-8593.
51. Tom Darden, Darrin York, Lee Pedersen. Particle mesh Ewald: An $N\cdot\log(N)$ method for Ewald sums in large systems. *The Journal of Chemical Physics* **1993,** 98, 10089.
52. Berk, Hess. P-LINCS: A Parallel Linear Constraint Solver for Molecular Simulation. *J. Chem. Theory Comput.*, **2008**, *4* (1), 116–122
53. Nosé S, Klein ML. Constant pressure molecular dynamics for molecular systems. Mol Phys. **1983**;50(5):1055-76.
54. Nosé S. A molecular dynamics method for simulations in the canonical ensemble. Mol Phys. **2002**;100(1):191-8.

Chapter 5: Mechanisms of Amyloid Inhibition: Redox State is a Key Determinant of the Activities of a Broad Class of Catechol-Containing Inhibitors

I acknowledge pleasant and fruitful collaborations with Dr. Sherry Hildreth and Dr. Rich Helm, who performed and analyzed LC-MS experiments for norepinephrine.

Abstract

Mechanisms of amyloid inhibition remain poorly understood, in part because most protein targets of amyloid assembly are initially partially unfolded or intrinsically disordered, which limits structural studies. Herein we employed a small molecule screening approach to identify inhibitors against tau 2N4R, $A\beta_{42}$ and human amylin to aid in mechanistic studies. One remarkable class of inhibitors identified against all three amyloid proteins were catechol containing compounds. Follow-up mechanistic studies confirm that autoxidation is critical to catecholamine anti-amyloid activities, but also enhances anti-amyloid activities for both catechol and catechol-containing compounds in general. Lastly, we also show that while autoxidation is essential for catechol mediated amyloid remodeling activities, these activities may represent epiphenomenon that are not required for anti-amyloid activities in general.

Introduction

Amyloid diseases represent some of the most debilitating and increasingly more common human diseases that include neurodegenerative diseases such as Alzheimer's disease and Parkinson's disease, as well as other chronic diseases including type 2 diabetes[1-3]. While there are currently no FDA approved anti-amyloid therapeutics available, decades of data continue to support the notion that one of the most viable therapeutic targets against amyloid disease continues to be the misfolding amyloid proteins themselves[4-6]. Recent high-resolution insights gained from several high-resolution amyloid structures, and atomic details on their interactions with amyloid inhibitors, has provided potentially exciting new avenues from which to identify, characterize and optimize lead candidates that could potentially reach the clinic[7-12]. Inevitably key to this process is achieving a better understanding of inhibitor mechanisms. Recent mechanistic insights have elucidated some of the key covalent and non-covalent forces responsible for determining small molecule-amyloidogenic protein interactions at various stages of amyloid formation[13]. Several examples have been described, such as stabilizing the soluble native conformations of some amyloidogenic proteins[14], perturbing or "remodeling" unaggregated or pre-aggregated amyloid species towards forming presumably innocuous, non-amyloidogenic aggregates[15-18], or even accelerating amyloid formation[19]. However, in many cases, a clear link between the chemical mode of action of an inhibitor and its macromolecular partner is poorly defined. Moreover, the biophysical and biochemical basis of inhibitor-perturbed amyloid aggregation pathways or alternate aggregate assemblies is not always clear.

Results/Discussion

In our studies, using a semi high throughput Thioflavin T screening platform, we performed a drug-repurposing screen on a library of 700 drugs or investigational compounds with diverse molecular scaffolds to identify broad classes of small molecule amyloid inhibitors that exhibited strong activities against three pathological amyloidogenic targets, these being tau 2N4R, $A\beta_{42}$, and amylin (Fig. 1). Analysis from this work identified several noteworthy classes of compounds that inhibited amyloid formation on all three targets. These included tetracyclines, anthraquinones and catechol-containing molecules amongst other miscellaneous structures (Figure S1). Secondary validation of a variety of lead candidates selected from each class was achieved by confirming that they exhibit dose response activities against amyloid formation and or prevented early oligomer interactions (Figure S2). Further inspection of the initial screening results indicated that catechol-containing compounds and redox-related anthraquinones comprised a high proportion of the top lead candidate inhibitors against each protein or peptide, as defined as exhibiting greater than three standard deviation of the (relative fluorescence units) RFU units below buffer treated amylin controls (Figure 1). In further support that the catechol functional group alone represents an important active component present within the group of catechol-containing compounds initially identified (Figure S1), ThT assays and preliminary transmission electron microscopy (TEM) data confirmed that catechol, but not phenol, exhibits strong anti-amyloid activities (Figure 1). These data support the hypothesis that the catechol functional group possess general anti-amyloid activities, which has also recently been suggested by individual case studies[18, 20-21], other small molecule screening experiments[20] and large scale data mining efforts.[13, 22] However, catechols and quinones are considered to be frequent Pan Assay Interference Compounds (PAINS)[28-29], therefore caution needs to be taken to validate

catechol-containing amyloid inhibitors using multiple orthogonal *in vitro* and cell-based assays as described in our previous work[18, 20]. Yet multiple catechol-containing compounds and other PAINS-like compounds, such as EGCG, curcumin, and oleuropein, demonstrated significant *in vivo* efficacies in reducing amyloid plaques[13]. We also demonstrated structure-activity relationship on two catechol-containing compounds, baicalein and oleuropein[18, 20], the criteria Baell and colleagues recommend using to exclude PAINS compounds. Furthermore, these same compounds are also commonly found in polyphenol-rich diets that are associated with numerous health benefits, and therefore, could potentially be developed as nutraceuticals. Thus, despite their classification as PAINS molecules, we argue that catechol-containing molecules represent a *bona fide* group of amyloid inhibitors as promising chemical biology tools to aid in future amyloid research.

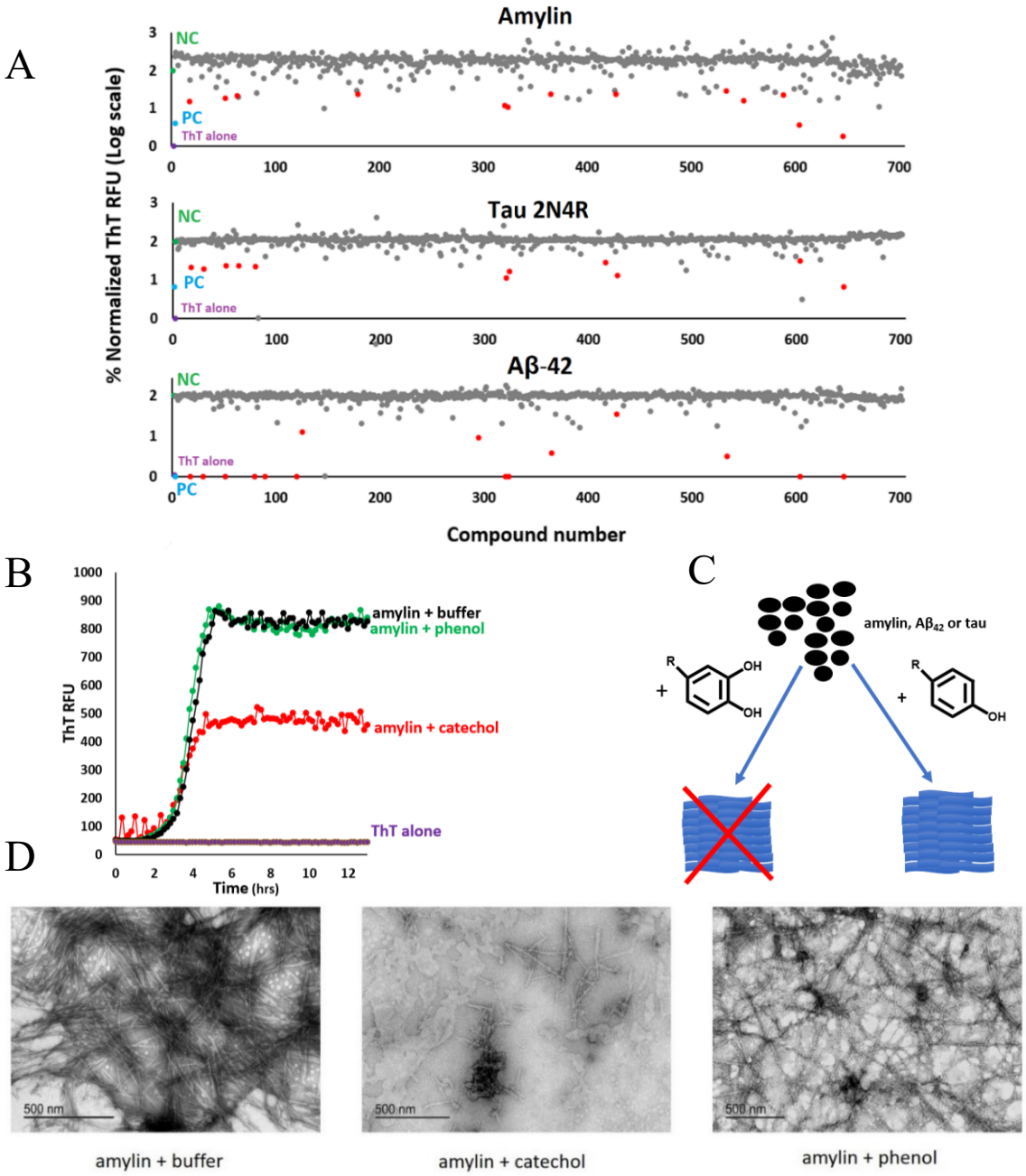

Figure 1: Small molecule anti-amyloid ThT screen identifies catechol-containing compounds and redox related anthraquinones as broad classes of potent amyloid inhibitors. (A) Catechol-containing compounds or anthraquinones (denoted by red dots) were observed to comprise 61%, 54% and 33% of the top lead candidates against tau 2N4R, Aβ and amylin, respectively. (top lead candidates were defined by exhibiting a ThT fluorescent signal ≥ three standard deviations below buffer treated negative controls identified against amylin. *(continued next page)*

Buffer treated negative controls (NC), are shown in green. Positive controls (PC, shown in magenta) included amyloid proteins treated with either rosmarinic acid (RA) or epigallocatechin gallate (EGCG), two previously confirmed amyloid inhibitors[13]. (B) Catechol but not phenol demonstrates strong anti-amyloid effects as exhibited by ThT (panel B) and TEM (panel D) assays. Typical molar ratios of compound to amyloidogenic protein were 2:1 for all ThT assays and 50:1 for TEM assays. For the model in (C) black circles represent monomeric amyloid protein; blue ribbon structures represent amyloid fibrils.

Accordingly, we sought to conduct mechanistic studies to clarify the chemical modes of action of the anti-amyloid activities of the catechol-containing compounds. Several recent case studies have indicated that autoxidation enhances or is even necessary for the observed anti-amyloid activities associated with certain catechol-containing amyloid inhibitors including baicalein, taxifolin and catecholamines[23-26]. Based on these data, and the fact that redox related anthraquinone compounds also exhibited strong anti-amyloid activities as indicated from our initial screening effort, we hypothesized that autoxidation represents a general factor that is linked to anti-amyloid activity of catechol-containing compounds. To test this hypothesis, numerous aged versus non-aged catechol-containing compounds were compared for their anti-amyloid activities. Under these conditions "aged" and "non-aged" terms define compounds that initially were prepared from the same powder stock but that were either incubated at 37 C° (i.e. "aged" condition) or -80 C° (i.e. "fresh" condition) for two days prior to being added to freshly dissolved solutions of amylin. In virtually all cases, aged catechol containing compounds but not negative control phenol and non-catechol containing amyloid inhibitor morin, exhibited greater activity than their non-aged counterparts (Figure 2). Moreover, these trends were recapitulated under aerobic but not anaerobic conditions for selected catecholamines and to a lesser extent for natural compound-catechol containing amyloid inhibitors (Figure S4). To show that the enhanced amyloid activities under aerobic but not anaerobic conditions were directly linked to the chemical change that occurs during autoxidation, UV-Visible time course spectra confirmed that oxidative chemical change only was detectable under aerobic conditions (Figure S3, Figure 3).

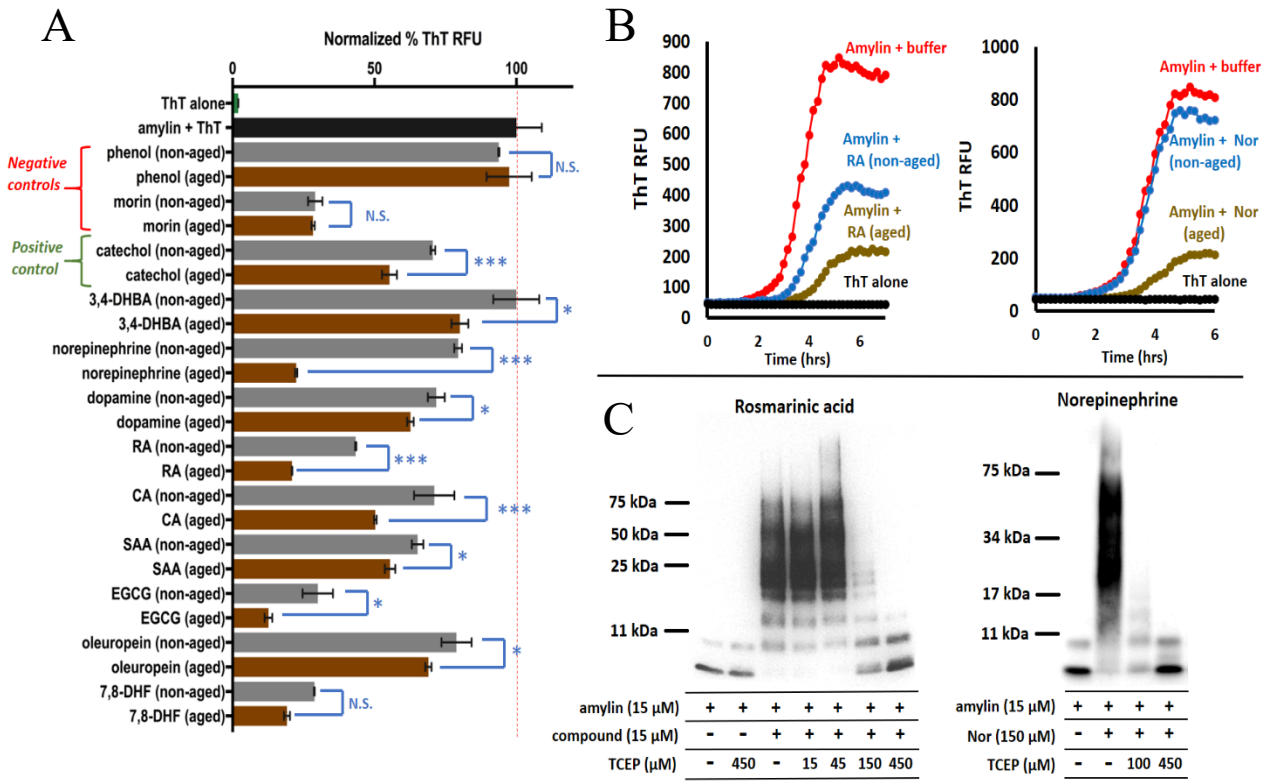

Figure 2: Autoxidation enhances anti-amyloid activities associated with a broad group of catechol-containing compounds. (A) Aged catechol containing compounds (brown bars), but not negative controls phenol (non-amyloid inhibitor) or morin (amylin amyloid inhibitor) display enhanced anti-amyloid activity compared to their non-aged counterparts (grey bars). All aged and non-aged treated amylin aggregation reactions were normalized to buffer treated amylin controls (black bar) indicated by the dashed red line. (B) ThT time course taken from data shown in (A) of aged versus non-aged RA and norepinephrine treated amylin aggregations reactions. (C) Dose response effects of TCEP on inhibiting RA and norepinephrine amyloid remodeling activity. Abbreviations: 7,8-dihydroxy flavone (7,8-DHF), rosmarinic acid (RA), caffeic acid (CA), salvianic acid A(SAA), 3,4-dihydroxybenzoic acid (3,4-DHBA). Statistics were conducted using one-way ANOVA, Sidak's multiple comparisons test: *p <0.05 ,** p <0.01, ***p < 0.001

While the mechanistic aims in this study were focused on broadly characterizing how autoxidation influences catechol mediated anti-amyloid activities, LC-MS data identified several oxidized byproducts within representative catecholamine, norepinephrine (Figure 3), that appeared during a similar time course observed for the anti-amyloid activities exhibited by norepinephrine as assessed by the gel remodeling, ThT and TEM assays (Figs. 3 and 4). Currently, ongoing studies are being employed to clarify the identity of these species. Collectively, these data suggest that autoxidation represents a general pathway that enhances catechol-containing compound anti-amyloid activities.

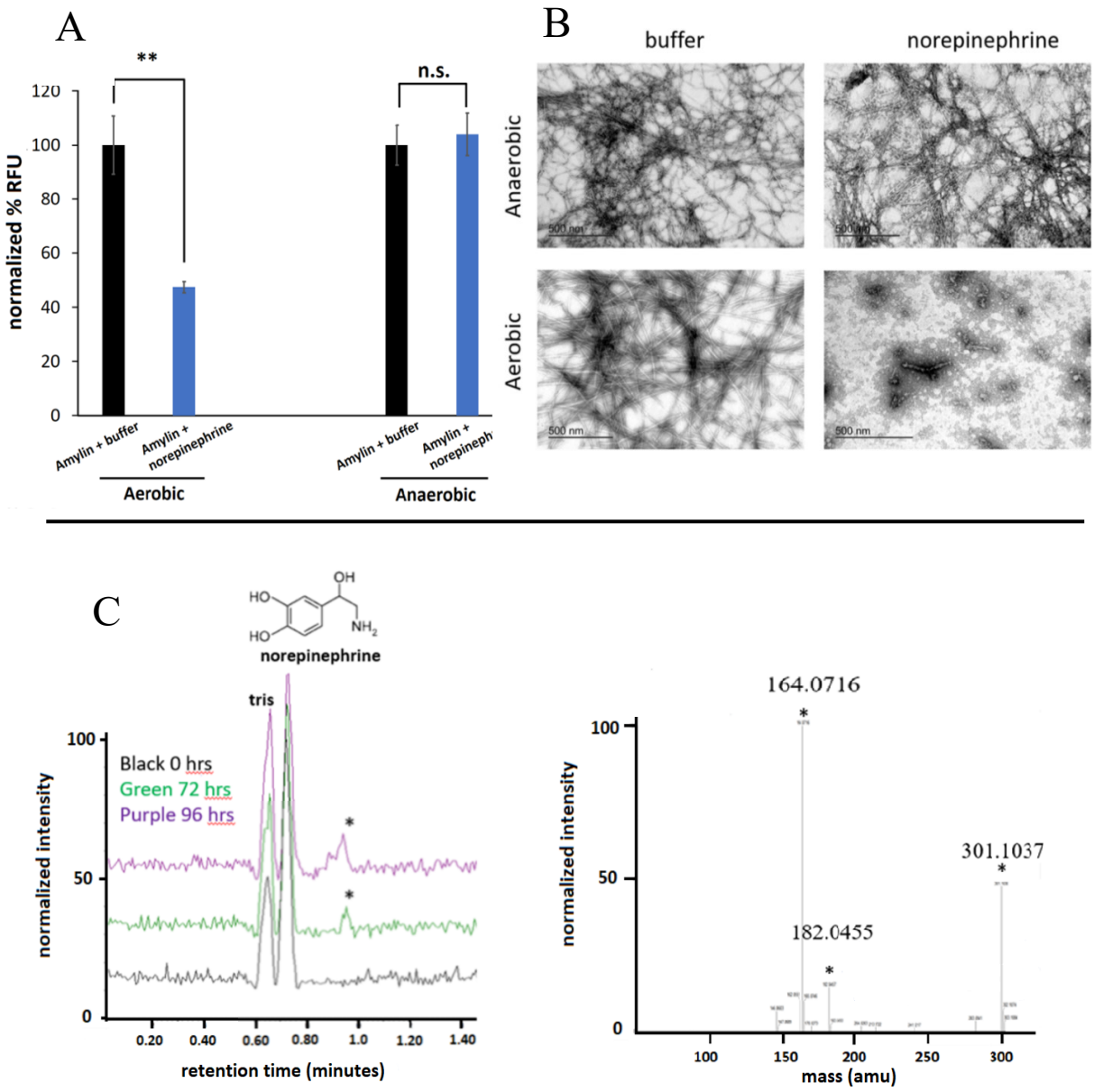

Figure 3: LC-MS identifies norepinephrine oxidized byproducts that are linked to norepinephrine anti-amyloid activity. (A,B) ThT and TEM data confirm that the anti-amyloid activity of norepinephrine requires aerobic conditions. (C) Freshly dissolved (time at 0 hour) or aged norepinephrine samples (time at 72 or 96 hours) were characterized by LC-MS. Visual inspection of the chromatograms showed a new peak at 0.97 minutes *(continued next page)*

in the 72 and 96-hour samples that was not present at 0 hours. MS (positive mode) of this fraction identified three species that are likely the oxidized byproducts of norepinephrine that include [M+ H^+] of 164.0716, 182.0455 and 182.1461. Norepinephrine samples aged under similar conditions to when these putative oxidized species were identified from LC-MS experiments also showed anti-amyloid activity as assessed by TEM, ThT and gel remodeling assays (Figure 3,4). Such activity was not associated with non-aged norepinephrine, that did not undergo oxidative chemical change. Thus, the oxidized norepinephrine byproducts identified by LC-MS are likely associated with and may contribute to norepinephrine anti-amyloid activities. Statistics were conducted using one-way ANOVA, Sidak's multiple comparisons test; *$p < 0.05$,** $p < 0.01$

Over the past decade several *in vitro* studies have reported that some small molecule amyloid inhibitors, many of which are catechol-containing polyphenols, perturb or "remodel" unaggregated and/or pre-aggregated amyloid species into aggregates that are resistant to protein denaturants[15-18, 27]. Consistent with these data and with the hypothesis that such phenomena are a general feature of catechol containing compounds, we confirmed that a variety of catechol containing natural compounds and catecholamines were all capable of remodeling freshly dissolved solutions of amylin into a distribution of protein aggregates that spanned the entire length of the separating gel in SDS-PAGE), which remained stable in presence of denaturing conditions (i.e., solutions containing 6.5M urea, 1X laemmli SDS sample buffer that were exposed to 95 C° for 5-10 minutes, data not shown). Moreover, a series of subsequent experiments confirmed that the general mechanism related to catechol-containing compound amyloid remodeling activity *requires compound autoxidation.* Using RA and norepinephrine, whose initial anti-amyloid activities were previously confirmed to be strongly influenced by autoxidation (Figs 1-3), we discovered that in a dose dependent manner, treatment with the reductant, TCEP, eliminated their amyloid remodeling activity (Figure 2). This effect was recapitulated in the presence of other reducing reagents including glutathione, cysteine and cystamine (Figure S5), and importantly, with many other catechol containing compounds, but not negative controls phenol and curcumin (Figure S6). Finally, under anaerobic conditions, we showed that remodeling activity mediated by catechol alone and catechol containing compounds are completely prevented (Figure S4).

A variety of covalent mechanisms can readily explain the observed requirement of autoxidation for catechol mediated remodeling and the corresponding strong stability of the observed remodeled aggregates. For example, free radical cycling occurring during catechol

autoxidation could directly cycle through nearby interacting amyloid proteins that subsequently leads to protein-protein and/or protein-compound adducts[21]. Alternatively, remodeled aggregates may also form through covalent interactions between electrophilic o-quinone oxidized byproducts of catechol parent compounds and amyloid protein side chain amines[17, 20-21, 23-26]. Regardless of the exact mechanism, these data are all consistent with the hypothesis that the presence of oxygen facilitates autoxidation which in turn enables all catechol containing compounds to engage in amyloid remodeling that likely involves a covalent mechanism.

While various reports indicate amyloid remodeling activities lead to what are presumably innocuous off-pathway aggregates that in some cases have even been reported to display anti-amyloid and/or cell rescue effects against amyloid induced cytotoxicity [15-18], it remains unclear whether amyloid remodeling is merely phenomenological in nature or if it represents a key mechanism responsible for anti-amyloid activity. To clarify this point, a variety of aerobic and or anaerobic compound pre-aging and amyloid aggregation conditions for select compounds catechol, RA and norepinephrine were developed that enabled an assessment of the relationship between amyloid remodeling and anti-amyloid aggregation activities. These data suggest that remodeling activity is not required for anti-amyloid activities in general nor is it an obligate determinant for enhancing catechol-containing compound anti-amyloid activity that occurs upon autoxidation (Figure 4).

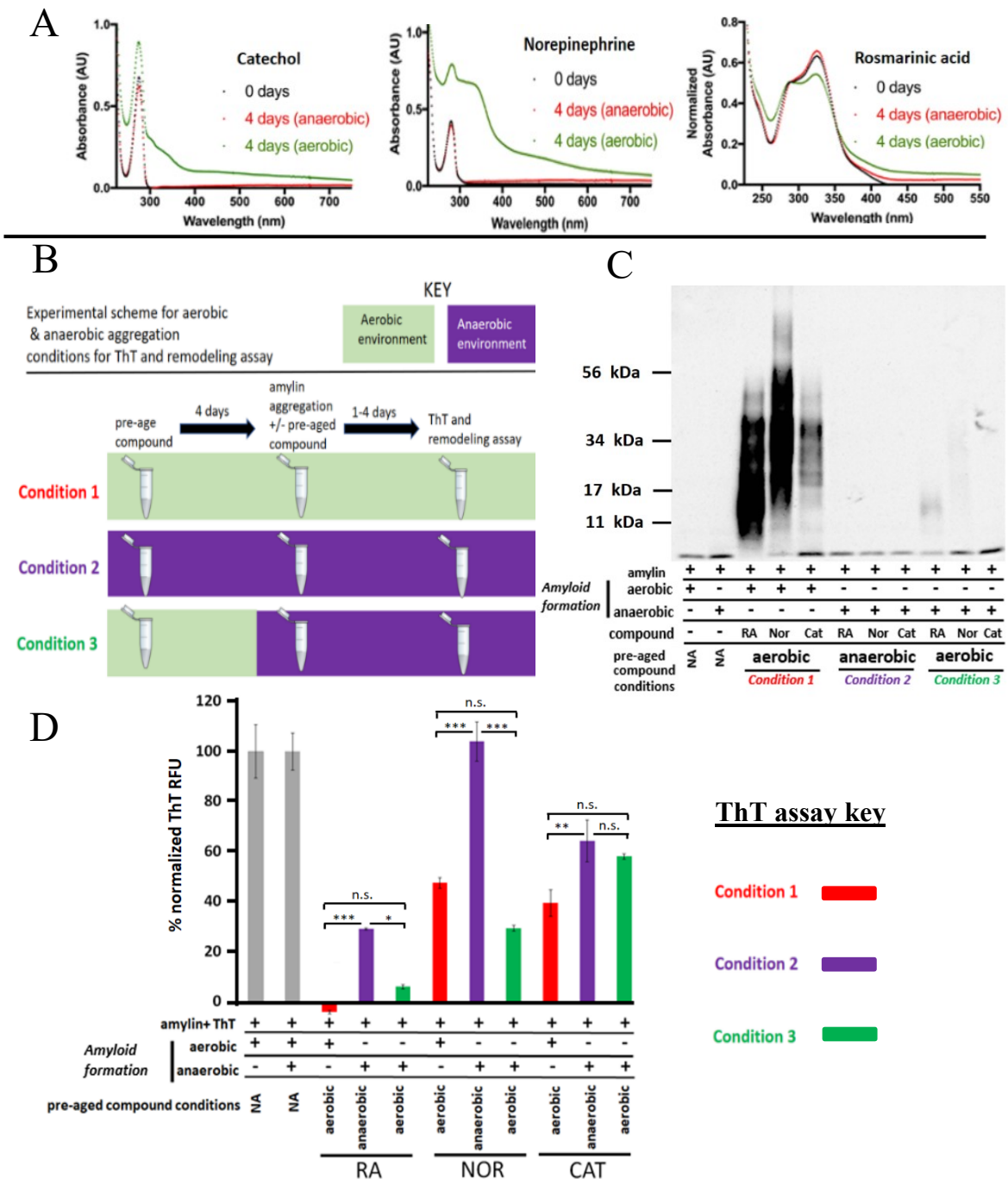

Figure 4: Amyloid remodeling is not required for catechol-containing compound anti-amyloid activity. (A) UV-Vis spectra reflect the oxidative changes incurred for aged catechol (cat), norepinephrine (nor) and rosmarinic acid (RA) under aerobic (green trace) but not anaerobic conditions (red trace). The zero-day (black trace) time point *(continued next page)*

represents the compound spectra taken prior to undergoing aging in either an aerobic or anaerobic environment (B) Experimental scheme for the ThT and remodeling assays under aerobic and anaerobic conditions. (C,D) When aerobically aged compounds are added to amylin amyloid mixtures maintained under aerobic conditions (condition 1, corresponding to red lettering in panel C and red bars in panel D) strong anti-amyloid and remodeling activity occurs. In contrast, when anaerobically aged compounds are added to amylin amyloid aggregation mixtures maintained under anaerobic conditions (condition 2, indicated by purple lettering in panel C and purple bars in panel D), compounds exhibit attenuated or no anti-amyloid aggregation activity coincident with a loss in remodeling activity. Finally, when compounds are aged under aerobic conditions and are added to amylin aggregation mixtures maintained under anaerobic conditions (condition 3, indicated by green lettering in panel C and green bars in panel D) strong amyloid inhibitory effects occur coincident with only minor to no remodeling activity. Statistics were conducted using one-way ANOVA, Sidak's multiple comparisons test; *$p < 0.05$,** $p < 0.01$, ***$p < 0.001$

Conclusions

Building on previous work [13, 17-18, 20-22, 24, 26, 30], our data suggest that catechol containing compounds in general, as well as their redox related anthraquinones, represent broad classes of amyloid inhibitors capable of targeting amyloid aggregation on multiple pathologically relevant amyloid forming proteins including tau 2N4R, $A\beta_{1-42}$, and amylin. Additionally, this work shows that (i) catechol but not phenol alone is an amyloid inhibitor (ii) autoxidation represents a general factor that plays a key role in enhancing the anti-amyloid activity of catechol-containing compounds and (iii) autoxidation is required for amyloid remodeling activity, a phenomenon that appears unnecessary for anti-amyloid activity. If indeed amyloid remodeling and the subsequent covalent process that is hypothesized to result in protein-compound adducts represent epiphenomenon, alternative reasoning is still needed to explain the overall enhanced amyloid activity observed upon catechol autoxidation. Future studies that use the structures of previously confirmed amyloid pharmacophores to explore the specific oxidized byproducts, whichpresumably produce enhanced anti-amyloid activities, , provides a facile approach from which to not only address this gap but also amplify the current pool of known potent small molecule amyloid inhibitors. Doing so will ultimately further uncover the key mechanisms and features that are pertinent to how catechol containing compounds and other broad classes of amyloid inhibitors function and potentially how such knowledge could be harnessed for translational applications. In this context, it would be desirable to find oxidized byproduct species that do not readily undergo potentially promiscuous (covalent) remodeling activity, which we suggest may not be necessary for anti-amyloid activity (Fig 4).

Material and Methods

Chemicals, Peptides and Other Reagents. Synthetic human amylin was purchased from AnaSpec (Fremont, CA) and the peptide quality was further validated by Virginia Tech core facility Mass Spectrometry Incubator. Amylin stocks were quantified by Pierce BCA protein assay kit (Thermo Fisher Scientific, Waltham, MA). Oleuropein (>98% purity; glycated form, Fig. 1A), tyrosol, 2-(3-hydroxyphenyl)ethanol, hexafluoro isopropanol (HFIP), and thioflavin T (ThT) were purchased from Sigma Aldrich (St. Louis, MO). Dimethyl sulfoxide (DMSO) and 2-Hydroxyphenethyl alcohol were purchased from Fisher Scientific (Pittsburgh, PA). 3-Hydroxytyrosol was purchased from Cayman Chemical (Ann Arbor, MI). Ligstroside and elenolic acid were purchased from Toronto Research Chemicals (Toronto, Ontario, Canada). Dulbecco's phosphate buffer saline (DBPS) was purchased from Lonza (Walkersville, MD).

Protein amyloid preparation for the 700 compound ThT screen

$A\beta_{42}$: Unaggregated solutions of $A\beta_{42}$ were typically prepared by dissolving lyophilized $A\beta_{42}$ powder (i.e., $A\beta_{42}$ is initially delivered from the vendor in this form) with 100% HFIP. Subsequent peptide quantification of this solution was estimated based on a standard microplate BCA assay. Initial stock solution preparation of $A\beta_{42}$ for the ThT assay were prepared by evaporating HFIP treated stocks followed by a modified two-step aqueous dissolution process as previously described[31]: Herein, HFIP evaporated stocks of $A\beta_{42}$ were dissolved in 60 mM NaOH. Next, these solutions were further diluted in 1X DPBS such that the final solution consisted of approximately 2.4 mM NaOH (i.e. ~4% 60 mM NaOH, 96% 1X DPBS). Immediately after the addition of 1X DPBS, 6.48 μL aliquots of $A\beta_{42}$ and 0.52uL aliquots of compound or buffer treated controls were distributed within a 384 microplate (i.e. reading plate).

The reading plate was sealed to prevent evaporation and allowed to incubate at 37° C until the estimated plateau of aggregation (~ 1 day). Next, the reading plate were centrifuged prior to receiving 14 uL of a 45 μM ThT solution prepared in 50 mM –Glycine-NaOH, 8.6 pH. Finally, all plates were read at excitation 444 nm/emission 490 nm to estimate plateau phase amyloid aggregation as indicated by ThT fluorescence. Note, the final concentration of $A\beta_{42}$ prior to being titrated with ThT, was approximately 12 μM, at a 3:1 molar ratio of compound to $A\beta_{42}$.

Amylin: Amylin stock preparation was initiated by dissolving lyophilized human amylin powder in 100% HFIP. After at least 2 hours of incubation at room temperature, HFIP was removed and the resulting amylin powder was re-dissolved in 100% DMSO and quantified by a standard BCA microplate assay (i.e. HFIP is extremely volatile and difficult to accurately pipette; thus, DMSO is a better solvent for peptide transfer; Initial HFIP dissolution was employed because it has been suggested to aid in removal of trace contaminants that may be present within lyophilized batches of peptide initially received from the vendor). Solutions of approximately 400 μM amylin (100% DMSO) were subsequently diluted with ThT in 1X DPBS and aliquoted to reading plate wells containing 0.45 μL of compound or vehicle buffer controls to a final volume of 15 μL. Final concentrations prior to amylin amyloid aggregation were 10 μM amylin, 30 μM compound and 30 μM ThT. All plates were continuously monitored for ThT fluorescence every 10 minutes (plates were shaken briefly prior to each read) at excitation 444 nm/emission 490 nm until the plateau phase was reached.

Tau 2N4R: Purified **r**ecombinant Batches of tau 2N4R initially dissolved in 100% 1X PNE buffer, were buffer exchanged with 1X HEPES buffer (10 mM HEPES, 30 mM NaCl, pH X) to

final concentration of 34.4 μM (quantified by standard BCA micro plate assay) in 92% 1X HEPES, 8% 1X PNE. Amyloid aggregation was initiated in the presence or absence of compound by diluting 6.48 μL of 34.4 μM tau 2N4R into the wells of the reading plates to a final volume of 21 μL containing 12.5 μM ThT and 0.06 mg-ml^{-1} Heparin. For compound treated wells, final molar concentration of compound to tau 2N4R was ~2:1. All aggregation reactions were incubated at 37 °C until the approximated plateau fluorescent readings were made at excitation 444 nm/emission 490 nm.

Anaerobic aggregating conditions

All reagents including buffers, protein and compounds were made anaerobic by flushing with nitrogen prior to being placed within an anaerobic bag. Oxygen concentration was maintained between 15-50 ppm within the anaerobic bag. Typical aggregating conditions within the bag were maintained between 25-30 °C.

Sample processing for ThT assays: after aggregation (>24 hrs.) , samples (amylin + compound, or amylin + buffer) were removed from the anaerobic bag and promptly added to ThT solutions contained within a 384 well plate (i.e., ThT solutions were added to the plate prior to taking out the samples form the anaerobic bag). End ThT fluorescence was measured at a 444 nm excitation/490 nm emission until a stable signal was reached (2-10 hr.).

Sample processing for gel remodeling assays: after aggregation (~3 days) samples were removed from the anaerobic bag, vacuumed dried (~30-45 minutes) and immediately quenched with ~6.5 M urea containing 15 mM tris and 1X SDS laemmeli sample buffer, heated at 95-100°C for 5-

10- minutes and subjected to SDS-PAGE followed by Western blot analysis with anti-amylin primary antibody (T-4157, 1:5000, Peninsula Laboratories, San Carlos, CA).

Sample processing for TEM: after aggregation (~3-4 days) samples were immediately removed from the anaerobic chamber and spotted on a 200-mesh formvar carbon coated grid within ~ 45 minutes. (see below for more details regarding TEM sample processing)

Transmission Electron Microscopy (TEM). Amylin fibrillation was initiated in 20 mM Tris-HCl, pH 7.4 and residual amount of DMSO at 1.5%. Final amylin concentration was 30 μM and the molar ratio of a compound to amylin ranged from 20:1 to 50:1. Samples were typically incubated at 27-37 °C without agitation for 3-4 days. Prior to imaging analyses, ~4 μl's of samples were blotted on a 200-mesh formvar-carbon coated grid for 5 minutes and wicked dry by filter paper. Dried samples were then immediately stained with uranyl acetate (1%) for 1-2 minutes, and again, wicked dry with filter paper before imaging. Prior to taking representative images (obtained from a JEOL 1400 operated at 120 kV, a qualitative assessment of the number of fibrils observed were made by scanning each grid quadrant for deposited material. TEM experiments were repeated at least twice.

Gel based remodeling activity. Vehicle control or specified pre-aged or non-pre-aged compounds were spiked into freshly dissolved amylin samples (containing amylin and buffer). Thereafter amylin aggregation was allowed to proceed for 3 days in the presence of reductant or under aerobic or anaerobic conditions. Final amylin concentration was 15 μM that included varying concentrations of compound and or reducing reagent depending upon the assay. After 3 days,

these samples were vacuum dried and re-dissolved in ~6.5 M urea containing 15 mM tris and 1X SDS laemmeli sample buffer, boiled at 95 °C for 5-10 minutes and subjected to SDS-PAGE followed by Western blot analysis with anti-amylin primary antibody (T-4157, 1:5000, Peninsula Laboratories, San Carlos, CA). All gel-based amyloid remodeling assays were repeated at least twice exception to remodeling experiments pertaining to reduced glutathione, cystamine and cysteine(Fig. S5). Herein, RA was chosen as the selected candidate to conduct at least two repeat assays with glutathione, cystamine and cysteine, whereas only single experiments were completed for Norepinephrine (Fig. S5).

Photo Induced Crosslinking of Unmodified Proteins (PICUP). Amylin aliquots from a master mix in 10 mM phosphate buffer, pH 7.4 were added separately to 0.6 mL eppendorf tubes containing small molecule inhibitors or DMSO vehicle loaded controls. Crosslinking for each tube was subsequently initiated by adding tris(bipyridyl)Ru(II) complex (Ruby) and ammonium persulfate (APS) (Typical Amylin:Rubpy:APS ratios were fixed at 1:2:20, respectively, at a final volume of 15-20 μL), followed by exposure to visible light, emitted from a 150-Watt incandescent light bulb, from a distance of 5 cm and for a duration of 5 seconds. The reaction was quenched by addition of 1X SDS sample buffer. PICUP was visualized by SDS-PAGE (16% acrylamide gels containing 6 M urea), followed by silver staining. Final concentrations for all PICUP reactions included 30 μM amylin, and 150 μM compound. The initial screening PICUP experiments depicted in Fig S6 were conducted once; similar trends were recapitulated in repeat PICUP experiments using selected catechol and anthraquinone candidates depicted in Fig S6 (data not shown).

Statistical Analyses. All ThT assay data are presented as the mean ± S.E.M. and the differences were analyzed with one-way ANOVA analyses multiple comparisons test ($p<0.05$ *, $p<0.01$ **, $p< 0.001$ ***) as implemented within GraphPad Prism software (version 6.0)

Supplemental Tables and Figures

compound number	% amylin amyloid inhibition	compound name
15	85	Epirubicin hydrochloride
49	82	Doxorubicin hydrochloride
61	79	Racepinephrine
145	90	Rifampicin
177	77	Hyperoside
318	88	Idarubicin hydrochloride
321	89	Daunorubicin hydrochloride
362	77	Taxifolin-(+)
425	77	(+/-)-Norepinephrine hydrochloride
531	72	Carbidopa
548	84	Rutin
601	96	Rifapentine
643	98	Epigallocatechin gallate
compound number	**% tau 441 amyloid inhibition**	**compound name**
15	80	Epirubicin hydrochloride
27	81	Methyldopa
49	78	Doxorubicin hydrochloride
61	77	Racepinephrine
77	78	Dopamine hydrochloride
145	65	Rifampicin
318	89	Idarubicin hydrochloride
321	84	Daunorubicin hydrochloride
414	73	Isoproterenol hydrochloride
425	87	(+/-)-Norepinephrine hydrochloride
601	69	Rifapentine
643	94	Epigallocatechin gallate
compound number	**% Aβ 1-42 amyloid inhibition**	compound name
15	100	Epirubicin hydrochloride
27	100	Methyldopa
49	100	Doxorubicin hydrochloride
77	100	Dopamine hydrochloride
87	100	Fenoldopam mesylate
117	100	Mitoxantrone hydrochloride
145	98	Rifampicin
292	91	Dihydrexidine hydrochloride
318	100	Idarubicin hydrochloride
321	100	Daunorubicin hydrochloride
362	96	Taxifolin-(+)
425	66	(+/-)-Norepinephrine hydrochloride
522	83	Resveratrol
531	97	Carbidopa
601	100	Rifapentine
643	100	Epigallocatechin gallate

Table S1:

Top lead catechol and anthraquinone candidates identified from the 700 compound ThT screen

against amylin, tau 2N4R and $A\beta_{42}$ (see Figure 1). The compound candidate name, number (corresponding to Figure 1) and percent amyloid inhibition is depicted. Any compounds that exhibited 3 standard deviation units of inhibition greater than observed for amylin + ThT controls were considered top candidates. Amylin was selected as the control amyloid protein standard because it exhibited greatest the deviation in the presence of buffer (compared to tau 2N4R and $A\beta_{42}$), which in turn conferred the most stringent criteria for defining top hits. The structures and total percent inhibition demonstrated from each compound relative to all proteins are shown in Fig. S1.

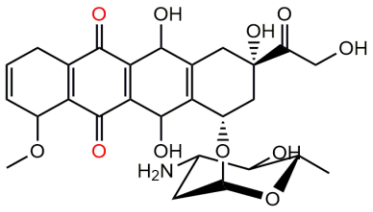

Epirubicin, compound # 15
% amyloid inhibtion
Amylin = 85.3%
Tau = 79.5%
Abeta $_{1-42}$ = 100%

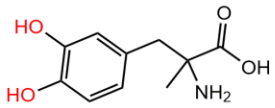

Methyldopa, compound # 27
% amyloid inhibtion
Amylin = 35.3%
Tau = 80.9 %
Abeta $_{1-42}$ =100 %

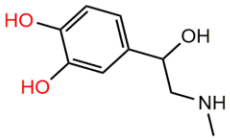

Racepinephrine, compound # 61
% amyloid inhibtion
Amylin = 78.5 %
Tau = 77.2 %
Abeta $_{1-42}$ = 53.1 %

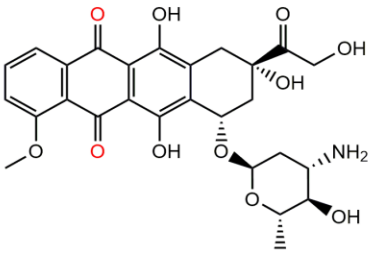

Doxorubicin, compound # 49
% amyloid inhibtion
Amylin = 81.6%
Tau = 77.6 %
Abeta $_{1-42}$ =99.8 %

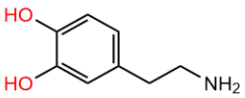

Dopamine, compound # 77
% amyloid inhibtion
Amylin = *37.0 %
Tau = 78.1 %
Abeta $_{1-42}$ = 100 %

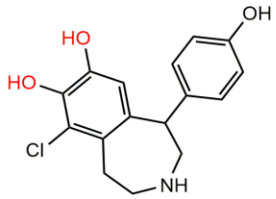

Fenoldopam mesylate, compound # 87
% amyloid inhibtion
Amylin = 39.0%
Tau = 61.0 %
Abeta $_{1-42}$ = 100 %

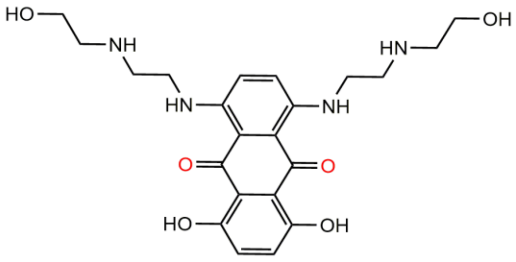

Mitoxantrone, compound # 117
% amyloid inhibtion
Amylin = 51.8%
Tau = 41.0%
Abeta $_{1-42}$ =100 %

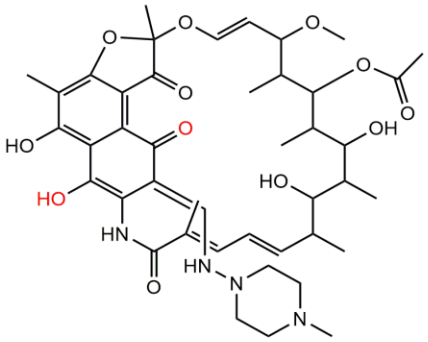

Rifampicin, compound # 145
% amyloid inhibtion
Amylin = 90.4 %
Tau = 65.0%
Abeta $_{1-42}$ = 98.4%

Figure S1
The compound name and number of each catechol and anthraquinone lead candidate identified form the 700 compound ThT assay against amylin, tau 2N4R and Aβ4$_2$ (Supplementary Table 1, Figure 1) along with its relative amyloid inhibition against each protein is depicted above and on the next page. In exceptional cases, compound activity was shown to be

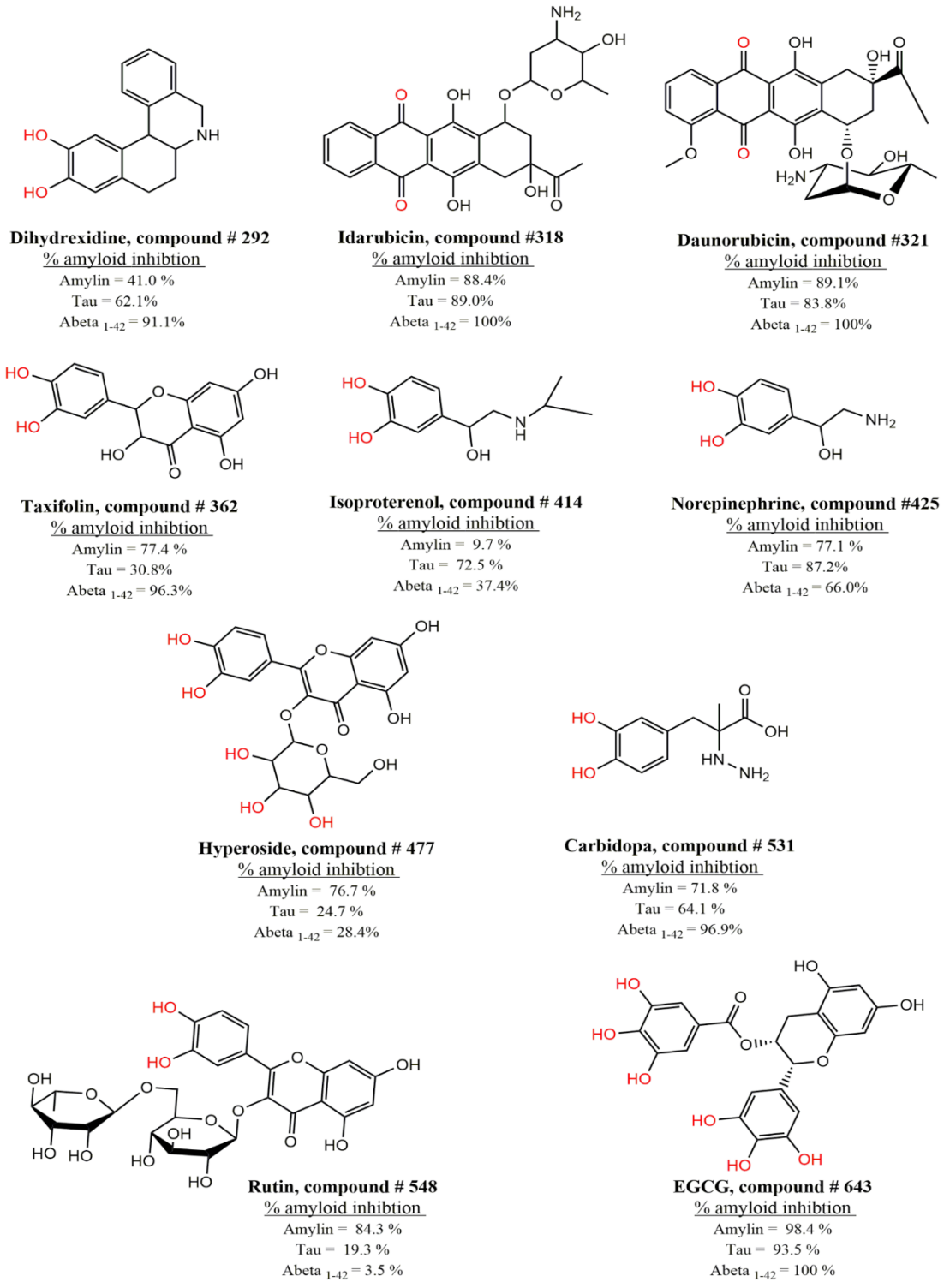

Figure S1 (continued from previous page) potentially protein specific: Isoproterenol inhibited tau 2N4R and $A\beta_{42}$ but not amylin amyloid formation; Rutin inhibited amylin and Tau 2N4R but not $A\beta_{42}$ amyloid formation. While protein specific or even amyloid polymorph specific affinity

within the same protein has been previously recognized [12, 32], further characterization to confirm the specificity of Isoproterenol and rutin was not conducted.

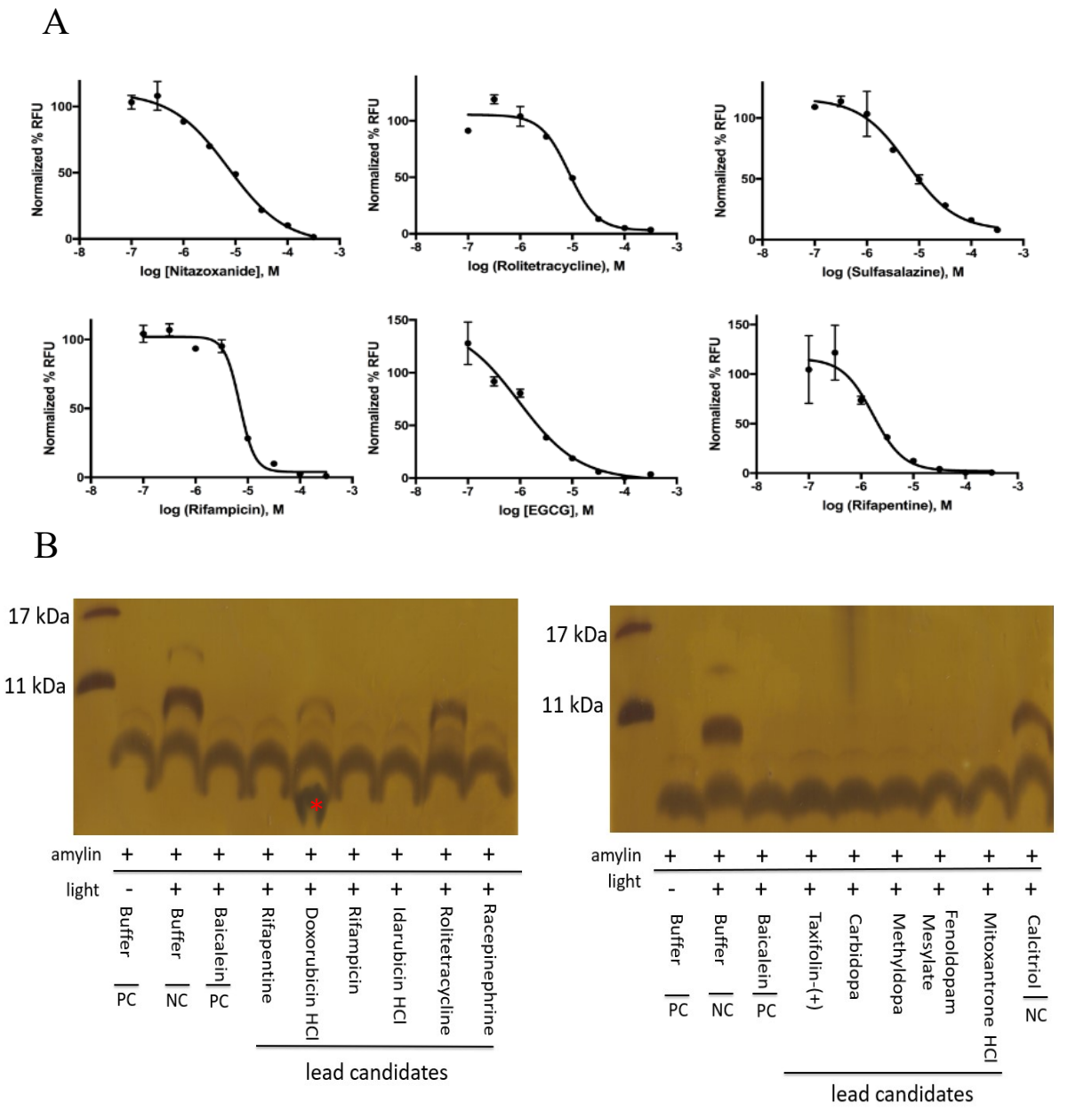

Figure S2. Selected compounds from a variety of classes of lead anti-amyloid candidates identified against tau 2N4R, $A\beta_{42}$ and amylin (Fig. 1, main text, compound structures S1-S5) also exhibit dose-response effects against amylin amyloid formation (ThT assay) (A) and prevent amylin oligomerization (Photo induced cross linking of unmodified proteins, PICUP assay) (B). ThT dose-response curves were conducted at an amylin concentration of 15 μM and all PICUP experiments were executed at an amylin concentration ranging from *(continued next page)*

25-30 μM at a fixed compound to amylin molar ratio of 5:1. Note: PICUP experiments that resulted in the observed band that ran below amylin monomer for doxorubicin treated-amylin (red asterisk) and the continuous distribution of bands observed for Rolitetracycline as well as carbidopa and fenoldopam mesylate (observed in duplicate repeat experiments, data not shown) treated-amylin PICUP reactions are phenomena that have been previously observed with other amylin amyloid inhibitors tested in our lab including rosmarinic acid, oleuropein and EGCG (data not shown). In these cases, follow up attempts to characterize the identities of these bands were unsuccessful. For PICUP experiments, baicalein served as a Positive control (PC)[20] and calcitriol was randomly selected from the list of compounds that displayed negligible activity against amylin from the initial repurposing screen (Fig 1, main text) to serve as the negative control (NC).

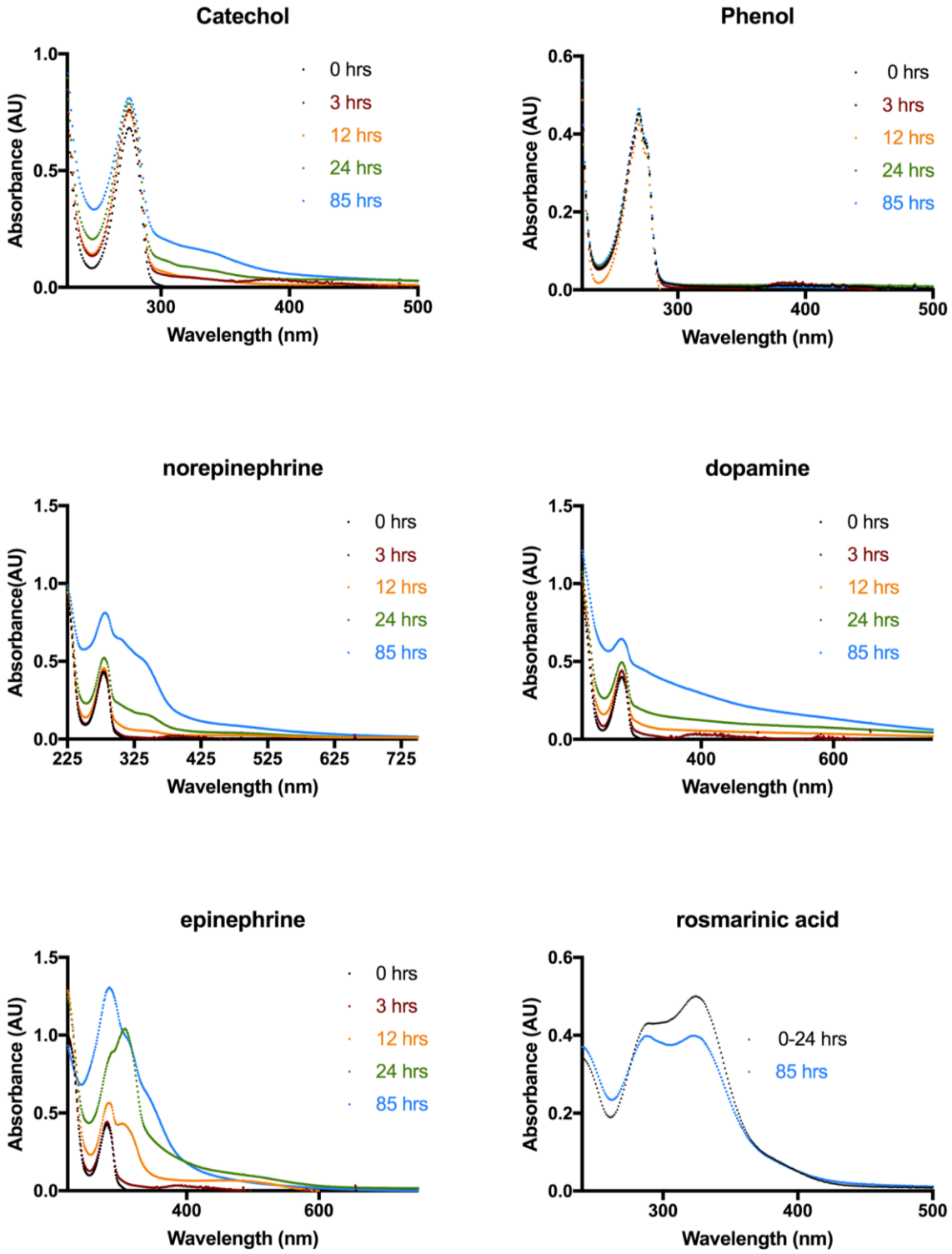

Figure S3: Representative UV-vis spectra depict the oxidative chemical change that occurs for catechol and catechol containing compounds under typical aerobic *(continued next page)*

pre-aging conditions. Multiple UV vis experiments confirmed that such chemical change does not occur under anaerobic conditions (data not shown).

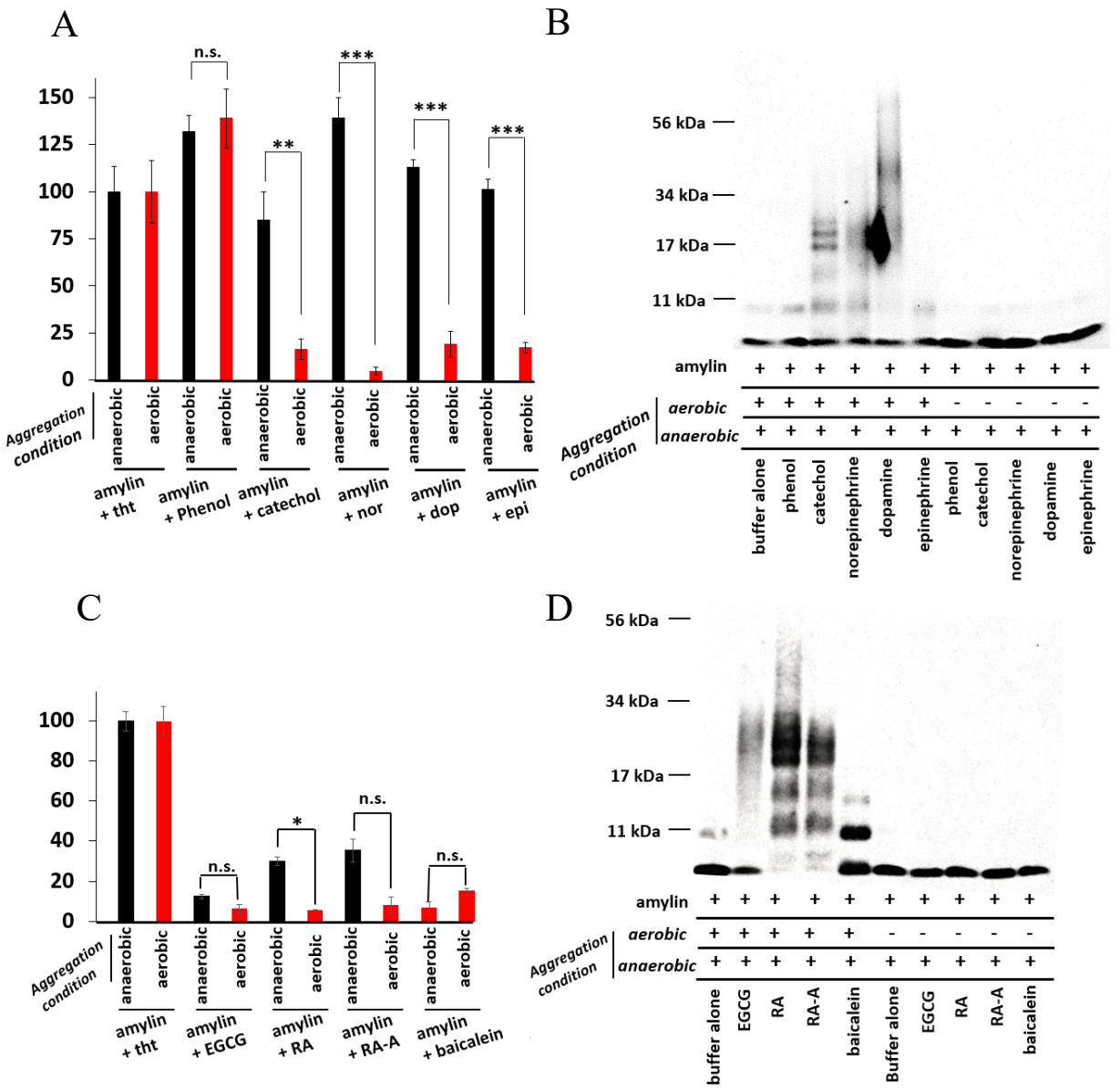

Figure S4. Aerobic conditions lead to enhanced anti-amyloid activity and is essential for amyloid remodeling phenomena by a select group of catechol containing amyloid inhibitors. (A,B) Aerobic but not anaerobically aged catechol and selected catecholamines, norepinephrine(nor), dopamine (dop) and epinephrine (epi) display strong anti-amyloid activities (A) and exhibit amyloid remodeling activities (B). No anti-amyloid activity or remodeling phenomena was observed for negative control phenol, regardless of the presence or absence of aerobic or anaerobic aging and aggregating conditions. *(continued next page)*

Aerobic but not anaerobically aged rosmarinic acid (RA) both exhibited enhanced anti-amyloid activity (C) and induced amyloid remodeling (D). This trend was also seen for EGCG and RA amide linked analogue (RA-A), albeit not statistically significant. The reverse trend for anti-amyloid activity was noted for baicalein (as has been previously observed under certain aging conditions[17, 24]), but remodeling effects of baicalein still required aerobic conditions. Statistics were conducted using one-way ANOVA, multiple comparisons test; $p<0.05$ *, $p<0.01$ **, $p<0.001$ ***

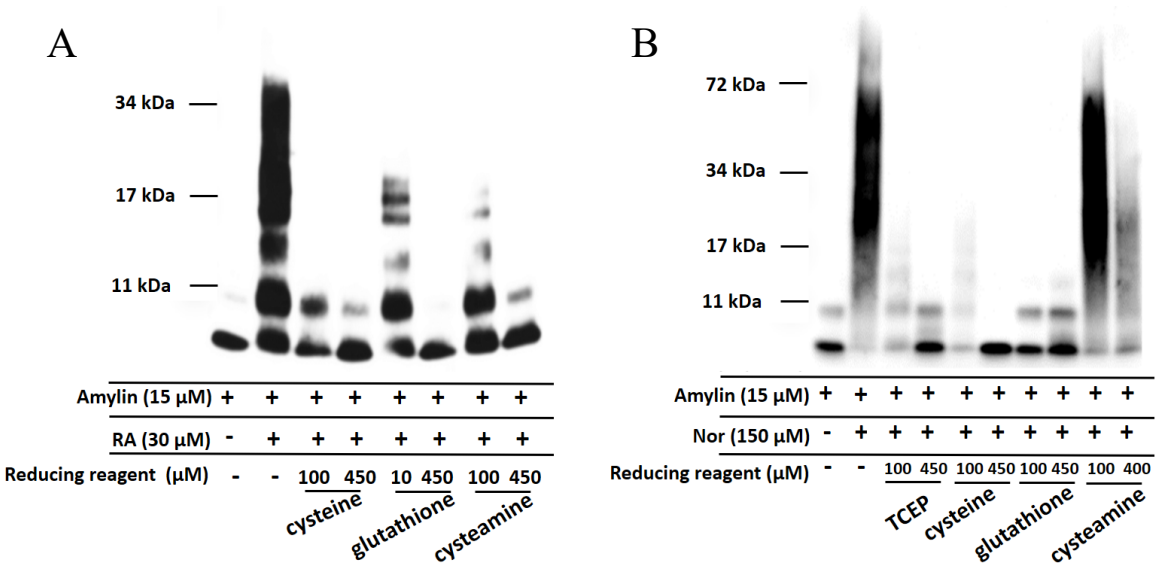

Figure S5: A reducing environment prevents amyloid remodeling phenomena induced by potent amylin amyloid inhibitors rosmarinic acid (RA) and norepinephrine(Nor). (A) In a dose dependent manner, low (10-100 μM) and high (450 μM) concentrations of various reducing reagents including TCEP, cysteine, glutathione and cysteamine eliminate remodeling activity by RA and Nor (For the effect of TCEP on RA-amyloid remodeling, see the main text of Fig. 2). We also observed similar activities for the disulfide forms of cysteine (i.e. cystine), glutathione, and cysteamine (i.e., cystamine) (data not shown).

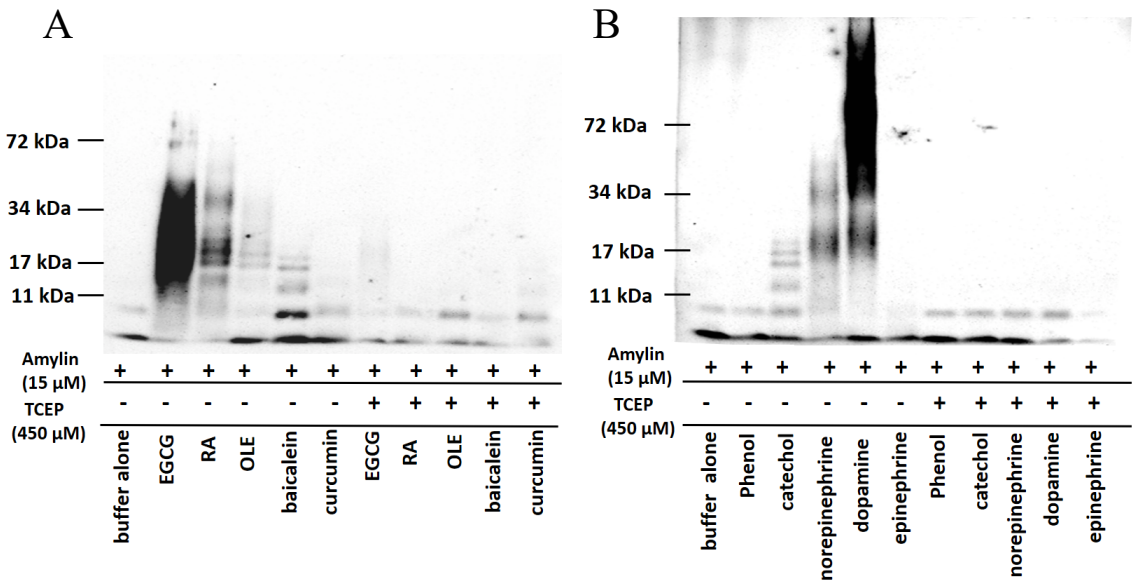

Figure S6: TCEP prevents amyloid remodeling effects observed by two classes of catechol-containing amyloid inhibitors. (A) remodeling activity of selected catechol containing natural compound amyloid inhibitors Epigallocatechin gallate (EGCG), rosmarinic acid (RA), oleuropein (OLE), baicalein (Bac) is significantly attenuated or completely prevented in the presence of 10:1 molar ratio of TCEP to compound (i.e., 450μM TCEP, 45μM natural compound). The negative control, curcumin, an amyloid inhibitor which lacks a catechol functional group, exhibits moderate remodeling activity, independent of the presence of TCEP. (B) The remodeling activity of selected catecholamine inhibitors norepinephrine, dopamine and epinephrine is completely prevented in the presence of a 10:1 molar ratio of TCEP to compound. Consistent with a remodeling mechanism linked to the catechol functional moiety present within the catecholamines, the same remodeling trend was seen for catechol but not phenol. Note that while under these conditions negligible remodeling activity is observed for epinephrine in the absence of TCEP (indicated by faint streak), some minor remodeling effects are observed at higher ratios of epinephrine to amylin (data not shown).

References

1. Knowles, T. P. J.; Vendruscolo, M.; Dobson, C. M., The amyloid state and its association with protein misfolding diseases. *Nat Rev Mol Cell Biol* **2014,** *15* (6), 384-396.
2. Chiti, F.; Dobson, C. M., Protein misfolding, functional amyloid, and human disease. *Annual review of biochemistry* **2006,** *75*, 333-66.
3. Westermark, P.; Andersson, A.; Westermark, G. T., Islet amyloid polypeptide, islet amyloid, and diabetes mellitus. *Physiological reviews* **2011,** *91* (3), 795-826.
4. Selkoe, D. J.; Hardy, J., The amyloid hypothesis of Alzheimer's disease at 25 years. *EMBO molecular medicine* **2016,** *8* (6), 595-608.
5. Eisenberg, D.; Jucker, M., The amyloid state of proteins in human diseases. *Cell* **2012,** *148* (6), 1188-1203.
6. Li, C.; Gotz, J., Tau-based therapies in neurodegeneration: opportunities and challenges. *Nature reviews. Drug discovery* **2017,** *advance online publication*.
7. Fitzpatrick, A. W. P.; Falcon, B.; He, S.; Murzin, A. G.; Murshudov, G.; Garringer, H. J.; Crowther, R. A.; Ghetti, B.; Goedert, M.; Scheres, S. H. W., Cryo-EM structures of tau filaments from Alzheimer's disease. *Nature* **2017,** *547* (7662), 185-190.
8. Sawaya, M. R.; Sambashivan, S.; Nelson, R.; Ivanova, M. I.; Sievers, S. A.; Apostol, M. I.; Thompson, M. J.; Balbirnie, M.; Wiltzius, J. J. W.; McFarlane, H. T.; Madsen, A. O.; Riekel, C.; Eisenberg, D., Atomic structures of amyloid cross-[bgr] spines reveal varied steric zippers. *Nature* **2007,** *447* (7143), 453-457.
9. Laganowsky, A.; Liu, C.; Sawaya, M. R.; Whitelegge, J. P.; Park, J.; Zhao, M.; Pensalfini, A.; Soriaga, A. B.; Landau, M.; Teng, P. K.; Cascio, D.; Glabe, C.; Eisenberg, D., Atomic view of a toxic amyloid small oligomer. *Science* **2012,** *335* (6073), 1228-31.
10. Nelson, R.; Sawaya, M. R.; Balbirnie, M.; Madsen, A. O.; Riekel, C.; Grothe, R.; Eisenberg, D., Structure of the cross-[beta] spine of amyloid-like fibrils. *Nature* **2005,** *435* (7043), 773-778.
11. Jiang, L.; Liu, C.; Leibly, D.; Landau, M.; Zhao, M.; Hughes, M. P.; Eisenberg, D. S., Structure-based discovery of fiber-binding compounds that reduce the cytotoxicity of amyloid beta. *eLife* **2013,** *2*, e00857.
12. Landau, M.; Sawaya, M. R.; Faull, K. F.; Laganowsky, A.; Jiang, L.; Sievers, S. A.; Liu, J.; Barrio, J. R.; Eisenberg, D., Towards a pharmacophore for amyloid. *PLoS biology* **2011,** *9* (6), e1001080.
13. Velander, P.; Wu, L.; Henderson, F.; Zhang, S.; Bevan, D. R.; Xu, B., Natural Product-Based Amyloid Inhibitors. *Biochemical pharmacology* **2017**.
14. Johnson, S. M.; Connelly, S.; Fearns, C.; Powers, E. T.; Kelly, J. W., The Transthyretin Amyloidoses: From Delineating the Molecular Mechanism of Aggregation Linked to Pathology to a Regulatory-Agency-Approved Drug. *Journal of molecular biology* **2012,** *421* (2), 185-203.
15. Ehrnhoefer, D. E.; Bieschke, J.; Boeddrich, A.; Herbst, M.; Masino, L.; Lurz, R.; Engemann, S.; Pastore, A.; Wanker, E. E., EGCG redirects amyloidogenic polypeptides into unstructured, off-pathway oligomers. *Nature structural & molecular biology* **2008,** *15* (6), 558-66.
16. Bieschke, J.; Russ, J.; Friedrich, R. P.; Ehrnhoefer, D. E.; Wobst, H.; Neugebauer, K.; Wanker, E. E., EGCG remodels mature α-synuclein and amyloid-β fibrils and reduces cellular toxicity. *Proceedings of the National Academy of Sciences of the United States of America* **2010,** *107* (17), 7710-7715.

17. Hong, D. P.; Fink, A. L.; Uversky, V. N., Structural characteristics of alpha-synuclein oligomers stabilized by the flavonoid baicalein. *Journal of molecular biology* **2008,** *383* (1), 214-23.
18. Wu, L.; Velander, P.; Liu, D.; Xu, B., Olive Component Oleuropein Promotes beta-Cell Insulin Secretion and Protects beta-Cells from Amylin Amyloid-Induced Cytotoxicity. *Biochemistry* **2017,** *56* (38), 5035-5039.
19. Jha, N. N.; Ghosh, D.; Das, S.; Anoop, A.; Jacob, R. S.; Singh, P. K.; Ayyagari, N.; Namboothiri, I. N.; Maji, S. K., Effect of curcumin analogs onalpha-synuclein aggregation and cytotoxicity. *Scientific reports* **2016,** *6*, 28511.
20. Velander, P.; Wu, L.; Ray, W. K.; Helm, R. F.; Xu, B., Amylin Amyloid Inhibition by Flavonoid Baicalein: Key Roles of Its Vicinal Dihydroxyl Groups of the Catechol Moiety. *Biochemistry* **2016**.
21. Meng, X.; Munishkina, L. A.; Fink, A. L.; Uversky, V. N., Molecular mechanisms underlying the flavonoid-induced inhibition of alpha-synuclein fibrillation. *Biochemistry* **2009,** *48* (34), 8206-24.
22. Joshi, P.; Chia, S.; Habchi, J.; Knowles, T. P. J.; Dobson, C. M.; Vendruscolo, M., A Fragment-Based Method of Creating Small-Molecule Libraries to Target the Aggregation of Intrinsically Disordered Proteins. *ACS Combinatorial Science* **2016,** *18* (3), 144-153.
23. Sato, M.; Murakami, K.; Uno, M.; Nakagawa, Y.; Katayama, S.; Akagi, K.; Masuda, Y.; Takegoshi, K.; Irie, K., Site-specific inhibitory mechanism for amyloid beta42 aggregation by catechol-type flavonoids targeting the Lys residues. *The Journal of biological chemistry* **2013,** *288* (32), 23212-24.
24. Zhu, M.; Rajamani, S.; Kaylor, J.; Han, S.; Zhou, F.; Fink, A. L., The flavonoid baicalein inhibits fibrillation of alpha-synuclein and disaggregates existing fibrils. *The Journal of biological chemistry* **2004,** *279* (26), 26846-57.
25. Popovych, N.; Brender, J. R.; Soong, R.; Vivekanandan, S.; Hartman, K.; Basrur, V.; Macdonald, P. M.; Ramamoorthy, A., Site specific interaction of the polyphenol EGCG with the SEVI amyloid precursor peptide PAP(248-286). *The journal of physical chemistry. B* **2012,** *116* (11), 3650-8.
26. Li, J.; Zhu, M.; Manning-Bog, A. B.; Di Monte, D. A.; Fink, A. L., Dopamine and L-dopa disaggregate amyloid fibrils: implications for Parkinson's and Alzheimer's disease. *FASEB journal : official publication of the Federation of American Societies for Experimental Biology* **2004,** *18* (9), 962-4.
27. Palhano, F. L.; Lee, J.; Grimster, N. P.; Kelly, J. W., Toward the Molecular Mechanism(s) by Which EGCG Treatment Remodels Mature Amyloid Fibrils. *Journal of the American Chemical Society* **2013,** *135* (20), 7503-7510.
28. Baell, J. B., Feeling Nature's PAINS: Natural Products, Natural Product Drugs, and Pan Assay Interference Compounds (PAINS). *Journal of natural products* **2016,** *79* (3), 616-28.
29. Baell, J. B.; Holloway, G. A., New substructure filters for removal of pan assay interference compounds (PAINS) from screening libraries and for their exclusion in bioassays. *Journal of medicinal chemistry* **2010,** *53* (7), 2719-40.
30. Pickhardt, M.; Gazova, Z.; von Bergen, M.; Khlistunova, I.; Wang, Y.; Hascher, A.; Mandelkow, E. M.; Biernat, J.; Mandelkow, E., Anthraquinones inhibit tau aggregation and dissolve Alzheimer's paired helical filaments in vitro and in cells. *The Journal of biological chemistry* **2005,** *280* (5), 3628-35.

31. Bitan, G., Structural Study of Metastable Amyloidogenic Protein Oligomers by Photo-Induced Cross-Linking of Unmodified Proteins. In *Methods in enzymology*, Indu, K.; Ronald, W., Eds. Academic Press: 2006; Vol. Volume 413, pp 217-236.
32. Krotee, P.; Rodriguez, J. A.; Sawaya, M. R.; Cascio, D.; Reyes, F. E.; Shi, D.; Hattne, J.; Nannenga, B. L.; Oskarsson, M. E.; Philipp, S.; Griner, S.; Jiang, L.; Glabe, C. G.; Westermark, G. T.; Gonen, T.; Eisenberg, D. S., Atomic structures of fibrillar segments of hIAPP suggest tightly mated beta-sheets are important for cytotoxicity. *eLife* **2017,** *6*.

Chapter 6: Conclusions and Future Perspectives

Summary

The work put forth in this dissertation has provided numerous mechanistic insights into the modes of action of several different catechol-containing small molecule anti-amyloid inhibitors. *Chapter 2* elucidated that the catechol functional group is essential for anti-amyloid effects of baicalein, that was mechanistically linked to forming adducts with amylin. *Chapter 3* highlighted the multifunctional capacity of oleuropein that included its anti-amyloid activities. The latter was linked to the presence of the catechol functional group present in the 3-hydroxytyrosol moiety within oleuropein. *Chapter 4* demonstrated that rosmarinic acid and its metabolites caffeic acid and salvianic acid A prevent amylin amyloid formation, consistent with a mechanism that was linked to the presence of RA's catechol functional groups. Moreover, RA and its amide linked analogue RA-A, which showed stronger anti-amyloid activities than RA in several assays, disrupted pre-formed amylin oligomers obtained from the sera of both HIP rats and humans; *Chapter 5* showed that catechol and redox related anthraquinones represent broad classes of amyloid inhibitors and that autoxidation is a determining factor for enhancing catechol containing amyloid inhibitor activities. Our data also indicate that while autoxidation is required for catechol mediated formation of (presumably non-toxic) denaturant resistant amylin aggregates, such a phenomenon may not be required for catechol mediated anti-amyloid activities.

Future perspectives

The focus of this dissertation has been the identification of small molecule amyloid inhibitors and mechanistic studies on how they modulate amylin amyloid formation, a hallmark characteristic of T2D. A critical issue that remains is determining the structural features present in oligomeric amyloid precursors or other amyloid species that are linked to their toxicity. To aid in these goals, recently solved high resolution amyloid structures and identification of a variety of structure and sequence-specific amyloid inhibitors including antibodies[1-7] as well as small molecules[8-13], together open powerful new avenues for potential amyloid diagnostic and drug discovery applications. For instance, over the last decade multiple amyloid-like crystal structures have been solved using truncated peptide sequences found within full length pathological amyloidogenic proteins[14-17]. The ability to co-crystalize small molecule amyloid inhibitors with some of these peptides has elucidated atomic details that clarify key interactions that define both sequence specific and non-sequence specific small molecule amyloid pharmacophores[15, 18]. Moreover, it now be possible to study amyloid inhibitors with full length amyloid proteins using cryo EM[19] or a combination of other high resolution structural techniques[15, 20-21]. As discussed in the literature review, these findings have paved the way for future structure-based amyloid inhibitor drug discovery[22].

One important group of amyloid structures that represent promising drug targets are seed competent or prion-like amyloids. Numerous data indicate that amyloid propagation *in vivo* in T2D as well as several other neurodegenerative amyloid diseases may be spread by prion like mechanisms, wherein a variety of conformational specific seeds (or strains) can serve as templates that accelerate amyloid formation and disease progression [23-30]. It is important to note that while infectious amyloid transmission has been confirmed between a variety of *in vivo* [23-24,

[27, 29-30] and or cell based systems [15, 26], the use of the phrases amyloid strains, or amyloid prions used in this context are not meant to be synonymous with prion proteins that cause transmissible spongiform encephalopathies, (i.e., that are infectious/transmissible between humans); rather, they are used to highlight the growing evidence that prion-like or seeded amyloid aggregation may be critical to how toxic amyloid formation is propagated in amyloid diseases. A major hurdle in improving and identifying the culprit amyloid prion strains that can be effectively targeted is to first delineate the specific structures that render these species seed-competent. While homotypic seeding is likely the main avenue for seeded amyloid assembly *in vivo* [23, 26-27, 29], given the polymorphic nature of amyloid formation [31-32], there may be multiple amyloid prion strains that exist for a given protein, some of which may be more relevant to disease progression than others. In fact, recent *in vivo* evidence supports this notion. In one study, α-synuclein exhibited prion activity that was specific to multiple system's atrophy, and that remarkably, the observed seeding propensity as reflected by *in vitro* biosensor cells (see below), differed according to the patient and brain tissue type.[23] In others studies, patient tissue samples obtained from both sporadic and familial forms of Alzheimer's disease (including Swedish and Artic forms) exhibit distinct amyloid beta prion conformations and propagate unique amyloid morphologies[24, 30] that are maintained upon serial passage within AD mice models[24]. In addition, recent characterization of tau prions suggests that their seeding propensity represents an early pathological indicator in P301S tauopathy mice model whose incidence precedes and may also contribute to increasing amounts of other observed pathological indicators such as phosphorylated tau [27]. Nonetheless, not all amyloid-prion strains seed cytotoxic amyloid formation [15]. Recently, it was confirmed that while amylin fragment 15-25 and 19-29 S20G both form fibrils, only those formed by 19-29 S20G were toxic; moreover, while both fragments

seeded full length amylin fibril assembly only 19-29S20G seeded-fibrils were toxic [15]. Thus, it may be advantageous to enhance seeded aggregation towards innocuous amyloids while at the same time preventing seeded amyloid assembly stemming from toxic precursor strains.

Numerous biosensor cell-based assays have been developed as sensitive tools that can reliably quantitate amyloid seeding activity of exogenously added amyloid prions [23, 26-27, 33]. Herein a variety of cell culture systems can be employed to recombinantly express an amyloidogenic protein of interest that is typically fused with a fluorescent reporter such as the yellow fluorescent protein, or in the case of FRET-based biosensor systems, differentially tagged with an acceptor/donor fluorescent pair. The fluorescently tagged amyloid proteins produced by these cells, normally remain soluble as reflected by a low intensity diffuse fluorescent signal; however, in the presence of an exogenously added amyloid seed, these fluorescently fused amyloid proteins will undergo amyloid aggregation. This results in punctate amyloid inclusions that emit an intense florescent signal, which can be easily quantified.

One potential application of this technology would be to utilize it in a high throughput manner to identify anti-amyloid inhibitors capable of disrupting cell to cell prion transmission from either *in vivo* or *in vitro* prepared amyloid samples. In addition, or even alternatively, one could use the same platform to select for seed competent strains only capable of propagating non-toxic amyloid polymorphs[15]. Initial candidates identified from the high throughput biosensor assays could further be examined with their interacting amyloid seeds to obtain high resolution structural data, that could in turn spur downstream rational drug design efforts in a similar fashion employed by Eisenberg and colleagues [22]. This approach would allow one to select for seed specific amyloid pharmacophore inhibitors or enhancers that could theoretically be tailored to a specific amyloid prion strain. Lead candidates emerging from these studies,

especially if the binding prion amyloid strain was obtained from a pathologically relevant *in vivo* preparation (i.e. human or animal model tissue samples) would represent promising anti-amyloid agents to test in animal models.

Currently our group is assessing the *in vivo* efficacy of rosmarinic acid's (RA) ability to prevent various pathologies that occur in T2D animal model (HIP rats) [34]. These include investigating RA's anti-amylin amyloid activities as well as its ability to halt or slow down progression of T2D and other related neurodegenerative complications that occur in HIP rats [35-36]. Based on previously confirmed RA efficacies against Aβ *in vitro* and in an AD mice model, [37-38] I hypothesize that RA will reduce toxic oligomeric and insoluble amylin amyloid burden in HIP rat's concomitant with attenuating HIP rat pathologies such as T2D progression. My work indicates that RA prevents amylin amyloid formation *in vitro* coincident with stabilizing, non-toxic amylin aggregates that presumably do not enhance or seed further amylin amyloid aggregation (Chapter 4) [12]. At the same time, data in Chapter 5 suggest that such activity may represent epiphenomena related to inhibitor mediated amyloid inhibition *in vitro*. In any case, it remains unclear what role these off pathway aggregates may play *in vivo*. Recently, Soto and colleagues showed that amylin prion propagation is critically important to potentiating amylin amyloid formation and T2D progression in transgenic mice that express human amylin[29]. Accordingly, development of the biosensor system for assessing amylin prion transmission could be employed to clarify if the RA-stabilized amylin aggregates formed *in vitro*, and more importantly, if the hypothesized anti-amyloid activity of RA-treated HIP rats are mechanistically linked to preventing seeded amylin prion transmission. Seeding assays using primary islets obtained from HIP rats and or experiments that assess amylin prion propagation between HIP rats, could be employed to further assess RA's ability to prevent serial propagation of amylin

prions [29]. These types of experiments will not only provide insights on the hypothesized modes of action of potent anti-amyloid inhibitors such as RA, but also provide an elegant chemical biology platform for future studies that could be used to better address the importance of a prion-like mechanism in determining amyloid propagation *in vivo*.

A major challenge in implementing any future anti-amyloid therapeutic will be determining when and how often it will be administered. Although improving amyloid diagnostic tools may eventually be able to help address these problems, it is likely that such a treatment plan would require regular doses for potentially dozens of years. Thus, an ideal alternative to an anti-amyloid drug therapeutic would be to discover an anti-amyloid vaccine. Below is a brief overview of recent and ongoing clinical trials involving select active immunotherapies against amyloid beta and tau. While adverse immune responses prematurely ended Phase II clinical trial for AN1792 (AN-1792 consists of synthetic full-length Aβ peptide with adjuvant; https://clinical trials.gov, identifier: NCT00021723) which targeted active immunity against $A\beta_{42}$, a silver lining in this study was that antibody responders (~20% of patients) showed favorable neuropsychological test battery scores and exhibited decreased amounts of tau in cerebral spinal fluid[39]. Second generation biological CAD106 (CAD106 combines multiple copies of Aβ1-6 peptide derived from the N-terminal B cell epitope of Aβ, coupled to a virus-like bacteriophage particle, called Qβ) has been engineered to induce active immunity against amyloid beta while avoiding the T cell mediated immune responses that plagued AN1792. Currently, CAD106 is in phase III human clinical trials that is testing efficacy against a sub population of non-cognitively impaired APOE carries that are at risk for developing AD (identifier: NCT02565511). This study is scheduled to finish in 2024. Additionally, the AADvac-1 vaccine that targets active immunity against pathological tau in populations of

individuals with mild AD, is also currently in phase II human clinical trials that is scheduled to conclude by 2019 (identifier NCT02579252). A more in-depth discussion of these or other recent clinical trials testing efficacies of anti-amyloid immunotherapies, or alternatively, small molecule amyloid inhibitors can be found elsewhere[7, 40] and in Chapter 1.

While modulating or preventing amyloid formation is currently thought to be important in curing amyloid diseases, given the multifactorial nature of amyloid disease pathogenesis, it's possible and even likely that a cure will require more than an effective anti-amyloid drug or vaccine. Accordingly, additional efforts to target non- amyloid agents and cellular processes linked to amyloid disease will also likely be important. In this context, an exciting application is the prospect of engineering multifunctional small molecules capable of inhibiting amyloid assembly as well as other specific targets or processes pertinent to amyloid disease progression (see literature review and Chapter 3 for more discussion)[9, 41]. In fact, in Chapter 3 using natural compound oleuropein, our group showed that multifunctional amyloid inhibitors may be harnessed against specific amyloid pathologies (i.e. enhancing glucose stimulated insulin secretion while concomitantly inhibiting amylin amyloid formation represents dual activities that are particularly important for preventing or protecting against T2D).

In addition to oleuropein, many anti-amyloid natural compound inhibitors have been shown to exhibit other activities that could be leveraged to address the multifactorial nature of amyloid disease. These include but are not limited to serving as antioxidants [41-45], preventing inflammation [41, 46], reducing mitochondrial stress [47-49], and enhancing autophagy [46]. In fact, these observed multifunctional activities may be linked to several epidemiological/population based studies that indicate regular consumption of the Mediterranean diet [50], that consists of a rich pool of polyphenols, is correlated with a reduced risk of developing neurodegeneration-linked

amyloid diseases as well as obesity-related cardiovascular dysfunction and T2D [41, 50-53]. These data suggest it may be possible to engineer a modulated formula of multifunctional anti-amyloid nutraceuticals that could be prophylactically and regularly consumed to combat the chronic development and progression of amyloid diseases. If so, the latter could represent a solution to bypass the otherwise daunting task of administering a therapeutic for a long duration, or to act in concert with a potential future anti-amyloid vaccine.

References

1. Kayed, R.; Pensalfini, A.; Margol, L.; Sokolov, Y.; Sarsoza, F.; Head, E.; Hall, J.; Glabe, C., Annular protofibrils are a structurally and functionally distinct type of amyloid oligomer. *The Journal of biological chemistry* **2009,** *284* (7), 4230-7.
2. Laganowsky, A.; Liu, C.; Sawaya, M. R.; Whitelegge, J. P.; Park, J.; Zhao, M.; Pensalfini, A.; Soriaga, A. B.; Landau, M.; Teng, P. K.; Cascio, D.; Glabe, C.; Eisenberg, D., Atomic view of a toxic amyloid small oligomer. *Science* **2012,** *335* (6073), 1228-31.
3. Glabe, C. G.; Kayed, R., Common structure and toxic function of amyloid oligomers implies a common mechanism of pathogenesis. *Neurology* **2006,** *66* (2 Suppl 1), S74-8.
4. Kayed, R.; Head, E.; Thompson, J. L.; McIntire, T. M.; Milton, S. C.; Cotman, C. W.; Glabe, C. G., Common Structure of Soluble Amyloid Oligomers Implies Common Mechanism of Pathogenesis. *Science* **2003,** *300* (5618), 486-489.
5. Kayed, R.; Head, E.; Sarsoza, F.; Saing, T.; Cotman, C. W.; Necula, M.; Margol, L.; Wu, J.; Breydo, L.; Thompson, J. L.; Rasool, S.; Gurlo, T.; Butler, P.; Glabe, C. G., Fibril specific, conformation dependent antibodies recognize a generic epitope common to amyloid fibrils and fibrillar oligomers that is absent in prefibrillar oligomers. *Molecular neurodegeneration* **2007,** *2*, 18.
6. Hatami, A.; Albay, R., 3rd; Monjazeb, S.; Milton, S.; Glabe, C., Monoclonal antibodies against Abeta42 fibrils distinguish multiple aggregation state polymorphisms in vitro and in Alzheimer disease brain. *The Journal of biological chemistry* **2014,** *289* (46), 32131-43.
7. van Dyck, C. H., Anti-Amyloid-beta Monoclonal Antibodies for Alzheimer's Disease: Pitfalls and Promise. *Biological psychiatry* **2017**.
8. Velander, P.; Wu, L.; Ray, W. K.; Helm, R. F.; Xu, B., Amylin Amyloid Inhibition by Flavonoid Baicalein: Key Roles of Its Vicinal Dihydroxyl Groups of the Catechol Moiety. *Biochemistry* **2016**.
9. Velander, P.; Wu, L.; Henderson, F.; Zhang, S.; Bevan, D. R.; Xu, B., Natural Product-Based Amyloid Inhibitors. *Biochemical pharmacology* **2017**.
10. Wu, L.; Velander, P.; Liu, D.; Xu, B., Olive Component Oleuropein Promotes beta-Cell Insulin Secretion and Protects beta-Cells from Amylin Amyloid-Induced Cytotoxicity. *Biochemistry* **2017,** *56* (38), 5035-5039.
11. Cao, P.; Raleigh, D. P., Analysis of the inhibition and remodeling of islet amyloid polypeptide amyloid fibers by flavanols. *Biochemistry* **2012,** *51* (13), 2670-83.
12. Ehrnhoefer, D. E.; Bieschke, J.; Boeddrich, A.; Herbst, M.; Masino, L.; Lurz, R.; Engemann, S.; Pastore, A.; Wanker, E. E., EGCG redirects amyloidogenic polypeptides into unstructured, off-pathway oligomers. *Nature structural & molecular biology* **2008,** *15* (6), 558-66.
13. Tatarek-Nossol, M.; Yan, L.-M.; Schmauder, A.; Tenidis, K.; Westermark, G.; Kapurniotu, A., Inhibition of hIAPP Amyloid-Fibril Formation and Apoptotic Cell Death by a Designed hIAPP Amyloid- Core-Containing Hexapeptide. *Chemistry & biology 12* (7), 797-809.
14. Wiltzius, J. J.; Sievers, S. A.; Sawaya, M. R.; Cascio, D.; Popov, D.; Riekel, C.; Eisenberg, D., Atomic structure of the cross-beta spine of islet amyloid polypeptide (amylin). *Protein science : a publication of the Protein Society* **2008,** *17* (9), 1467-74.
15. Krotee, P.; Rodriguez, J. A.; Sawaya, M. R.; Cascio, D.; Reyes, F. E.; Shi, D.; Hattne, J.; Nannenga, B. L.; Oskarsson, M. E.; Philipp, S.; Griner, S.; Jiang, L.; Glabe, C. G.; Westermark,

G. T.; Gonen, T.; Eisenberg, D. S., Atomic structures of fibrillar segments of hIAPP suggest tightly mated beta-sheets are important for cytotoxicity. *eLife* **2017,** *6*.
16. Nelson, R.; Sawaya, M. R.; Balbirnie, M.; Madsen, A. O.; Riekel, C.; Grothe, R.; Eisenberg, D., Structure of the cross-[beta] spine of amyloid-like fibrils. *Nature* **2005,** *435* (7043), 773-778.
17. Sawaya, M. R.; Sambashivan, S.; Nelson, R.; Ivanova, M. I.; Sievers, S. A.; Apostol, M. I.; Thompson, M. J.; Balbirnie, M.; Wiltzius, J. J. W.; McFarlane, H. T.; Madsen, A. O.; Riekel, C.; Eisenberg, D., Atomic structures of amyloid cross-[bgr] spines reveal varied steric zippers. *Nature* **2007,** *447* (7143), 453-457.
18. Landau, M.; Sawaya, M. R.; Faull, K. F.; Laganowsky, A.; Jiang, L.; Sievers, S. A.; Liu, J.; Barrio, J. R.; Eisenberg, D., Towards a pharmacophore for amyloid. *PLoS biology* **2011,** *9* (6), e1001080.
19. Fitzpatrick, A. W. P.; Falcon, B.; He, S.; Murzin, A. G.; Murshudov, G.; Garringer, H. J.; Crowther, R. A.; Ghetti, B.; Goedert, M.; Scheres, S. H. W., Cryo-EM structures of tau filaments from Alzheimer's disease. *Nature* **2017,** *547* (7662), 185-190.
20. Fitzpatrick, A. W. P.; Debelouchina, G. T.; Bayro, M. J.; Clare, D. K.; Caporini, M. A.; Bajaj, V. S.; Jaroniec, C. P.; Wang, L.; Ladizhansky, V.; Müller, S. A.; MacPhee, C. E.; Waudby, C. A.; Mott, H. R.; De Simone, A.; Knowles, T. P. J.; Saibil, H. R.; Vendruscolo, M.; Orlova, E. V.; Griffin, R. G.; Dobson, C. M., Atomic structure and hierarchical assembly of a cross-β amyloid fibril. *Proceedings of the National Academy of Sciences of the United States of America* **2013,** *110* (14), 5468-5473.
21. Wälti, M. A.; Ravotti, F.; Arai, H.; Glabe, C. G.; Wall, J. S.; Böckmann, A.; Güntert, P.; Meier, B. H.; Riek, R., Atomic-resolution structure of a disease-relevant Aβ(1–42) amyloid fibril. *Proceedings of the National Academy of Sciences* **2016,** *113* (34), E4976-E4984.
22. Jiang, L.; Liu, C.; Leibly, D.; Landau, M.; Zhao, M.; Hughes, M. P.; Eisenberg, D. S., Structure-based discovery of fiber-binding compounds that reduce the cytotoxicity of amyloid beta. *eLife* **2013,** *2*, e00857.
23. Woerman, A. L.; Stöhr, J.; Aoyagi, A.; Rampersaud, R.; Krejciova, Z.; Watts, J. C.; Ohyama, T.; Patel, S.; Widjaja, K.; Oehler, A.; Sanders, D. W.; Diamond, M. I.; Seeley, W. W.; Middleton, L. T.; Gentleman, S. M.; Mordes, D. A.; Südhof, T. C.; Giles, K.; Prusiner, S. B., Propagation of prions causing synucleinopathies in cultured cells. *Proceedings of the National Academy of Sciences* **2015,** *112* (35), E4949-E4958.
24. Watts, J. C.; Condello, C.; Stöhr, J.; Oehler, A.; Lee, J.; DeArmond, S. J.; Lannfelt, L.; Ingelsson, M.; Giles, K.; Prusiner, S. B., Serial propagation of distinct strains of Aβ prions from Alzheimer's disease patients. *Proceedings of the National Academy of Sciences* **2014,** *111* (28), 10323-10328.
25. Yanamandra, K.; Kfoury, N.; Jiang, H.; Mahan, T. E.; Ma, S.; Maloney, S. E.; Wozniak, D. F.; Diamond, M. I.; Holtzman, D. M., Anti-tau antibodies that block tau aggregate seeding in vitro markedly decrease pathology and improve cognition in vivo. *Neuron* **2013,** *80* (2), 402-414.
26. Frost, B.; Jacks, R. L.; Diamond, M. I., Propagation of Tau Misfolding from the Outside to the Inside of a Cell. *Journal of Biological Chemistry* **2009,** *284* (19), 12845-12852.
27. Holmes, B. B.; Furman, J. L.; Mahan, T. E.; Yamasaki, T. R.; Mirbaha, H.; Eades, W. C.; Belaygorod, L.; Cairns, N. J.; Holtzman, D. M.; Diamond, M. I., Proteopathic tau seeding predicts tauopathy in vivo. *Proceedings of the National Academy of Sciences* **2014,** *111* (41), E4376-E4385.

28. Westermark, P.; Andersson, A.; Westermark, G. T., Islet amyloid polypeptide, islet amyloid, and diabetes mellitus. *Physiological reviews* **2011,** *91* (3), 795-826.
29. Mukherjee, A.; Morales-Scheihing, D.; Salvadores, N.; Moreno-Gonzalez, I.; Gonzalez, C.; Taylor-Presse, K.; Mendez, N.; Shahnawaz, M.; Gaber, A. O.; Sabek, O. M.; Fraga, D. W.; Soto, C., Induction of IAPP amyloid deposition and associated diabetic abnormalities by a prion-like mechanism. *The Journal of experimental medicine* **2017,** *214* (9), 2591-2610.
30. Lu, J.-X.; Qiang, W.; Yau, W.-M.; Schwieters, Charles D.; Meredith, Stephen C.; Tycko, R., Molecular Structure of β-Amyloid Fibrils in Alzheimer’s Disease Brain Tissue. *Cell 154* (6), 1257-1268.
31. Annamalai, K.; Guhrs, K. H.; Koehler, R.; Schmidt, M.; Michel, H.; Loos, C.; Gaffney, P. M.; Sigurdson, C. J.; Hegenbart, U.; Schonland, S.; Fandrich, M., Polymorphism of Amyloid Fibrils In Vivo. *Angewandte Chemie (International ed. in English)* **2016,** *55* (15), 4822-5.
32. Tycko, R.; Wickner, R. B., Molecular structures of amyloid and prion fibrils: consensus versus controversy. *Accounts of chemical research* **2013,** *46* (7), 1487-96.
33. Jackrel, M. E.; Shorter, J., Potentiated Hsp104 variants suppress toxicity of diverse neurodegenerative disease-linked proteins. *Disease Models & Mechanisms* **2014,** *7* (10), 1175-1184.
34. Butler, A. E.; Jang, J.; Gurlo, T.; Carty, M. D.; Soeller, W. C.; Butler, P. C., Diabetes due to a progressive defect in beta-cell mass in rats transgenic for human islet amyloid polypeptide (HIP Rat): a new model for type 2 diabetes. *Diabetes* **2004,** *53* (6), 1509-16.
35. Despa, S.; Sharma, S.; Harris, T. R.; Dong, H.; Li, N.; Chiamvimonvat, N.; Taegtmeyer, H.; Margulies, K. B.; Hammock, B. D.; Despa, F., Cardioprotection by controlling hyperamylinemia in a "humanized" diabetic rat model. *Journal of the American Heart Association* **2014,** *3* (4).
36. Despa, S.; Margulies, K. B.; Chen, L.; Knowlton, A. A.; Havel, P. J.; Taegtmeyer, H.; Bers, D. M.; Despa, F., Hyperamylinemia contributes to cardiac dysfunction in obesity and diabetes: a study in humans and rats. *Circulation research* **2012,** *110* (4), 598-608.
37. Hamaguchi, T.; Ono, K.; Murase, A.; Yamada, M., Phenolic compounds prevent Alzheimer's pathology through different effects on the amyloid-beta aggregation pathway. *The American journal of pathology* **2009,** *175* (6), 2557-65.
38. Ono, K.; Li, L.; Takamura, Y.; Yoshiike, Y.; Zhu, L.; Han, F.; Mao, X.; Ikeda, T.; Takasaki, J.; Nishijo, H.; Takashima, A.; Teplow, D. B.; Zagorski, M. G.; Yamada, M., Phenolic compounds prevent amyloid beta-protein oligomerization and synaptic dysfunction by site-specific binding. *The Journal of biological chemistry* **2012,** *287* (18), 14631-43.
39. Gilman, S.; Koller, M.; Black, R. S.; Jenkins, L.; Griffith, S. G.; Fox, N. C.; Eisner, L.; Kirby, L.; Rovira, M. B.; Forette, F.; Orgogozo, J. M., Clinical effects of Abeta immunization (AN1792) in patients with AD in an interrupted trial. *Neurology* **2005,** *64* (9), 1553-62.
40. Wang, Y.; Yan, T.; Lu, H.; Yin, W.; Lin, B.; Fan, W.; Zhang, X.; Fernandez-Funez, P., Lessons from Anti-Amyloid-beta Immunotherapies in Alzheimer Disease: Aiming at a Moving Target. *Neuro-degenerative diseases* **2017,** *17* (6), 242-250.
41. Stefani, M.; Rigacci, S., Beneficial properties of natural phenols: highlight on protection against pathological conditions associated with amyloid aggregation. *BioFactors (Oxford, England)* **2014,** *40* (5), 482-93.
42. Liu, T.; Jin, H.; Sun, Q. R.; Xu, J. H.; Hu, H. T., The neuroprotective effects of tanshinone IIA on beta-amyloid-induced toxicity in rat cortical neurons. *Neuropharmacology* **2010,** *59* (7-8), 595-604.

43. Han, M.; Liu, Y.; Zhang, B.; Qiao, J.; Lu, W.; Zhu, Y.; Wang, Y.; Zhao, C., Salvianic borneol ester reduces beta-amyloid oligomers and prevents cytotoxicity. *Pharmaceutical biology* **2011,** *49* (10), 1008-13.
44. Savelieff, M. G.; DeToma, A. S.; Derrick, J. S.; Lim, M. H., The ongoing search for small molecules to study metal-associated amyloid-beta species in Alzheimer's disease. *Accounts of chemical research* **2014,** *47* (8), 2475-82.
45. Yin, F.; Liu, J.; Ji, X.; Wang, Y.; Zidichouski, J.; Zhang, J., Silibinin: a novel inhibitor of Abeta aggregation. *Neurochemistry international* **2011,** *58* (3), 399-403.
46. Grossi, C.; Rigacci, S.; Ambrosini, S.; Ed Dami, T.; Luccarini, I.; Traini, C.; Failli, P.; Berti, A.; Casamenti, F.; Stefani, M., The polyphenol oleuropein aglycone protects TgCRND8 mice against Ass plaque pathology. *PloS one* **2013,** *8* (8), e71702.
47. Qu, M.; Jiang, Z.; Liao, Y.; Song, Z.; Nan, X., Lycopene Prevents Amyloid [Beta]-Induced Mitochondrial Oxidative Stress and Dysfunctions in Cultured Rat Cortical Neurons. *Neurochemical research* **2016,** *41* (6), 1354-64.
48. Sawmiller, D.; Li, S.; Mori, T.; Habib, A.; Rongo, D.; Delic, V.; Bradshaw, P. C.; Shytle, R. D.; Sanberg, C.; Bickford, P.; Tan, J., Beneficial effects of a pyrroloquinolinequinone-containing dietary formulation on motor deficiency, cognitive decline and mitochondrial dysfunction in a mouse model of Alzheimer's disease. *Heliyon* **2017,** *3* (4), e00279.
49. Cheng, B.; Gong, H.; Li, X.; Sun, Y.; Chen, H.; Zhang, X.; Wu, Q.; Zheng, L.; Huang, K., Salvianolic acid B inhibits the amyloid formation of human islet amyloid polypeptide and protects pancreatic beta-cells against cytotoxicity. *Proteins* **2013,** *81* (4), 613-21.
50. Hardman, R. J.; Kennedy, G.; Macpherson, H.; Scholey, A. B.; Pipingas, A., Adherence to a Mediterranean-Style Diet and Effects on Cognition in Adults: A Qualitative Evaluation and Systematic Review of Longitudinal and Prospective Trials. *Frontiers in Nutrition* **2016,** *3*, 22.
51. Anastasiou, C. A.; Yannakoulia, M.; Kosmidis, M. H.; Dardiotis, E.; Hadjigeorgiou, G. M.; Sakka, P.; Arampatzi, X.; Bougea, A.; Labropoulos, I.; Scarmeas, N., Mediterranean diet and cognitive health: Initial results from the Hellenic Longitudinal Investigation of Ageing and Diet. *PloS one* **2017,** *12* (8), e0182048.
52. Martinez-Lapiscina, E. H.; Clavero, P.; Toledo, E.; Estruch, R.; Salas-Salvado, J.; San Julian, B.; Sanchez-Tainta, A.; Ros, E.; Valls-Pedret, C.; Martinez-Gonzalez, M. A., Mediterranean diet improves cognition: the PREDIMED-NAVARRA randomised trial. *Journal of neurology, neurosurgery, and psychiatry* **2013,** *84* (12), 1318-25.
53. Berr, C.; Portet, F.; Carriere, I.; Akbaraly, T. N.; Feart, C.; Gourlet, V.; Combe, N.; Barberger-Gateau, P.; Ritchie, K., Olive oil and cognition: results from the three-city study. *Dementia and geriatric cognitive disorders* **2009,** *28* (4), 357-64.